## Biophysical Studies on the Structure, Conformational Dynamics and Carbohydrate Binding of Cucurbitaceae Phloem Exudate Lectins

#### A Thesis

Submitted for the Degree of

#### **DOCTOR OF PHILOSOPHY**

# By SARADAMONI MONDAL



School of Chemistry
University of Hyderabad
Institute of Eminence
Hyderabad-500046

India

December 2021

### Biophysical Studies on the Structure, Conformational Dynamics and Carbohydrate Binding of Cucurbitaceae Phloem Exudate Lectins

#### A Thesis

Submitted for the Degree of

#### DOCTOR OF PHILOSOPHY

# By SARADAMONI MONDAL



School of Chemistry
University of Hyderabad
Institute of Eminence
Hyderabad-500046
India
December 2021

# DEDICATED TO MY BELOVED FAMILY.....

## **Contents**

Statement		i
Certificate		ii
Declaration		iii
Acknowledgem	ents	iv
Abbreviations		v
Chapter 1:	Introduction	1
Chapter 2:	DSC and FCS Studies Reveal the Mechanism of Thermal and Chemical Unfolding of CIA17, a Polydisperse Oligomeric Protein from <i>Coccinia indica</i>	32
Chapter 3:	Effect of pH on the Local/Global Structure of CIA17 and its Carbohydrate Binding. Presence of a Molten Globule-Like State at Low pH	56
Chapter 4:	Macromolecular Crowding Significantly Affects the Conformational Features and Carbohydrate Binding Properties of CIA17, a PP2-type Lectin from <i>Coccinia indica</i> .	82
Chapter 5:	Purification, Biochemical/Biophysical Characterization and Chitooligosaccharide Binding to BGL24, a New PP2- Type Phloem Exudate Lectin from Bottle Gourd ( <i>Lagenaria siceraria</i> )	102
Chapter 6:	General Discussion and Conclusions	131
References		139
Plagiarism Repo	ort	162
Curriculum vita	e	176



#### **STATEMENT**

I hereby declare that the matter embodied in this thesis is the result of investigations carried out by me in the School of Chemistry, University of Hyderabad, Hyderabad, under the supervision of **Prof. Musti J. Swamy**.

In keeping with the general practice of reporting scientific observations, due acknowledgements have been made whenever the work described is based on the finding of other investigators. Any omission which might have occurred by oversight or error is regretted.

Hyderabad

December 2021

Saradamoni Mondal

Saradamon, Mondal



This is to certify that the thesis entitled "Biophysical Studies on the Structure, Conformational Dynamics and Carbohydrate Binding of Cucurbitaceae Phloem Exudate Lectins" submitted by Saradamoni Mondal bearing registration number 16CHPH23 in partial fulfilment of the requirements for award of the Doctor of Philosophy (Ph.D.) is a bonafide work carried out by him under my supervision and guidance in the School of Chemistry, University of Hyderabad. This thesis is free from plagiarism and has not been submitted previously in part or in full to this or any other University or Institution for award of any degree or diploma.

Further, the student has six publications before submission of the thesis for adjudication and has produced evidences for the same in the form of reprints.

Parts of this thesis have been published in the following two publications:

- S. Mondal, K. Bobbili, S. Paul, M. J. Swamy J. Phys. Chem. B. 2021, 125, 7117–7127. (Chapter 2)
- 2. <u>S. Mondal</u>, M. J. Swamy *Int. J. Biol. Macromol.* **2020**, *164*, 3656–3666. (Chapter 5)

He has also made presentations in the following conferences:

- 1. Poster presentation in the Symposium on "FCS 2021 12th National Workshop on Fluorescence and Raman Spectroscopy", 29<sup>th</sup> November–5 December, 2021 at IISER and RGCB Thiruvananthapuram Kerala.
- Oral presentation at "CHEMFEST-2021" Annual in-house Symposium of School of Chemistry, University of Hyderabad.
- Poster presentation at "CHEMFEST-2020" Annual in-house Symposium of School of Chemistry, University of Hyderabad.
- 3. Poster presentation in the ""43<sup>rd</sup> Indian Biophysical Society Annual Meeting" 22–25 February, 2019 at IISER Kolkata.

Further the student has passed the following courses towards fulfillment of the coursework requirement for Ph. D. degree:

Sl. No.	Course	Title	Credits	Grade/Status
1.	CY-801	Research Proposal	3	B <sup>+</sup> /Pass
2.	CY-802	Chemistry Pedagogy	3	B/Pass
3.	CY-805	Instrumental Methods-A	3	B/Pass
4.	CY-806	Instrumental Methods-B	3	A/Pass

Prof. Musti J. Swamy Thesis Supervisor

Prof. Musti J. Swamy School of Chemistry University of Hyderabad Hyderabad – 500 046, India Kumara Swamylle
Dean

School of Chemistry University of Hyderabad

Dean
SCHOOL OF CHEMISTRY
University of Hyderabad
Hyderabad-500 046



#### **DECLARATION**

I, Saradamoni Mondal hereby declare that the thesis entitled "Biophysical Studies on the Structure, Conformational Dynamics and Carbohydrate Binding of Cucurbitaceae Phloem Exudate Lectins" submitted by me under the supervision of Prof. Musti J. Swamy is a bonafide research work which is free from plagiarism. I also declare that it has not been submitted previously in part or in full to this University or any other University or Institution for the award of any degree or diploma. I hereby agree that my thesis can be deposited in Shodganga/INFLIBNET.

A report on plagiarism from the University Library is enclosed.

Saradamoni Mondal

Saradamoni Mondal

Reg. No.:16CHPH23

Prof. Musti J. Swamy

**Thesis Supervisor** 

Prof. Musti J. Swamy School of Chemistry University of Hyderabad Hyderabad – 500 046, India

#### **ACKNOWLEDGEMENTS**

The thesis could be a summary of five years of efforts, but the journey started when I was first introduced to science. From that day to date several people have inspired me and also contributed across the road with ups and downs. The thesis wouldn't be complete without thanking their contribution.

First and foremost, I would like to express my deep gratitude to my PhD supervisor, Prof. Musti J. Swamy, for his constant guidance and enormous support. I am very grateful to him for giving me the freedom to think the projects, plan and work independently but he was always accessible to discuss about the problems at any instant. His continuous encouragements helped me to keep positive even when things were not going smoothly. It has been a tremendously educative experiences to work with him.

I extend my gratitude to the present and former Deans, and Faculty members, School of Chemistry for their valuable suggestions at various stages and for the infrastructure available at the school. My sincere thanks to my doctoral committee members, Prof. Lalitha Guruprasad and Prof. A. K. Bhuyan for their cooperation and support throughout.

I am particularly grateful to Prof. Anunay Samanta of our school for giving me access of time-correlated single-photon counting instrument and his students Mr. Somnath Das and Sumanta Paul for their help with the TCSPC and FCS measurements. I would also like to acknowledge Prof. Nadimpalli Siva Kumar, University of Hyderabad and his lab members especially Kavyashree Ranganatha for their help in any need.

I would like to thank all the non-teaching staff of the School of Chemistry for providing me their valuable services at the appropriate time. I am also grateful to the Central Instrumental Laboratory, University of Hyderabad for providing an excellent instrumentation facility and my special thanks to Mr. Prasad for his kind cooperation.

I have been very fortunate to work in a lab where the atmosphere has always been friendly and enjoyable. I am grateful to my senior, Dr. Debparna Datta for introducing me the techniques of biophysical chemistry and for her timely suggestions on various things. I would also like to acknowledge Dr. Sudheer Kumar Cheppali, Dr. D. Sivaramakrishna, Dr. Kishore K. Bobbili and Dr. Pavan K. Nareddy for their fruitful suggestions and discussions. I have been enjoying my association with Sk. Alim, the most organised and responsible person in lab, who has looked after me throughout our association in the MJS lab including making tea and also with Ch. Ravidar, my partner in sports and fun. I am extremely thankful to Dr. Mohini Yarra, Dr. Venu Gopal and Dr. Debasree Das. I would like to appreciate Suman Kumar Chowdhury for his immense efforts for maintaining a cheerful enjoyment in lab. I also thank Konga Manasa, Sneha Banerjee, Tejaswini and Sonali for providing a good working atmosphere in the lab.

I would like to thank "Bangla UOH Samsad" and "HCU Bong Connection" for organising Parichiti, Bhasa, Saraswati Puja, Mahalaya, and Diwali which have helped me to overcome my homesickness particularly during festivals.

I treasure the moments shared with "NRS Core committee' Soutrik, Subham, Anupam, Suman da, Sumanta, Alamgir and "Divader Diwali" Sneha di, Sabari di, Moumita di, Tasnim di, Debika and Olivia. I also express my thanks to Debu, Somratan, Arunava, Sampita, Shilpa, Somdatta (Rudra), Liton, Manorama, Priyanka.

I would like to cherish my friendship with Mahmood da, Md. Ishtiyak, Somedutta (Maity) and Daradi not only helping me mentally in my ups and downs but also help me in my research work in many ways. I am thankful to friends and seniors Sugata da, Sudipta da Subhobrata da, Kollol da, Mou di, Arijit (Saha) da, Apurba da, Saddam da, Hafijur, Mr. Ankit, Senthin anna, Tanmay da, Arun anna, Anupam da, Suriya anna, Anil anna, Samita di, Shipra di, Arosmita di, Abu Taher da, Arijit (Mukherjee) da, Bappaditya da, Kuntal da, Najir and Mujahid who have always been there to help me and made my stay in Hyderabad a memorable one.

I would like to cherish the bonding with all my Ph.D. batchmates: Jyotsna, Mamina, Prachi, Soumya, Hema Kumari, Jayakrushna, Pritam, Akram, Irfan, Gorachand, Santi Swarupini, Subham (Datta), Nilanjan, Kalyani, Laxman.

I always reminisce the time spent with Tina, Jayashri, Sayantika, Sampreeti, Manisha di, Pratima di, Barnali di, Sarbani, Rituparna who made my B.Sc. days special. I would also like to thank Arijit, Devraj, Sovan, Tanmay, Nurul, Abhisekh and all my M.Sc. friends for their help during those days.

I convey my sincere regards and gratefulness to all my teachers who steered me towards the direction at various stages in my life. I specially thank my childhood teachers Govinda Babu, Ujjwal Kaku, Sudip Kaku, Shyamoli Kakima, Rajesh da, Tarun Kundu (Sir) whose affection as well as teaching will always be very dear to me.

It is difficult to put into words how much I owe for my best friend Somnath. His unwavering belief in my abilities, support and encouragements helped me to overcome my weakness and led to achieve things which seemed impossible to me. Thank you, Somnath, for being my pillar of support.

I express my eternal gratefulness to my late grandparents. "Dadu" was the first person who had a dream of my prosperous future and always encouraged me in my education and co-curricular activities. The maximum credit goes to my parents for whatever I have been able to accomplish so far. I acknowledge the love and support of my brother, Ramkamal, Sister-in-law, Susmita and Nephew, Sourish. I also acknowledge my cousins, Rammoy, Ram da, Ramjiban Da, Rammohan Da, Sampa di, Tumpa Di, Nabarun Da, Santanu Da, Sudeshna (Boudi), Laboni, Dolon di and relatives. for their endless love and support.

My deepest apologies if I have forgotten your name to mention but I wish to express my heartful gratitude to everyone who has played a role in my life in some way or other.

Saradamoni Mondal

#### **ABBREVATIONS**

ACN Acetonitrile

ANS 1, 8-anilinonapthalenesulfonic acid

BSA Bovine Seram Albumin

CBD Carbohydrate binding domain

CD Circular dichroism

Con A Concanavalin A

DSC Differential scanning calorimetry

Da Dalton

DTT Dithiothreitol

DNA Deoxyribonucleic acid

EDTA Ethylenediaminetetraaceticacid

Gdn.HCl Guanidine hydrochloride

Gdn.SCN Guanidine thiocyanate

 $\Delta G$  Change in free energy

GlcNac N-acetyl glucosamine

 $\Delta H$  Change in enthalpy

HCl Hydrochloric acid

His Histidine

HPLC High performance liquid chromatography

ITC Isothermal titration calorimetry

*K*<sub>a</sub> Association constant

 $\beta$ Me  $\beta$ -mercaptoethanol

MRE Mean residue ellipticity

MRW Mean residue weight

PAGE Polyacrylamide gel electrophoresis

PAMP Pathogen-associated molecular pattern

PB Phosphate buffer

Pro Proline

PDB Protein data bank

PI Protease inhibitor

PNA Peanut agglutinin

PP1 Phloem protein 1

PP2 Phloem protein 2

RIP Ribosome inactivating protein

RNA Ribonucleic acid

SBA Soybean agglutinin

SDS Sodium dodecylsulphate-

 $\Delta S$  Change in entropy

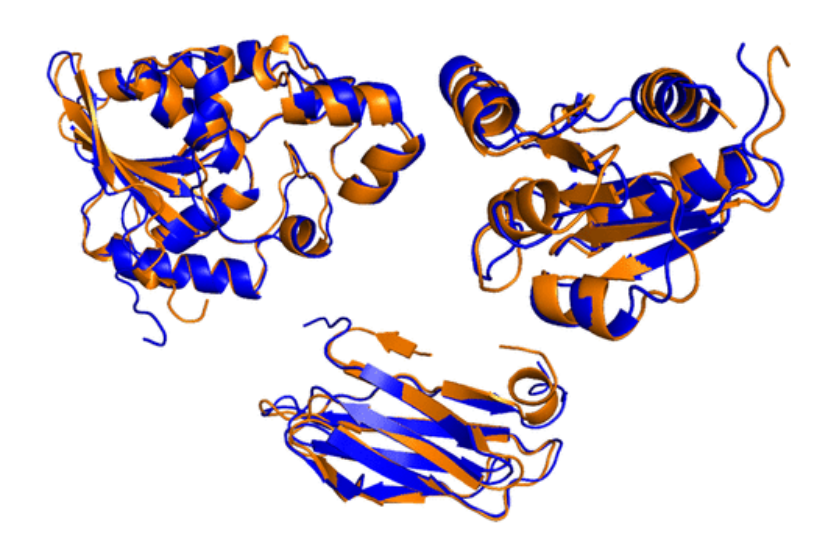
TFA Trifluoroacetic acid

T<sub>m</sub> Transition temperature

Trp Tryptophan

Tyr Tyrosine

## Introduction



"Proteins hold the key to the whole subject of the molecular basis of biological reactions."

- Linus Pauling

#### 1.1. Proteins

#### 1.1.1 Structure and Function of Proteins

Proteins, the most abundant and versatile among macromolecules, serve crucial role to sustain life [Berg et al., 2002]. All Proteins, regardless of the diversity in their biological functions, are made up of long polypeptide chains composed of the same set of 20 amino acid residues. Each protein contains a distinctive number of amino acid residues arranged in a unique sequence which folds up into a specific 3-D structure in order to optimize the maximum activity of the protein. In nature, four levels of architecture are found in proteins [Lehninger et al., 2004].

- (A) **Primary structure** includes the polypeptides made up of covalently bonded amino acids and the disulphide bonds. Specific sequence for a given protein is dictated by the corresponding 3-codon genes and is inextricably linked to its structure and function [Lehninger et al., 2004; Voet et al., 2011].
- (B) **Secondary structure** refers to some local arrangements of amino acid residues in the polypeptide chain which is dictated by steric constrains and several weak interactions.  $\alpha$ -helix and  $\beta$ -conformations ( $\beta$ -sheets and  $\beta$ -turns) are the most prominent secondary structures found in most of the fibrous and globular proteins. Similarly charged amino acid residues in adjacent position prevent the formation of  $\alpha$ -helix [Nelson et al., 2004]. The rest unstructured part is referred to the random coiled structure.
- (C) **Tertiary structure** is the three-dimensional spatial arrangements of polypeptides and the secondary structural elements in a protein. Folding in polypeptide chains to achieve the more stable structure of the protein is held by various kinds of weak interactions, e.g., hydrogen bonding, electrostatic interactions, salt bridge formation, hydrophobic and pi-pi stacking interaction and sometimes by the formation of covalent disulfide cross-linkages.
- (D) **Quaternary structure** refers to the spatial arrangements of two or more subunits (each polypeptide chain is called as subunit) within the protein. In multi-subunit proteins weak interactions between the subunits provide more stability to the overall structure.

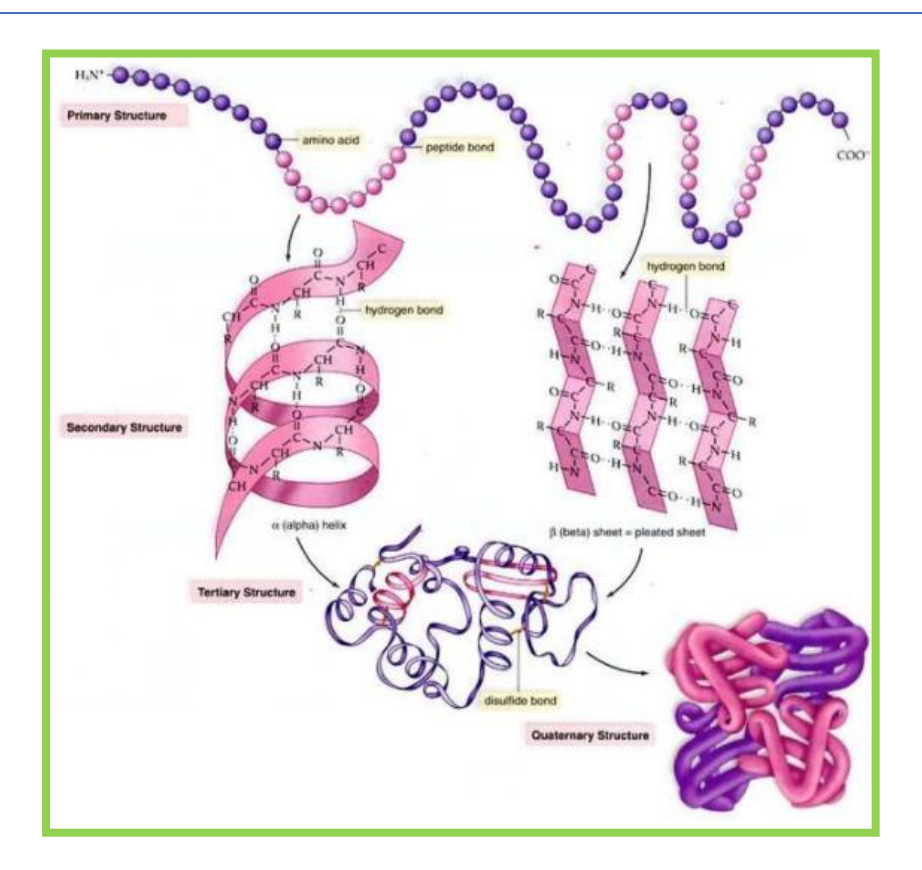


**Fig. 1.1.** Cartoon representation of the structural levels of proteins (primary, secondary, tertiary and quaternary structures). Image was taken from S. Mader, Biology. Mcgraw Hill, 2010.

#### 1.1.2. Protein Stability

The nascent polypeptide chain synthesized in ribosome immediately folds into the compact native conformation which is functionally active and essential for certain biological processes. Protein stability can be defined as the difference in free energy ( $\Delta G$ ) between the native (folded) and unfolded states obtained from the Gibbs–Helmholtz equation [Kumar and Venkatesu, 2012; Lehninger et al., 2004]:

$$\Delta G = -RT \ln K_a = -RT \ln [U] / [F]$$

The energy difference between the folded and unfolded states is small, in the range of  $\sim 20$  to 65 kJ/mol, which suggests that the native protein is marginally more stable under

physiological conditions. The predominant factors that contribute to the protein stability include the hydrophobic effect, and van der Waals and steric interactions along with conventional H-bonding and electrostatic interactions within itself and with solvent molecules [Kumar and Venkatesu, 2012; Lehninger et al., 2004]. A large increase in heat capacity upon unfolding of protein has been attributed to the exposure of nonpolar residues to the aqueous solvent during the unfolding process i.e., the reorganisation of the solvent [Robertson and Murphy, 1997]. The stability of a globular protein, in general, is the result of a balance between the intramolecular interactions and with the cosolvent molecules [Kumar and Venkatesu, 2012; Lehninger et al., 2004]. Other contributing factors are  $n \rightarrow \pi^*$  interactions, aromatic rings interactions involving  $\pi$ - $\pi$ , cation- $\pi$ , anion- $\pi$ , X-H--  $\pi$ , and sulphur-arene bonds, as well as C-H- - O and C5 hydrogen bonding, chalcogen bonding etc. These noncanonical secondary contributions can be divided into two general classes: (1) weak but abundant interactions involving the peptide backbone and (2) less frequent but strong interactions involving side chains of the protein [Newberry and Raines, 2019].

#### 1.1.3. Protein Structural Dynamics and (Un)Folding

Proteins are dynamic entities and undergo several changes leading to the formation of multiple conformational states. The structural transitions of proteins span over a magnitude of femto-second (that resulting from vibrations and rotations of the chemical bonds) and pico- to nano-second (resulted from fluctuation of the orientations of bond vectors) time scale and adopt unique conformations by a series of quasi-equilibrium processes that allow proteins to perform specific functions [Henzler-Wildman and Kern, 2007]. The motion of side-chain rotamers and fluctuations of the polypeptide backbone occurs in several nanoseconds. According to free energy landscape (FEL) theory, structural dynamics of proteins are characterized by **thermodynamics** i.e., the relative populations/probabilities and/or lifetimes of the conformational states and **kinetics** that involves the conformational transition leading to the population redistribution among those conformational states of the protein [Henzler-Wildman and Kern, 2007; Ma et al., 2001].

The protein (un)folding pathway often involves the formation of folding intermediates. Characterizing the nature of such intermediate states is crucial to determine

whether the protein will refold robustly to the native conformation or will undergo misfolding and/or aggregation [Tsytlonok and Itzhaki, 2013; Wagner and Kiefhaber, 1999]. 'Molten globule', an equilibrium/kinetic intermediate that possesses native-like secondary structure with perturbed tertiary structure compared to the native state, is one of the commonly observed intermediate states [Redfield et al., 1994; Wu et al., 1995]. These folding intermediates are transient in nature and structural characterization of them is difficult. Extreme conditions such as low pH, high temperature, denaturants or co-solvent are used frequently in order to populate such an intermediate state sufficiently to allow detailed structural analysis [Feige et al., 2008; Tsytlonok and Itzhaki, 2013].

#### 1.1.4. Protein Oligomerization

Oligomeric proteins, comprising of two or more inter-connected polypeptide chains make up 30-35% of total cellular proteins in both eukaryotic and prokaryotic organisms and are accountable for many biological processes [Griffin and Gerrard, 2012]. Protein oligomerization can be defined as an arrangement of monomeric unit of protein i.e., protomer into homo- or hetero-oligomers with a majority of the proteins forming homodimers or tetramers [Hashimoto and Panchenko, 2010]. Oligomerization can take place either naturally or by artificial means which arises through covalent bonding (e.g., disulphide bond formation) or weak non-covalent associations in an irreversible or reversible manner, respectively. Oligomerization allows proteins to form larger structures which reduces the surface area of the protomer in a protein complex and can offer extra stability and protection against denaturation [Liu, 2015]. The association of subunits differs in strength and duration depending on the system and the local environment. Some proteins are found to exist primarily in oligomeric forms which have dissociation constants  $(K_d)$  in the nanomolar range while others have a weak tendency to associate, with a higher  $K_d$  value in the micromolar or even millimolar range. The weaker complexes demonstrate smaller contact areas between the monomers and the interfaces are more planar and polar when compared to the "strong" complexes which mostly undergo large conformational modulations upon association/dissociation and are associated with the larger, less planar and often more hydrophobic interfaces [Ali and Imperiali, 2005; Nooren and Thornton, 2003]. Proteins oligomerize dynamically in response to the change in physiological environment, such as a change in pH, temperature, effective concentration of protein and/or ligand, upon nucleotide binding, phosphorylation state etc which can induce a dramatic effect on the affinity for the subunits association by several orders of magnitude. Since protein oligomerization is inextricably related to the protein activity, modulating this process is a highly promising therapeutic strategy for the treatment of several human diseases [Kumari and Yadav, 2019; Liu, 2015].

#### 1.2. Protein Glycosylation

Glycosylation is a complex co- or post-translational modification process by which glycans are attached to either proteins or lipids through the formation of glycosidic linkage by enzymes called glycosyltransferases and/or glycosidases in eukaryotes. Glycosylation usually takes place in the endoplasmic reticulum (ER) and golgi bodies apparatus with sequential addition of sugar residues occurring in the *cis-*, *medial-* and *trans-*Golgi compartments of the cell. Glycosylation plays a major role in the formation of cell membrane in determining the proper conformation of many membrane proteins and also in cell-cell adhesion [Lodish et al., 2000; Reily et al., 2019; Spiro, 2002]. The diversity in protein glycosylation arises due to the glycans comprising of linear or branched oligosaccharides, the amino acid residues to which the glycan is attached and the cellular/environmental condition as well [Ohtsubo and Marth, 2006; Pilobello and Mahal, 2007].

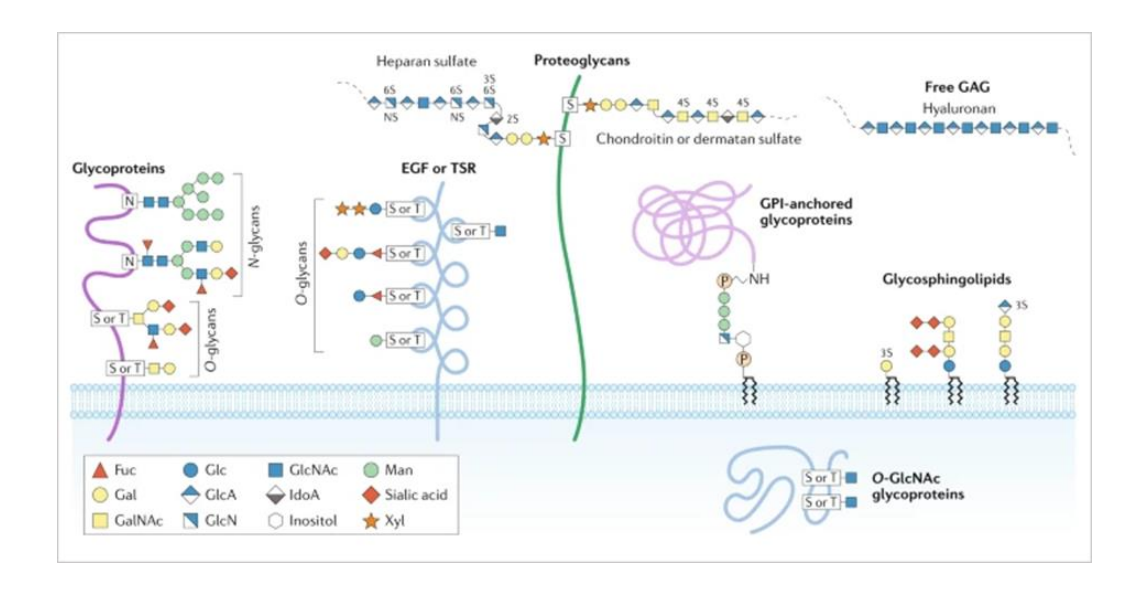


**Fig. 1.2.** Major types of glycosylations observed in human. (Image taken from Reily et al., 2019.)

Glycosylation of proteins includes the addition of N-linked and O-linked glycans, phosphorylated glycans, as well as glycosaminoglycans and glycosylphosphatidylinositol (GPI) anchors to protein backbones and sometimes C-mannosylation of tryptophan residues [Mitra et al., 2006; Reily et al., 2019; Spiro, 2002]. In glycoproteins, the glycan chains linked to N- and O- atoms of amino acid residues are termed as N-glycans and O-glycans, and are attached by a  $\beta$ 1-glycosidic linkage at the consensus glycosylation motif Asn-X-Ser/Thr (in which X denotes any amino acid except for Pro) [Lodish et al., 2000; Moremen et al., 2012].

#### 1.3. Lectins

Lectins are a unique class of proteins or glycoproteins of non-immune origin that bind carbohydrates in a highly specific and reversible manner but are devoid of enzymatic activity. Lectins are able to precipitate different glycans and glycoproteins present on the cell surface, known as 'glycocalyx' and were also termed as 'agglutinins' [Sharon and Lis, 2004]. They are ubiquitously found in all possible living organisms and are often

categorized based on their sources, e.g., animal lectins, plant lectins, fungal, or bacterial lectins. Animal lectins are found in serum, intra- and extracellular matrix as well as membranes and fulfil specific endogenous functions [Drickamer and Taylor, 1993]. Plant lectins are present in different vegetative storage organs including seeds (Concanavalin A, ricin, jacalin), bark (MornigaG, MornigaM), leaves (mistletoe lectin/viscumin), roots/tubers (*Urtica dioica* agglutinin), bulb (*Solanum tuberosum* lectin), latex (mulberry, *Morus indica*) and phloem sap (*Cucurbita maxima, Cucumis sativus*) with the seed lectins being extensively studied [Datta et al., 2016; Narahari and Swamy, 2010; Patel et al., 2011; Rüdiger and Gabius, 2001]. The viral lectins attach to the sialic acid on the plasma membrane and mediate several infections in the host cells, such as influenza virus hemagglutinin [Varki et al., 2009]. Numerous bacterial lectins are produced on the cell surface in the form of filamentous assemblies, commonly known as fimbriae and adhere to epithelial cells initiating bacterial infections [Sharon, 1987].

Lectins are also divided into various types according to their carbohydrate-binding specificities, such as gluocose/mannose binding, galactose binding, fucose binding, *N*-glycan binding etc. Lectins are also grouped based on the homology in their amino acid sequences. Fujimoto and coworkers classified lectins into 48 families based on their three-dimensional structure determined by X-ray crystallography or NMR analysis [Fujimoto et al., 2014].

#### 1.3.1. Lectin-Carbohydrate Interaction

Lectins interact with carbohydrates primarily via a network of hydrogen bonds, van der Waals and hydrophobic interactions, electrostatic interactions; coordination bonds with metal ions sometimes play a major role. Selectivity towards sugar and affinity result from hydrogen bonding with hydroxyl groups of the sugar that can act both as a hydrogen bond donor as well as an acceptor [Elgavish and Shaanan, 1997; Komath et al., 2006; Sharma and Surolia, 1997; Sharon, 1993; Weis and Drickamer, 1996]. Water mediated bonds often strengthen the interactions. Based on the monosaccharide specificity, lectins can be classified into five groups as well: mannose-, galactose/N-acetylgalactosamine-, sialic acid-, fucose- and N-acetylglucosamine-specific, all of which are building blocks for

animal cell surface glycans. The affinity of lectins towards monosaccharides is usually weak (dissociation constant in the milimolar range). However, affinity often increases several folds for the oligosaccharides of cell surface glycoproteins or glycolipids. For example, Con A shows about 100-fold higher affinity towards a synthetic mannose polymer than simple methyl-α-mannopyranoside [Mortell et al., 1996]. Subsite binding or an extended binding region, ligand multivalency and conformational heterogeneity contribute for the high affinity and specificity towards oligosaccharides [Bundle and Young, 1992; Sharma and Surolia, 1997; Sharon, 1993]. This high affinity of lectins towards multivalent ligands is termed as 'cluster glycoside effect' [Dimick et al., 1999; Lis and Sharon, 2003].

#### 1.3.2. Lectin-Noncarbohydrate Interaction

Several lectins have been found to possess distinct hydrophobic, non-carbohydrate ligand binding sites that are remote from the carbohydrate binding site [Komath et al., 2006]. Widely used hydrophobic fluorescent probes such as ANS (1, 8-anilino-naphthalene sulfonic acid) and TNS (2,6-toluidinylnaphthalenesulfonic acid), several phytohormones like abscisic acid, zeatin, cytokinin, kinetin, gibberellic acid, as well as adenine and its derivatives were found to bind several lectins with an affinity of 10<sup>3</sup> -10<sup>6</sup> M<sup>-1</sup> [Gegg et al., 1992; Maliarik and Goldstein, 1988; Roberts and Goldstein, 1982, 1983a, b]. For example, lima bean lectin binds with ANS with a binding constant  $3.9 \times 10^3 \, M^{-1}$  [Roberts and Goldstein, 1982] The binding constant for the interaction of WGA with adenine and adenine related phytohormones were in the range of 1.6 -  $2.3 \times 10^6$  M<sup>-1</sup> [Bogoeva et al., 2004]. Momordica charantia seed lectin, MCL, a galactose specific lectin was also reported to bind adenine and cytosine with moderate binding affinity ( $K_a \sim 1.1$  and  $1.5 \times 1.5$ 10<sup>4</sup> M<sup>-1</sup>) [Kayitha et al., 2009a]. In addition, several lectins bind porphyrins which are potential photosensitizers in photodynamic therapy. For example, jacalin and snake-gourd lectin bind porphyrins with association constants in a range of 10<sup>3</sup> -10<sup>5</sup> M<sup>-1</sup> and Con A and pea lectin interacted with the binding constants in the range of  $1.2 - 6.3 \times 10^4 \,\mathrm{M}^{-1}$  [Bhanu et al., 1997; Komath et al., 2006]. Porphyrins or other similar hydrophobic drugs complexed with several lectins can be used in a variety of fields including cell biology and medicine.

#### 1.3.3. Plant Lectins

Plants lectins are most thoroughly studied among the lectins owing to their vast distribution among the plant kingdom and their ease of purification. Based on structural heterogeneity they have been classified into seven distinct families; legume lectins, chitin binding lectins, type-2 ribosome inactivating proteins and related lectins, jacalin related lectins, monocot mannose binding lectins, amaranthin lectins and cucurbitaceae phloem lectins [Van Damme et al., 1998]. Based on differences in the extent of agglunating ability or the number of carbohydrate binding domains (CBD) each family is further subdivided into four groups, such as merolectins, which contain a single CBD, hololectins that have at least two identical carbohydrate binding domains with the same specificity, and chimerolectins, which are fusion proteins consisting of a lectin domain linked to some other domain which has an independent functional activity that is from the carbohydrate binding (e.g., Type-II RIPs) and super lectins, which possess more than one CBD but with different specificities, e.g., the tulip bulb lectin [Van Damme et al., 1998].

The function of plant lectins is still unclear. Many lectins are present in the vegetative storage organs and are thought to behave primarily as storage proteins [Van Damme et al., 2002]. Most plant lectins are cytotoxic and several evidences support their involvement in protecting the plants from attack by fungi, insects, phytophagous invertebrates or herbivorous animals [Datta et al., 2016; Peumans et al., 2001]. The lectins in leguminous plants play a key role in the establishment of symbiosis between the plant and nitrogen-fixing bacteria. The presence of lectins in roots mediates the specific association of bacteria and the root hair surface which is termed as the "lectin recognition hypothesis" [Hirsch, 1999; Kijne, 1996].

#### 1.4. Phloem

Phloem, the major integral component of the entire plant communication system is comprised of phloem fibres, sieve elements, companion cells, and phloem parenchyma [Heo, et al., 2014]. Sieve elements, the major conducting cells in phloem tissue, are elongated and are connected in end-to-end fashion to form Sieve tubes which are interconnected with each other through sieve plates, the membrane-like cell wall which facilitate the passage of materials through the pores known as sieve pores. Sieve tubes lack nuclei and other organelles and are inextricably associated with the companion cells via plasmodesmata. Companion cells are the "Power suppliers" for the sieve elements as proteins and other molecules which are synthesized in companion cells are translocated into the sieve elements [Jiang et al., 2019]. Phloem parenchyma are the parenchyma cells made up of cellulose and function as the storage compartments for starch, fats and proteins as well as tannins and resins in certain plants. Overall, phloem consists of a facinating collection of distinct cells (see Fig. 3A) which fecilitate the phloem tissue to play a major rule in long distance trafficcing in plants as well as in plant defence responses.

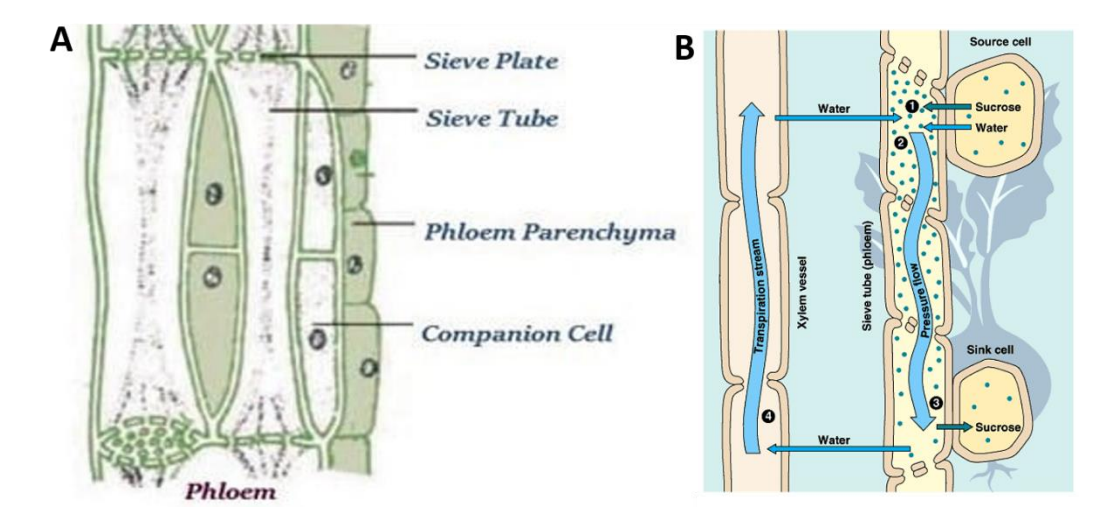


**Fig. 1.3.** (A) Cross section of phloem tissue and (B) transport in phloem tissue. Images taken from <a href="https://qsstudy.com/biology/phloem-tissue-describe-different-types-phloem-tissue">https://qsstudy.com/biology/phloem-tissue-describe-different-types-phloem-tissue</a> and <a href="http://biology4alevel.blogspot.com/2014/11/41-transport-in-phloem.html">http://biology4alevel.blogspot.com/2014/11/41-transport-in-phloem.html</a>.

#### 1.4.1. Translocation in Phloem

Among several models proposed for the translocation of the photo-assimilates produced on the leaves and other organic molecules from the source to the sink tissues e.g., stems, roots, fruits etc, the mass flow theory proposed by Ernest Münch [Münch, 1930] is now widely accepted. The process is accomplished by the mechanism of **phloem loading** and **unloading** (see Fig. 3B). Organic substances and macromolecules are loaded in to sieve elements from companion cells or mesophyll cells by active energy processes. The pressure gradient in the sieve tubes, generated by the accumulation (loading) of sugars and other osmotic substances at the sources draws water into the cell and creates a positive hydrostatic pressure which pushes the saps towards the sink and their release (unloading) at the sinks occurs by lowering the turgor pressure [Knoblauch et al., 2010; Schepper et al., 2013].

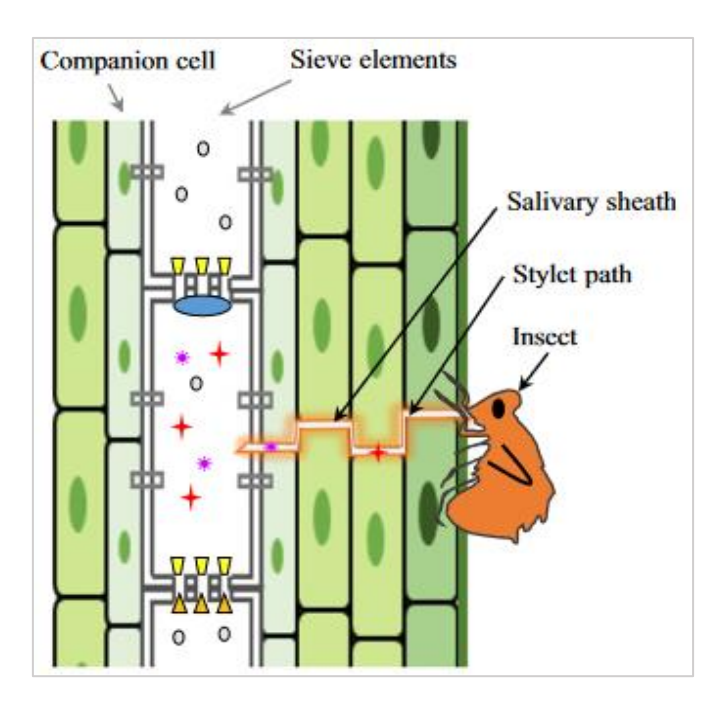


**Fig. 1.4.** A longitudinal diagram of phloem–insect/pathogen interactions. An insect is shown with its stylet piercing the plant tissue in order to reach a phloem sieve cell (Image taken from Jiang et al., 2019).

#### 1.4.2. Phloem in Plant Defence Responses

Phloem sap plays a key role in rapid sealing of the wound caused by the phloem feeding insects [Jiang et al., 2019]. Damage of sieve tubes disturbs the existing pressure conditions resulting in a turgor shift which induces the occlusion of sieve tubes via the plugging of sieve pores. Following injury, phloem exudate oozes out from their parietal position and forms plugs at sieve plates to block further translocation, thus generating a barrier which seals the wound. Indeed, the defence response is essentially the expression of some proteins known as **phloem proteins** which can interact with the pathogen and its associated molecular patterns (PAMP) and transmit the alarm signals from the injured parts to the entire plant [Will and Van Bel, 2006; Will et al., 2013].

#### 1.5. Phloem Proteins and Their Function

In most angiosperms, phloem sap contains many ultra-structurally distinct protein bodies, collectively called as phloem proteins (P-proteins) [Esau and Cronshaw, 1967; Kehr, 2006; Kleining, 1975]. These proteins are the fundamental component of the parietal cytoplasmic contents of sieve elements and often disperse as filamentous network [Thompson and Schulz, 1999]. P-proteins appear as amorphous, crystalline, filamentous, tubular and fibrillar structures under microscopy depending on the source plant species [Dinant et al., 2003; Thompson and Schulz, 1999]. The functions of most of the P-proteins are poorly understood. Many phloem proteins have been predicted to play a major role in wound sealing and defence responses, and represent a class of proteins which influence plantinsect interactions. They are thought to accumulates at the sieve plate upon injury and block the translocation by forming P-protein plugs [Golecki et al., 1999; Kehr, 2006; Oparka and Cruz, 2000; Thompson and Schulz, 1999]. The P-proteins are primarily composed of phloem protein 1 (PP1) and phloem protein 2 (PP2). In Cucurbita maxima PP1 is a 96 kDa structural protein and forms P-protein filaments by the formation of disulfide bridges with PP2 proteins [Dinant et al., 2003; Read and Northcote, 1983; Will et al., 2013]. PP2 proteins in various Cucurbitaceae species are 32-52 kDa homo-dimers which appear to play a major role in wound sealing, protect the plants from pathogenic attack, and also interact with different RNA molecules to form ribonucleoprotein (RNP) complexes and transport them from cell to cell and exhibit lectin activity as well.

#### 1.5.1. PP2 Type Lectins

PP2 proteins are one of the most abundant proteins among the phloem proteins. PP2 proteins are synthesized in the companion cells and are thought to associate with the polymers of PP1 and subsequently transported into the sieve elements via plasmodesmata pores. PP2 proteins are reported to exist as homodimer with a subunit molecular weight of 16-26 kDa and specifically binds chitooligosaccharides [ $\beta$ (1-4) linked oligomers of *N*-acetylglucosamine (GlcNAc)].

#### 1.5.2. Occurrence

#### 1.5.2.1. Cucurbitaceae Phloem Lectins

The PP2 type lectins are highly abundant in Cucurbitaceae fruits (Sabnis & Hart, 1978) and are purified from the phloem exudate of several Cucurbitaceae species such as ridge gourd (Luffa acutangula), pumpkin (Cucurbita maxima), snake gourd (Trichosanthes anguina), cucumber (Cucumis sativus), ivy gourd (Coccinia indica) and are characterized in considerable detail [Anantharam et al., 1986; Bobbilli et al., 2014, 2018a, b, 2019; Bostwick et al., 1999; Kumar et al., 2015; Narahari and Swamy, 2010; Narahari et al., 2011a, b; Nareddy et al., 2017, 2018; Read and Northcote, 1983; Sanadi and Surolia, 1994; Sanadi et al., 1998]. The PP2 lectins from various Cucurbitaceae species are highly homologous with respect to their amino acid sequence and contain a highly conserved "chitin binding domain" whose conformation is locked by a disulfide bond between two cysteine residues. In the early days these lectins were believed to exist as homodimers containing un-glycosylated subunit of molecular mass of 24-26 kDa and show high affinity towards chitooligosaccharides. Recent studies showed that many of these lectins form higher oligomers at higher concentration [Bobbili et al., 2018a; 2018b]. Most interestingly, intrageneric as well as intergeneric divergence in their occurance, structure and carbohydrate binding affinity were found among the Cucurbitaceae PP2 lectins. Some Cucurbitaceae genus contain another PP2-type lectin of Mr~ 17 kDa along with the 24-26 kDa. For example, multiple 17 kDa PP2 proteins (CmsLec17 and CmmLec17 from cucumber and melon) were found in *Cucumis spp* with minor variations in their amino acid sequence [Dinant et al., 2003]. Two lectins (CIA24 and CIA17) with distinct chitooligosaccharide binding affinities have been purified from the phloem exudate of *Coccinia indica* [Bobbili et al., 2018a, b]. The 24/26 kDa PP2 lectins contains an N-terminal segment comprising of ~62-65 amino acid residues which is absent in the 17 kDa phloem lectins. The fundamental role of this small region in the structural stability and/or in lectin activity is not clearly understood. The ligand binding affinity remains almost unaltered in proteins lacking this *N*-terminal peptide. A chitooligosaccharide specific lectin, SGPL was also purified from snake gouard (*Trichosanthes anguina*) phloem exudate which exists as a heterodimer of Mr ~105 kDa, with subunit molecular weights of 57 kDa and 48 kDa [Narahari et al., 2011a, b].

#### 1.5.2.2. Non-Cucurbitaceae Phloem Lectins

PP2 like domains are also found beyond Cucurbitaceae fruits. For example, two PP2 like genes from Apiacae and 30 PP2 like genes from Arabidopsis genome were isolated among which AgPP2-1 and AgPP2-2 from celery and AtPP2-A1 and -A2 from Arabidopsis exhibit highest sequence identity (30-40%) with those from *Cucurbitaceae* family. PP2 like genes were identified in 21 species including eight dicot families, like Solanaceae, Fabaceace, Malcaceae and Aizoaceae, and in four monocot species from Poaceae [Dinant et al., 2003]. Although conservation of these domains is highly specialised in the vascular angyosperms, PP2 like genes were identified in vascular gymnosperms including several cereals and *Pinus taeda*, *Pinus sabiniana* [Schulz et al., 1989] and were also found in nonvascular plant like *P. patens*. The presence of genes encoding PP2 like proteins in almost all plant kingdoms with significant probability indicates that these genes are ancient [Dinant et al., 2003].

#### 1.5.3. Role of the Phloem Exudate Lectins

#### 1.5.3.1. Chitin Binding Properties

All PP2-type lectins have a unique property to bind chitin and N-linked oligosaccharides containing core chitobiose structure. Chitin is the primary component of the fungal cell wall and most importantly, plants do not contain chitin in it but possess the enzymes those can degrade it [Bueter et al, 2013; Chen et al., 2018; Kasprzewska, 2003]. Binding between PP2-type lectins and N-linked oligosaccharides is possibly mediated by the interaction of the lectins with core chitobiose moiety of the N-linked glycoconjugates. Their capacity of chitin binding reflected the involvement PP2-lectins in anti-pathogenic responses in plants.

#### 1.5.3.2. Anti-pathogenic Responses and Wound Sealing

Upon biological stress and/or wounds made by insects, the phloem sap oozed out through the wound which quickly forms elastic-jelly-like substance, possibly due to disulfide bond formation (oxidation) with other PP2 lectins and also with the PP1 filamentous proteins upon exposure to air. The PP2 lectins thus form insoluble cross-linked filaments, and immobilize microorganisms and fungi in it which results in a sealing of the wounded sieve tubes and protect the plants from the insecticidal and pathogenic attack.

#### 1.5.3.3. Possible Involvement in RNA Binding and Transport of RNP Complexes

The Cucurbitaceae PP2 type lectins are thought to involve in the interaction with several RNA molecules, form the ribonucleoprotein (RNP) complexes and mediate transport of RNP complexex from cell to cell and thus play a key role as *super highway* to deliver RNA based information signals in the entire plants [Jorgensen et al., 1998; Lucas et al., 2001]. They can bind a variety type of RNA molecules such as mRNAs, siRNAs, miRNAs and viroid RNA. PP2 protein from *Cucurbita maxima* phloem exudate i.e., CmPP16 (*Cucurbita maxima* Phloem Protein16) was found to bind both endogenous and exogenous RNAs in a nonspecific manner. *Cucumis sativus* (Cucumber) phloem protein 2 (CsPP2) is a homodimeric lectin with an apparent molecular weight of ~26 kDa which is similar to CPL and CmsLec17 were found to interact with viroid RNA *in vitro* [Gómez and Pallás,

2001, 2004; Owens et al., 2001]. Two homodimeric phloem lectins, CmmPP2 and CmmLec17 with Mr ~24 and 17 kDa, and an unchracterized ~14 kDa protein isolated from water melon (*Cucumis melo*) were also reported to exhibit RNA binding activity, with CmmLec17 exhibiting higher RNA binding affinity than the other two [Balachandran et al., 1997; Golecki et al., 1999; Gomez and Pallas, 2001; Gomez et al., 2005; Owens et al., 2001; Pallas and Gomez 2013]. Since PP2 proteins have allelic variants like histone proteins [Kamakaka and Biggins, 2005] their functions may also be similar to those of the histone proteins in that they complex with RNA and help in protecting them from degradation as well as in their transport.

#### 1.5.3.4. Chaperone Like Activity

A recent study suggested that the PP2 lectins can possibly act as molecular chaperones during stress condition. A recombinant protein of AtPP2-A1 which encodes a phloem lectin exhibits dual functions including both molecular chaperone activity and antifungal activity under external stresses such as attack by pathogens, and other signalling molecules [Lee et al., 2014]. These results suggest that the AtPP2-A1 molecular chaperone protein plays a critical role in Arabidopsis defence system against diverse external stresses including fungal pathogenic attack and heat shock.

#### 1.6. Purification of PP2 Type Lectins

PP2-type lectins have been purified from the phloem exudate of several cucurbit species by various approaches. Sabnis and Hart (1978) purified the phloem exudate proteins from *Cucurbita maxima*, *Cucumis sativus* and *Cucumis melo* using gel filtration on Sephedex G100 followed by ion-exchange chromatography on CM Sepharose CL-6B. Beyenback et al. (1974) purified a 30 kDa protein from *Cucurbita maxima* by a combination of ammonium sulfate precipitation, and chromatographic tecniques such as ion-exchange chromatography on CM cellulose and gel filtration. Read and Northcote (1983) also purified the *C. maxima* lectin by a combination of ammonium sulfate precipitation and ion-exchange chromatography on CM Sepharose CL-6B. Another phloem exudate lectin from vegetable marrow (*Cucurbita pepo*) was purified by ammonium sulfate precipitation,

followed by affinity chromatography on chitooligosaccharides covalently coupled to Sepharose (Allen, 1979). Surolia and coworkers purified phloem exudate lectin from ridge gourd (*Luffa acutangula*) and ivy gourd (*Coccinia indica*) using affinity chromatography where soybean lectin coupled to Sepharose 6B and Sepharose 4B were used as the affinity matrices, respectively [Anantharam et al., 1986; Sanadi and Surolia, 1994]. In these methods, the affinity of those lectins for the *N*-linked oligosaccharide of soybean agglutinin, which contains an internal chitobiose unit, was exploited. Later, Swamy and colleagues reported the purification of several Cucurbitaceae phloem exudate lectins including pumpkin (*Cucurbita maxima*), snake gourd (*Trichosanthes anguina*), cucumber (*Cucumis sativus*), and ivy gourd (*Coccinia indica*) [Narahari and Swamy, 2010; Narahari et al., 2011; Nareddy et al., 2017; Bobbili et al., 2018 a&b] employing affinity chromatography on chitin.

#### 1.7. Physiochemical Properties

Several PP2 like lectins have been isolated, purified and characterized with respect to their primary and secondary structures, stability against thermal, pH and chemical unfolding as well as carbohydrate specificity in considerable detail. These proteins contain 152-218 amino acid residues in each subunit of Mr ~17 kDa – 26 kDa in their primary structure. The amino acid sequence of the 24 or 26 kDa phloem exudate lectin is significantly conserved in the 17 kDa phloem exudate lectins except for the *N*-terminal 62 amino acid residues which is absent in the 17 kDa proteins. Most of the PP2 type lectins e.g., PPL, SGPL, CPL, CIA17 and CIA24 are predominantly β-sheet proteins with very little α-helical content in their secondary structure [Bobbili et al., 2018 a, b; Narahari and Swamy, 2010; Narahari et al., 2011a; Nareddy et al., 2017]. These are multi-tryptophan proteins where Trp residues are partially exposed to the surface and some of the Trp residues are involved in the ligand binding site [Bobbili et al., 2014; Narahari et al., 2009, 2011b]. There have been no reports of crystal structure determination of phloem lectins till date. However, three-dimensional modeled structures of PPL (see Fig. 1.5) and CIA17 predicted by homology modelling have been reported recently.

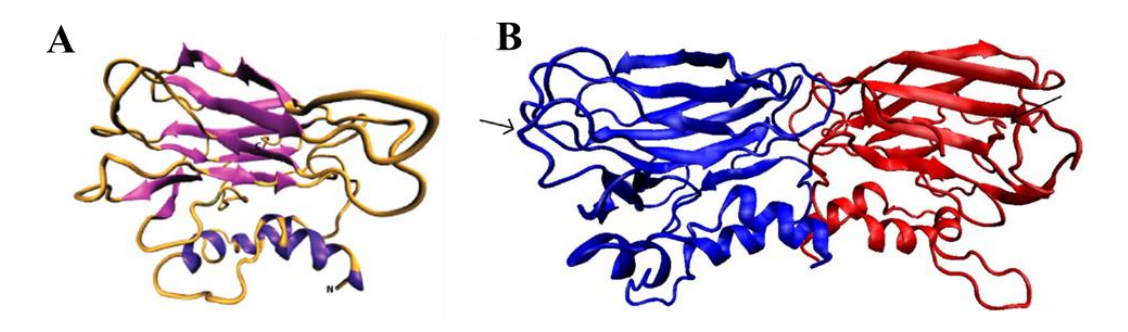


**Fig. 1.5.** Homology modeled structure of (A) PPL monomer generated by I-TASSER and (B) PPL dimer generated by SymmDock. The two monomers are shown in blue and red and the putative binding sites, identified by molecular docking and MD simulations are indicated by the arrow (Images were taken from Narahari et al., 2011b).

Cucurbitaceae PP2 type lectins contain several cysteine residues which form covalent intra- and/or inter-molecular disulphide linkages and provide extra stability to the protomers as well as oligomers. For example, CIA17 contains three cysteine residues among which C32 and C49 form an intra-molecular disulfide bond, whereas C125 near the C-terminal end remains exposed to the surface and most likely participates in the formation of intermolecular disulfide linkages with other molecules of CIA17 or PP1 proteins [Bobbili et al., 2019] leading to the formation of cross-linked, extended structures that seals the injuries inflicted by the insects.

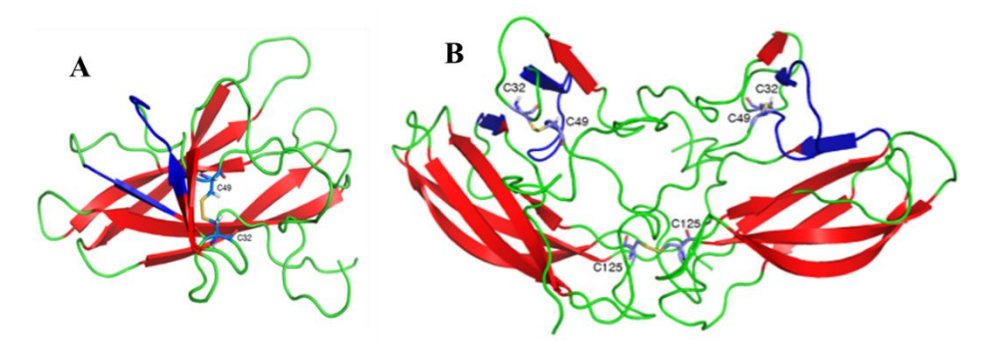


**Fig. 1.6.** Modelled structure of (A) CIA17 monomer with the intramolecular disulfide linkage between C32 and C49 and (B) CIA17 dimer with the disulphide bond between C125 residues of two CIA17 subunits. Putative sugar binding region is shown by blue arrow (Images were taken from the supplementary material of Bobbili et al., 2019).

Plant lectins are quite thermo stable. Among plant lectins, PP2 lectins specifically have shown the highest thermal stability. Temperature dependent CD spectra indicated that the secondary structure of SGPL was almost unaltered between 30 and 60 °C and that for PPL was uninfluenced up to 80 °C. Both the secondary and tertiary structures of CIA17, CIA24 as well as for CPL were unchanged even at 95 °C. Differential scanning calorimetric studies demonstrated that PP2 lectins undergo thermal transition in a two-state manner whereas the unfolding process of some others involves 3 or 4 states depending on the oligomeric form. For example, thermal transition of PPL, SGPL and CPL occurs at 81, 73 and 97.6 °C and the unfolding is a two state (native → unfolded) irreversible process [Narahari and Swamy, 2010; Narahari et al., 2011a; Nareddy et al., 2018;] while CIA17 and CIA24 exhibits considerably higher thermal stability, with the complete unfolding transition being observed at 109 and 105 °C. The unfolding thermogram of CIA17 consists of three overlapping endotherms centred at 98, 106 and 109 °C [Mondal et al., 2021, work reported in chapter 2] whereas for CIA24, DSC thermogram consisted of two overlapping endotherms at 101 and 105 °C suggesting that thermal unfolding of CIA17 is a four state (oligomer→ dimer→ monomer →unfolded) and CIA24 is a three-state process (dimer→ monomer →unfolded) [Bobbili et al., 2018b, 2019]. High antiparallel β-sheet content in their secondary structure, as well as their high propensity to form large oligomeric structures possibly can contribute to their high thermal stability. Thermal unfolding and thermal inactivation are broadly correlated for these lectins. The hemagglutination activity of PPL remains unaltered when incubated at different temperatures up to 70 °C. The activity decreased quite sharply between 75 and 85 °C and incubation at 90 °C led to the complete loss of activity of the lectin [Narahari et al., 2010]. SGPL retained about 50% and 10% hemagglutination activity when incubated at 70 °C and 80 °C [Narahari et al., 2011] and complete loss of activity occurs when incubated at 90 °C. In case of CPL and CIA17 the hemagglutination activity was fully retained even after incubation at 90 °C [Bobbili et al., 2018a; Nareddy et al., 2017]. The thermal stability of CPL was highest in the pH range 5.0 to 7.0 and was found to decrease below pH 5.0 [Nareddy et al., 2018].

## 1.7.1. Carbohydrate Specificity, Stoichiometry and Thermodynamics of Carbohydrate binding

Cucurbitaceae PP2-type lectins are highly specific for chitooligosaccharides. Detailed energetics and thermodynamics of chitooligosaccharide binding have been investigated for several of them, namely PPL, CPL, LAA, CIA17, CIA24 and SGPL using isothermal titration calorimetry (ITC), fluorescence and circular dichroism spectroscopy [Anantharam et al., 1986; Bobbili et al., 2018a, b, and 2019; Narahari et al., 2011a, b; Nareddy et al., 2017; Sanadi and Surolia, 1994; Sanadi et al., 1998]. Association constants, thermodynamic parameters and stoichiometry for the binding obtained in these studies have been summarized in Table 1.1.

A PPL dimer binds to  $(GlcNAc)_{3.5}$  with a binding constant of  $1.26 - 1.53 \times 10^5$  M<sup>-1</sup> at  $25^{\circ}$ C and a binding stoichiometry ~2.0 whereas for chitohexaose, the binding constant is  $6.16 \times 10^6$  which is approximately 48-fold higher affinity than that for chitotriose. Moreover, the binding stoichiometry decreased from 1.96 for chitotriose to 1.08 for chitohexaose molecule per dimeric PPL. The decrease in stoichiometry suggests that one chitohexaose molecule can bind two different PPL molecules simultaneously leading to the formation of higher order complexes [Narahari et al., 2011a, b]. Thus, while chitotriose interacts with the combining site of one protomer, chitohexaose molecules most likely interact with two binding sites from two independent protein molecules. PPL forms very weak complexes with chitobiose where the binding affinity was in the milimolar range ( $K_b = 2.3 \times 10^3$  M<sup>-1</sup>).

Chitooligosaccharide binding of CPL, CIA24 and CIA17 follows a similar pattern as observed for PPL with the exception that CIA24 does not bind chitobiose at all. The binding stoichiometry for di, tri, tetra and penta-oligosaccharides was found to be close to unity with respect to the protomer for all the lectins mentioned above. For CPL, the association constants were in the range of  $1.11-1.92 \times 10^5 \, \text{M}^{-1}$  for [(GlcNAc)<sub>2-5</sub>] but a dramatic increase was observed for chitohexaose binding with a value of  $17.5 \times 10^5 \, \text{M}^{-1}$  [Nareddy et al., 2017].

**Table 1.1.** Binding constants ( $K_b$ ) and thermodynamic parameters for the association of chitooligosaccharides with PPL, SGPL, CPL, CIA17 and CIA24 estimated from isothermal titration calorimetry (reproduced from Bobbili et al., 2018b, 2019; Narahari et al., 2011a, b; Nareddy et al., 2017).

Lectin	Sugar	n	$K_b \times 10^{-5}$ (M <sup>-1</sup> )	$-\Delta G$ (kcal.mol <sup>-1</sup> )	-Δ <i>H</i> (kcal.mol <sup>-1</sup> )	$-\Delta S$ (cal.mol <sup>-1</sup> .K <sup>-1</sup> )
	(GlcNAc) <sub>2</sub>	1.0*	0.023	4.58	11.6	23.3
	(GlcNAc) <sub>3</sub>	0.98 (± 0.07)	1.53 (± 0.19)	7.06	16.5 (± 0.3)	31.73 (± 1.4)
PPL	(GlcNAc) <sub>4</sub>	0.91	1.26	6.84	21.8	50.2
	(GlcNAc) <sub>5</sub>	$0.79 (\pm 0.07)$	1.43 (± 0.2)	7.03	$23.7 (\pm 0.8)$	56.0 (± 2.9)
	(GlcNAc) <sub>6</sub>	$0.54 (\pm 0.09)$	61.6 (± 2.2)	9.26	$30.7 (\pm 0.3)$	71.9 (± 1.1)
	(GlcNAc) <sub>3</sub>	0.98 (±0.21)	1.75 (±0.07)	7.11	12.6 (±0.1)	23.1 (±1.1)
g G DY	(GlcNAc) <sub>4</sub>	1.19 (±0.2)	1.39 (±0.03)	7.02	15.3 (±0.1)	27.6
SGPL	(GlcNAc) <sub>5</sub>	1.18 (±0.04)	1.45 (±0.16)	7.06	16.6 (±0.3)	32.1
	(GlcNAc) <sub>6</sub>	0.92 (±0.01)	3.70 (±0.1)	7.56	17.4 (±0.1)	32.7
CPL	(GlcNAc) <sub>2</sub>	1.0 (±0.00)	0.01 (±0.00)	4.32	8.1 (±0.1)	12.5 (±0.6)
	(GlcNAc) <sub>3</sub>	0.96 (±0.01)	1.11 (±0.12)	6.88	14.2 (±0.7)	24.5 (±2.4)
	(GlcNAc) <sub>4</sub>	0.84 (±0.00)	1.77 (±0.27)	7.13	17.2 (±0.8)	33.6 (±2.9)
	(GlcNAc) <sub>5</sub>	0.86 (±0.03)	1.92 (±0.07)	7.23	20.1 (±0.5)	43.3 (±1.7)
	(GlcNAc) <sub>6</sub>	0.42 (±0.02)	17.5 (±3.08)	8.52	35.4 (±1.6)	90.3 (±5.8)
	(GlcNAc) <sub>2</sub>	1.2	0.05	5.08	18.7	45.8
	(GlcNAc) <sub>3</sub>	1.18 (±0.05)	3.53 (±0.22)	7.58	25.6 (±1.3)	60.5 (±4.4)
CIA17	(GlcNAc) <sub>4</sub>	1.16 (±0.05)	4.05 (±0.01)	7.65	27.2 (±0.7)	65.6 (±2.4)
	(GlcNAc) <sub>5</sub>	0.99 (±0.03)	4.31 (±0.25)	7.69	33.9 (±0.3)	87.5 (±0.9)
	(GlcNAc) <sub>6</sub>	0.64 (±0.02)	180.0 (± 30)	9.94	45.9 (±1.8)	120.5(±6.5)
CIA24	(GlcNAc) <sub>3</sub>	1.51 (±0.49)	0.27 (±0.05)	6.13	15.7 (±0.6)	31.7
	(GlcNAc) <sub>4</sub>	1.20 (±0.05)	1.07 (±0.04)	6.97	20.4 (±0.3)	44.3 (±1.2)
	(GlcNAc) <sub>5</sub>	1.20 (±0.05)	1.13 (±0.02)	7.0	20.2 (±1.2)	43.6 (±2.4)
	(GlcNAc) <sub>6</sub>	0.48 (±0.01)	1.83 (±0.07)	7.2	51.3 (±2.4)	145.5 (±7.8)

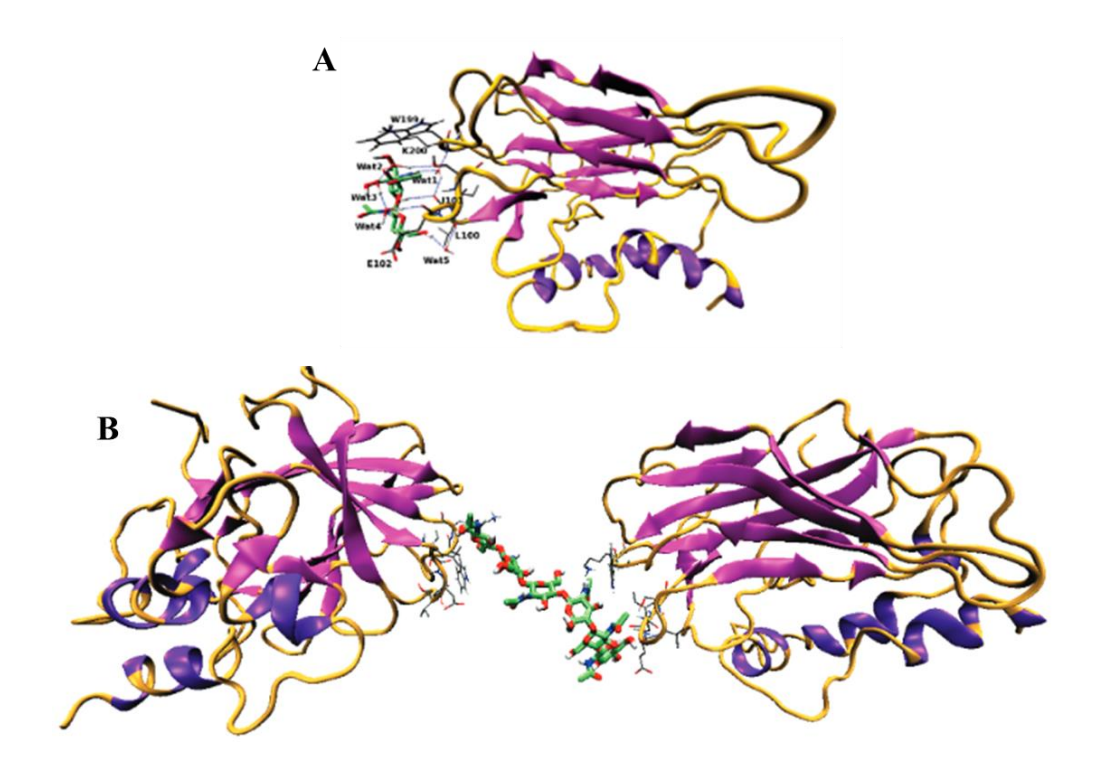


**Fig. 1.7.** Mode of chitooligosaccharide binding to PPL. (A) Chitobiose docked at the putative binding site of PPL. (B) Complex of chitohexaose with PPL dimer obtained from molecular docking studies and optimized by molecular dynamics simulations (Images were taken from Narahari et al., 2011b).

For both CPL and CIA17, the stoichiometry of binding was almost unaltered up to chitopentaose. However, the binding affinity was found to increase by ~100 fold for chitotriose as compared to chitobiose while for chitotetraose and chitopentaose marginal changes in binding affinity were observed. Chitohexaose, on the other hand, could bind to two CPL or CIA17 molecules at the same time as evidenced by a decrease in stoichiometry to 0.42. The binding affinity was ~10-fold and ~70-fold higher for CPL and CIA17, respectively, than that of chitotriose [Nareddy et al., 2017; Bobbili et al., 2019]. CIA24 also binds to [(GlcNAc)<sub>3-6</sub>] in a similar fashion with the exception that CIA24 does not bind chitobiose at all [Bobbili et al., 2018b]. Therefore, similar to PPL, the extended carbohydrate binding sites of CPL, CIA17 and CIA24 can also accommodate up to a

trisaccharide and hexasaccharide binding leads to the formation of higher order proteincarbohydrate complex. This is schematically depicted in Fig. 1.8.



**Fig. 1.8.** Schematic diagram depicting the oligomerization of CIA17 dimers by the simultaneous binding of chitohexaose molecules to two CIA17 molecules (Image taken from Bobbili et al., 2019).

In case of SGPL, the saccharides of all chain lengths [(GlcNAc)<sub>2-6</sub>] bind with the same stoichiometry and similar binding affinity with hexasaccharide being the best ligand, suggesting that it has a very large extended binding site that can accommodate a hexasaccharide or even a higher chitooligosaccharide [Narahari et al., 2011a, b].

Binding constants of chitooligosaccharides to LAA were estimated from the increase in fluorescence intensity as well as the molar ellipticity in the near UV region. The binding constants obtained are  $1.4 \times 10^3$ ,  $1.26 \times 10^4$ ,  $9.7 \times 10^4$  and  $6.5 \times 10^5$  M<sup>-1</sup> for chitobiose, chitotriose, chitotetraose and chitopentaose, respectively [Anantharam et al., 1986]. Binding of 4-methylumbelliferyl- $\beta$ -D-N,N',N''-triacetylchitotrioside and unlabeled sugars to *Coccinia indica* agglutinin was studied by fluorescence spectroscopy. The binding constant and thermodynamic parameters obtained suggested that the combining site of CIA can accommodate one chitotetraose molecule and the fourth sugar residue of tetrasaccharide is in close proximity to the fluorescent Trp residues [Sanadi and Surolia, 1994; Sanadi et al., 1998].

In summary, results of chitooligosaccharide binding studies indicate that PPL binding site can accommodate up to a trisaccharide whereas in CIA and LAA the binding site is extended and can accommodate up to a tetrasaccharide. In SGPL, the ligand binding site appears to be further extended and possibly accommodate a pentasaccharide, or even a hexasaccharide.

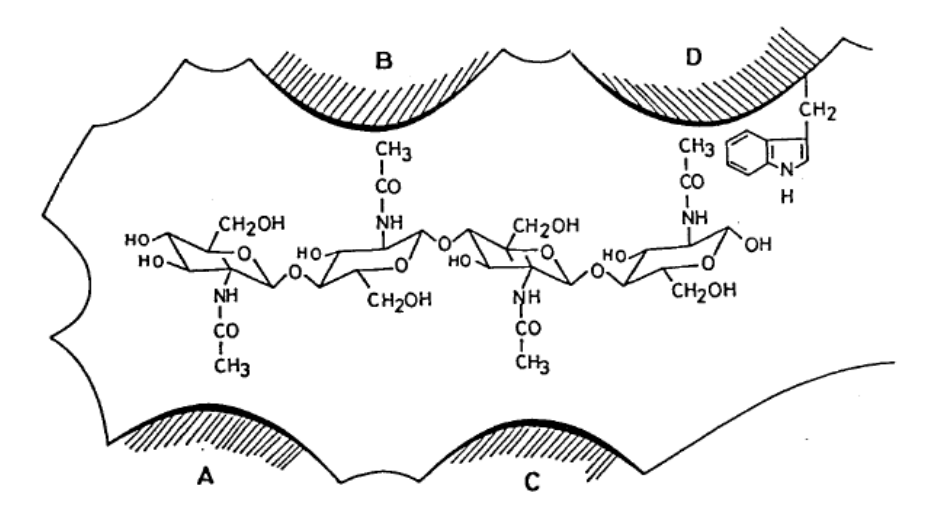


**Fig. 1.9.** Schematic model of the binding site of CIA with chitotetraose. A, B, C, and D refer to the different subsites (Image taken from Sanadi et al., 1998).

Association of chitoloigosaccharides to the PP2 lectins was essentially enthalpy driven. Thermodynamic parameters obtained for the binding of chitologosaccharide to several PP2 lectins, namely LAA, PPL, CPL, CIA17, and CIA24 indicated that the binding process is accompanied with a favourable increase in enthalpy whereas the entropic contribution to the binding is negative [Anantharam et al., 1986; Bobbili et al., 2018b, 2019; Narahari et al., 2011b; Nareddy et al., 2017; Sanadi et al., 1998].

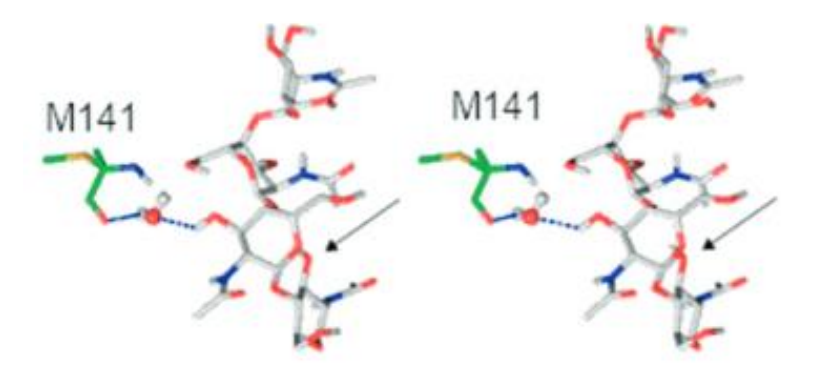


**Fig. 1.10.** Stereo view of the CIA17-chitotetraose interactions mediated by water molecules. The amino acid residues forming water mediated H-bonds with sugar molecules are shown (Images were taken from Bobbili et al., 2019).

The changes in enthalpy and entropy associated with the binding are compensatory in nature which is generally explained in terms of reorganization of water structure around the binding site of the protein and the ligand. Molecular docking studies for PPL and CIA17 indicated that the interaction of chitooligosaccharides involves several direct and water mediated hydrogen bonds (shown in Fig. 1.10) besides van der Waals' interactions between the functional groups on the ligand molecules and the protein [Bobbili et al., 2019; Narahari et al., 2011].

Site directed mutagenesis has been performed on PPL to validate the carbohydrate binding pocket predicted by molecular docking and molecular dynamics studies [Bobbili et al., 2014]. The docked chitooligosaccharides showed major interactions with Leu-100 and Glu-102 (subsite 1), Ile-101, Ser-104, and Trp-199 (subsite 2), and Trp-199 and Lys-200 (subsite 3). Among these, mutation of Ser-104 led to ~ 90 % loss of activity suggesting that it is crucial for carbohydrate binding by PPL. Mutation of Leu-100 and Lys-200 lead to 40 % decrease in the lectin activity indicating that they are also important for the sugar binding activity of this lectin. These residues were found to be largely conserved in several other phloem proteins.

# 1.8. Macromolecular Crowding

Most of the biophysical and biochemical studies have been performed in research laboratories in aqueous buffer solution maintaining the physiological pH, ionic strength etc. The intracellular environment is quite different from the dilute buffer solution. The living cell contains several macromolecules such as proteins, nucleic acids, polysaccharides etc, which occupies almost 40% (by wight) of the cellular volume and makes the free available space limited for other biomolecules (see Fig. 1.11). This is termed as 'excluded volume effect' which increases the effective concentrations of macromolecules (thus increasing their chemical activity), which in turn alters the rates and equilibrium constants of the reactions [Ellis, 2001; Minton, 2001; Zhou et al., 2008]. Inside a cell, the density and viscosity is significantly higher and also the crowded milieu alters the dielectric properties of the media [Puchkov, 2013; Rajendran et al., 2010].

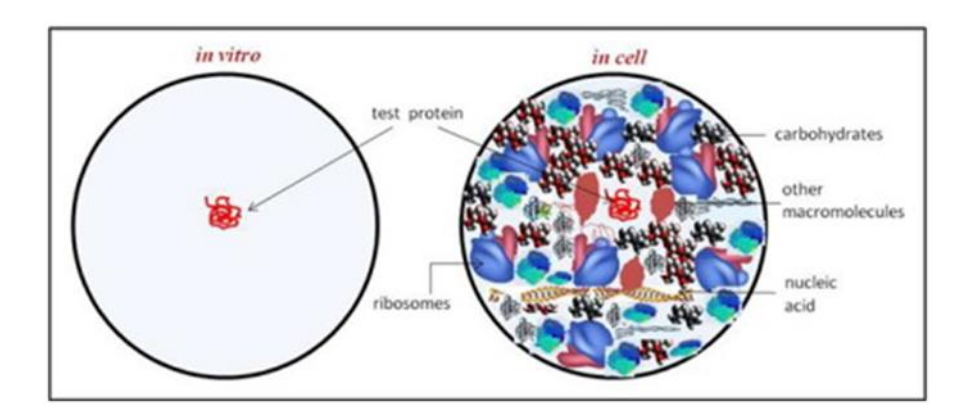


**Fig. 1.11.** The difference in macromolecular crowding between *in vitro* and *in vivo* (inside the cell). Panel (a) represents the presence of the test protein in dilute buffer solution and panel (b) represents the presence of test protein along with other biomolecules in the cytoplasm (Image is taken from Sahid et al., 2017).

Molecular crowding is known to exert profound effect in modulating many biological processes including the structure and function of the proteins [Zimmerman and Minton, 1993; Zhou et al., 2008]. There have been several theoretical and experimental studies investigating the effect of molecular crowding on the structure and dynamics of proteins, protein stability, (un)folding pathway, binding kinetics and equilibria, aggregation behaviour as well as enzymatic activity [Cheung et al., 2005; Christiansen et al., 2010; Hong and Gierasch, 2010; Harada et al., 2012; Samiotakis et al., 2009; Senske et al., 2014]. In order to mimic the 'crowded' cell environment the buffer solutions in laboratory experiments are usually modified by adding high concentrations of different synthetic agents such as polyethylene glycols (PEG), dextrans, ficolls and poly vinyl pyrrolidines (PVPs) of different molecular weights and larger protein-based crowding agents eg., HSA, BSA etc. The results from such experiments have demonstrated that macromolecular crowding shifts the equilibrium towards the more compact transition state of protein. Crowding can either increase or decrease the reaction rate of an association reaction. For instance, the self-association of human spectrin is enhanced in the presence of high concentrations of PEG and the amyloid formation by human apolipoprotein C-II is accelerated in crowded milieu [Cole and Ralston, 1994; Hatters et al., 2002; Kim and Yethiraj, 2011]. On contrary, the association rate of TEM1- $\beta$ -lactamase (TEM) and the  $\beta$ lactamase inhibitor protein (BLIP) depends strongly on the concentration of PEG. A lower concentration of PEG i.e., in the dilute regime TEM-BLIP association rate becomes slower but faster association was observed when PEG concentration crossed the semidiluted regime [Kozer et al., 2007]. The presence of crowding agents leads to a reduction in the diffusion constant of the reactants while equilibrium constant for the association increases. Therefore, the overall rate of the reaction results from a balance between the decreased probability of a collision between the reacting species and an increased thermodynamic driving force for association [Kim and Yethiraj, 2011]. Crowding is mostly expected to decelerate fast association reactions but accelerate slow associations [Zhou et al., 2008]. Crowding favours the more compact folded state of proteins and promotes the compaction of the more expanded denatured state. Addition of PEG 4K increases the transition temperature (T<sub>m</sub>) by ~15 °C for thermal denaturation of DNase I [Sasaki et al., 2007]. Both Ficoll 70K and dextran 70K increase the T<sub>m</sub> of apo- and holo-flavodoxin [Perham et al., 2007; Stagg et al., 2007]. The structural changes of native enzymes in the crowded environment result in enhancing enzymatic activity. For example, addition of PEG 6K increases enzyme activity of Escherichia coli AspP [Moran-Zorzano et al., 2007] with a six-fold increase in V<sub>max</sub> and addition of dextran 70K, Ficoll 70K, or PEG 6K increases enzyme activity of isochorismate synthase [Jiang and Guo, 2007].

Howerver, recent works have suggested that protein-crowding interaction may be stabilizing or destabilizing in nature [Inomata et al., 2009; Mittal et al., 2013]. For example, Macromolecular crowding exerts destabilizing effect on the stability of myoglobin [Malik et al., 2012]. The activity of the recombinant human brain-type creatine kinase decreases under crowded environment [Fan et al., 2012]. Synthetic crowders, PVPs and Ficoll 70 stabilize chimotrypsin inhibitor 2 (CI2) against thermal and chemical denaturation while protein crowders such as *E. coli* cytoplasm, lysozyme or BSA acts in opposite direction and destabilize CI2 to different extents [Benton et al., 2012; Miklos et al., 2010, 2011]. All these evidences suggest that the effect of crowding on macromolecules is obvious but the question that arises is whether the molecular crowding is a friend or foe?

While the excluded volume effect is purely stabilizing, the nonspecific soft chemical interactions between crowding agents and the target protein may be stabilizing or destabilizing [Das and Sen, 2018]. The soft interactions can be attractive or repulsive depending on the source of the chemical interaction e.g., charge-charge interactions, hydrogen bonding, hydrophobic effect etc., which can add to or subtract from the excluded volume effect [Sarkar et al., 2013a, b].

### 1.9. Motivation and Outline of the Present Work

Lectins are amazing tools in glycomic research and have potential applications in biological, biomedical and clinical research. Their unique capability to recognize simple and/or complex carbohydrate structures with distinct specificity made them important to investigate their structural and functional properties from past 4-5 decades. In particular, plant lectins are widely studied owing to their high abundance and availability, ease of purification as well as diversity in structure and carbohydrate specificity. Among plant lectins, legume lectins are extensively studied and a great deal of information including primary structure and crystal structure of many of them is available.

Despite the fact that the presence of PP2 lectins in the phloem exudate of Cucurbitaceae species and their potential role in plant defence mechanism, wound sealing against insect attack, lectin activity as well as the formaton of RNP complexes and their long-distance trafficking have been documented over 40 years ago, only a few proteins from this family have been purified and characterized with respect to ligand binding properties, primary and secondary structures. Moreover, no 3-dimensional structure of a member of this family is known so far. The Cucurbitaceae fruits are produced in large quantities and form a major part of the Indian diet. A detailed knowledge of structure, function and carbohydrate specificity is a prerequisite in order to understand their role in living systems. Therefore, purification and biophysical characterization of new lectins from this family is very important.

In the present study, we have investigated the detailed mechanism of thermal and chaotrope-induced unfolding of *Coccinia indica* agglutinin (CIA17), a homo-dimeric

protein with a subunit mass of 17 kDa, which exists as a soluble, polydisperse aggregate in aqueous solution. Thermal unfolding involves three distinct steps: i) dissociation of oligomeric aggregates of the protein into the constituent dimers, ii) dissociation of the dimers into monomers, and iii) unfolding of the monomers, whereas chaotrope induced denaturation pathway consists of two distinct steps which could be assigned to dissociation of the dimeric protein into monomers and unfolding of the monomers. Our results demonstrated that CIA17 forms higher oligomeric structures which are soluble aggregates at the physiological concentration (6 to 8 mg/mL) and forms jelly like substrates by forming disulfide bond (oxidation) upon exposure to air. These results are relevant for understanding the role of the phloem proteins in protecting the plant from insect/pest attack.

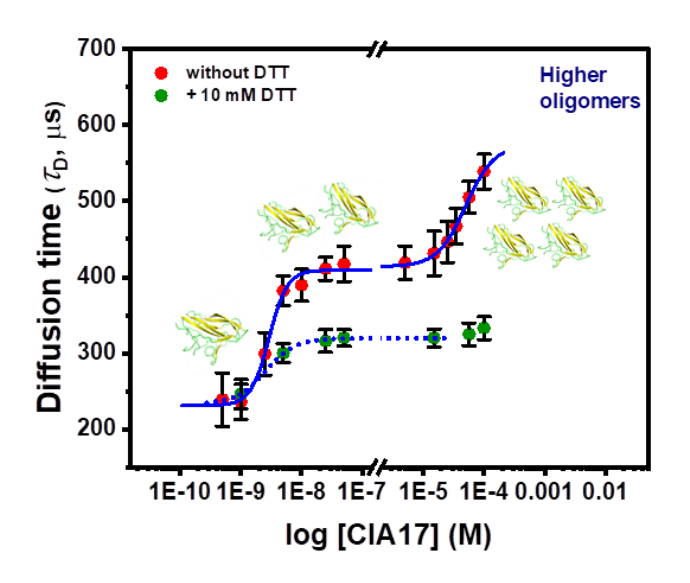
We further investigated the pH induced changes in the conformation, structural dynamics as well as carbohydrate-binding activity of CIA17. The results obtained indicated that CIA17 exists as partially unfolded, molten globule like state at pH  $\leq$  2.0 with the secondary structure almost unaltered but the local conformation has been modulated significantly. The molten globule observed at pH 2.0 retains adequate ability to bind chitooligosachharides when compared to the native protein but is restricted with regard to forming higher oligomers except the formation of homodimer at relatively high concentration. The detailed investigation on thermal, chemical and pH unfolding of such a polydispersed oligomeric protein will give a new insight in the context of protein (un)folding dynamics.

The effect of macromolecular crowding on the structure as well as carbohydrate binding properties of CIA17 was also studied using various spectroscopic techniques. The different shape and size of the synthetic crowders plays an important role on the structure/conformation of CIA17 mainly through 'excluded volume effect' though some nonspecific soft interactions seem to be present which in turn modulates the carbohydrate binding activity of the protein.

In the present work, a chitooligosaccharide binding PP2-type lectin (BGL24) was also purified from the phloem exudate of bottle-gourd (*Lagenaria siceraria*) by affinity

chromatography. We also investigated its structural and carbohydrate binding properties as well as its cytotoxicity towards normal splenocytes and epithelial, triple negative breast cancer cells (MDA-MB-231) using various biophysical and biochemical techniques. Further, the accessibility and exposure of the Trp residues as well as chemical, acidic and thermal unfolding were investigated by fluorescence and circular dichroism spectroscopy.

# DSC and FCS Studies Reveal the Mechanism of Thermal and Chemical Unfolding of CIA17, a Polydisperse Oligomeric Protein from *Coccinia indica*



The work was published as

Saradamoni Mondal, Kishore Babu Bobbili, Sumanta Paul, Musti J. Swamy\*

J. Phys. Chem. B 2021, 125, 26, 7117-7127

# 2.1. Summary

The mechanism of thermal and chemical unfolding of Coccinia indica agglutinin (CIA17), a chitooligosacharide-specific phloem exudate lectin, was investigated by biophysical approaches. DSC studies revealed that the unfolding thermogram of CIA17 consists of three components (T<sub>m</sub> ~98, 106 and 109°C) which could be attributed to dissociation of protein oligomers into constituent dimers, dissociation of the dimers into monomers, and unfolding of the monomers. Intrinsic fluorescence studies on the chemical denaturation by guanidinium thiocyanate and guanidinium chloride indicated the presence of two distinct steps in the unfolding pathway, which could be assigned to dissociation of the dimeric protein into monomers and unfolding of the monomers. Results of fluorescence correlation spectroscopic studies could be interpreted in terms of the following model: CIA17 forms oligomeric structures in a concentration dependent manner, with the protein existing as a monomer below 1 nM concentration, but associating to form dimers at higher concentrations ( $K_D \approx 2.9 \text{ nM}$ ). The dimers associate to yield tetramers with a  $K_D$  of ~47  $\mu$ M, which further associate to form higher oligomers with further increase in concentration. These results are consistent with the proposed role of CIA17 as a key player in the defense response of the plant against microbes and insects.

### 2.2. Introduction

Despite numerous studies on protein (un)folding dynamics, a detailed understanding of the complexity of structural/conformational changes that occur during protein folding/unfolding is still an important and largely unsolved problem [Choi et al., 2011; Pace, 1986; Royer, 2006]. Although the pathway of protein folding is often described by a simple two state model (Native ↔ Unfolded), recent studies employing different single molecule techniques revealed the presence of intermediate state(s) even for singledomain, monomeric proteins [Basak and Chattopadhyay, 2014; Privalov, 1996; Yadav et al., 2014]. Characterizing the nature of such intermediate states is crucial for understanding protein folding since the intermediate states can direct folding and accelerate the transition to the native state restricting the conformational space available for the unfolded state [Bhuyan and Udgaonkar, 2001; Bonetti et al., 2016; Privalov, 1996]. While a number of studies have been reported on the unfolding of single domain/subunit proteins, unfolding studies on oligomeric proteins have been rather limited. The stability of oligomeric proteins can be greatly influenced by inter-subunit interaction as well as intramolecular interactions. In this context, while some oligomeric legume lectins showed two-state unfolding with folded multi-subunit native protein and unfolded polypeptides in equilibrium, several globular proteins are known to deviate from the two-state behavior and exhibit well populated intermediate states [Gaikwad, et al., 2002; Reddy et al., 1999; Sen and Mandal, 2014; Sinha et al., 2005]. Although unfolding of several legume lectins has been investigated, there have been no reports on the folding/unfolding processes of phloem exudate lectins, several of which have been shown to exist as polydisperse aggregates in solution [Bobbili et al., 2018a, b].

The phloem proteins (P-proteins) are highly abundant in Cucurbitaceae *genere* and appear as amorphous, crystalline or tubular structures under microscopy [Esau and Cronshaw, 1967; Golecki et al., 1999; Kehr, 2006; Kleining et al. 1975; Oparka and Cruz, 2000; Thompson and Schulz, 1999]. PP2 proteins together with the filamentous phloem protein, PP1 appear to be synthesized in companion cells and transported into the sieve elements via plasmodesmata pores [Dinant et al., 2003]. Under oxidative conditions, e.g., when the tissue is wounded by insects and phloem exudate is exposed to

air, PP1 and PP2 proteins associate to form cross-linked filaments connected via disulfide bonds and finally yield an insoluble gel which seals the wound and prevents microorganisms and fungi from entering the plant tissue, thus protecting the plants from pathogenic attack [Beneteau et al., 2010; Gómez and Pallás, 2004; Gómez et al., 2005; Read and Northcote, 1983; Will and Van Bel, 2006; Will et al., 2013; Zhang et al., 2013]. While PP1 proteins do not exhibit any ligand binding ability, PP2 proteins have been shown to exhibit lectin activity and also interact with different RNA molecules to form ribonucleoprotein (RNP) complexes and transport them from cell to cell [Gómez et al., 2005; Owens, et al., 2001; Pallás & Gómez, 2013]. Therefore, it is important to carry out systematic investigations on them in order to obtain a molecular level understanding of their biological functions.

In view of the above, PP2-type phloem exudate lectins have been purified from several Cucurbitaceae species such as ridge gourd (*Luffa acutangula*) [Anantharam et al., 1986; Kumar et al., 2015], pumpkin (*Cucurbita maxima*) [Bobbili et al., 2014; Bostwick et al., 1994; Narahari and Swamy, 2010; Narahari et al., 2011b; Read and Northcote, 1983;], snake gourd (*Trichosanthes anguina*) [Narahari et al., 2011a], cucumber (*Cucumis sativus*) [Nareddy and Swamy, 2018; Nareddy et al., 2017;], ivy gourd (*Coccinia indica*) [Bobbili et al., 2019; Sanadi and Surolia, 1994; Sanadi et al., 1998] and are characterized in considerable detail. The PP2 lectins from various Cucurbitaceae species are highly homologous with respect to their amino acid sequence and contain a highly conserved "chitin binding domain" whose conformation is locked by a disulfide bond between two cysteine residues.

Coccinia indica agglutinin (CIA17), purified from the phloem exudate of unripe ivy gourds (Coccinia indica) is a homodimeric PP2-type lectin with a subunit molecular mass of  $\sim$ 17 kDa [Bobbili et al., 2018a]. This protein exists in a polydisperse, oligomeric form with the size of the oligomer increasing with concentration. Each subunit of the lectin is made up of 152 amino acid residues and contains an extended binding site which specifically recognizes chitooligosaccharides [Bobbili et al., 2018a, 2019]. CIA17 is a predominantly  $\beta$ -sheet protein and exhibits high thermal stability with its secondary and

tertiary structures remaining essentially unaltered up to 90 °C as indicated by CD spectroscopic investigations reported earlier [Bobbili et al., 2018a].

In the present study, thermal unfolding of CIA17 was further investigated in the absence as well as in the presence of ligand (chitooligosaccharides) using differential scanning calorimetry (DSC). Since CIA17 contains eight tryptophan residues in its primary structure [Bobbili et al., 2018a], chaotrope-induced unfolding of this protein was studied using fluorescence spectroscopy by monitoring changes in the tryptophan emission characteristics in the presence of varying concentrations of chemical denaturants. In addition, the concentration dependent oligomerization as well as guanidinium chloride (GdmCl) induced unfolding pathway of CIA17 were probed using fluorescence correlation spectroscopy (FCS).

### 2.3. Materials and Methods

### 2.3.1. Materials

Unripe ivy gourds were purchased from local vendors.  $\beta$ -Chitin from squid pen (Sigma) was a kind gift from Prof. A. R. Podile, School of Life Sciences, University of Hyderabad. 2-Mercaptoethanol ( $\beta$ ME),  $\alpha$ -chitin, chitooligosaccharides, ammonium persulphate, acrylamide, GdmCl, guanidinium thiocyanate (GdmSCN), urea, and dithiothreitol (DTT) were purchased from Sigma (St. Louis, MO, USA). All other chemicals and reagents were procured from local suppliers and were of the highest purity available.

# 2.3.2. Purification of CIA17

CIA17 was purified by sequential affinity chromatography on  $\alpha$ -chitin and  $\beta$ -chitin as described earlier and was found to be pure by sodium dodecyl sulfate-polyacrylamide gel electrophoresis (SDS-PAGE) [Bobbili et al., 2018a]. Concentration of the purified protein was estimated from its  $A_{280nm}$  value of 3.08 for a 1.0 mg/mL solution at 1.0 cm path length [Bobbili et al., 2018a]. This would correspond to a molar extinction coefficient of 53,658  $M^{-1}$  cm<sup>-1</sup>.

# 2.3.3. Differential Scanning Calorimetry

DSC measurements were carried out on a Nano DSC equipment from TA systems (New Castle, DE, USA). Protein samples of 0.125-1.0 mg/mL (7.5 - 58  $\mu$ M) concentration, dialyzed against 10 mM phosphate buffer, pH 7.0 were heated from 10 to 120 °C at a scan rate of 30 or 60 degrees per hour. The dialysate was used as the reference. To investigate the effect of ligand binding on the thermal unfolding of the protein, CIA17 was pre-incubated with 4.37 mM chitotriose before the DSC scan. Sample and reference solutions were properly degassed prior to the DSC experiment to eliminate bubbling effects. Reproducibility of baselines was verified by multiple scans, and reversibility of protein unfolding was monitored by scanning the samples twice in succession. After correcting for buffer contribution, the thermograms were analyzed using the Gaussian Modeler software supplied by TA Systems.

# 2.3.4. Fluorescence Spectroscopy

Fluorescence spectra were recorded on a Spex Fluoromax-4 fluorescence spectrometer (Jobin-Yvon Ltd., Edison, NJ, USA). CIA17 samples of 1.11  $\mu$ M concentration were irradiated with 295 nm light to excite tryptophan residues selectively and emission spectra were recorded in the wavelength range of 300-400 nm using excitation and emission slits of 5 nm width.

Chemical unfolding of CIA17 induced by various chaotropic agents was studied by monitoring changes in the intrinsic fluorescence properties of the protein when the concentration of denaturants was varied. In these experiments, CIA17 samples were incubated overnight with different concentrations of various denaturants (GdmCl, GdmSCN and urea) and emission spectra of the protein were recorded as described above for the native protein. All spectra were corrected by subtracting buffer scans recorded under identical conditions. To investigate the role of disulfide bonds in stabilizing the protein structure, studies were also performed in the presence of 10 mM DTT.

# 2.3.5. Fluorescence Correlation Spectroscopy (FCS)

FCS measurements were carried out with an Alexa 488 labeled CIA17 (A488-CIA17). The lectin was labeled with Alexa Fluor 488 carboxylic acid succinimide ester (A488) following the procedure provided by the manufacturer (Molecular probes, Invitrogen). The labeling reaction was carried out in 0.1 M carbonate buffer, pH 8.3 at room temperature by incubating a mixture of CIA17 and A488 at a dye/protein ratio of 2 for 2 hours in dark. To stop the labelling reaction, the reaction mixture was incubated with freshly prepared 1.2 M hydroxylamine, pH 8.5. The labeled protein (A488-CIA17) was separated from the free dye by passing the reaction mixture through a Sephadex G-25 column (30 × 1.3 cm), pre-equilibrated with 20 mM sodium phosphate buffer, pH 7.4. Concentrations of the protein and dye were estimated by measuring the absorbance of the conjugate in phosphate buffer at 495 nm and 280 nm using their molar extinction coefficients of 73000 M<sup>-1</sup> cm<sup>-1</sup> (A488) and 53,658 M<sup>-1</sup> cm<sup>-1</sup> (CIA17). The degree of labeling ([dye]/[protein]) was estimated as 0.44.

### 2.3.5.1. FCS Instrumentation and Methods

FCS measurements were carried out using a time resolved confocal fluorescence microscope, Micro Time 200, PicoQuant. A pulsed diode laser ( $\lambda_{ex}$  = 485 nm with fwhm 144 ps) was used as the excitation source. The excitation light was reflected by a dichroic mirror and focused onto the sample placed on a coverslip using a water immersion objective (Olympus UPlansApo 60X/1.2 NA). Fluorescence signal of the sample collected by the same objective was directed to pass through the same dichroic mirror and a 510 LP filter followed by a pinhole of 50  $\mu$ m diameter. The signal was then passed through a 50/50 beam splitter and entered into two PDM series single photon avalanche diodes (SPADs) from PicoQuant. FCS measurements were performed by placing a highly diluted (0.5-50 nM) solution of A488-CIA17 on a coverslip placed on the top of the objective. For denaturation study, the labeled protein (25 nM concentration) was incubated with increasing concentrations (0-7.5 M) of GdmCl. To investigate oligomer formation by the lectin at higher concentrations, labeled protein (10 nM) was mixed with different concentrations of unlabeled protein (final concentration 20 nM-100  $\mu$ M) and

incubated for 30-120 minutes before FCS measurements. The duration of each measurement was 600 s and each point represented in the plot is the average of three independent measurements.

### 2.3.5.2. FCS Data Analysis

The fluctuations of fluorescence intensity were measured within a small detection volume (1.2 fL) and a temporal range from nanoseconds to seconds by using a focused laser beam and pinhole. All the FCS data were analyzed using SymphoTime software provided by PicoQuant. Fluorescence fluctuations detected by two SPAD detectors were then cross correlated via the second order autocorrelation function, given by:

$$G(\tau) = \frac{\langle \delta F(t) \delta F(t+\tau) \rangle}{\langle F(t) \rangle^2}$$
 (2.1)

where  $\langle F(t) \rangle$  is the average fluorescence intensity,  $\delta F(t)$ , and  $\delta F(t+\tau)$  are the fluctuations of fluorescence intensity from the mean value at time t and  $t+\tau$  which are given by:

$$\delta F(t) = F(t) - \langle F(t) \rangle$$
 and  $\delta F(t + \tau) = F(t + \tau) - \langle F(t) \rangle$ 

The correlation function of a molecule diffusing freely is given by:

$$G(\tau) = \frac{1}{N} \left( 1 + \frac{\tau}{\tau_D} \right)^{-1} \left( 1 + \frac{\tau}{\kappa^2 \tau_D} \right)^{-\frac{1}{2}}$$
 (2.2)

and the correlation function of a molecule undergoing conformational changes (or any other reactions/changes) that result in changes in the fluorophore brightness along with diffusion is given by:

$$G(\tau) = \frac{1 - I + I \exp(\tau/\tau_R)}{N(1 - I)} \left(1 + \frac{\tau}{\tau_D}\right)^{-1} \left(1 + \frac{\tau}{\kappa^2 \tau_D}\right)^{-\frac{1}{2}}$$
 (2.3)

In the above equations, N represents the number of molecules in the observation volume,  $\tau_D$ ,  $\tau$ , and  $\tau_R$  are the diffusion time, lag time and relaxation time, respectively.  $\kappa$  (=  $\omega_z/\omega_{xy}$ ) is the structural parameter where  $\omega_z$  and  $\omega_{xy}$  are the longitudinal and transverse radii of the observation volume and I is the associated amplitude. The excitation volume was estimated as 1.2 fL using the known diffusion coefficient of Rhodamine 6G in water

(426  $\mu$ m<sup>2</sup> s<sup>-1</sup>) [Kapusta, 2010]. All the measurements were carried out at room temperature (~25 °C). The diffusion coefficient (*D*) was calculated employing  $\tau_D$  value in equation (2.4):

$$\tau_D = \frac{\omega_{xy}^2}{4D} \tag{2.4}$$

According to the Stokes-Einstein equation, hydrodynamic radius  $(R_h)$  can be estimated from the measured value of D of the species diffusing in the smaller volume as follows:

$$D = \frac{k_B T}{6\pi \eta R_h} \tag{2.5}$$

where  $\eta$  is the viscosity and T is the temperature at which measurements were carried out.

The progressive addition of GdmCl changes the viscosity and refractive index of the solution that affect the actual determination of size and relaxation time of the protein. Hence the hydrodynamic radius was estimated using the following equations 2.6 and 2.7, respectively, after correcting the viscosity and refractive index mismatch [Sherman et al., 2008; Chattopadhyay et al., 2005; Mojumdar et al., 2012].

$$\frac{R_h^{Sample}}{R_h^{A488}} = \frac{\tau_D^{Sample}}{\tau_D^{A488}} \tag{2.6}$$

$$\tau_R^{corr} = \tau_R^{uncorr} \times \frac{\tau_D^{buff}}{\tau_D^{sample}}$$
 (2.7)

where  $\tau_R^{corr}$  and  $\tau_R^{uncorr}$  are the viscosity corrected and uncorrected relaxation time component, respectively, and  $\tau_D^{buff}$  and  $\tau_D^{sample}$  correspond to the diffusion time of free Alexa 488 in buffer and in different experimental conditions, respectively. The  $R_h$  of A488 was estimated as 5.63 (± 0.23) Å from the diffusion coefficient of 435 (± 19)  $\mu$ m<sup>2</sup>s<sup>-1</sup> which was estimated from the cross-correlation data.

# 2.4. Results and Discussion

# 2.4.1. DSC Studies on Thermal Stability of CIA17

In order to investigate thermal unfolding of CIA17 and the effect of ligand binding on it DSC studies were performed on the protein in 10 mM phosphate buffer, pH 7.4 in the absence and in presence of 1 mM chitotriose. The thermogram of native CIA17 consists of three overlapping endothermic components centered at 98.3, 105.9 and 108.6 °C (Fig. 2.1A), where the lowest temperature component was found to be the broadest and least energetic among them. The broad transition is consistent with the polydisperse nature of the oligomeric structures as observed from AFM studies [Bobbili et al., 2018a].

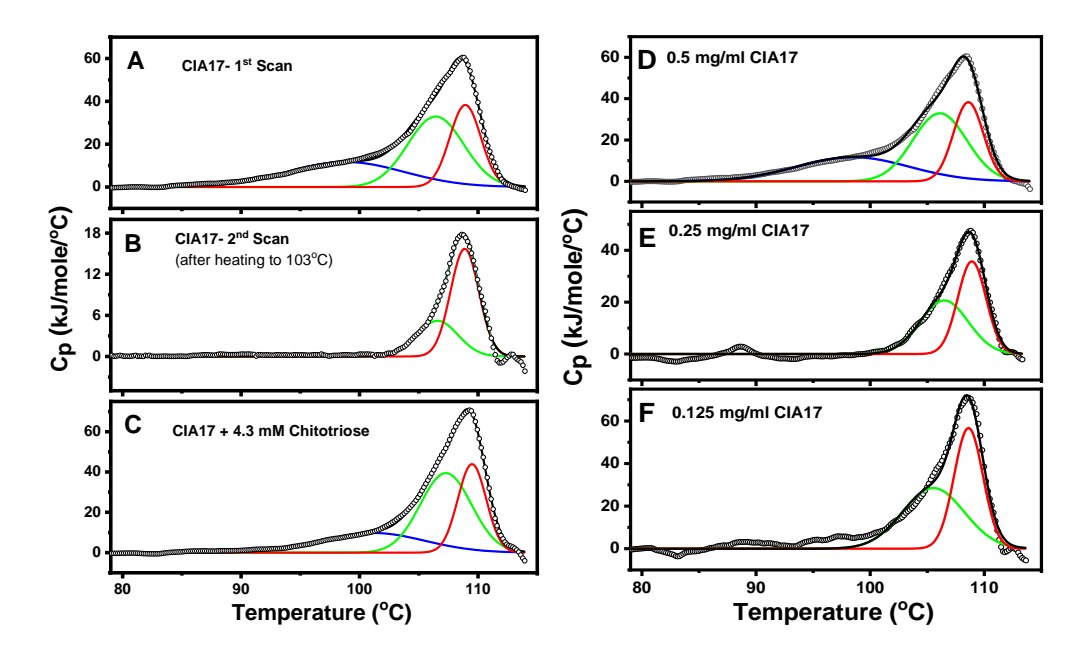


**Fig. 2.1.** DSC thermograms of CIA17 at pH 7.4. A) First heating scan. B) Second heating scan of the protein that was heated up to 103 °C and cooled to 10 °C. C) First heating scan in presence of 4.37 mM chitotriose. The concentration of protein was 1mg/mL for A, B and C. (D, E, F) DSC thermograms of CIA17 at different protein concentrations. The concentration of the protein is indicated in each panel. The data points are shown as open circles. The blue, green and red lines indicate the three

individual transitions obtained from the fit, whereas the black line corresponds to the sum of the three individual transitions.

When the native protein was heated to 110 °C and immediately cooled down to 10°C and reheated, no endotherm was observed indicating that the unfolding process is irreversible. However, when the sample was heated up to 103 °C (midpoint of transition 2), and cooled to 10 °C and reheated, only two peaks were seen; the first peak centered at 98.3 °C was not observed (Fig. 2.1B). Although thermograms obtained in presence of chitotriose could also be resolved into three components similar to native CIA17, small but distinct shifts to higher temperatures were observed in the position of all the three endotherms (Fig. 2.1C). Thermodynamic parameters obtained by analyzing the thermograms are given in Table 2.1.

**Table 2.1:** Transition temperatures of different transitions in the thermal unfolding of CIA17 observed by differential scanning calorimetriy. Buffer: 10 mM sodium phosphate, pH 7.0.

Sample/scan description	Transition assignment	T <sub>m</sub> (°C)
Native CIA17		
Transition 1	Oligomer to dimer	98.3
Transition 2	Dimer to monomer	105.9
Transition 3	Monomer unfolding	108.6
Second heating scan after cooling from 103 °C		
Transition 1	Dimer to monomer	106.7
Transition 2	Monomer unfolding	108.9
CIA17 + 4.3 mM chitotriose		
Transition 1	Oligomer to dimer	101.1
Transition 2	Dimer to monomer	107.3
Transition 3	Monomer unfolding	109.5

The complex thermogram of CIA17 containing three underlying components can be explained as follows. Our previous AFM studies have shown that in the concentration range used in the present DSC studies (0.5 - 1.0 mg/mL), which is approximately 29 - 58 μM of the protein) CIA17 exists as a mixture of soluble, large aggregates [Bobbili et al., 2018a]. Therefore, we assign transition 1 to reversible dissociation of the oligomeric aggregates into dimers. Transition 1 is not seen in DSC scans performed with low concentrations of the protein (see Fig. 2.1E, F), which is in agreement with our previous AFM studies, which indicated that oligomerization of CIA17 is concentration dependent [Bobbili et al., 2018a]. Further, this transition is not seen when the sample is heated to 103 °C (midpoint of the second transition), cooled to 10 °C and reheated, suggesting that most likely formation of the soluble aggregates is a slow process. Transition 2, centered at ~105.9 °C, can be assigned to the dissociation of dimers into monomers, whereas transition 3, centered at ~108.6 °C, is assigned to irreversible unfolding of the monomers. Oligomerization could be responsible for the hyper thermal stability of CIA17, with the residues at the interface of oligomerization acting as hot spots, which enhance thermal stability via oligomerization [Tanaka et al., 2008].

Thermal stability of CIA17 was not significantly affected in the presence of chitooligosaccharides, which could be due to a relatively weak association between the lectin and the oligosaccharides at the high temperatures where these transitions occur. The three transitions that are observed in the DSC thermograms of CIA17 (see Fig. 2.1A) can be represented by *Scheme I*:

$$(A_2)_n \leftrightarrow nA_2 \rightarrow 2nA \rightarrow 2nU$$

where n is the degree of oligomerization, A and U represent the native and unfolded forms of the protein. A plausible pictorial representation of these thermal transitions is given in Fig. 2.2.

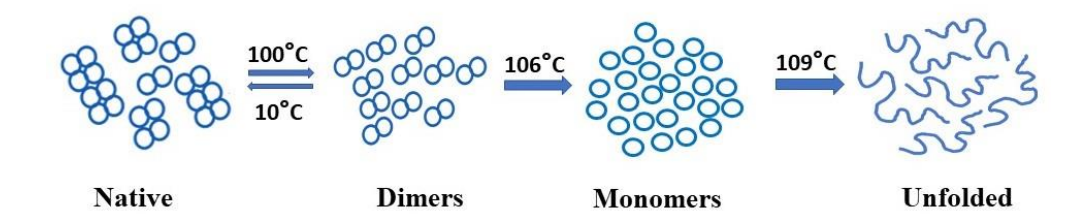


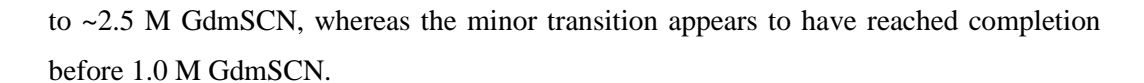
**Fig. 2.2.** A schematic representation of thermal unfolding of CIA17. In the first transition, centered at ~98.3 °C, the oligomers reversibly dissociate into dimers. In the second transition, centered at ~105.9 °C, the dimers irreversibly dissociate into monomers. In the final transition, centered at 108.6 °C, the monomers undergo complete, irreversible unfolding.

# 2.4.2. Chemical Unfolding of CIA17

Addition of chaotropic agents to protein solutions in aqueous media disrupt the hydrogen bond network between water molecules both in the bulk as well as in the hydration shells around hydrophobic amino acids, which weakens the hydrophobic effect and destabilizes the protein structure, resulting in its unfolding. We have investigated the effect of three chemical denaturants, namely urea, GdmCl and GdmSCN on the structure of CIA17 by monitoring fluorescence emission characteristics of the protein. Chemical Unfolding of several proteins was studied by monitoring changes in the tryptophan fluorescence characteristics such as fluorescence intensity, quantum yield, emission maximum, fluorescence lifetime, pre-exponential factor, fluorescence anisotropy, and rotational correlation time when the concentration of denaturants was varied [Eftink, 1994]. Although fluorescence intensity exhibits proportionality to the population of the microstates (i.e., folded, unfolded), which is crucial to derive thermodynamic parameters from the spectroscopic data, complexity arises in many cases, e.g., the intrinsic temperature dependence or a pronounced protein concentration dependence of the tryptophan fluorescence emission or in some cases the differences in intensity signals from folded and unfolded states are very small, which make precise measurements difficult [Duy and Fitter, 2006; Tan et al., 1998]. Native CIA17 shows an emission maximum ( $\lambda_{max}$ ) at 335 nm upon excitation at 295 nm, suggesting that the tryptophan

residues in CIA17 are neither totally buried inside the hydrophobic core of the protein nor fully exposed on the hydrophilic surface, but exist in a partially buried state. CIA17 contains 9 Trp residues which are located in different microenvironments and the fluorescence emission of some of these could be quenched by neighboring amino acid residues such as Lys, Arg, Asp, Glu, Asn and His by excited state proton transfer and/or electron transfer mechanism [Chen and Barkley, 1998]. Further, different denaturants may affect the fluorescence intensity differently as each of the chaotropic agents used here was reported to affect the lifetime of the indole moiety differently [Swaminathan et al., 1994]. In view of these considerations, which make it difficult to study the chemical unfolding of CIA17 by monitoring changes in the fluorescence intensity, we have monitored changes in the emission  $\lambda_{max}$  of the lectin in presence of denaturants. While the emission maximum also does not give a true picture of the unfolding process when the emission intensities exhibit changes during the unfolding process, at least the general trends can be assessed more reliably since the emission  $\lambda_{max}$  only increases when the protein unfolds, whereas the emission intensity can increase, decrease or remain unaltered.

Fluorescence spectra of CIA17 incubated with different concentrations of GdmSCN and a plot depicting the emission maximum of CIA17 as a function of the denaturant concentration are shown in Fig. 2.3A and 2.3B, respectively. Similar data corresponding to GdmCl-induced unfolding are presented in Fig. 2.3C and 2.3D, respectively. The main unfolding event appears to be a two-state transition with a transition midpoint at 3.1 M GdmSCN and the  $\lambda_{max}$  of the protein exhibits a red shift to 349 nm as the concentration of the chaotrope is gradually increased to ~4 M, indicating complete exposure of Trp residues to the aqueous solvent (Figs. 2.3A, 2.3B). Interestingly, a smaller, yet distinct event is seen between 0 and 2 M GdmSCN. Considering that this event is associated with only a small shift (~2 nm) in  $\lambda_{max}$  (Fig. 2.3B), this transition can be ascribed to the dissociation of the dimeric protein into monomers, which does not change the structure of the folded protomers and hence not expected to significantly alter the emission  $\lambda_{max}$ . Incubation of the protein with 10 mM DTT prior to treatment with GdmSCN lowered the midpoint of the main unfolding event



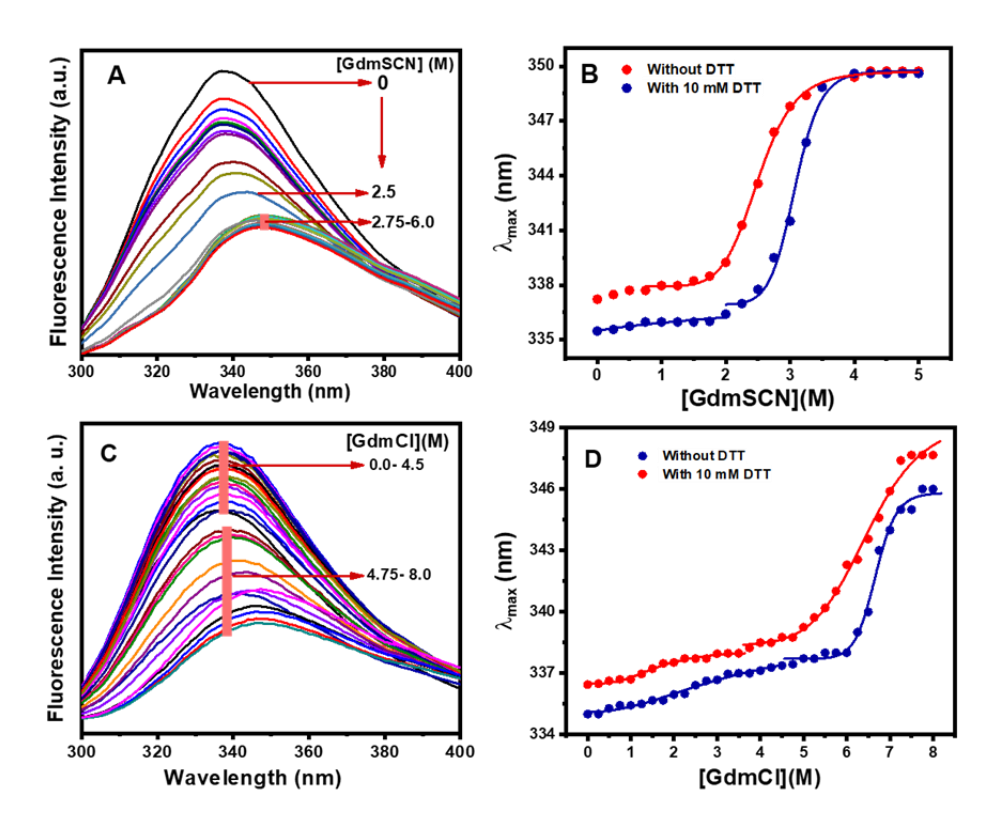


Fig. 2.3. Fluorescence emission spectra of CIA17 in the absence and in the presence of GdmCl (A) and GdmSCN (C). Emission maxima ( $\lambda_{max}$ ) vs denaturant concentration for (B) GdmCl and (D) GdmSCN. Blue ( $\bullet$ ) and red ( $\bullet$ ) symbols represent data points for experiments performed in the absence and in the presence of 10 mM DTT. Solid lines in B and D correspond to sigmoidal fits of the data obtained using Botzmann model and Levenberg-Marquardt iteration algorithm available in MicroCal Origin software.

Qualitatively very similar results were obtained with GdmCl (Fig. 2.3C, 2.3D), excepting that the midpoint of the main unfolding transition was observed at significantly higher concentrations of the chaotrope for the studies conducted in the presence and absence of 10 mM DTT (~6.4 and 6.8 M, respectively). The corresponding minor transitions, attributed to the dissociation of the dimeric CIA17 into monomers were

found to be centered at around 1.4 and 2.5 M GdmCl, respectively (Fig. 2.3D). Urea was found to be the least effective in denaturing CIA17. In the absence of DTT, incubation with 10 M urea led to only 2-3 nm red shift in the emission maximum, although upon reduction with 10 mM DTT the emission  $\lambda_{max}$  of CIA17 shifted to 345 nm (data not shown). These observations are consistent with the general understanding that urea is a weaker chemical denaturant than guanidinium salts [Tanford, 1968].

Results obtained from chemical unfolding studies on CIA17, performed in the absence and presence of DTT, can be explained in terms of additional stability imparted by the disulfide bonds connecting cysteine residues to the overall structure of the protein. CIA17 contains three cysteine residues among which C34 and C51 form an intramolecular disulfide bond, whereas C125 near the C-terminal end remains exposed to the surface and most likely participates in the formation of intermolecular disulfide linkages with PP1 proteins, which promote the formation of cross-linked, extended structures that seal the wounds inflicted by insect bites. The present results, obtained from the chaotrope-induced unfolding studies suggest that these intra- and intermolecular disulfide bonds undergo cleavage when incubated with 10 mM DTT, which facilitates complete unfolding of CIA17 upon treatment with the chaotropic agents, GdmSCN and GdmCl. Thus, the present studies indicate that disulfide linkages play an important role in the tertiary and quaternary structure of CIA17.

It is instructive to compare results of thermal unfolding studies with those obtained from the chemical denaturation studies. While the DSC studies indicated that the thermal unfolding of CIA17 involves three distinct steps, only two well-resolved steps could be identified in the chemical unfolding studies with both GdmCl and GdmSCN. This difference can be explained on the basis of differences in the concentrations of CIA17 used in the DSC and fluorescence studies, employed in the thermal and chemical unfolding studies, respectively. Our previous AFM studies have shown that at the relatively high concentration of 0.5-1.0 mg/mL (~29-58  $\mu$ M) used in the DSC studies CIA17 exists as relatively large, yet soluble aggregated structures, whereas at the concentration of ~1-2  $\mu$ M used in the fluorescence studies it exists as small globular structures [Bobbili et al., 2018a]. Therefore, it appears that the first component in the

DSC thermogram of native CIA17, centered at ~98.3 °C is the dissociation of such large soluble aggregates of the protein into dimers. Since such large aggregates are not present in the low concentration protein samples used in the fluorescence measurements, only two transitions have been observed in the chemical denaturation studies. Formation of higher oligomers or aggregation at higher concentrations was further investigated by probing the size of the native protein using fluorescence correlation spectroscopy (FCS).

### 2.4.3. Fluorescence Correlation Spectroscopic Studies

The fluorescence correlated data for CIA17-A488 conjugate in 15 mM phosphate buffer is shown in Fig. 2.4. The cross-correlation data was better fitted to eq. (2.3) which includes the contribution of an exponential term in addition to the simple diffusion to the fluorescence intensity fluctuation, than to equation (2.2), which corresponds to a single diffusion component model.

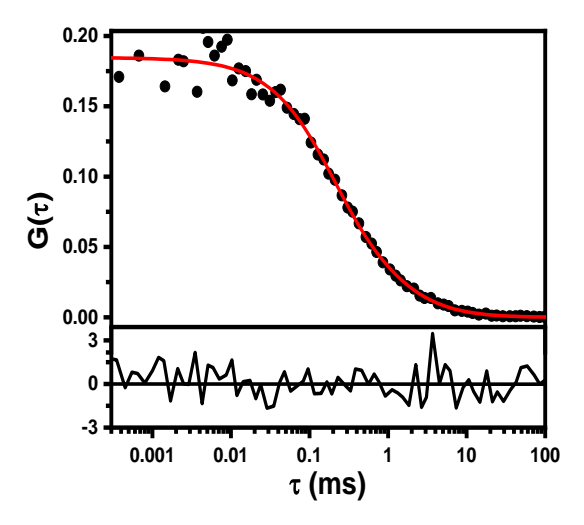


**Fig. 2.4.** Correlation data of A488-labeled CIA17. The red solid line is the fit to eq (2.3), corresponding to simple diffusion with a second order exponential component. The bottom panel shows the residual distribution for the fit.

The correlation data for free Alexa488 was well fitted to the single diffusion model and the laser intensity used for all the FCS measurements was ~10-12  $\mu$ W, which rules out the possibility of fluorescence fluctuation due to intersystem crossing. Considering these aspects, the  $2^{nd}$  term ( $\tau_R$ ) in the correlation function can be attributed to

the conformational fluctuations in the protein that modulate the interaction between amino acid residues Trp and Tyr of the protein and the fluorophore because side chains of these two amino acids have been demonstrated to efficiently quench the fluorescence emission of Alexa fluorophores when they come in close proximity [Mojumdar et al., 2012; Chen et al., 2010; Pabbathi et al., 2013]. Besides 9 Trp and 3 Tyr residues, each CIA17 subunit also has 2 His and 6 Met residues, which can quench the fluorescence emission intensity of the dye to different degrees when the protein undergoes conformational fluctuations. This in turn can lead to fluctuations in the observed fluorescence intensity.

From FCS measurements performed on labeled CIA17 in the concentration range of 5-50 nM, the average hydrodynamic radius ( $R_h$ ) of the native protein was estimated as 2.91 ( $\pm 0.23$ ) nm, which is significantly higher than 2.04 nm predicted for the monomeric protein by the following empirical equation [Wilkins et al., 1999]:

$$R_h = 4.75 \ n^{0.29} \ \text{Å} \tag{2.8}$$

where n is the number of amino acid residues in the protein.

The higher  $R_h$  value obtained from the FCS measurements suggests that the lectin exists in an oligomeric form in the concentration range of 5-50 nM. A significant change in average diffusion time  $(\tau_D)$  from 332  $(\pm 23)$  to 236  $(\pm 21)$   $\mu s$  was observed with the progressive dilution of the labeled protein to  $\leq 0.8$  nM. Consequently,  $R_h$  value decreases to ~2.13  $(\pm 0.15)$  nm indicating that CIA17 exists essentially as a monomer at concentrations below 1 nM.

In order to investigate the formation of higher oligomers or aggregates at higher concentrations, CIA17-A488 conjugate (10 nM) was mixed with unlabeled CIA17 to yield varying concentrations (250 nM to 100  $\mu$ M) of the total protein. FCS measurements were carried out after 30-120 minutes incubation with the same experimental set up. The normalized correlation curves and the variation of hydrodynamic radius of the native protein as a function of total protein (labeled + unlabeled) concentration are shown in Fig. 2.5. Despite the complexity of oligomerization, all the correlation data could be fitted satisfactorily to Eq. (2.3). The  $R_h$  value increases to 3.4 ( $\pm$ 0.33) nm at  $\geq$  5 $\mu$ M of

total protein. Only a marginal change was observed over the concentration range of 5-40  $\mu$ M. The R<sub>h</sub> value increases to 4.3 ( $\pm$ 0.2) nm at 57  $\mu$ M and 4.97 ( $\pm$ 0.25 nm) nm when the protein concentration reached 100  $\mu$ M.

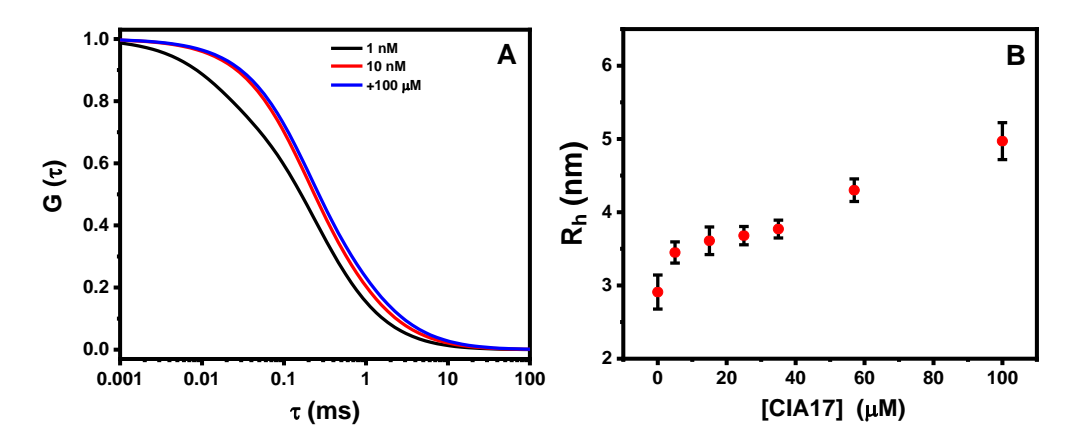


**Fig. 2.5.** (A) Normalized correlation curves of A488-CIA17 conjugate with increasing concentration of unlabeled CIA17. (B) Variation of R<sub>h</sub> with increasing concentration of protein. Error bars represent SD values estimated from a minimum of 4 measurements.

The average degree of oligomerization (k) was determined from the relative diffusion coefficients ( $D_k$ , k =1, 2, 3,...) of different oligomers. According to the Stokes-Einstein equation, diffusion coefficient of a spherical particle is inversely proportional to the cubic root of its volume. The AFM images of CIA17 reported earlier indicate that small oligomers are nearly spherical, and at higher concentrations they further self-assemble leading to the formation of filamentous structures [Bobbili et al., 2018a]. Considering the near-spherical shape of the oligomers, it can be written as  $D_k = D_1 k^{-1/3}$  where k is the number of subunits present in the oligomer [Chakraborty et al., 2012]. The diffusion coefficient was found to decrease to 84 (± 14)  $\mu$ m<sup>2</sup>s<sup>-1</sup> when the concentration of the total protein (labeled + unlabeled) was varied between 5 and 50 nM, whereas it was estimated as 115 (±21)  $\mu$ m<sup>2</sup>s<sup>-1</sup> at concentrations  $\leq$  0.8 nM. The  $D_k/D_1$  value remained nearly unchanged within error at an average value of 0.86 over the wide concentration range of 5 nM–5  $\mu$ M, implying that CIA17 exists as homodimer over this concentration

range. The ratio decreases to 0.71 ( $\pm 0.12$ ) in the concentration range of 10-40  $\mu M$  of the unlabeled protein suggesting the formation of tetramers (dimer of dimers).

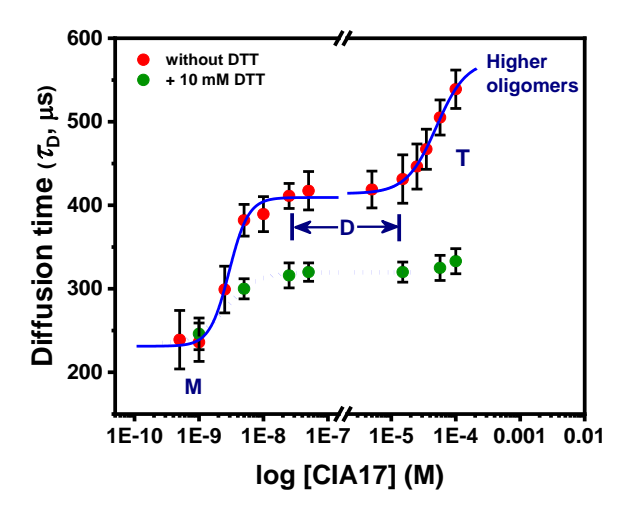
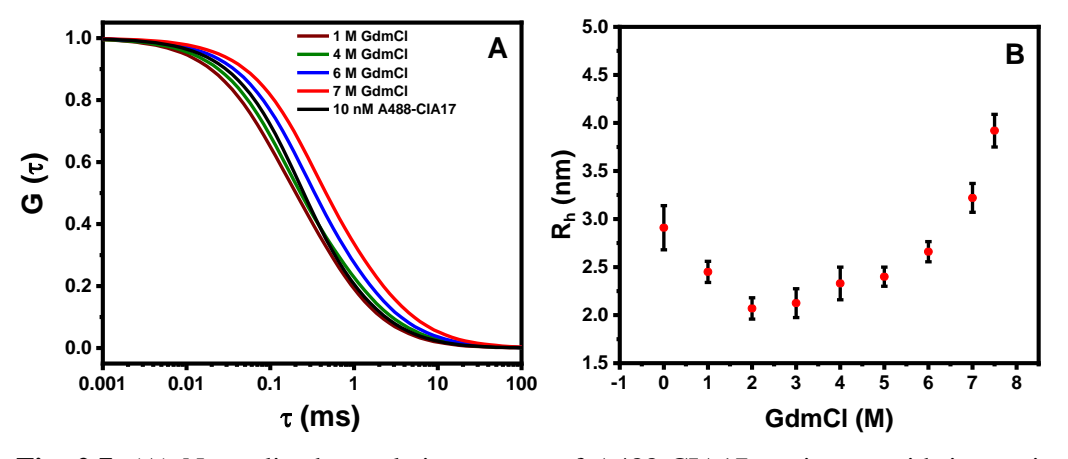


Fig. 2.6. Binding curves showing the M  $\leftrightarrow$  D and D  $\leftrightarrow$  T equilibrium of CIA17. The change in diffusion time is plotted against logarithm of the total protein concentration. From a nonlinear regression of the data (blue lines) the dissociation constants ( $K_D$ ) for the M  $\leftrightarrow$  D and D  $\leftrightarrow$  T equilibria were estimated as 2.92 nM and 47.2  $\mu$ M.

Fig. 2.6 shows a plot of diffusion time of CIA17 as a function of log [CIA17]. For the native protein in the absence of any reducing agent, the plot shows two well-separated equilibria corresponding to association of monomers (M) to give dimer (D) and dimers combining to yield tetramers (T). Sigmoidal fits of the data using Botzmann model and Levenberg-Marquardt iteration algorithm available in MicroCal Origin software yielded the dissociation constants ( $K_D$ ) for the  $M \leftrightarrow D$  and  $D \leftrightarrow T$  equilibria as 2.92 nM and 47.2  $\mu$ M, respectively. The diffusion coefficient was found to be  $56 \mu m^2 s^{-1}$  at a protein concentration of 57  $\mu$ M and 49.3  $\mu$ m<sup>2</sup>s<sup>-1</sup> at 100  $\mu$ M of the unlabeled protein with corresponding  $D_k/D_1$  ratios of 0.54 and 0.48, respectively. The k value was estimated to be ~8-12 when the concentration of the unlabeled protein was varied between 50 and 100  $\mu$ M, which suggests that the homodimeric CIA17 self assembles leading to the formation of larger aggregates at higher protein concentrations. Very interestingly, when the CIA17 samples were preincubated with 10 mM DTT, only one

equilibrium was observed which overlapped with the monomer-dimer equilibrium seen in the absence of the reducing agent. While the diffusion time observed for the monomer in the presence of DTT was similar to that determined for the native protein, the  $\tau_D$  value corresponding to the dimer, however, was considerably lower than that determined for the native protein dimer. This suggests that reduction of the disulfide bonds leads to changes in the shape of the protein, which in turn alters its diffusion time. Additionally, it is seen that presence of DTT prevents the formation higher oligomers (beyond dimer), clearly indicating that disulfide bond formation is required for the formation of large oligomeric structures of the protein that take part in the formation of polymeric structures that may play a role in wound sealing on the surface of the fruit.

The dissociation constants of ~2.9 nM estimated here for the CIA dimer dissociating into monomers and ~47  $\mu$ M estimated for the tetramer to dissociate to yield dimers are about one and three orders of magnitude higher than the values of 0.55 nM and 50 nM, respectively, estimated for corresponding equilibria of the tumor suppressor protein p53 [Rajagopalan et al., 2011]. Additionally, it is also interesting to note that in the case of p53 the  $K_D$  values for the dimer  $\leftrightarrow$  tetramer equilibrium is approximately 100 fold higher than that estimated for the monomer  $\leftrightarrow$  dimer equilibrium, whereas for CIA17 the  $K_D$  values for the two equilibria differ by ~1600 fold.



**Fig. 2.7.** (A) Normalized correlation curves of A488-CIA17 conjugate with increasing concentration of unlabeled CIA17. (B) Variation of  $R_h$  value with increasing concentration of GdmCl.

# 2.4.5. Effect of GdmCl on the Size and Conformational Dynamics of CIA17

The normalized fluorescence correlation profile and the variation of hydrodynamic radius of the native protein with increase in denaturant (GdmCl) concentration is shown in Fig. 2.7. In contrast to what is expected for a monomeric protein,  $R_h$  value decreases with increase in the concentration of GdmCl up to 2 M, followed by a steady increase in  $R_h$  value with gradual increase in concentration (3 to 7.5 M) of the denaturant. For the native protein, an  $R_h$  value of ~2.91 ( $\pm$ 0.23) nm was calculated from the diffusion time of 25 nM A488-CIA17. At 2 M GdmCl,  $R_h$  decreases to ~2.07 nm which is close to the  $R_h$  value of 2.04 nm predicted for the monomer by Eq. (2.8). With further increase in denaturant concentration,  $R_h$  increases steadily and a sharp change to a value of 3.92 nm occurred at 7.5 M concentration. This matched well with the  $R_h$  value of 3.87 nm predicted for the unfolded protein (with n amino acid residues) from the following empirical equation [Wilkins et al., 1999]:

$$R_{h} = 2.21 \, n^{0.57} \, \text{Å} \tag{2.9}$$

This clearly suggests that the lectin completely unfolds when incubated with 7.5 M GdmCl. Results of steady state fluorescence measurements (section 2.4.2) suggested that chemical unfolding of CIA17 by GdmCl is a three-state process. Similarly, the FCS data could be interpreted as follows: in the first transition (0-2 M GdmCl) the dimeric protein dissociates to give monomers and the second transition (3-7.5 M GdmCl) is the denaturation of monomers to yield the unfolded protein. The above changes in the hydrodynamic radius of the protein as the concentration of the denaturant is varied are consistent with the following model. CIA17 exists as homodimer at the concentration used in these studies (25 nM) and its chaotrope-induced denaturation can be described by the three-state model shown in *Scheme II*:

$$A_2 \stackrel{K_1}{\leftrightarrow} 2I \stackrel{K_2}{\leftrightarrow} 2U \tag{II}$$

where  $A_2$  is the dimeric native protein, I is the monomeric intermediate and U is the unfolded protein.

The variation of relaxation time ( $\tau_R$ ) monitored as a function of GdmCl concentration is shown in Fig. 2.8. The figure indicates that  $\tau_R$  decreases from 126 ( $\pm 12$ ) to 78 ( $\pm 13$ )  $\mu$ s upon the addition of 1 M GdmCl and then gradually increases and finally

reaches a value of 126 ( $\pm 16$ )  $\mu s$  at 7.5 M of GdmCl. The sharp decrease in relaxation time at low GdmCl concentrations (0-1 M) may be due to the partial dissociation of dimer to monomer. The constant increase in  $\tau_R$  as the concentration of GdmCl increases is possibly due to the increase in average distance of the fluorophore and Trp residues during the unfolding process.

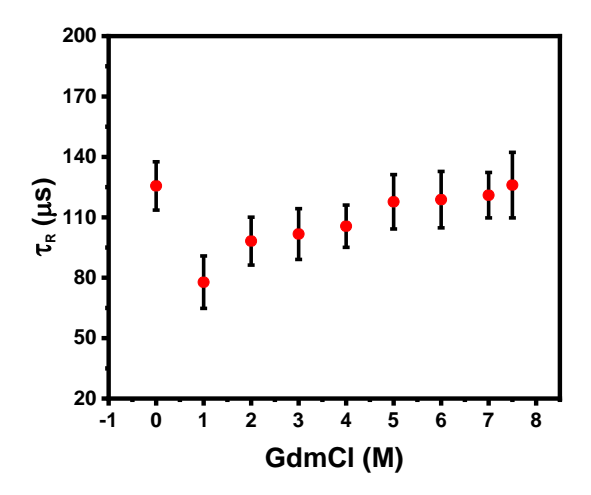


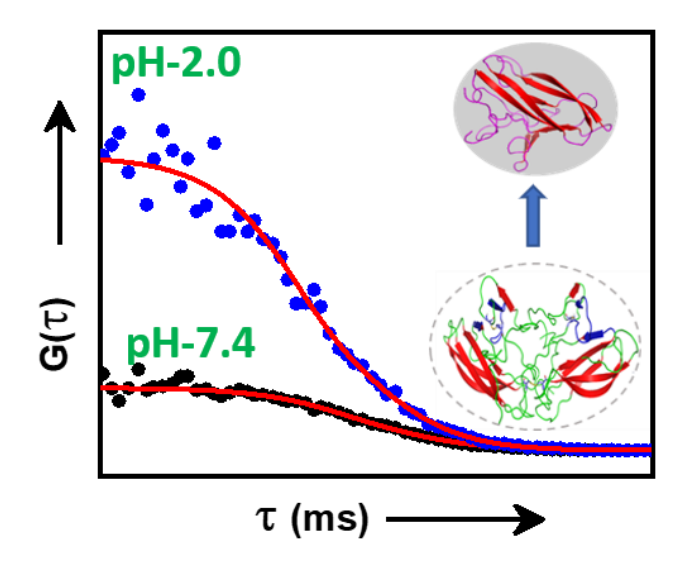
**Fig. 2.8.** Variation of  $\tau_R$  as a function of GdmCl concentration.

It is interesting to compare the results of thermal and chemical unfolding studies on CIA17 with those obtained with cucumber (*Cucumis sativus*) phloem lectin (CPL), another dimeric phloem exudate lectin isolated from the Cucurbitaceae [Nareddy et al., 2017; Nareddy and Swamy, 2018]. While the present studies have shown that unfolding thermograms of CIA17 could be resolved into three components, suggesting the presence of intermediate states in the unfolding process, thermal unfolding of CPL could be analyzed in terms of a single transition from a fully folded state to a completely unfolded state. Similarly, chemical unfolding of CIA17 by GdmCl and GdmSCN could be resolved into two transitions, whereas denaturation of CPL by GdmCl could be explained in terms of a single unfolding transition [Nareddy and Swamy, 2018].

### 2.5. Conclusion

In summary, the present DSC studies on the thermal unfolding of CIA17 show that it is a highly thermostable protein with a  $T_{\rm m}$  of ~109 °C for complete unfolding of the protein at physiological pH. The overall thermal unfolding of the protein is a complex process involving dissociation of oligomeric aggregates into dimers, followed by further dissociation of the dimers into monomers which then undergo complete unfolding to yield the fully denatured protein. Fluorescence spectroscopic studies on the chaotropeinduced unfolding of CIA17 by GdmSCN and GdmCl revealed at least two components in the unfolding process, which could be attributed to dissociation of the dimeric protein into monomers and complete unfolding of the monomeric subunits. Results of fluorescence correlation spectroscopic studies show CIA17 exists in the monomeric form below 1 nM and the monomers associate to give dimers at higher concentrations (K<sub>D</sub> ~2.9 nM), which again associate to tetramers with further increase in concentration (K<sub>D</sub> ~47 µM). Higher oligomers are formed when the concentration is increased. The concentration of CIA17 under physiological conditions is ~6-8 mg/ml (S. Mondal & M. J. Swamy, unpublished observations). This is considerably higher than the concentrations required for the formation of higher oligomers (≥ tetramer). However, since the phloem fluid oozing out of the wound (or cut) on the fruit is a clear liquid, these oligomers must be soluble. However, upon exposure to air the proteins in the phloem fluid associate to form a jelly like substance which seals the wound. The exposure to air must involve disulfide bond formation (oxidation), and our above results show that blocking the disulfide bond formation by using DTT in the sample prevents the formation of higher oligomers. These results are relevant for understanding the role of the phloem proteins in protecting the plant from insect/pest attack.

# Effect of pH on the Local/Global Structure of CIA17 and its Carbohydrate Binding. Presence of a Molten Globule-Like State at Low pH



**Saradamoni Mondal,** Somnath Das, Sumanta Paul, Shilpa Barik, Musti J. Swamy\*

Manuscript under preparation

# 3.1. Summary

pH induced changes in the conformation, structural dynamics as well as carbohydratebinding activity of Coccinia indica agglutinin (CIA17) were investigated employing biophysical approaches. The secondary structure of CIA17 remains almost unaltered over a wide pH range (2.0-8.5) while the tertiary structure of the protein exhibits considerable changes. The decrease in fluorescence intensity and the excited state lifetime at low pH indicated the perturbation in the local conformation (near Trp residues) of the lectin which was further demonstrated by the enhancement in Trp accessibility towards the external charged quenchers under acidic condition. Results of fluorescence correlation spectroscopic (FCS) studies indicate that at pH 2.0 the lectin exists as a monomer over the concentration range of 10 nM-200 nM and forms dimers at higher concentrations (KD ≈ 387 nM) but couldn't form higher oligomers even at ~150-fold higher concentrations unlike the native protein (at pH 7.4). Thermal unfolding of the low pH intermediate involves two distinct steps: dissociation of dimer to monomer, followed by the unfolding of the monomer. The intermediate retains a considerable degree of chitooligosaccharide binding. These results significantly implicate that the pH induced unfolding pathway involves the formation of a monomeric molten globule like intermediate which retains appreciable carbohydrate binding ability.

### 3.2. Introduction

The intracellular pH of each compartment of the living cell is strictly controlled. Regulation of the cellular pH is fundamental for homeostatic control of physiological processes, such as synthesis of proteins, DNA and RNA, vesicular trafficking, control of the cell cycle and ion transport across membranes [Gout et al., 1992; Ishizawa, 2014; Roberts et al., 1980,1982]. Cells of higher plants contain two main compartments, cytoplasm, which is slightly alkaline (pH  $\sim$ 7.4-7.5) and the vacuole which is considerably acidic with a pH range of  $\sim$ 4.5-6.0 [Alexov, 2004; Roberts et al., 1982]. Proteins are sensitive to changes in the pH of organelles and are found to have different pH optima with respect to stability and activity. Changes in pH can modify the protonation state (p $K_a$ ) of ionizable side chains, which in turn induce conformational changes of the folded proteins [Alexov, 2004; O'Brien et al., 2012; Russo et al., 2012; Talley and Alexov, 2010; Yang and Honig, 1993].

The molten-globule-like state is a kinetic intermediate in protein (un)folding pathway that is quite different from native or denatured state but is a compact denatured state with native-like secondary structure and slightly distorted tertiary structure compared to the native state [Redfield et al., 1994; Wu et al., 1995; Zohu et al., 2000]. The molten globule (MG) state, which has been detected during protein folding in in vitro studies, is thought to be involved in protein translocation and membrane insertion in vivo and is implicated in genetic diseases, such as cystic fibrosis and emphysema [Bychkova and Ptitsiyn, 1995; Prajapati et al., 2007]. Equilibrium and/or kinetic intermediates resembling MG state have been reported for several globular proteins including cytochrome C [Colón and Roder, 1996; Goto et al., 1990], α-lactalbumin [Kuwajima et al., 1996], lysozyme [Radford et al., 1992], barstar [Khurana and Udgaonkar, 1994] etc. Molten globule-like structures were reported to be present as folding intermediates in a few lectins e.g., lentil lectin [Marcos et al., 2000] peanut agglutininin [Reddy et al., 1999], banana lectin [Khan et al., 2013] and Fusarium solani lectin [Khan et al., 2007]. Although a number of phloem exudate lectins have been purified and characterized in the last 4 decades or so, there are no reports on the presence

of MG-like intermediates involved in the (un)folding pathways of phloem exudate lectins. Importantly, the 3-dimensional structure is not known for any of these lectins.

Coccinia indica agglutinin (CIA17), an oligomeric PP2-type lectin with subunit mass of ~17 kDa and each subunit contains 152 amino acid residues with one extended binding site for chtooligosacharide [Bobbili et al., 2019]. The detailed mechanism of thermal and chemical unfolding of CIA17 is reported in Chapter 2 which showed that Cia17 has high thermal ( $T_{\rm m}$  ~110 °C) and chemical stability ( $C_{\rm m}$  ~ 7.5 M GdmCl) at physiological pH. CIA17 exists as a polydisperse oligomeric protein and self assembles to form higher oligomeric structure in a concentration dependent manner [Mondal et al., 2021].

In the work presented in this chapter, pH induced changes in the conformation and/or structural dynamics of the lectin have been investigated using CD spectroscopy, steady-state and time-resolved fluorescence spectroscopy and fluorescence correlation spectroscopy. Thermal stability of the lectin at different pH was investigated using differential scanning calorimetry. The results obtained indicate the formation of a MG-like state of the protein monomer at pH 2.0, which retains considerable carbohydrate binding ability as assessed by isotheral titration calorimetry.

## 3.3. Materials and methods

#### 3.3.1. Materials

Unripe ivy gourd (*Coccinia indica*) fruits were purchased from local vendors.  $\beta$ -chitin, 2-mercaptoethanol ( $\beta$ ME),  $\alpha$ -chitin, chitooligosaccharides, ammonium persulphate, acrylamide, guanidine hydrochloride (GdmCl), guanidine thiocyanate (GdmSCN), urea, and dithiothreitol (DTT) were purchased from Sigma (St. Louis, MO, USA). All other chemicals and reagents were procured from local suppliers and were of the highest purity available.

CIA17 was purified from the phloem exudate of unripe ivy gourd by sequential affinity chromatography on  $\alpha$ -chitin followed by  $\beta$ -chitin as described in chapter 2.

## 3.3.2. Circular Dichroism (CD) Spectroscopy

CD spectroscopic measurements were performed on a Jasco J-810 spectropolarimeter. CIA17 samples of 1.57  $\mu$ M and 15.7  $\mu$ M monomer concentrations were used for measurements in the far-UV (250-190 nm) and near-UV (300-250 nm) regions, respectively. A rectangular quartz cuvette of 0.2 cm path-length was used for all measurements. Protein samples were dialyzed against the following buffers to obtain the desired pH: 10 mM KCl-HCl (pH 2.0, 2.5), 10 mM glycine-HCl (pH 3.0, 3.5), 10 mM sodium acetate (pH 4.0, 5.0), 10 mM sodium phosphate (pH 6.0-7.4), 10 mM tris-HCl (pH 8.5). All spectra reported are averages of 7 consecutive scans recorded at a scan rate of 100 nm/min. Spectral data were collected at 1 nm intervals.

## 3.3.3. Steady State Fluorescence Spectroscopy

Fluorescence emission spectra were recorded on a Jasco FP-8500 spectrofluorometer. CIA17 samples ( $OD_{280} < 0.10$ ) were irradiated at 295 nm to excite tryptophan residues selectively and emission spectra were recorded in the wavelength range of 300-400 nm. Fluorescence quenching titrations were performed using neutral (acrylamide), anionic (iodide) and cationic (cesium ion) quenchers as described earlier [Narahari et al., 2009]. Briefly, fluorescence emission spectra were recorded after each addition of small aliquots from a 5 M stock solution of the quencher to the protein under native and denatured conditions (in presence of 4 M GdmSCN), at different pH, and in presence of 1 mM chitotetraose. Fluorescence intensities were corrected by subtracting the buffer spectra recorded at the same condition following volume correction. Further, inner filter correction to the fluorescence intensity was done using the following equation:

$$F_{corr} = F_{obs} \times antilog \left[ \frac{oD_{ex} + oD_{em}}{2} \right]$$
 (3.1)

Here,  $F_{corr}$  and  $F_{obs}$  are the corrected and observed fluorescence intensities, respectively and  $OD_{ex}$  and  $OD_{em}$  are the absorbance values measured at excitation wavelength (295 nm) and corresponding wavelengths of emission maximum ( $\lambda_{max}$ ). The steady state

fluorescence quenching data were analyzed using Stern-volmer Eq (3.2) as well as modified Stern-Volmer Eq (3.3):

$$F_0/F = 1 + K_{SV}[Q] (3.2)$$

$$F_0/\Delta F = f_a^{-1} + (K_a f_a)^{-1} [Q]^{-1}$$
(3.3)

where  $F_0$  and F are the relative fluorescence intensities in the presence and absence of quencher respectively, [Q] is the quencher concentration,  $K_{SV}$  is the Stern-Volmer quenching constant for a given quencher,  $\Delta F$  (= $F_0$ -F) is the change in fluorescence intensity after each titration,  $f_a$  is the fraction of total fluorescence intensity that is accessible to the quencher and  $K_a$  is the corresponding Stern-Volmer quenching constant for the accessible fraction of the fluorophores. The slope of  $F_0/F$  vs [Q] plot corresponds to the Stern-Volmer constant ( $K_{SV}$ ) and from the slope and intercept of  $F_0/\Delta F$  vs [Q] plot,  $K_a$  and  $f_a$  values are calculated.

## 3.3.3.1 Analysis of the Steady State Quenching

The static and dynamic components involved in the Stern-Volmer plot for acrylamide quenching of denatured CIA17 were resolved using the following equations:

$$F_0/F = (1 + K_{SV}[Q]) (1 + K_S[Q])$$
(3.4)

$$\tau_o/\tau = 1 + K_{SV}[Q] \tag{3.5}$$

where  $K_{SV}$  and  $K_S$  are the collisional and static quenching constants, [Q] is the quencher concentration,  $\tau_o$  and  $\tau$  are the average lifetimes of the protein obtained from the time resolved fluorescence measurements in the absence and presence of quencher at different concentrations. Eq. (3.4) yielded a slope ( $K_{SV}$ ) of a plot of  $\tau_o/\tau$  vs [Q] which corresponds to the dynamic quenching constant. The static quenching constant ( $K_S$ ) was then calculated by incorporating the  $K_{SV}$  value in eq. (3.5).

#### 3.3.4. Fluorescence Lifetime Measurements

Fluorescence lifetimes were measured on a time correlated single photon counting (TCSPC) spectrometer from Horiba Jobin Yvon IBH (Glasgow, UK) equipped with a

delta diode laser source as described in Das et al. (2020). Samples of CIA17 (OD<sub>280</sub>  $\sim$  0.07) were excited at 285 nm and the decay was monitored at the respective emission maxima. The instrument response function was 860 ps. and excitation and emission slit widths used for the experiment ranged between 6 and 12 nm. A dilute solution of Ludox in water was used as the scatterer to record the lamp profile. The fluorescence decay curves obtained were analyzed by a multiexponential iterative program provided by the manufacturer.

## 3.3.5. Fluorescence Correlation Spectroscopy (FCS)

FCS measurements were carried out with an Alexa488 labeled CIA17 (A488-CIA17) using a time-resolved confocal fluorescence microscope, MicroTime 200, PicoQuant. The lectin was labeled with Alexa fluoro 488 carboxylic acid succinimide ester (A488) following the procedure as described in Chapter 2. A pulsed diode laser ( $\lambda_{ex} = 485$  nm with fwhm 144 ps) was used as the excitation source.

The average degree of oligomerization (k) was determined from the relative diffusion coefficients ( $D_k$ , k =1, 2, 3,...) of different oligomers. According to the Stokes-Einstein equation, diffusion coefficient of a spherical particle is inversely proportional to the cubic root of its volume,  $D_k = D_1 k^{-1/3}$  where k is the number of subunits present in oligomer.

## 3.3.6. Differential Scanning Calorimetry

DSC measurements were carried out on a Nano DSC equipment from TA systems (New Castle, DE, USA). Protein samples of 0.5-1.0 mg/mL (29-58  $\mu$ M) concentration, dialyzed against buffers of desired pH (see Section 3.3.2 for details of the buffers) were heated from 10 to 120 °C at a scan rate of 1 degree/min. The dialysates were used as the reference. Sample and reference solutions were properly degassed prior to the DSC measurements. Thermograms obtained were analyzed using the Gaussian Modeler software supplied by TA Systems.

## 3.3.7. Isothermal Titration Calorimetry

Calorimetric titrations were carried out at 25 °C on a PEAQ-ITC instrument (Malvern Instrument Ltd., UK). Protein samples of concentration ~ 75-100  $\mu$ M were taken in the sample cell and titrations were carried out by injecting 1.5  $\mu$ L of chitoteraose (GlcNAc)<sub>4</sub> at a concentration of 0.75-1.15 mM with a 2-minute interval between successive injections. During entire titration the sample in the calorimeter cell was stirred at 750 rpm. The titrations were carried out at pH 2.0 and 7.4. Blank titrations were also performed by injecting aliquots of the ligand solution in to the buffer, which yielded insignificant heats of dilution. The binding isotherms were analyzed by using analysis software provided with the instrument. Thermodynamic parameters, viz., binding stoichiometry (n), change in enthalpy ( $\Delta$ H) and association constant ( $K_a$ ) were obtained by nonlinear least-squares fittings of experimental data using the 'one set of sites' binding model. Free energy of binding ( $\Delta$ G) and change in entropy ( $\Delta$ S) were deduced from the association constant and enthalpy of binding using the following standard thermodynamic equation:

$$-RT \ln K_a = \Delta G = \Delta H - T\Delta S \tag{3.4}$$

#### 3.4. Results and Discussion

## 3.4.1. CD Spectroscopic Studies

In the present study, we employed CD spectroscopy to investigate the effect of changing pH on the secondary and tertiary structure of CIA17. Far- and near-UV CD spectra of CIA17 samples that were dialyzed against buffers of different pH between 2.0 and 8.5 are shown in Figs. 3.1A and 3.1B, respectively. While far-UV CD spectra exhibited very few changes with change in pH, suggesting that the secondary structure of CIA17 is quite stable over a broad pH range, significant changes were observed in the near-UV CD spectra, indicating that tertiary structure of the protein is altered considerably with change in pH. In this respect, CIA17 is similar to CPL, another Cucurbitaceae PP2 type lectins isolated from cucumber (*Cucumis sativus*) whose secondary structure remains unaltered over a wide range of pH [Nareddy and Swamy, 2018].

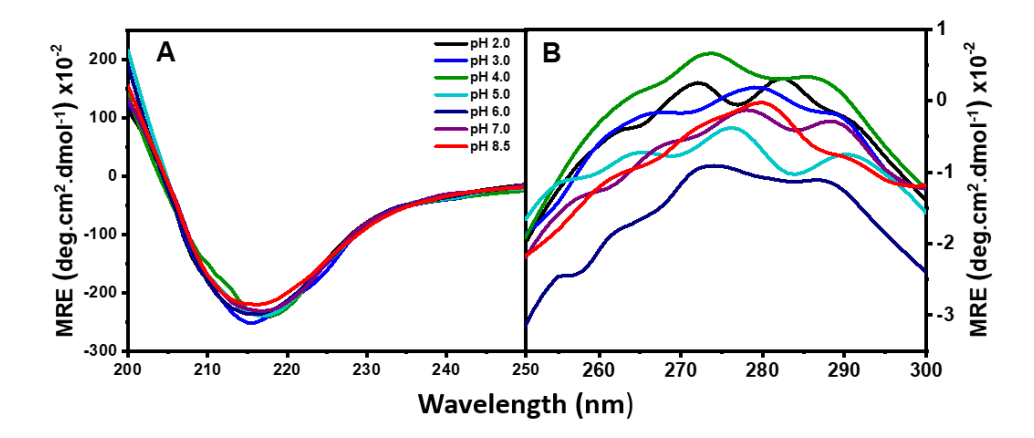


**Fig. 3.1.** CD spectra of CIA17 recorded at different pH. (A) Far-UV region, (B) near UV region. Color code in A indicates the pH at which each spectrum was recorded (for both panels A and B).

## 3.4.2. Steady-state Fluorescence Studies

Native CIA17 showed an emission  $\lambda_{max}$  at 340 nm when the tryptophan residues of the lectin were selectively excited at 295 nm, indicating that tryptophan residues are neither totally buried inside the hydrophobic interior of the protein nor completely exposed on the hydrophilic surface, but are most likely distributed across various degrees of exposure to the aqueous medium [Mondal et al., 2021]. A blue shift in the  $\lambda_{max}$  to 335 nm upon binding of chitooligosaccharides indicates a more compact structure on ligand binding whereas in presence of 4 M GdmSCN, the emission  $\lambda_{max}$  shifted to 350 nm indicating complete unfolding of the protein as reported in our previous study [Mondal et al., 2021]. Fluorescence intensity decreases gradually with decrease in pH from 7.4 to 2.0 although the  $\lambda_{max}$  remains essentially unaltered as shown in Fig. 3.2.

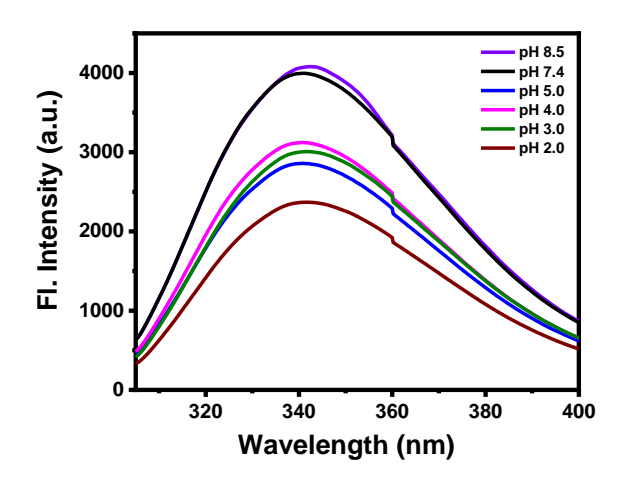
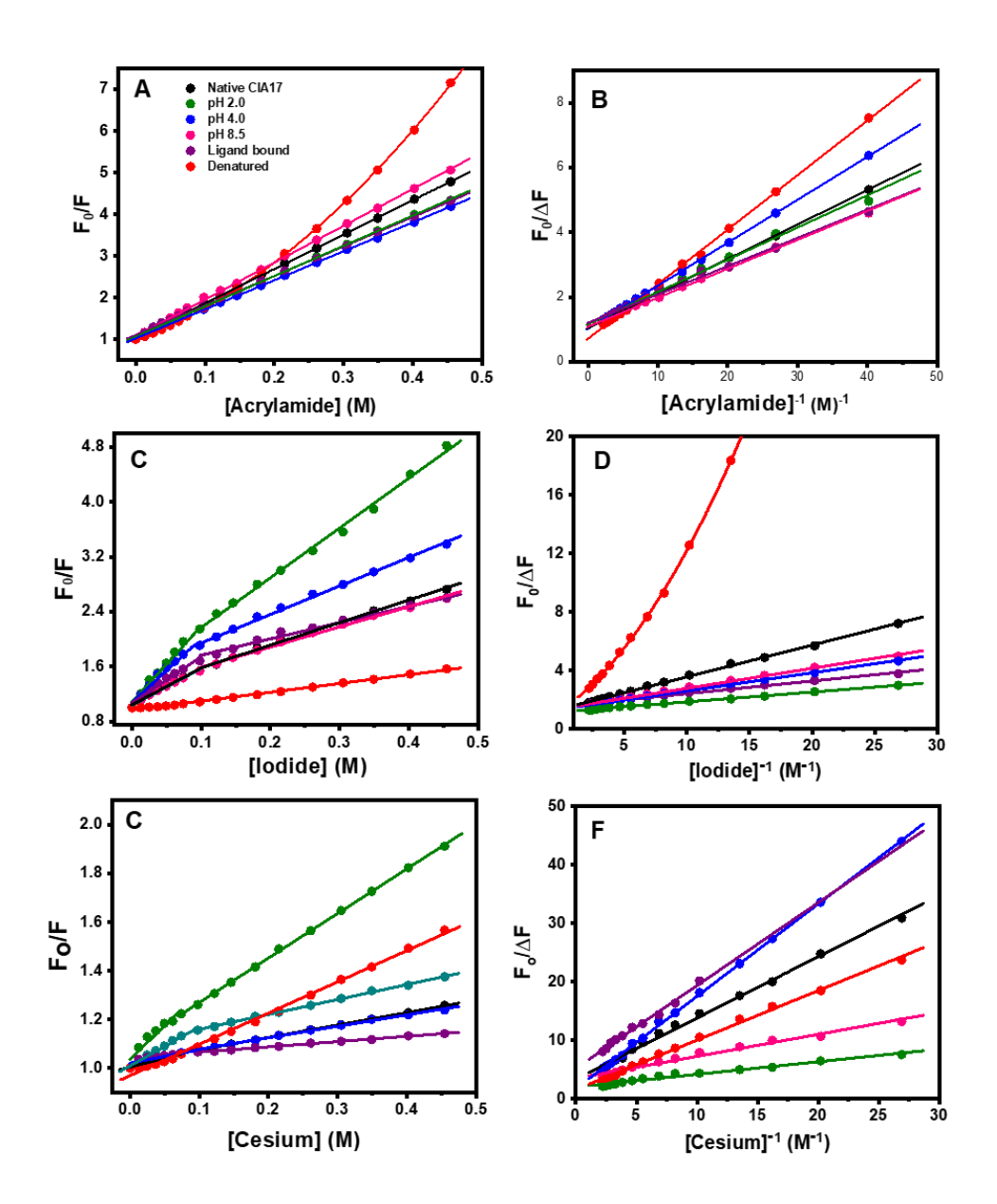


Fig. 3.2. Fluorescence emission spectra of CIA17 at different pH.

Conformational changes induced by change in pH of the lectin were investigated by probing Trp accessibility of the protein at different pH by monitoring quenching of the protein intrinsic fluorescence intensity by external quenchers, viz. acrylamide, iodide ion and cesium ion. Quenching studies were also performed in the presence of saturating concentrations of chitotetraose and upon denaturation with 4 M GdmSCN. For the native protein, acrylamide induced the maximum quenching (~81%) followed by iodide ion (~56%) which is again higher than the quenching due to cesium ion (~26%). Acrylamide being a neutral polar molecule can penetrate better into the hydrophobic interior of the protein and hence induces maximum quenching. The lower quenching efficiency of the ionic quenchers can be ascribed to the lower accessibility of some of the Trp residues that are located in the hydrophobic core of the protein. Between the two ionic quenchers, Γ showed a higher degree of quenching as compared to Cs<sup>+</sup>, which could be due to the better quenching efficiency of Γ as compared to Cs<sup>+</sup>. Additionally, electrostatic attraction/repulsion exerted by specific charged amino acid residues in the vicinity of some Trp residues to these ionic quenchers may also play a role.



**Fig. 3.3.** Stern-Volmer and modified Stern-Volmer plots for the fluorescence quenching of CIA17. (A, C, E) Stern-Volmer plots. (C, D, F) Modified Stern-Volmer plots. The quenchers used are: (A, B) acrylamide; (C, D) iodide; (E, F) cesium ion. Color code in (A) indicates conditions under which the quenching experiments were performed.

The quenching data were analysed by the Stern-Volmer approach (Eq. 3.2 & Eq. 3.3) and the Stern-Volmer and modified Stern-Volmer plots are shown in Fig. 3.3. The Stern-Volmer plot for acrylamide is linear for the native protein suggesting that the quenching of native CIA17 involves either dynamic or static quenching process, whereas upon denaturation, the plot is initially linear but tends to show upward curvature at higher quencher concentrations, indicating the contribution of both the dynamic and static quenching processes. The static and dynamic components involved in the Stern-Volmer plot were resolved using the equations (3.4) and (3.5) where a plot of  $\tau_o/\tau$  vs [Q] yielded a straight line (Fig. 3.4) with a slope of 3.79 that corresponds to the dynamic quenching constant (K<sub>SV</sub>) and the static quenching constant (K<sub>S</sub>) was obtained as 3.55. Similar to the native protein, linear dependence in the Stern-Volmer plots was observed for acrylamide quenching at all pH values (Fig. 3.3A).

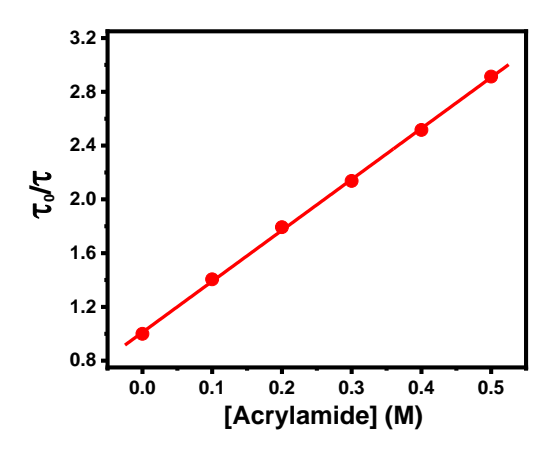


Fig. 3.4. Plot for  $\tau_0/\tau$  versus [Q]. The resolution of the dynamic component involved in acrylamide quenching of intrinsic fluorescence of CIA17 under denatured condition.

The Stern-Volmer plot for both the ionic quenchers (Fig. 3.3C and 3.3E) showed a biphasic curve for the native protein whereas a nearly linear plot was obtained upon denaturation which again suggests that the micro-environment surrounding all the fluorophores is not homogeneous and some of the buried Trp residues become exposed to the solvent upon denaturation. The reduction of the excited state lifetime of fluorophores with increase in quencher concentration (see Table 3.3) implies that the

fluorescence quenching occurs by the involvement of dynamic quenching mechanism for both the ionic quenchers. The Stern-Volmer plots for charged quenchers showed biphasic nature irrespective of the pH (Fig. 3.3C and 3.3E). Tryptophan accessibility to the quenchers ( $f_a$ ) and the corresponding Stern-Volmer constant ( $K_a$ ), determined from the intercept and the slope of the modified Stern-Volmer plots, respectively, are summarized in Table 3.1. The data presented in Table 3.1 clearly shows that in the native protein about ~91, 75 and 45% of the Trp residues are accessible to acrylamide,  $\Gamma$  and  $\Gamma$  cs, respectively. Ligand binding resulted in a significant decrease in the accessible fraction and the extent of quenching for all three quenchers, possibly due to the attainment of more compact structure of the lectin when bound to the ligand or because the ligand blocks the access to the quencher or both. Denaturation of CIA17 enhanced the Trp accessibility to ~100% and 91% to acrylamide and  $\Gamma$  cs. Surprisingly, the accessible fraction decreases to 39.1% towards  $\Gamma$  for the lectin denatured with 4 M GdmSCN. The possible explanation is that unfolding results in negatively charged amino acid residues coming in close proximity of Trp residues.

Acrylamide induced quenching was almost unaltered with change in pH (2.0-8.5). Only marginal variations were observed in the fraction of accessible fluorophores towards both the charged quenchers under slightly basic (pH~ 8.5) and acidic (pH~ 4.0) conditions which results in only a marginal change (within a range of 10%) in the extent in quenching for Γ and Cs<sup>+</sup>. At pH~ 2.0, Trp accessibility increases to~ 82% and 75% for Γ and Cs<sup>+</sup>, respectively and consequently, the extent of quenching increases almost ~1.3 and 1.8-fold respectively for ionic quenchers. The dramatic increase in the tryptophan accessibility as well as large enhancement in the extent of quenching indicate considerable modulation in the local conformation of the protein at pH 2.0 which makes the Trp residues more exposed towards the ionic quenchers.

**Table 3.1.** Extent of fluorescence quenching of CIA17 by different quenchers and different quenching parameters obtained by the analysis of Stern Volmer and modified Stern Volmer plot.

Sample condition	quenching (%)	K <sub>SV1</sub> (M <sup>-1</sup> )	K <sub>SV2</sub> (M <sup>-1</sup> )	f <sub>a</sub> (%)	K <sub>a</sub> (M <sup>-1</sup> )
		Acrylan	nide		
pH 8.5	79.9	8.33	_	91.6	12.3
pH 7.4	79.1	8.25	_	91.4	9.91
pH 4.0	76.0	6.95	_	92.1	7.8
pH 2.0	76.9	7.26	_	88.9	11.8
Chitotetraose	76.6	7.07	_	83.3	13.9
Denatured	88.4	5.86	16.7	~100	5.63
		<b>Iodide</b>	ion		
pH 8.5	60.6	5.1	2.9	68.2	11.5
pH 7.4	62.7	6.7	3.2	75.2	7.4
pH 4.0	67.5	9.2	4.2	75.2	10.5
pH 2.0	78.6	11.1	7.3	82	17.2
Chitotetraose	59.5	6.7	2.4	64.7	18.6
Denatured	36.2	1.3	_	39.1	0.78
		Cesium	ion		
pH 8.5	34.5	1.6	0.61	61.7	1.99
pH 7.4	26.4	0.74	0.51	45.3	1.7
pH 4.0	26.3	0.71	0.47	43.5	0.75
pH 2.0	47.6	2.74	1.82	74.6	3.69
Chitotetraose	12.4	0.66	0.22	19.3	3.64
Denatured	38.4	1.3	_	90.8	1.19

#### 3.4.3. Time-resolved Fluorescence Studies

Fluorescence lifetime decay profiles of CIA17 under various conditions were recorded using an excitation laser source at 285 nm. The decay profiles of Trp fluorescence of the native protein and upon ligand bounding could be best fitted to a biexponential function as shown in Fig. 3.5A. For native CIA17, two lifetime components were obtained as 2.81 ns and 5.02 ns where the two components contribute 61 and 39%, respectively to the total fluorescence intensity. In the presence of 1 mM chitotetraose, two lifetime components 2.7 ns and 5.93 ns were obtained with respective contributions of 62 and 38%.

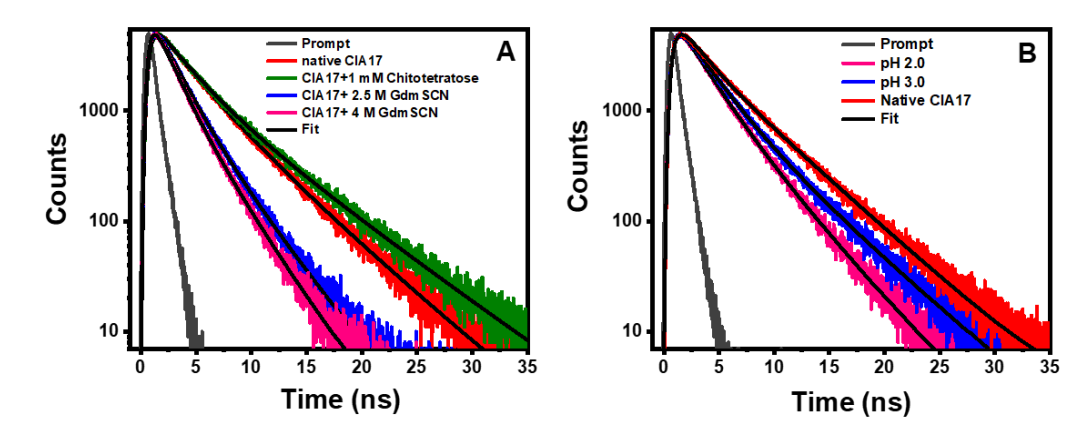


**Fig. 3.5.** Time resolved fluorescence decay profiles of CIA17. (A) Under native and ligand bound conditions as well as in presence of denaturant. (B) at different pH. Color code in the panels indicates different experimental conditions at which the decay was recorded.

The average lifetime  $(\tau)$  of protein fluorescence was calculated using the following equation:

$$\tau = \sum_{i} \alpha_{i} \tau_{i} / \sum_{i} \alpha_{i} \tag{3.11}$$

where i=1, 2, 3 and  $\alpha_i$  is the pre-exponential weighting factor of each lifetime component  $(\tau_i)$ . All the factors  $(\tau_i, \alpha_i, \text{ and } \tau)$  obtained from the decay curve after fitting have been summarized in Table 3.2. The table clearly indicates that the average

fluorescence lifetime of CIA17 slightly increases to 3.93 ns when it binds to chitooligosaccharides as compared to that observed in its native state (~3.67 ns). Analysis of the decay profiles with triexponential function yielded a better fit for the data obtained in the presence of GdmSCN (Fig. 3.4A). In presence of 2.5 M and 4 M GdmSCN, the three lifetime components obtained were: 1.83 ns, 3.59 ns, 0.45 ns, and 1.4 ns, 2.8 ns, 0.30 ns, respectively. The unfolding of the lectin as a function of denaturant concentration is accompanied by the diminution of lifetime of the longer components with the rise of another component with shorter lifetime (32% and 23% for 2.5 M and 4 M GdmSCN, respectively) leading to an overall decrease in average lifetime of the lectin in presence of the chaotropic agent.

**Table 3.2.** Results obtained from time-resolved fluorescence measurements on CIA17 under varying conditions.

Sample	$\alpha_1$	$\tau_1$	$\alpha_2$	$\tau_2$	$\alpha_3$	τ <sub>3</sub>	τ
Native CIA17	0.61	2.81	0.39	5.02	-	-	3.67
pH~ 2.0	0.51	2.22	0.26	3.92	0.23	0.57	2.28
pH~ 3.0	0.51	2.39	0.26	4.77	0.23	0.43	2.55
pH~ 4.0	0.43	2.38	0.34	4.26	0.23	0.56	2.60
pH~ 8.5	0.42	1.47	0.58	4.56	-	-	3.26
+1 mM chitotetraose	0.62	2.7	0.38	5.93	-	-	3.93
+ 2.5 M GdmSCN	0.51	1.83	0.17	3.59	0.32	0.45	1.69
+4.0~M~GdmSCN	0.42	1.4	0.35	2.8	0.23	0.30	1.64

Similar to the results obtained upon chaotrope induced unfolding, decay profiles of the lectin obtained at lower pH (pH  $\leq$  4.0) could be best fitted to a triexponential function (see Fig. 3.4B). At pH 3.0, the average lifetime of the protein decreased to ~2.6

ns which further decreases to  $\sim$ 2.3 ns at pH 2.0. The decrease in average lifetime of the protein is accompanied by an increase in contribution of the shorter component ( $\sim$  0.57 ns) with a concomitant decrease in the lifetime of the longer components (2.81 ns to 2.22 ns, and 5.02 ns to 3.92 ns). Such reduction in the average lifetime of the lectin at low pH again indicates structural and/or conformational change of the protein.

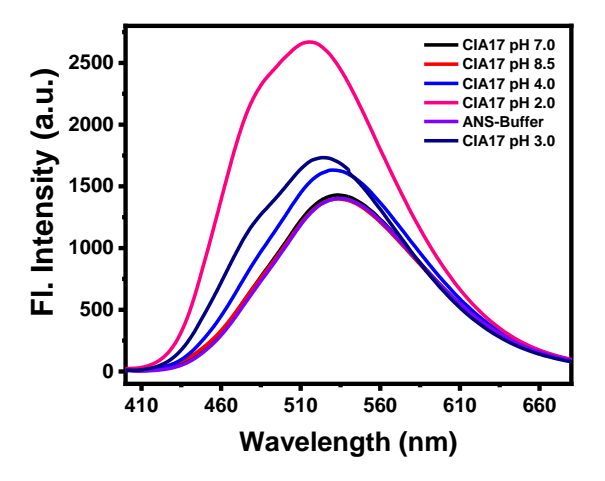
The average lifetime of the native protein as well as under denaturation is reduced in presence of the external quenchers like acrylamide, iodide and cesium ion. The average lifetime of the native protein decreases to 0.99 ns and 1.25 ns in presence of 0.5 M acrylamide and iodide ion respectively whereas in presence of 0.5 M Cesium ion  $\tau$  decreases only to 2.5 ns. The  $\tau$  value of the protein decreased even further to 0.36 ns in presence of 0.5 M acrylamide under denatured condition. The decrease in average lifetime of the protein in presence of all three quenchers indicates the involvement of the collisional quenching process under both the native and denatured condition although static quenching process also contributes in higher concentration of acrylamide for the unfolded protein.

Table.3.3: Results obtained from the time-resolved fluorescence measurements on CIA17 under varying conditions.

Sample	$\alpha_1$	$\tau_1$	$\alpha_2$	$\tau_2$	$\alpha_3$	$\tau_3$	τ
CIA17+0.1 M acrylamide	0.66	2.5	0.34	0.91			1.99
CIA17+0.3 M acrylamide	0.59	1.73	0.41	0.62			1.7
CIA17+0.5 M acrylamide	0.50	1.44	0.50	0.53			0.99
CIA17+0.2 M KI	0.62	2.36	0.38	0.8			1.77
CIA17+ 0.5 M KI	0.51	1.86	0.49	0.63			1.25
CIA17+0.1M CsCl	0.41	1.48	0.59	4.23			3.10
CIA17+0.3 M CsCl	0.43	1.4	0.57	3.94			2.85
CIA17+0.5 M CsCl	0.44	1.37	0.56	3.73			2.69

#### 3.4.4. ANS Fluorescence

Conformational changes induced in CIA17 by varying the pH were further investigated by monitoring the fluorescence emission characteristics of 1-anilinonaphthalene-8-sulphonic acid (ANS), a widely used extrinsic fluorescence probe. ANS binding has been extensively used to characterize changes in the hydrophobicity of a variety of proteins [Kundu et al., 2016; Kumar and Swamy, 2016]. As shown in Fig. 3.6, ANS exhibits relatively weak fluorescence intensity with an emission  $\lambda_{max} \sim 535$  nm in water or aqueous buffer, pH 7.4, which doesn't change in the presence of CIA17 in the pH range of 5.0-8.5. Interestingly, when the pH is decreased to 4.0, 3.0 and 2.0, the fluorescence intensity increases ~1.15, 1.2 and 1.9-fold, with concomitant blue shifts in the emission  $\lambda_{max}$  to 531, 525 and 517 nm, respectively. These observations indicate that CIA17 undergoes distinct conformational changes at low pH, which result in an exposure of hydrophobic regions on the surface of the lectin, which are sensed by ANS.



**Fig. 3.6.** Fluorescence spectra of ANS in the absence and in presence of CIA17 at different pH. Color code in the panel indicates the pH of the protein sample.

# 3.4.5. Size and Conformational Dynamics of CIA17 at Different pH

FCS is a powerful tool to study the size and conformational dynamics of proteins. FCS measures fluctuations in the fluorescence intensity of fluorophore attached to a protein as the protein of nM to pM concentration diffuses in and out of the confocal volume. In this

study, FCS experiments were carried out to investigate the change in size and conformational dynamics of CIA17 at low pH. Fluorescence correlated data for Alexa Fluor 488 carboxylic acid succinimide ester labeled CIA17 (A488-CIA17) under native folded condition (in 20 mM phosphate buffer, pH 7.4) and at low pH ~ 2.0 is shown in Fig. 3.6. The cross-correlation data was better fitted to Eq. (3.9) which includes the contribution of conformational relaxation term along with the simple diffusive component to the fluorescence intensity fluctuation as discussed earlier [Mondal et al., 2021]. The correlation data for free Alexa 488 (A488) was well fitted to the single diffusion model irrespective of pH of the buffer.

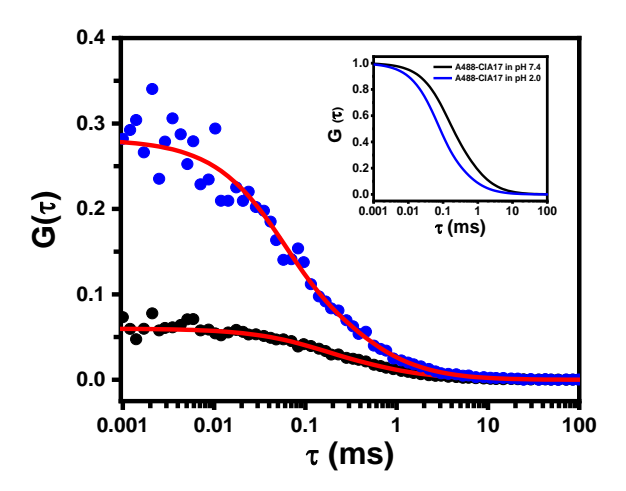


**Fig. 3.6.** Auto-correlation curves of A488-CIA17 conjugate at pH 7.4 and 2.0. Normalized correlation curves of A488-CIA17 conjugate are shown in the inset.

The hydrodynamic radius ( $R_h$ ) of the native protein was estimated as 2.98 (± 0.21) nm from the diffusion time of 25 nM A488-CIA17 which is in good agreement with our previous report that CIA17 exists as a homodimer over the wide concentration range of 5 nM–5  $\mu$ M [Mondal et al., 2021]. At pH ~ 2.0, A488-CIA17 was found to diffuse faster followed by a dramatic decrease in average diffusion time ( $\tau$ <sub>D</sub>) to 194 (± 23)  $\mu$ s from 332 (±21) that was estimated under the native condition and the  $R_h$  value was estimated as

~1.75 ( $\pm$  0.18) nm which is even less than the  $R_h$  value ~2.04 nm predicted for the monomeric protein by the following empirical equation [Wilkins et al., 1999]:

$$R_{h} = 4.75 \ n^{0.29} \ \text{Å} \tag{3.12}$$

Protein unfolding at low pH usually appears through the formation of an extended transition state due to the repulsion between the positively charged residues and is expected to increase the  $\tau_D$  as well as  $R_h$  value. Interestingly, Kundu et al. (2016) reported the formation of a more compact low-pH (at pH~ 1.25) intermediate of MPT63, a major secreted protein from *Mycobacterium tuberculosis*, which diffuses faster as compared to the native state as a result of helical structure accumulation at pH 1.25. CIA17 contains  $\beta$ -sheet predominantly in its secondary structure which remains almost unaltered up to pH - 2.0 as indicated by the far-UV CD spectra. The anomalous behavior of CIA17 at low pH thus can be envisioned as follows: the acid induced unfolding of the homo-dimeric lectin involves the formation of the monomeric molten globule like intermediate state at pH ~2.0 which is significantly contracted in size and diffuse faster. GdmCl induced unfolding also involves the formation of monomeric intermediate at 1-2 M GdmCl concentration which undergoes complete unfolding at 7-7.5 M of GdmCl [Mondal et al., 2021].

**Table 3.3:** Parameters obtained from the FCS measurements (cross correlated data) on CIA17 under varying conditions.

CIA17	$\tau_{\mathrm{D}}\left(\mu \mathrm{s}\right)$	R <sub>h</sub> (nm)	$\tau_{\rm R} \ (\mu  {\rm s})$
At pH 7.4	332 (±21)	2.91(±0.23)	124(±5)
At pH 2.0	194 (±23)	1.75 (±0.18)	55 (±3)
2M GdmCl	412(±19)	$2.07(\pm0.23)$	78 (±13)
7.5M GdmCl	883 (±55)	$3.87(\pm0.23)$	126 (±16)

The  $2^{nd}$  term  $(\tau_R)$  in the correlation function associated with the exponential term which presumably arises from the short- and long-range conformational fluctuations in

the protein structure in microsecond time regime. As shown in Table 3.3, for the native homodimeric protein,  $\tau_R$  is observed as  $124\pm 5~\mu s$  and  $\tau_R$  decreases to 55 ( $\pm 3$ )  $\mu s$  at pH 2.0. The variation of relaxation time ( $\tau_R$ ) was monitored as a function of GdmCl concentration in our previous work [Mondal et al., 2021] and chaotrope-induced denaturation was found to involve dissociation of the dimeric protein into monomers with  $\tau_R \sim 78~(\pm 13)~\mu s$ . The marked difference observed in the  $\tau_D$  and  $\tau_R$  values indicate that the monomeric intermediate formed in the GdmCl induced unfolding is most likely different in shape and size when compared to the low pH molten globule state.

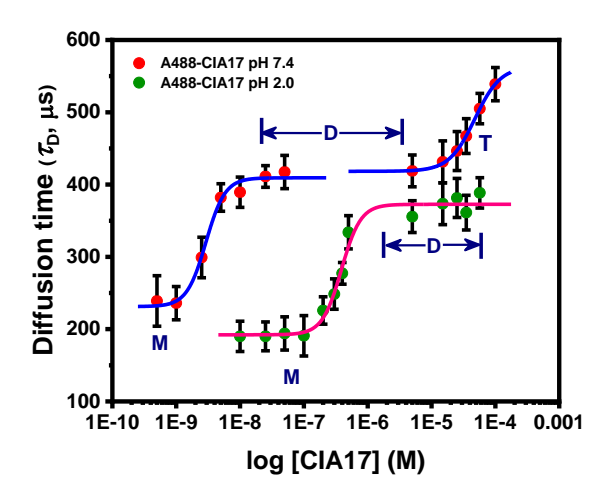
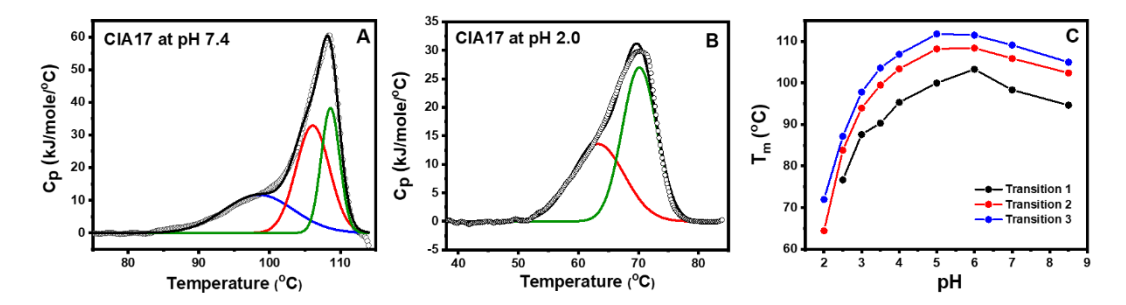


Fig. 3.7. Binding curves showing the equilibrium  $M \leftrightarrow D$  and  $D \leftrightarrow T$  for CIA17 at pH 7.4 and pH 2.0. The change in diffusion time is plotted against logarithm of the total protein concentration.

#### 3.4.6. Concentration Dependent Oligomerization of CIA17 at Molten Globule State

Fig. 3.7 shows a plot of diffusion time as a function of log [CIA17] for the protein at pH 2.0 and we have compared that with the results obtained from measurements performed at pH 7.4, reported in our previous study [Mondal et al., 2021]. At pH 7.4, the plot shows two well-separated regions corresponding to two equilibria with dissociation constants ( $K_D$ ) of 2.92 nM ( $M \leftrightarrow D$  equilibrium) and 47.2  $\mu M$  ( $D \leftrightarrow T$  equilibrium), whereas a single equilibrium was found at pH 2.0 with a  $K_D \sim 387$  ( $\pm 24.4$ ) nM. At pH 2.0 the

diffusion time of A488-CIA17 is almost unchanged over the concentration range of 10-200 nM.  $\tau_D$  was found to increase from 194 to 388  $\mu$ s  $\mu$ m<sup>2</sup>s<sup>-1</sup> when concentration of the unlabeled protein was increased gradually 5  $\mu$ M and remains almost unaltered even at 57  $\mu$ M, indicating that CIA17 exists as a dimer over this concentration range and that it doesn't form higher oligomers beyond dimers even at very high concentration.



**Fig. 3.8.** DSC thermograms of CIA17 (A)at pH 7.4 and (B) pH 2.0. The blue, red and green lines indicate the three individual transitions obtained from the fit, whereas the black line corresponds to the sum of the three individual transitions. (C) Plot of three transition temperature  $(T_m)$  vs pH.

## 3.4.7. Effect of pH on Thermal Unfolding of CIA17

Effect of pH on the thermal unfolding of CIA17 was investigated by recording the DSC thermograms after dialyzing the protein samples against the buffer of desired pH. It was observed that final unfolding temperature ( $T_{\rm m}$ ) shifts from 109 °C to 71 °C when pH of the protein sample is decreased from 7.4 to 2.0 (Fig. 3.8 A, B). The thermogram of native CIA17 consists of three overlapping endothermic components centered at 98.3, 105.9 and 108.6 °C which was assigned to the dissociation of protein oligomers into constituent dimers followed by the dissociation of the dimers into monomers and unfolding of the monomers (Mondal et al., 2021). DSC thermograms for the lectin at pH-2.0 consisted of two overlapping endotherms which could be attributed to the partial dissociation of dimer into monomer followed by the complete unfolding of the monomer. Since, the protein concentration used for each DSC measurements is 25-57  $\mu$ M and the lectin at pH-2.0 exists as a dimer over the concentration range of 400 nM to 57  $\mu$ M as estimated

from the FCS measurements. A plot depicting variation of  $T_{\rm m}$  as a function of change in pH is shown in Fig. 3.8C and transition temperatures obtained by analyzing the thermograms are given in Table 3.4.

Little change of transition temperature from 111.8 °C to 111.5 °C with a negligible change in unfolding enthalpy in the pH range ~5.0 to 6.0 suggested that no protonation or deprotonation occurs upon unfolding in this pH range. The isoelectric point (pI) of CIA17, estimated as ~5.42 from its amino acid sequence [Bobbili et al., 2018a] also suggests that the protein exists mostly as zwitterion around pH 5.0-6.0 and the protein does not lose or gain any proton in this pH range.

**Table 3.4.** Transition temperatures of the different transitions in the thermal unfolding of CIA17 at different pH obtained from differential scanning calorimetry.

pН	$T_{ m m}$	$T_{ m m}$	$T_{ m m}$
	(Transition 1)	(Transition 2)	(Transition 3)
2.0	-	64.4	71.94
2.5	76.67	83.8	87.2
3.0	87.6	93.97	97.82
3.5	90.31	99.5	103.6
4.0	95.33	103.4	106.9
5.0	99.99	108.2	111.8
6.0	103.3	108.4	111.5
7.0	98.32	105.9	108.6
8.0	94.66	102.4	105.0
9.2	91.78	98.28	101.2

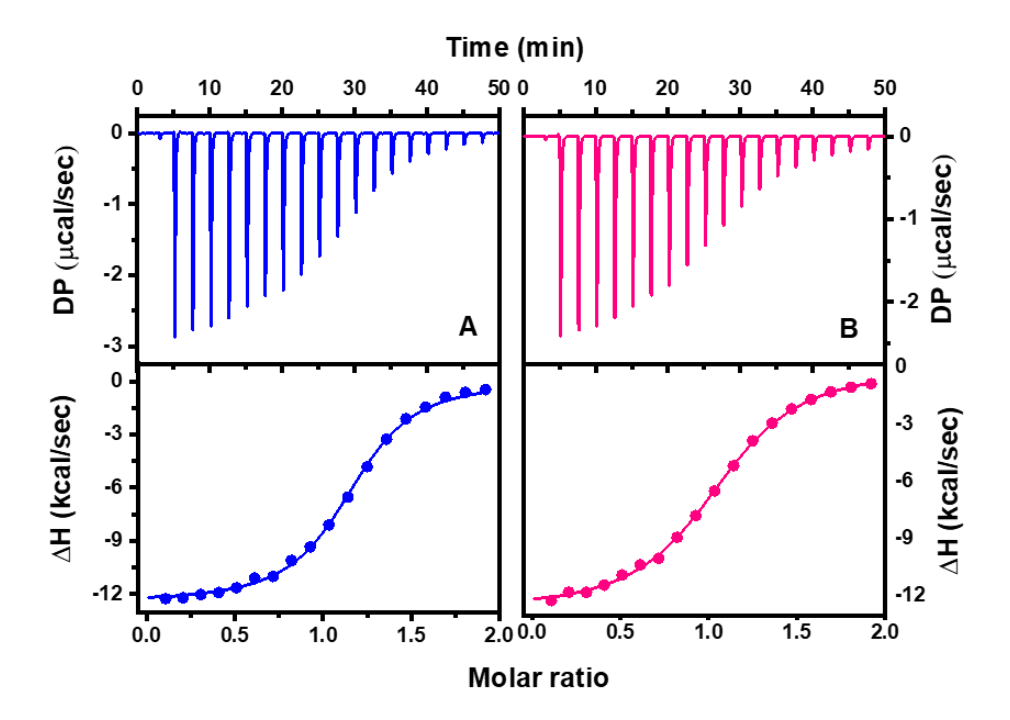


Fig. 3.9. Calorimetric titration of CIA17 with chitotetraose at different pH. (A) CIA17 in phosphate buffer pH ~7.4 and (B) pH~2.0. Upper panels, raw ITC profile obtained from the titration of 114  $\mu$ M of CIA17 against 1.14 mM of chitotetrose. Lower panels, binding isotherm as a function of molar ratio obtained by integrating the peak area from the raw data after correction of the heat of dilution. The solid line indicates the fit to the experimental data. T = 25 °C.

#### 3.4.8. Isothermal Titration Calorimetric Studies

ITC is the most powerful technique to characterize the energetics of molecular interactions, including protein-ligand interactions. Representative ITC profiles for the binding of chitotetraose to CIA17 at pH 7.4 and pH 2.0 are shown in Fig. 3.9A and B, respectively. In the upper panels, the individual peak corresponds to the exothermic heat released for the interaction at each injection of the ligand and the lower panel shows the plot of incremental heat liberated as a function of chitotetraose to the protein molar ratio. The solid line in the lower panel shows a non-linear-least squares fit of the data to 'one

set of sites' binding model. Various thermodynamic parameters associated with the binding obtained from the fit have been summarized in Table 3.5.

**Table 3.5.** Association constants and thermodynamic parameters derived obtained for chitotetraose binding of CIA17 at different pH obtained from ITC experiment.

pН	n	$K_{\rm a} \times 10^{-5}$	$-\Delta G^0$	-ΔH <sup>0</sup>	$-\Delta S^0$
		( M <sup>-1</sup> )	(kcal/mol)	(kcal/mol)	(cal.mol <sup>-1</sup> . K <sup>-1</sup> )
7.4	1.14 (±0.053)	3.15	7.5	12.5 (±0.081)	16.64 (±0.081)
2.0	0.995 (±0.014)	1.34	7	12.4 (±0.157)	18.09 (±0.081)

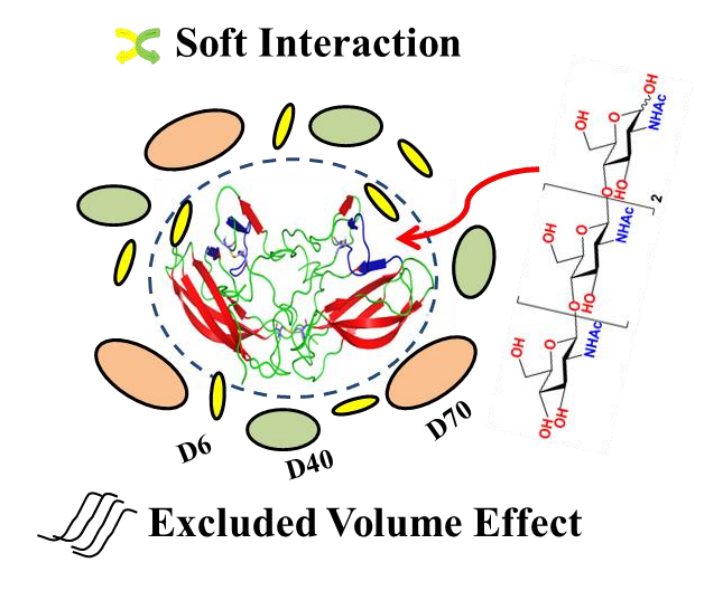
CIA17 under native condition (pH 7.4) binds to chitotetraose with an association constant of  $3.15 \times 10^5 \, \text{M}^{-1}$ . The association constants obtained for the lectin at pH ~ 2.0 was  $1.34 \times 10^5 \, \text{M}^{-1}$  with a stoichiometry (n) for the chitotetraose-CIA17 interaction close to unity for the intermediate. The binding enthalpy and entropy at pH 2.0 was almost similar to that of the native protein. The results suggested that CIA17 retains almost 80% of the lectin activity of the native protein in the molten globule like state irrespective of the structural or conformational change of the protein at low Ph (pH - 2.0).

## 3.5. Conclusions

In the present work, we investigated the pH induced changes in the conformation, structural dynamics as well as carbohydrate-binding activity of CIA17. The secondary structure of CIA17 remains almost unaltered over a wide pH range (8.5-2.0) while the tertiary structure of the protein was modulated significantly. The large enhancement in Trp accessibility towards the external charged quenchers under such acidic condition indicated that the low pH perturbed the the local conformation near the Trp residues considerably. Results of fluorescence correlation spectroscopic (FCS) studies indicate that the lectin at pH 2.0 exists as a monomer over the concentration range of 10 nM-200 nM and forms dimers at higher concentrations ( $K_D \approx 387$  nM) but couldn't form higher oligomer even high concentrations ( $\sim 57$   $\mu$ M) unlike the native protein (at pH 7.4). The

 $T_{\rm m}$  of the main unfolding transition is pH dependent, and decreases from 109 °C to 72 °C as the pH decreases from 7.4 to 2.0. Interestingly, unlike the native protein (at pH 7.4), the unfolding of the pH 2.0 intermediate occurs in a three steps process: homo-dimeric lectin dissociates into monomeric molten globule like state followed by the complete unfolding of the monomers. The results obtained indicated that CIA17 exists as a monomeric molten globule like state at pH - 2.0 which retains almost 80% of the lectin activity of the native protein irrespective of the change in structure and conformation of the lectin.

# Macromolecular Crowding Significantly Affects the Conformational Features and Carbohydrate Binding Properties of CIA17, a PP2-type Lectin from Coccinia indica



**Saradamoni Mondal,** Somnath Das, Musti J. Swamy\*

Manuscript submitted for publication

## 4.1. Summary

The effect of macromolecular crowding on the conformational features and carbohydrate binding properties of CIA17, a PP2-type lectin, was investigated employing polymeric dextrans D6, D40 and D70 (M<sub>r</sub> ~6, 40 and 70 kDa, respectively) as crowding agents. While the secondary structure of CIA17 was significantly affected by D6, only marginal changes were induced by D40 and D70. While addition of larger dextrans, D70 and D40 induced modest quenching (~10%) of the protein fluorescence by a static pathway, a high degree of quenching (37%) was induced by D6 and involved both static and collisional quenching processes. Association constant for the CIA17-chitooligosacciaride interaction increased by 33% and 260% in the presence of D40 and D70, whereas it decreased by 33% in presence of D6. The higher binding affinity can be attributed to excluded volume effect, i.e., increased effective concentration of the protein in presence of D40 and D70, whereas D6 being smaller, possibly penetrates into the protein interior, disrupting water structure around the protein and also inducing conformational changes, resulting in weaker binding. These observations demonstrate that molecular crowding significantly affects the carbohydrate binding characteristics of lectins, which can modulate their physiological function.

#### 4.2. Introduction

Living cells typically contain approximately 60% water by weight, whereas macromolecules such as proteins, nucleic acids and polysaccharides constitute the remaining 40%. This limits the free space available for other biomolecules, resulting in the 'excluded volume effect' that increases the effective concentrations of macromolecules, which in turn increases their chemical activity and alters the rates and equilibrium constants of reactions [Minton, 2001; Ellis, 2001; Zhou et al., 2008]. Crowding also affects the density, viscosity and dielectric properties of the medium [Puchkov, 2013; Rajendran et al., 2010; Zimmerman and Minton, 1993]. The restricted and crowded environment in the cytoplasm modulates biochemical and biophysical processes in the intracellular milieu [Zhou et al., 2008; Zimmerman and Minton, 1993]. To mimic the 'crowded' cell environment, laboratory experiments are usually modified by adding high concentrations of crowding agents (synthetic polymers/proteins). Extensive experimental and theoretical studies have been carried out to investigate the effect of molecular crowding on the structure, stability, dynamics, folding-unfolding pathways as well as enzymatic activity of proteins [Charlton et al., 2008; Cheung et al., 2005; Christiansen et al., 2010; Dhara et al., 2010; Hong and Gierasch, 2010; Kim and Yethiraj, 2011; Moran-Zorzano et al., 2007; Samiotakis et al., 2009; Sasaki et al., 2007; Stagg et al., 2007; Zhou et al., 2008]. While in most cases macromolecular crowding shifts the protein structure towards a more compact state which could be explained on the basis of excluded volume effect, some recent studies suggest that the crowded environment may lead to both stabilization and destabilization of the native protein structure, possibly due to non-specific soft interactions [Inomata et al., 2009; Malik et al., 2012; Senske et al., 2014]. For example, while synthetic crowders such as poly vinyl pyrrolidines (PVPs) and Ficoll 70 were reported to stabilize chimotrypsin inhibitor 2 (CI2) against thermal and chemical denaturation, protein crowders such as E. coli cytoplasm, lysozyme or bovine serum albumin destabilized CI2 to different extents [Benton et al., 2012; Miklos et al., 2010, 2011]. While the excluded volume effect is always stabilizing, the nonspecific chemical interactions between crowders and the target

protein can be either stabilizing or destabilizing [Das and Sen, 2018; Sarkar et al., 2013a, b].

Although, as can be gleaned from the above cited studies, the effect of molecular crowding on a variety of proteins has been investigated, the structure, conformation and activity of lectins, the non-enzymatic carbohydrate binding proteins in the crowded environment still remain unexplored. Lectins, a unique class of ubiquitous carbohydrate binding proteins of non-immune origin, are found in various kinds of living organisms such as plants, animals, microbes and fungi [Sharon and Lis, 1972, 2004]. Lectins are structurally quite diverse and are involved in numerous biological processes. In plants, lectins are present in different parts including seeds, bark, leaves, roots/tubers, latex as well as the phloem exudate and these have been extensively studied [Lis and Sharon, 2003; Van Damme et al., 1998]. Phloem is the major integral component of the whole plant communication system by which photo-assimilates and other vital nutrients are transported over long distances [Kehr, 2006; Oparka and Cruz 2000; Thompson and Schulz, 1999]. In the phloem exudate, phloem protein 2 (PP2) is the most abundant protein and exhibits lectin activity. The PP2 proteins also play a major role in long distance trafficking of nutrients, wound sealing and anti-pathogenic responses. They also form ribonucleoprotein (RNP) complexes by interacting with different RNA molecules and transport them from cell to cell [Dinant et al., 2003; Gómez and Pallás, 2004; Owens et al., 2001; Pallás and Gómez, 2013; Read and Northcote, 1983; Will and Van Bel, 2006;].

Coccinia indica agglutinin (CIA17), a PP2-type chitooligosachaide-specific lectin, is a major protein in the phloem exudate of Coccinia indica fruits [Bobbili et al., 2018a]. The work reported in chapters 2 and 3 and previous work from this lab have shown that CIA17 exists as a homo-dimer at an intermediate concentration and forms oligomeric and filamentous structures at higher concentrations under native conditions at neutral pH whereas at lower pH further association of the dimeric protein to form larger oligomers is not observed [Bobbili et al., 2019; Mondal et al., 2021]. In previous work, we also reported detailed investigations on the primary and secondary structure, thermal and chemical unfolding as well as thermodynamics of chitooligosaccharide binding to

CIA17 in aqueous buffer [Bobbili et al., 2018a; Bobbili et al., 2019; Mondal et al., 2021]. In the present study, we investigated the effect of macromolecular crowding on the structure and conformation of this lectin using CD spectroscopy, as well as various fluorescence spectroscopic techniques, viz., steady-state and time-resolved fluorescence spectroscopy and fluorescence quenching by neutral and charged quenchers. Finally, the effect of molecular crowding on the association constants and thermodynamic parameters governing carbohydrate binding was assessed by isothermal titration calorimetry.

#### 4.3. Materials and Methods

#### 4.3.1. Materials

Unripe ivy gourd (*Coccinia indica*) fruits were purchased from local vendors.  $\alpha$ -chitin,  $\beta$ -chitin, chitooligosaccharides, ammonium persulphate, acrylamide, potassium iodide, dextran 70 (D70), dextran 40 (D40) and dextran (D6) were purchased from Sigma (St. Louis, MO, USA). All other chemicals and reagents were procured from local suppliers and were of the highest purity available.

CIA17 was purified from the phloem exudate of unripe ivy gourd by sequential affinity chromatography on  $\alpha$ -chitin followed by  $\beta$ -chitin as described in chapter 2 and 3.

## 4.3.2. Circular Dichroism (CD) Spectroscopy

CD spectroscopic measurements were carried out on a Jasco J-810 spectropolarimeter (Jasco Corporation, Tokyo, Japan). CIA17 samples of 1.57  $\mu$ M monomer concentration were used for measurements in the far-UV (250-200 nm) region. A rectangular quartz cuvette of 0.1 cm path-length was used for all measurements. CD spectra of the lectin were recorded in the absence and presence of different crowding agents (D70, D40 and D6) at varying concentration (0-200 mg/mL). All spectra reported are averages of 7 successive scans recorded at a scan rate of 50 nm/min. Spectral data were collected at 1 nm intervals.

## 4.3.3. Steady-state Fluorescence Spectroscopy

Fluorescence emission spectra were recorded on a Jasco FP-8500 fluorescence spectrometer. CIA17 samples ( $OD_{280} < 0.1$ ) in the absence and presence of crowding agents at different concentrations (0-200 mg/mL) were irradiated at 295 nm to excite tryptophan residues selectively and emission spectra were recorded in the wavelength range of 300-400 nm.

Acrylamide, a neutral quencher and iodide, a charged quencher were used in the fluorescence quenching studies with CIA17 in the native state and upon incubation with various concentrations (50-200 mg/mL) of the crowding agents essentially as described in chapter 3.

#### 4.3.4. Time-resolved Fluorescence Measurements

Fluorescence lifetime was measured on a time correlated single photon counting (TCSPC) spectrometer from Horiba Jobin Yvon IBH (Glasgow, UK) equipped with a delta diode laser source and a thermocube chiller as described previously in chapter 3. Samples of CIA17 ( $OD_{280} \sim 0.07$ ) were excited at 285 nm and the decay was monitored at the emission maxima for the native and denatured protein in the absence and presence of crowding agents at different concentrations (100 and 200 mg/mL).

## 4.3.5. Isothermal Titration Calorimetry

Calorimetric titrations were carried out at 25 °C on a PEAQ-ITC instrument (Malvern Instruments Ltd., UK) essentially as described in chapter 3. CIA17 samples of concentration 75-100 µM (protomer) were taken in the sample cell and titrations were carried out by injecting 2.0 µL of chitotetraose (GlcNAc)<sub>3</sub> at a concentration of 1-1.2 mM. To investigate the protein-carbohydrate interaction under different crowded environments, protein and ligand solutions containing varying concentrations of the three crowders (50 and 100 mg/mL) were used. A 10-minute interval was given between successive injections in order to ensure that equilibrium is attained before the next aliquot is added. During the titration the sample in the calorimeter cell was stirred at 750 rpm. Blank titrations were also performed by injecting aliquots of the ligand solution into

the buffer (or buffer containing crowder); these injections yielded insignificant heats of dilution.

#### 4.4. Results and Discussion

## 4.4.1. CD Spectroscopic Studies

Far-UV CD spectra of CIA17 recorded in the absence and presence of varying concentrations of D40, D70 and D6 are shown in Fig. 4.1. The spectrum of native CIA17 with a broad negative band centered at  $\sim$  216 nm is consistent with a predominance of  $\beta$ -sheets in its secondary structure as reported earlier [Bobbili et al., 2018a]. Addition of D40 and D70 led to only minor changes in the far-UV CD spectra of the protein, indicating that these two dextrans induce only moderate changes in the secondary structure of the protein. Addition of D6, on the other hand, resulted in considerably larger changes in the CD spectra and the magnitude of these changes increased with increase in the concentration of the crowder, indicating that addition of D6 significantly altered the secondary structure of the protein.

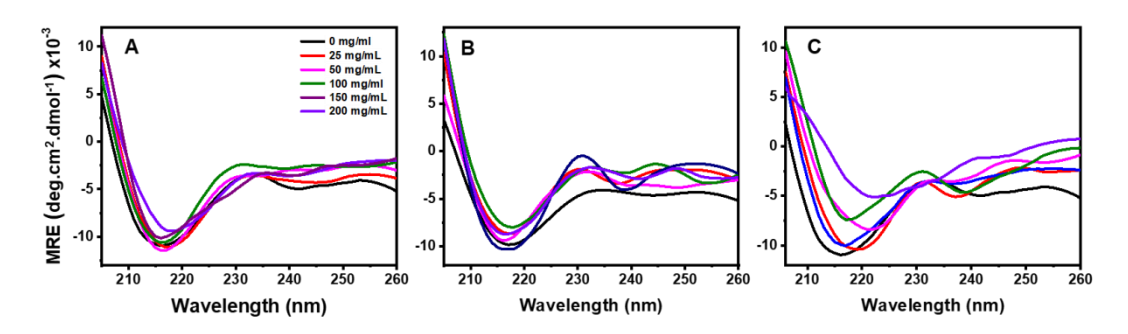


**Fig. 4.1.** CD spectra of CIA17 recorded in the absence and presence of different crowders. The crowders used are: (A) D40, (B) D70 and (C) D6. Color code in panel A indicates the specific concentration of crowder at which each spectrum was recorded (for all three panels).

# 4.4.2. Steady-state Fluorescence Spectroscopy

CIA17 has nine tryptophan residues and exhibits an emission maximum ( $\lambda_{max}$ ) at ~ 339 nm under native condition indicating that on an average the Trp residues exist in a

partially buried state, although the degree of exposure of individual Trp residues is likely to be different.

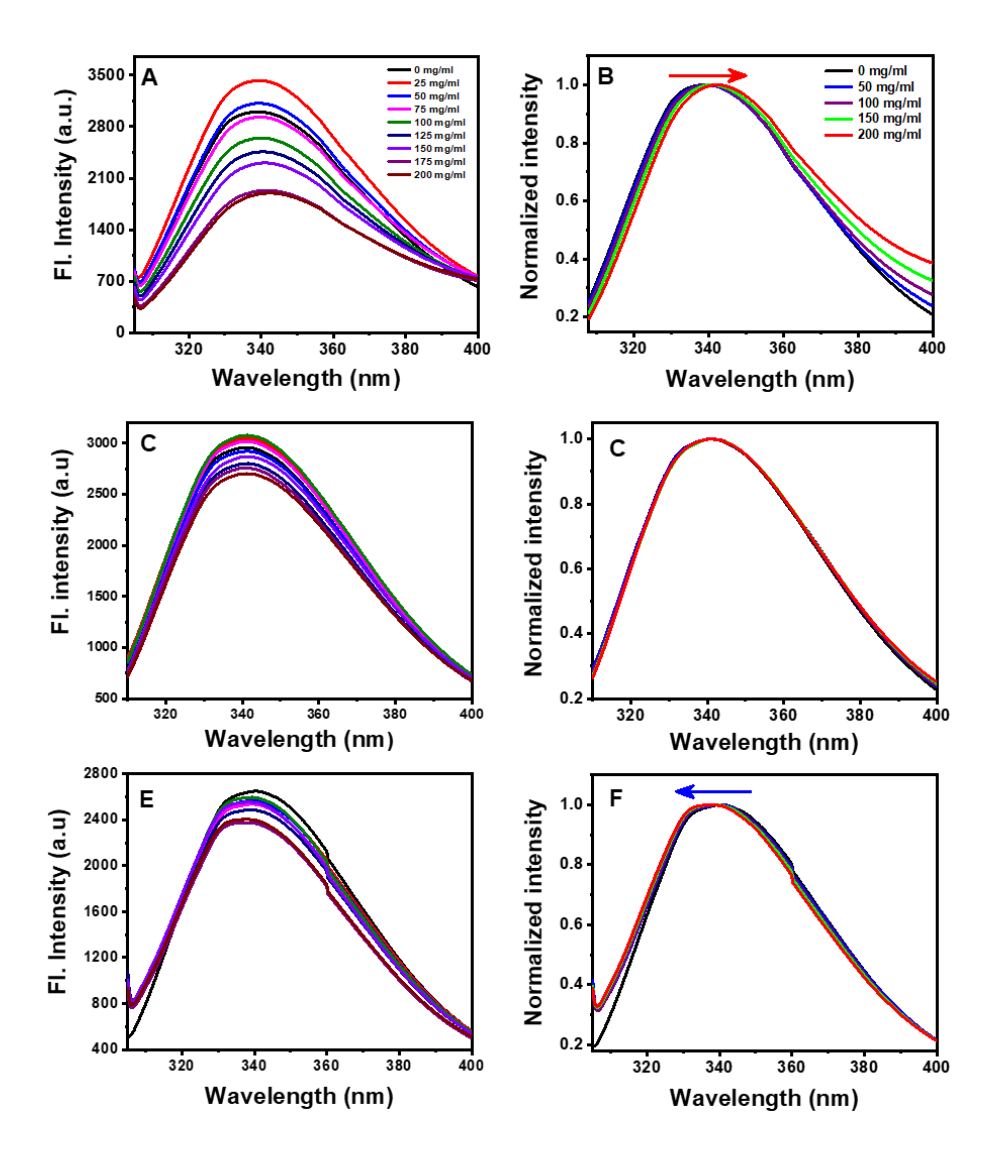


**Fig. 4.2.** (A, C, E) Fluorescence emission spectra and (B, D, F) normalized emission spectra of CIA17 in the absence and presence of (A, B) D6, (C, D) D40 and (E, F) D70 at different concentrations.

In order to investigate the effect of molecular crowding on the tertiary structure of the lectin, the Trp fluorescence of the native protein was monitored as a function of the concentration of different crowding agents. The fluorescence emission spectra obtained in the presence of increasing concentrations of D6, D40 and D70 are shown in Fig. 4.2. Careful observation of spectra clearly indicated that increasing the concentration of all three dextrans leads to a decrease in the fluorescence intensity of the protein, but to varying degrees in each case. While the addition of 200 mg/mL D6 led high quenching (37%), the extent of quenching observed at the same concentration of D40 (12%) and D70 (10%) was considerably lower. Further, addition of D6 also induced ~4 nm red shift in the emission maximum ( $\lambda_{max}$ ) whereas addition of D40 did not induce any shift in the  $\lambda_{max}$  while addition of D70 led to a ~2 nm blue shift. These observations suggest that the presence of various crowders brings about distinct changes in the microenvironment of the Trp residues to different extents.

# 4.4.3. Time-resolved Fluorescence Spectroscopy

In order to gain further insights into the mechanism of the crowder-induced quenching of protein intrinsic fluorescence, the fluorescence decay profiles of CIA17 were recorded in the absence and presence of crowders and the results obtained are shown in Fig. 4.3. The decay curve for the native protein alone could be best fitted to a bi-exponential function with lifetime components of 2.04 ns and 4.76 ns, which contribute 39 and 61%, respectively, to the total fluorescence intensity. The average lifetime of the protein fluorescence was calculated by using the following equation:

$$\tau = \sum_{i} \alpha_{i} \tau_{i} / \sum_{i} \alpha_{i} \tag{4.1}$$

where  $i=1,\,2,\,3$  and  $\alpha_i$  is the pre-exponential weighting factor of each lifetime component  $(\tau_i)$  and  $\tau$  is the amplitude average lifetime. Values of all these parameters  $(\tau_i, \alpha_i, \text{ and } \tau)$  obtained from the multi-exponential fits have been summarized in Table 4.1. The average lifetime of CIA17 (3.69 ns) was almost unaltered in presence of D40 (3.67 ns) and D70 (3.65 ns) even at very high concentration ~200 mg/mL (as shown in Fig. 4.3), suggesting that the influence of dynamic quenching is negligible and the quenching process occurs mostly through the static pathway. In contrast,  $\tau$  value decreases to 2.78

ns in the presence of 100 mg/mL of D6 which further decreases to 2.44 ns at 200 mg/mL of D6. Fitting to a triexponential function yielded a better fit for the lectin in the presence of D6, and the three lifetime components obtained are: 2.6 ns, 5.57 ns and 0.43 ns (at 100 mg/mL), and 2.46 ns, 5.71 ns, and 0.43 ns (at 200 mg/mL). These results clearly indicate that the decrease in average fluorescence lifetime of the lectin in the presence of D6 is accompanied by the diminution of lifetime of the longer components with the rise of another shorter lifetime component (0.43 ns), implying the involvement of dynamic pathway.

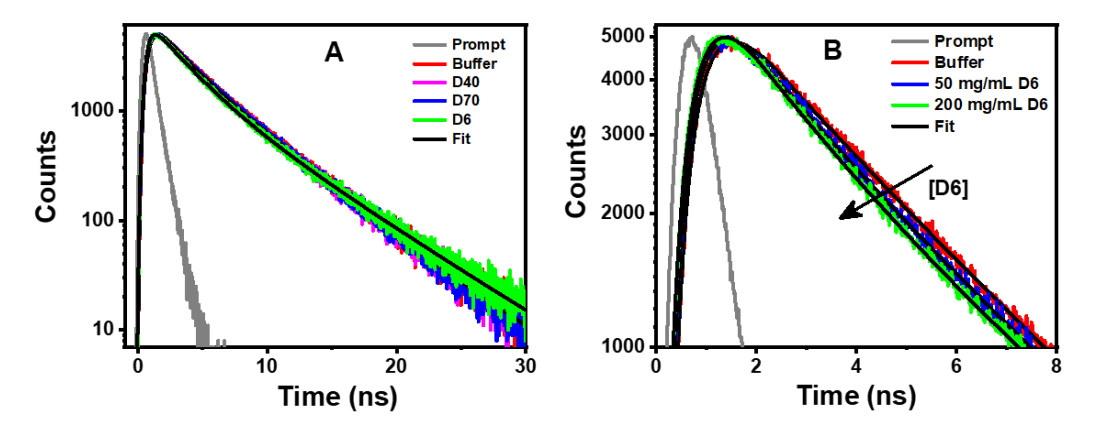


**Fig. 4.3.** Time resolved fluorescence decay profiles of CIA17 in the absence and presence of crowders. (A) In the presence of 200 mg/mL D6, D40 and D70. (B) A zoomed-in view of the decay profile at different concentrations of D6. Color code in the panels indicates different crowded environments at which the fluorescence decay was recorded.

Quenching of the intrinsic fluorescence of CIA17 induced by D40 and D70 appears to follow a predominantly static pathway by the ground state complex formation between the indole side chains of Trp residues and neighboring amino acid residues in the immediate vicinity, which becomes more facile under crowded environment where the protein experiences excluded volume effect that leads to even closer approach of the amino acid residues in close proximity, resulting in increased quenching of the Trp fluorescence. Interestingly, quenching induced by D6 appears to involve both

collisional/dynamic and static mechanisms. These observations can be envisioned as follows: D6 being smaller in size, can partially penetrate into the interior of the protein, resulting in its closer approach to the Trp residues leading to collisional quenching in addition to static quenching as explained above. D40 and D70 are larger than the protein and hence face steric hindrance while approaching the protein interior for accessing the Trp residues and hence cannot quench the protein fluorescence by the collisional mechanism.

**Table 4.1.** Results obtained from the time-resolved fluorescence measurements on CIA17 under varying conditions.

Sample (Condition)	$\alpha_1$	$\tau_1$	$\alpha_2$	$\tau_2$	$\alpha_3$	$\tau_3$	τ
Native CIA17	0.39	2.04	0.61	4.76	-	-	3.67
+D40 (100 mg/mL)	0.39	2.12	0.61	4.75	-	-	3.72
+D40 (200 mg/mL)	0.43	2.12	0.57	4.81	-	-	3.65
+D70 (100 mg/mL)	0.42	2.17	0.58	4.77	-	-	3.68
+D70 (200 mg/mL)	0.43	2.11	0.57	4.77	-	-	3.63
+D6 (100 (mg/mL)	0.42	2.6	0.28	5.57	0.30	0.43	2.78
+D6 (200 (mg/mL)	0.39	2.46	0.23	5.71	0.38	0.43	2.44

Our time resolved fluorescence data is quite interesting to interpret the quenching of the protein fluorescence in presence of crowding agents as it is the first report of the involvement of collision between Trp residues of the protein and the crowder molecules. Previous studies have shown that macromolecular crowders induce appreciable quenching of the tryptophan fluorescence in proteins such as lysozyme, human serum albumin (HSA) and bovine serum albumin (BSA) by static mechanism [Singh and Chowdhury, 2013, 2017]. Although for all these proteins, similar to CIA17, the more pronounced effect was seen in the presence of D6, major differences were observed in the extent of quenching. In addition, differences were also observed in the quenching profiles, with linear Stern-Volmer plots obtained for both the serum albumins, whereas an upward curvature was seen in the quenching profile for lysozyme (which was

explained by the *sphere of action* model). This heterogeneity observed in the conformational modulations of different proteins by D6 strongly indicates that the effect of the crowding agents on the protein structure is obvious but depends considerably on the nature of the biomolecules under investigation.

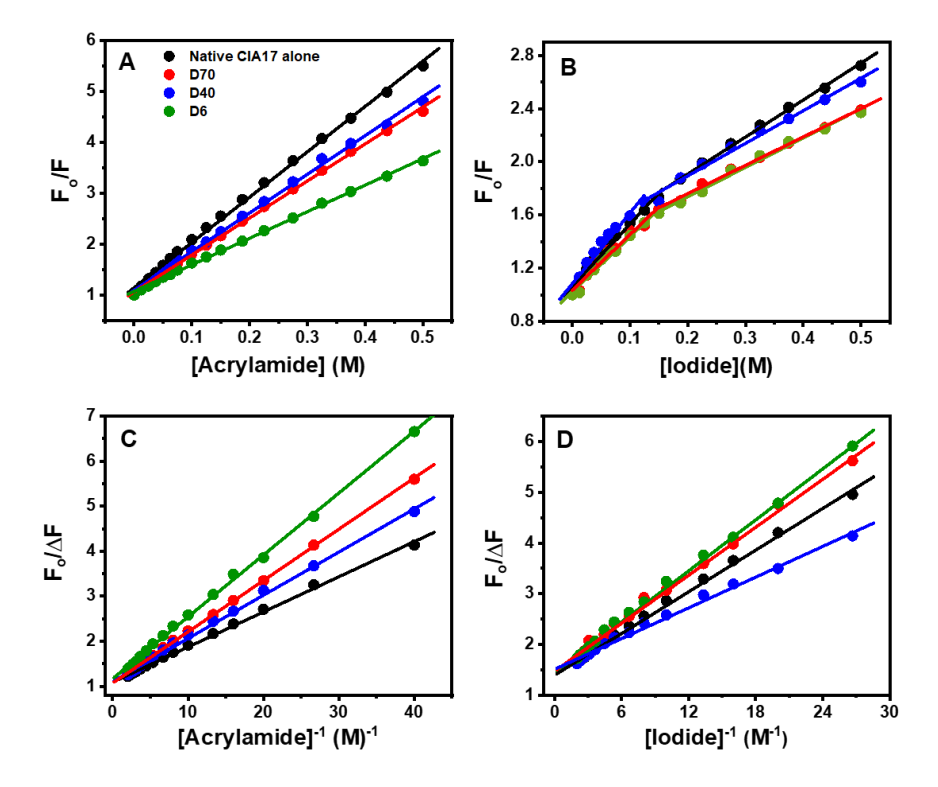


**Fig. 4.4.** Stern-Volmer (A, B) and modified Stern-Volmer (C, D) plots for the fluorescence quenching of CIA17 by neutral and ionic quenchers in the absence and presence of crowding agents at 100 mg/mL. (A, C) Acrylamide and (B, D) Iodide ion. Color code in A indicates the crowding agents used in all the quenching experiments.

## 4.4.4. Tryptophan Fluorescence Quenching by Neutral and Ionic Quenchers

Crowder-induced changes in the protein conformation, assessed from the changes observed in the protein intrinsic fluorescence (due to the indole side chains of Trp residues), have been discussed in the above section. Perturbations in the protein structure were further investigated by measuring the Trp accessibility towards external

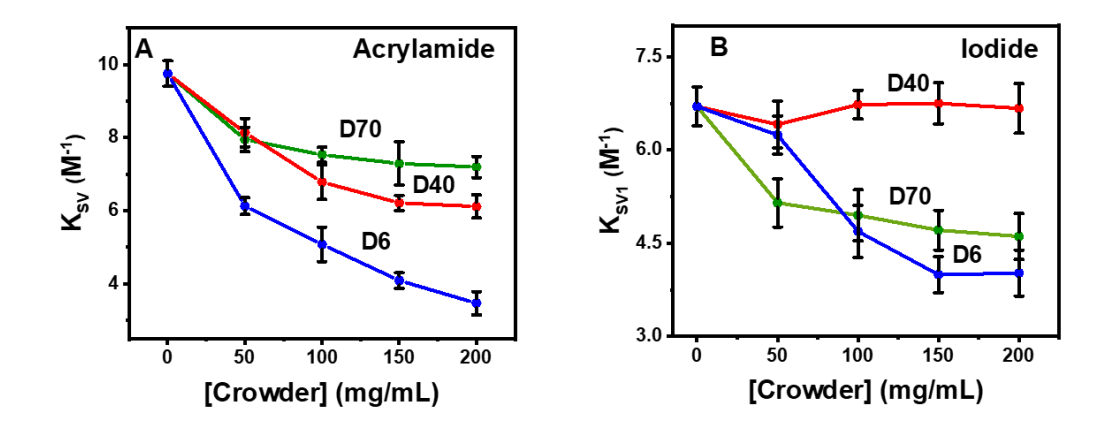
quenchers such as acrylamide and iodide ion under such crowded environment. Acrylamide, being a neutral polar molecule, can penetrate into the hydrophobic interior of proteins. Hence it can access both surface-located as well as buried Trp residues, whereas iodide ion, being a charged species, has a lower accessibility to the Trp residues that are located in the hydrophobic core of the protein and mostly gives insight about the residues on the surface.

**Table 4.2.** Results of steady-state quenching of CIA17 obtained in the absence and presence of different crowders. Crowder concentration in each case was 100 mg/mL. The final quencher concentration used in each case was 0.5 M.

Sample (condition)	Quenching (%)	K <sub>SV1</sub> (M <sup>-1</sup> )	K <sub>SV2</sub> (M <sup>-1</sup> )	f <sub>a</sub> (%)	K <sub>a</sub> (M <sup>-1</sup> )					
Acrylamide										
NativeCIA17	80.9	9.75	-	91.4	14.0					
+ <b>D70</b>	78.0	7.53	-	90.0	11.6					
+ <b>D40</b>	75.2	6.78	-	91.2	10.0					
+ <b>D</b> 6	67.0	5.08	-	87.0	8.1					
		Iodide								
Native CIA17	62.7	6.70	3.20	75.2	5.9					
+ <b>D70</b>	57.5	4.95	2.54	67.6	9.3					
+ <b>D40</b>	62.0	6.73	2.87	65.0	15.9					
+ <b>D</b> 6	57.7	4.69	2.59	69.0	8.5					

Stern-Volmer and modified Stern-Volmer plots for the quenching by acrylamide are shown in Fig. 4.4A for CIA17 in the native state and in the presence of 100 mg/mL concentration of D6, D40 and D70. All Stern-Volmer plots for quenching by acrylamide are linear. At 0.5 M concentration, acrylamide quenches ~81% of the Trp fluorescence of native CIA17 with a  $K_{SV}$  value ~ 9.75  $M^{-1}$ . Although similar linear trend was observed

in the Stern-Volmer plots even in the presence of crowding agents, the extent of quenching as well as the K<sub>SV</sub> values decreased with increase in crowder concentration for all three crowders (see Fig. 4.5A), suggesting that the protein structure becomes more compact under crowded environment, which results in a decrease in the accessibility of the Trp residues to acrylamide. Interestingly, the Stern-Volmer plots for iodide ion quenching of the native protein alone and in presence of different crowding agents were biphasic (see Fig. 4.4B), indicating that the charged iodide ion is able to distinguish between Trp residues that are surface exposed and those that are buried in the hydrophobic core of the protein. At 0.5 M concentration, iodide ion quenches 62.7% of the intrinsic fluorescence of native CIA17. The degree of quenching remains almost unaltered for iodide ion in presence of D40 even at 200 mg/mL, while the extent of quenching as well as K<sub>SV</sub> values decreased gradually with increase in concentration for both D70 and D6 (Fig. 4.5B), indicating that both the exposed and buried Trp residues become less accessible in the 'compact conformation' of the protein induced by D70 and D6.



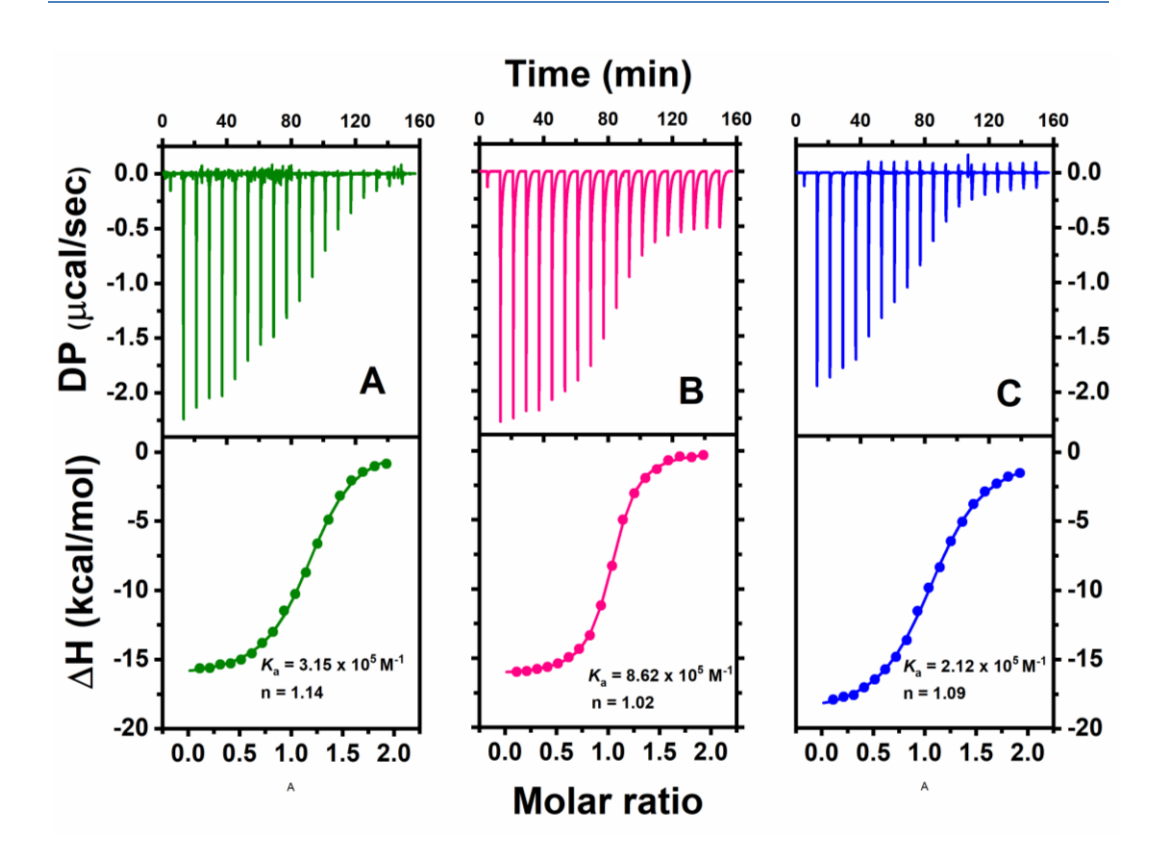
**Fig. 4.5.** Plot of  $K_{SV}$  as a function of crowder concentration for intrinsic fluorescence quenching of CIA17 by (A) acrylamide and (B) iodide ion.

Table 4.2 clearly indicated that quenching by both acrylamide and iodide was lowest in presence of D6 among the three crowders employed. This observation is contrary to what is expected since quenching process is diffusion controlled and the bulk

viscosity of the dextran solutions at any given concentration (mg/mL) follows the order  $\eta_{D70} > \eta_{D40} > \eta_{D6}$  [Singh and Chowdhury, 2013]. The anomaly can be explained as follows: (i) having the lowest molecular weight among the three crowders, D6 contains the highest molar concentration at a fixed wt% value (e.g., 200 mg/mL). Therefore, it exerts maximum excluded volume effect, due to which the protein adopts a more compact structure resulting in a decreased accessibility of the Trp residues to the quencher, and (ii) D6 molecules partially penetrate the protein matrix and hinder the external quencher from approaching the Trp residues, which in turn reduces the collisional quenching of the Trp fluorescence.

#### 4.4.5. Isothermal Titration Calorimetric Studies

ITC is a highly powerful method, which allows a detailed characterization of the energetics of molecular interactions and has been widely used for investigating lectincarbohydrate interactions [Bobbili et al., 2019; Dam and Brewer, 2002; Nareddy et al., 2017; Sultan and Swamy, 2005; Surolia et al., 1996]. In this study, the association constant and thermodynamic parameters associated with the binding of chitotetraose to CIA17 in buffer alone and in the presence various crowders, namely D6, D40 and D70 were investigated by ITC measurements. Three representative calorimetric titrations for the binding of chitotetraose to CIA17 are shown in Fig. 6A-C. The profiles shown in these figures correspond to titrations performed in the absence of any crowder, and in the presence of 100 mg/mL concentrations of D70 and D6. In each figure, the upper panel shows the raw ITC data where the individual peak corresponds to the heat liberated after each injection of the ligand to the protein and the lower panel represents the incremental heats released as a function of chitotetraose/protomer molar ratio. The non-linear least squares data was fit (shown as solid line) to the 'one set of sites' model using the in-built analysis software. The thermodynamic parameters and binding constants associated with the ligand binding obtained from this analysis are presented in Table 4.3.



**Fig. 4.6.** Calorimetric titration of CIA17 with chitotetraose in the absence and presences of different crowders. (A) CIA17 in phosphate buffer, pH  $\sim$ 7.0, (B) in presence of 100 mg/mL D70, and (C) in presence of 100 mg/mL D6. Upper panels; raw ITC profiles obtained from the titration of 114  $\mu$ M CIA17 with 1.14 mM chitotetraose. Lower panels; binding isotherms as a function of molar ratio obtained by integrating the peak area from the raw data after correction of the heat of dilution. Solid lines indicate the fits of the experimental data to 'one set of sites' binding model. T = 25°C.

The binding stoichiometry of the chitotetraose-CIA17 interaction was found to be close to unity with respect to the protein monomer for titrations carried out in the absence as well as in the presence of different crowding agents. CIA17 under native conditions in phosphate buffer (pH  $\sim$  7.0) binds to chitotetraose in phosphate buffer with an association constant of  $3.15 \times 10^5$  M<sup>-1</sup>. The binding strength increases to  $4.13 \times 10^5$  M

 $^{1}$  in the presence of D40 (~33% higher), and to 8.67  $\times$  10 $^{5}$  M $^{-1}$  in presence of D70 (~260% higher), but decreases to  $2.12 \times 10^{5}$  M $^{-1}$  (~33% decrease) in the presence of D6.

**Table 4.3.** Association constants ( $K_a$ ) and thermodynamics parameters associated with the binding of chitotetraose to CIA17 in presence of crowders at different concentrations. T = 25 °C.

Sample (Condition)	n	$K_{\rm a} \times 10^{-5}$ (M <sup>-1</sup> )	$-\Delta G^{\circ}$ (kcal/mol)	-ΔH° (kcal/mol)	-ΔS° (cal.mol <sup>-1</sup> .K <sup>-</sup>
Buffer	1.14	3.15 (±0.13)	7.50	12.5 (±0.1)	16.6 (±0.1)
D70	1.01	8.34 (±0.28)	8.10	17.5 (±0.3)	31.4 (±0.3)
D40	1.12	4.21(±0.11)	7.67	25.2 (±0.3)	58.7 (±0.4)
D6	1.09	2.05 (±0.19)	7.27	19.2 (±0.3)	39.9 (±0.2)

The increase in binding constant in presence of larger crowders like D70 and D40 may be due to the increase in effective concentration of the protein and/or the more compact structure of the lectin as a result of the excluded volume effect exerted by the crowding agents. The unexpected decrease of  $K_a$  value in presence of D6 even at low concentrations is possibly due to some soft chemical interaction between the protein and the crowder that destabilizes the protein structure. This explanation is consistent with results obtained from CD and fluorescence spectroscopic studies, which showed that increasing the concentration of D6 led to large changes in the secondary structure as well as tertiary structure of CIA17. It may be noted that the association constant of  $3.15 \times 10^5$  M<sup>-1</sup> for the chitotriose-CIA17 interaction is somewhat lower than the  $K_a$  value of  $4.03 \times 10^5$  M<sup>-1</sup> obtained earlier by ITC studies [Bobbili et al., 2019]. This difference could be due to the differences in the activity of the different batches of protein used in these two studies. However, it may be noted that all the binding parameters reported here have been obtained from a single batch of protein and the values have been quite reproducible as can be assessed from the standard deviations indicated in Table 4.3.

In general, lectin-carbohydrate interactions are exothermic, i.e., they are enthalpically favored with unfavorable change in entropy [Lemieux, 1996; Narahari et al., 2011b]. CIA17-chitooligosaccharide interaction was found to follow this trend and the compensatory nature in the change in enthalpy and entropy was explained in terms of the reorganization of water around the binding site of the protein and the ligand [Bobbili et al., 2018a; Swaminathan et al., 1998]. The change in the binding constant of the CIA17-chitotetraose interaction in the crowded milieu is accompanied by the large increase in enthalpy ( $-\Delta H^{\circ}$ ) and entropy ( $-\Delta S^{\circ}$ ). A plot of the enthalpy vs entropy values (Fig. 4.7) exhibits a linear dependence indicating that the negative entropy contribution is compensated by the increase in enthalpy as a consequence of the reorganization of water molecules in the crowded milieu.

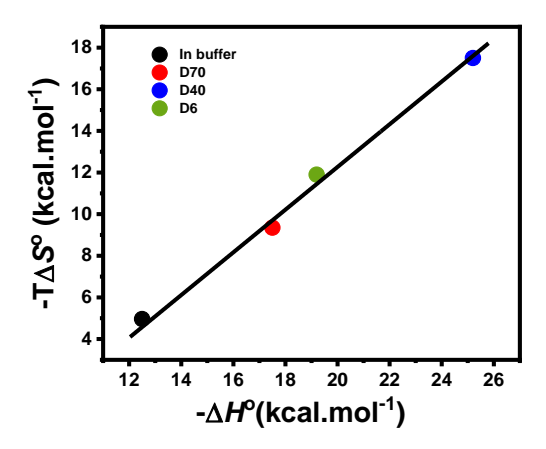


**Fig. 4.7.** Enthalpy  $(\Delta H^{\circ})$ -entropy  $(T\Delta S^{\circ})$  compensation plot for the binding of chitotetraose to CIA17 in the absence and in the presence of 100 mg/mL of D6, D40 and D70.

The crowder molecules can replace water molecules from the bulk as well as from the surroundings of the binding pocket depending on the nature of the crowding agents. The relatively larger size of D70 and D40 make their approach to the core of the protein matrix sterically hindered. So, they can affect the structure of the lectin as well as the carbohydrate binding ability possibly by displacing the water molecule only from bulk, which reduces the available volume for the protein as well as for chitotetraose,

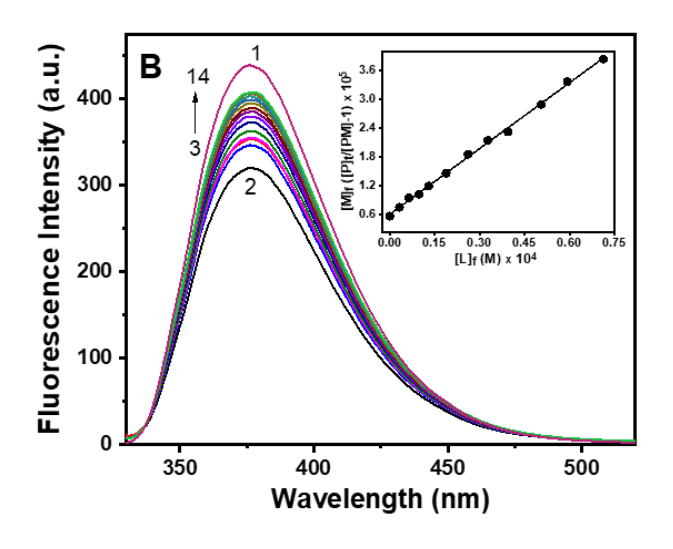
thereby increasing the specific activity of the biomolecules under investigation which in turn increases the association constant. In contrast, D6 molecules are comparatively smaller, with a rod-like structure. Therefore, they can possibly penetrate partially into the interior of the protein and can potentially disrupt the water structure surrounding the binding pocket. Results of molecular docking and MD-simulation studies showed that the sugar moiety (GlcNAc residues) interacts with the amino acid residues of CIA17 through the formation of direct and water mediated hydrogen bonds besides van der Waals interactions [Bobbili et al., 2019]. It is likely that removal of some of the water molecules that interact with the protein surface by D6 weakens/reduces the water mediated hydrogen bonds, which in turn results in a decrease of the binding constant.

#### 4.5 Conclusions

In summary, the studies presented in this chapter demonstrates that macromolecular crowding modulates the conformational features and carbohydrate binding properties of CIA17. Dextrans of various sizes (D70, D40 and D6) were found to influence the structure and conformation of the lectin to different extents which in turn leads to alterations in the carbohydrate binding characteristics, vis-a-vis the native protein. The secondary structure of CIA17 remains essentially unaffected by the presence of higher molecular weight dextrans (D70 and D40) while appreciable changes were observed in the presence of D6, with the magnitude of change increasing with increase in concentration. All the crowders modulate the tertiary structure of the protein significantly as indicated by the crowder-induced quenching of the intrinsic protein fluorescence. D6 induced maximum quenching of Trp fluorescence among all the crowders employed, with the involvement of both static as well as dynamic quenching processes, whereas quenching induced by D70 and D40 was predominantly static in nature. Trp fluorescence quenching with acrylamide and iodide ion gave further insights regarding the crowderinduced perturbation of the local conformation of the lectin. Quenching by both acrylamide and iodide was lowest in presence of D6 among the three crowders employed due to the highest excluded volume effect and lower availability of some of the fluorophores which are quenched directly by D6 molecules via a collisional pathway.

The association constants ( $K_a$ ) for chitotetraose-CIA17-interaction increases significantly (~30-250 %) with D40 and D70 whereas a ~ 40-60% decrease was observed in presence of D6. Overall, the studies reported here indicate that molecular crowding significantly affects the carbohydrate binding property of lectins, which is relevant to understanding how protein-carbohydrate interactions can be modulated under physiological conditions in vivo.

# Purification, Biochemical/Biophysical Characterization and Chitooligosaccharide Binding to BGL24, a New PP2Type Phloem Exudate Lectin from Bottle Gourd (Lagenaria siceraria)



The work was published as

Saradamoni Mondal, Musti J. Swamy\*

Int. J. Biol. Macromol. 2020, 164, 3656-3666.

#### 5.1. Summary

Phloem Protein 2 (PP2), highly abundant in the sieve elements of plants, plays a significant role in wound sealing and anti-pathogenic responses. In this study, we report the purification and characterization of a new PP2-type lectin, BGL24 from the phloem exudate of bottle gourd (Lagenaria siceraria). BGL24 is a homodimer with a subunit mass of ~24 kDa and exhibits high specificity for chitooligosaccharides. The isoelectric point of BGL24 was estimated from zeta potential measurements as 5.95. Partial amino acid sequence obtained by mass spectrometric studies indicated that BGL24 exhibits extensive homology with other PP2-type phloem exudate lectins. CD spectroscopic measurements revealed that the lectin contains predominantly  $\beta$ -sheets, with low  $\alpha$ helical content. CD spectroscopic and DSC studies showed that BGL24 exhibits high thermal stability with an unfolding temperature of ~82 °C, and that its secondary structure is essentially unaltered between pH 3.0 and 8.0. Fluorescence titrations employing 4-methylumbelliferyl-β-D-N,N',N''-triacetylchitotrioside as an indicator ligand revealed that the association constants for BGL24-chitooligosaccharide interaction increase considerably when the ligand size is increased from chitotriose to chitotetraose, whereas only marginal increase was observed for chitopentaose and chitohexaose. BGL24 exhibited moderate cytotoxicity against MDA-MB-231 breast cancer cells, whereas its effect on normal splenocytes was marginal.

#### 5.2. Introduction

The Cucurbitaceae phloem exudate lectins (PP2 proteins) are soluble cytoplasmic proteins with extended binding sites for chitooligosaccharides [ $\beta$ (1-4) linked oligomers of *N*-acetylglucosamine (GlcNAc)] [Peumans et al., 2001].

Lagenaria siceraria, commonly known as bottle gourd, belongs to the Cucurbitaceae family [Yetişir et al., 2008]. L. siceraria is a rich wellspring of dietary prebiotics and is believed to improve the probiotic populaces that influence enteric microbial metabolism prompting synthesis and release of beneficial biomolecules [Ahmad et al., 2011; Schlumbaum and Vandorpe, 2012; Vigneshwaran et al., 2016; Yetişir et al., 2008]. Recently Vigneswaran and coworkers have reported the anti-proliferative activity of crude L. siceraria latex sap [Vigneshwaran et al., 2016]. The potential pharmacological activity of the different parts of L. siceraria to treat various diseases made them important for detailed biochemical and biophysical characterization.

Upon biological stress and/or injury, Cucurbitaceae plants ooze the phloem through the wound, which very quickly coagulates to form elastic-like substance. Analysis of the biochemical composition of the phloem exudate revealed that it contains a variety of macromolecules including lectins.

In the present work, we report the purification of a PP2-type lectin (bottle gourd lectin, BGL24) from the phloem exudate of bottle gourd by affinity chromatography on chitin. Information on the primary and secondary structure of the lectin was obtained by mass spectrometric and circular dichroism (CD) spectroscopic studies, whereas its identified to carbohydrate binding specificity was be directed towards chitooligosaccharides by hemagglutination-inhibition assay. The effect of temperature and pH on the stability as well as on the lectin activity of BGL24 was also explored. Additionally, thermodynamic parameters governing the binding of a fluorescently labeled chitooligosaccharide, 4-methylumbelliferyl-β-D-N,N',N''-triacetylchitotrioside [MeUmbβ(GlcNAc)<sub>3</sub>] to this lectin were characterized by fluorescence titrations monitoring changes in the fluorescence intensity of the 4-methlyumbelliferyl moiety upon titration with BGL24, whereas the binding of unlabeled chitooligosaccharides was investigated by using MeUmb $\beta$ (GlcNAc)<sub>3</sub> as an indicator ligand [Sanadi and Surolia, 1994].

#### 5.3. Materials and Methods

#### 5.3.1 Materials

Unripe bottle gourds (*Lagenaria siceraria*) were purchased from local vegetable vendors. Chitin (from crab shells), dithiothreitol (DTT), galactose, glucose, mannose, fucose, methyl- $\alpha$ -D-glucopyranoside, methyl- $\alpha$ -D-galactopyranoside, methyl- $\alpha$ -D-mannopyranoside, N-acetyl-D-glucosamine, cellobiose, lactose, melibiose, lactulose, 4-methylumbelliferyl- $\beta$ -D-N, N', N''-triacetylchitotrioside and all the chitooligosaccharides were obtained from Sigma Chemical Co. (St. Louis, MO, USA). All other chemicals and reagents used were of the highest purity available from local suppliers.

#### 5.3.2. Extraction and Purification of BGL24

Bottle gourd fruits were washed thoroughly with double distilled water and dried. Then 2-3 mm deep longitudinal incisions were made on the clean surface of the fruit as described earlier for other Cucurbitaceae fruits [Anantharam et al., 1986; Bobbili et al., 2018a; Narahari and Swamy, 2010; Sanadi and Surolia, 1994] and the phloem exudate oozing out from the incisions was collected immediately into previously prepared icecold 20 mM sodium phosphate buffer (pH 7.4) containing 150 mM NaCl and 3 mM DTT (PBS-DTT) [Nareddy et al., 2017]. The phloem exudate collected in PBS-DTT was centrifuged at 4057 g for 20 minutes at 4 °C in an Eppendorf 5810R centrifuge. The supernatant was directly subjected to affinity chromatography on a chitin column which was pre-equilibrated with PBS-DTT. The flow-through obtained was reloaded to ensure complete binding of the protein. The column was then washed with PBS-DTT extensively to remove unbound proteins, monitoring absorbance of the eluent at 280 nm. When absorbance fell below 0.05 at 280 nm, the proteins bound to the chitin column were eluted with 16 mM acetic acid at room temperature and fractions of ~6 mL were collected. The absorbance of each fraction was assessed at 280 nm. Fractions of higher absorbance were pooled and dialyzed against distilled water followed by 20 mM phosphate buffer. Homogeneity of the affinity-purified protein was assessed by native PAGE as well as by SDS-PAGE under reducing/denaturing and non-reducing conditions [Laemmli, 1970].

#### **5.3.3. Size Exclusion Chromatography**

The affinity purified protein dialyzed against 20 mM sodium phosphate buffer (pH 7.4) containing 150 mM NaCl (PBS) was further subjected to gel-filtration chromatography. About 100 mL of Sephadex G-100 matrix was packed in a long glass column (1.5 cm  $\times$  100 cm) and equilibrated with PBS. The void volume (V<sub>o</sub>) and the resolution of the column were previously measured by the passage of blue-dextran and the standard protein marker successively. About 1 mL of BGL24 sample (2.5 mg/mL) was loaded on the column and eluted with the extraction buffer. After discarding the void volume, 1 mL fractions were collected and the absorbance of each fraction was measured at 280 nm. The molecular weight (MW) of the native protein was determined from a plot of log MW vs V<sub>e</sub>/V<sub>o</sub> and comparing the elution volume of the protein with that of standard proteins as described earlier [Tejavath and Nadimpalli, 2014]. In this plot V<sub>o</sub> is the void volume and V<sub>e</sub> is the elution volume.

#### **5.3.4. Reverse Phase HPLC**

Reverse phase HPLC was performed on a Shimadzu UFLC system (Kyoto, Japan) equipped with a diode array detector. Affinity purified BGL24 was dialyzed against water and subjected to chromatography on a semi-preparative C-18 column (250 mm  $\times$  10 mm) of 10  $\mu$ m particle size [Tejavath and Nadimpalli, 2014]. The column was eluted with an increasing gradient of 0.1% trifluoroacetic acid (TFA) as solvent A and 66% acetonitrile in 0.1% TFA as solvent B using a 70-minute program with a constant flow rate of 5 mL/min. The purity of the protein was assessed by SDS-PAGE [Laemmli, 1970].

#### 5.3.5. Zeta Potential Measurements

In order to determine the isoelectric point of BGL24, zeta potential of the protein was measured at different pH using a Malvern Zetasizer Nano ZS (Malvern Instrument Ltd.,

UK) fitted with red laser light ( $\lambda = 632.8$  nm) [Datta et al., 2016]. A 10 µg/mL concentration protein solution in PBS was titrated with 0.1 M HCl to obtain the desired pH within the range of 2.0-8.0 at 25 °C. For every sample of different pH, measurements were done in triplicate using a disposable folded capillary cell (DTS1070) provided by Malvern and average values have been reported.

# 5.3.6. Hemagglutination and Hemagglutination-Inhibition Assays

Hemagglutination and hemagglutination-inhibition assays were carried out in 96 well ELISA microtiter plates as described earlier [Datta et al., 2016]. In brief, BGL24 was serially two-fold diluted into successive wells in each row of the ELISA plate. To each well containing 50 μL of serially diluted lectin in PBS, 50 μL of 4% of human erythrocyte suspension (A, B, O) were added and mixed, which resulted in a final volume of 100 μL. After incubation at 4 °C for 1 h, the hemagglutination titer was visually scored. The effect of divalent metal ions on the lectin activity was assessed by performing the hemagglutination assay in the presence of 1 mM concentration of various divalent metal ions (Ca<sup>2+</sup>, Mg<sup>2+</sup>, Mn<sup>2+</sup>, Sn<sup>2+</sup>, Zn<sup>2+</sup>). Activity of the protein was also assessed after dialyzing against 10 mM EDTA, followed by dialysis against PBS. To investigate the effect of temperature on the lectin activity, samples were preincubated at the desired temperature (25-95 °C) for 60 minutes, cooled to room temperature and the hemagglutination assay was performed as above. To investigate the effect of pH, lectin samples used were dialysed against the buffer of desired pH (3.0-8.0) together with erythrocytes that were suspended in the same buffer.

Hemagglutination-inhibition assays were performed in a similar manner using a stock solution of sugar which was serially two-fold diluted to give a final volume of 40  $\mu$ L in each well. Then 10  $\mu$ L of lectin was added, mixed and incubated at 4 °C for ~15 min. Then 50  $\mu$ L of 4% erythrocyte suspension was added and mixed. After incubation for 1 h at 4 °C, the hemagglutination titer was visually scored. The following sugars were used in the hemagglutination-inhibition assay: galactose, glucose, mannose, fucose, methyl- $\alpha$ -D-glucopyranoside, methyl- $\alpha$ -D-galactopyranoside, methyl- $\alpha$ -D-galactopyranoside, methyl- $\alpha$ -D-galactopyranoside, methyl- $\alpha$ -D-galactopyranoside,

mannopyranoside, N-acetyl-D-glucosamine, cellobiose, lactose, melibiose, lactulose and chitooligosaccharides, (GlcNAc)<sub>3-6</sub>.

#### **5.3.7.** Mass Spectrometric Studies

Partial amino acid sequence of BGL24 was obtained by MALDI-TOF mass spectrometry. Samples for MS analysis were prepared as follows. Bands corresponding to BGL24 were excised from SDS-PAGE gels (electrophoresis being performed under reducing conditions) and cut into small pieces and the protein was subjected to in-gel digestion by trypsin according to Shevchenko et al. (2006). In-gel digestion and peptide extraction have been performed as described in earlier [Nareddy et al., 2017]. In the final step, the proteolytic peptides were extracted by adding extraction buffer (water/acetonitrile, 1:2 v/v with 5% formic acid added) to each tube and incubating for 15 min at 37 °C in a shaker. The supernatant was collected into a fresh tube and dried *in vacuo*.

The residue obtained in the above step was dissolved in TFA and ACN buffer and spotted along with  $\alpha$ -cyano-4-hydroxycinnamic acid (HCCA) matrix onto the target plate. After air drying of the spot, mass spectra were recorded using a Bruker Ultraflex III MALDI-TOF/TOF mass spectrometer (Bruker Daltonics) which was calibrated with peptide standards (bradykinin, angiotensin-I, angiotensin-II, bombesin, ACTH and somatostatin). Peaks with high relative abundance were further analysed by Mascot search.

The intact molecular mass of BGL24 was determined from the mass spectrum recorded on an Autoflex II MALDI TOF-TOF instrument from Bruker Daltonics as described earlier [Junqueira et al., 2008]. Protein sample extracted from a reducing SDS-PAGE gel band corresponding to 24 kDa was used for estimating the exact mass. The following instrumental settings were employed. Laser frequency: 60 Hz (laser power 90%); acceleration voltage: 20 kV; lens voltage: 6 kV; mass range: 20000 to 30000 m/z. The instrument was calibrated using a high molecular weight standard (Protein standard II, Bruker).

## **5.3.8.** Multiple Sequence Alignment

Amino acid sequences of several tryptic peptides of BGL24 were obtained from Mascot analysis by matching their masses with those predicted for tryptic peptides of phloem lectin 2 of *Cucurbita argyosperma*. Amino acid sequences of other homologous proteins were obtained from the NCBI protein database (www.ncbi.nlm.nih.gov/protein). Pairwise sequence alignment was done with *Cucurbita argyrosperma ssp.* phloem protein using bioinformatics (https://www.ebi.ac.uk/Tools/psa/). Multiple sequence alignment with other PP2-type lectins and phloem proteins was carried out using Clustal Omega software (https://www.ebi.ac.uk/Tools/msa/clustalo/).

## 5.3.9. Circular Dichroism Spectroscopy

All CD spectral data were recorded on an Aviv 420 spectropolarimeter (Lakewood, NJ, USA) that was connected with a Peltier thermostat for temperature regulation [Nareddy et al., 2017; Datta et al., 2016]. The concentration of BGL24 used was ~0.1 OD and 1.0 OD for measurements in the far UV (250-190 nm) and near UV (300-250 nm) regions, respectively. Samples were placed in a rectangular quartz cuvette of 2 mm path length and the slit width was 2 nm. All spectra reported are the averages of 5 scans obtained at a scan rate of 20 nm/min. In order to investigate the thermal unfolding as well as the pH-induced unfolding of BGL24, CD spectra were recorded at different temperatures (30-90 °C) and at different pH (3.0-8.0). To obtain the desired pH condition, the BGL24 samples were dialyzed against the appropriate buffer among the following: 20 mM KCl-HCl (pH 2.0), 20 mM glycine-HCl (pH 3.0), 20 mM sodium acetate (pH 4.0-5.0), 20 mM sodium phosphate (pH 6.0-7.0), 20 mM Tris-HCl (pH 8.0-9.0).

#### **5.3.10. Differential Scanning Calorimetry**

DSC measurements were performed on a NanoDSC differential scanning calorimeter from TA instruments (New Castle, Delaware, USA) equipped with a sample cell and a reference cell. BGL24 in water was taken in the sample cell whereas water was loaded in the reference cell. DSC scans were also run with BGL24 that was preincubated with 1 mM chitotetraose. Thermograms obtained were analyzed by fitting the data to a Gaussian

model available in the NanoAnalyze DSC analysis software provided by the manufacturer.

# 5.3.11. Fluorescence Studies on the Binding of MeUmb $\beta$ (GlcNAc) $_3$ to BGL24 and Reversal Titrations with Chitooligosaccharides

All the fluorescence spectroscopic measurements were performed on a Jasco FP-8500 spectrofluorometer equipped with a Jasco ETC-815 Peltier device for temperature regulation. A 2.0 mL solution of 3.81  $\mu$ M 4-methylumbelliferyl- $\beta$ -D-N,N',N''-triacetylchitotrioside [MeUmb $\beta$ (GlcNAc) $_3$ ] in a 1  $\times$  1  $\times$  4.5-cm quartz cuvette was excited at 318 nm and emission spectra were recorded between 330 and 520 nm. Slit widths of 2.5 nm were used on both the monochromators. The umbelliferyl sugar was titrated by the addition of small aliquots from a 4.75 mg/mL ( $\sim$ 81  $\mu$ M) BGL24 stock solution and emission spectra were recorded in the wavelength range of 330-520 nm after 2 min incubation. In order to obtain the thermodynamic parameters of binding, titrations were carried out at five different temperatures between 15 and 35 °C. The association constants were determined from Chipman plots as described earlier [Chipman et al., 1967; Komath et al., 2001; Sanadi and Surolia,1994].

Binding of unlabeled chitooligosaccharides to BGL24 was investigated by studying their ability to reverse the binding of MeUmb $\beta$ (GlcNAc)<sub>3</sub> from its complex with BGL24. In these experiments, the fluorescence spectrum of MeUmb $\beta$ (GlcNAc)<sub>3</sub> (3.81  $\mu$ M) was recorded first and then it was incubated with a defined quantity of BGL24 (~3.5  $\mu$ M), following which the fluorescence spectrum of the sample was recorded again. The mixture was then titrated by adding small aliquots of the unlabeled chitooligosaccharide from a concentrated (1.5 – 3.0 mM) stock solution at a constant temperature. This led to an increase in the fluorescence intensity of the indicator ligand due to its dissociation from the complex with BGL24. The association constants for both the indicator and inhibitory ligands were obtained by analyzing the titration data (changes in the fluorescence intensity of the indicator ligand) as described earlier

[Chipman et al., 1967; Komath et al., 2001]. In order to obtain the thermodynamic parameters some of the titrations were performed at different temperatures.

#### 5.3.12. Cell Culture

Normal splenocytes and triple negative breast cancer cells (MDA-MB-231) were maintained in a 37 °C incubator (Sanyo MCO-19AIC, Panasonic Biomedical Sales Europe BV, AZ Etten Leur, Netherlands) in 5%  $CO_2$  and humid atmosphere. Both types of cells were cultured in 9.6 cm<sup>2</sup> culture flasks in MEM medium supplemented with 2 mM glutamine, 10% foetal bovine serum (FBS) and 1% penicillin-streptomycin. Cells were counted and seeded at a density of  $1 \times 10^4$  cells/cm<sup>2</sup> in each well of a 96 well cell culture plate.

## 5.3.13. MTT Cell Viability Assay

The cytotoxicity of BGL24 towards normal splenocytes and MDA-MB-231 cells was assessed by MTT cell-viability assay as described previously [Datta et al., 2016], and the results were compared with those obtained with jacalin (*Artocarpus integrifolia* lectin). Briefly, in each well of a 96-well cell culture plate, 100  $\mu$ L of cell suspension was transferred and kept overnight. Then 100  $\mu$ L of each lectin was added in different concentrations (0-1 mg/mL) to different wells. After incubation at 37 °C for 72 h, the supernatant was removed from the cells and 100  $\mu$ L of fresh medium was added, followed by the addition of 25  $\mu$ L of 5 mg/mL MTT in PBS. The plates were then incubated for 4 h and the supernatant was removed. Then 100  $\mu$ L of DMSO was added to each well and after 15 min of shaking at 300 rpm the absorbance was measured at 570 nm. The respective untreated medium was used as the negative control.

# 5.4. Results and Discussion

# 5.4.1. Affinity Chromatographic Purification of BGL24

BGL24 was purified from the phloem exudate of bottle gourd (*Lagenaria siceraria*) by affinity chromatography on  $\alpha$ -chitin. A single peak was obtained when the lectin was eluted with 16 mM acetic acid from the  $\alpha$ -chitin column in about 85% overall yield (Fig.

5.1A). In native PAGE under non-reducing and non-denaturing condition, the affinity purified protein showed a single band (Fig. 5.1C). SDS-PAGE under non-reducing condition showed an intense band corresponding to ~44 kDa (Fig. 5.1D, lane 2). When larger amounts of the protein were loaded, weaker bands corresponding to higher molecular weights were also seen (Fig. 5.1D, lane 3), suggesting that BGL24 self-assembles noncovalently to form higher oligomeric structures similar to another Cucurbitaceae phloem exudate lectin, CIA17 [Bobbili et al., 2018a].

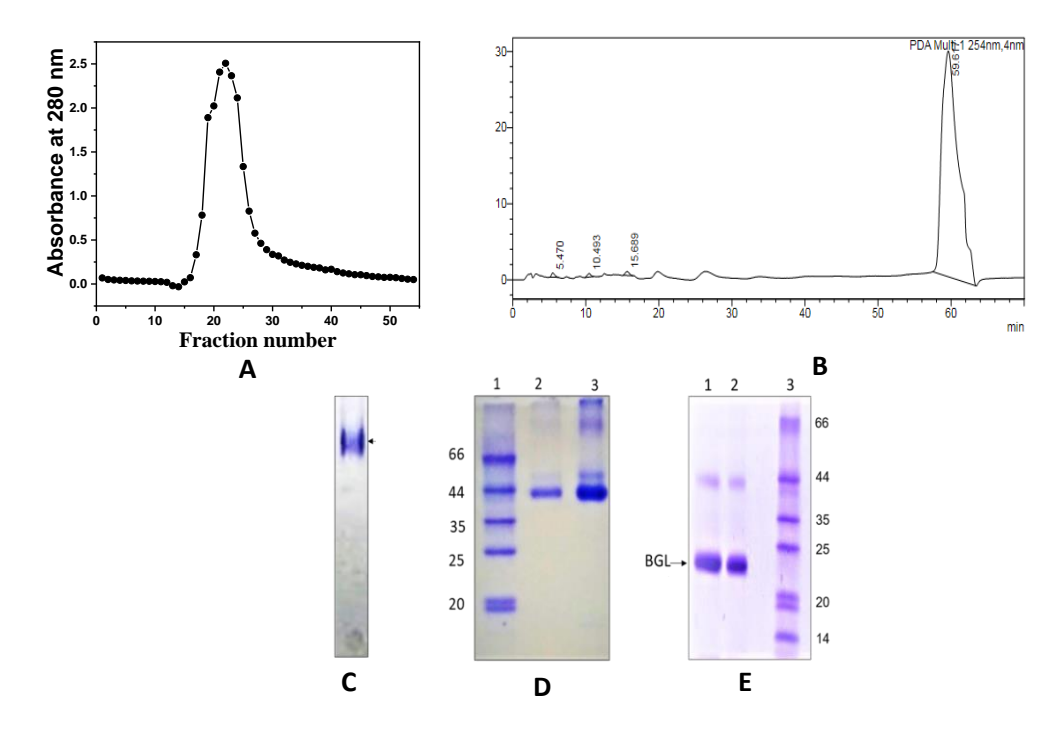


**Fig. 5.1.** Chromatographic purification and gel electrophoresis analysis of BGL24. (A) Elution profile of BGL24 from α-chitin affinity chromatography. Protein bound to α-chitin was eluted with 16 mM acetic acid and 6 mL fractions were collected. (B) Reverse phase HPLC chromatogram of affinity purified BGL24. The major peak eluting at 59.6 minutes corresponds to BGL24. (C) Native-PAGE of affinity purified BGL24 on 10% resolving gel and 2.5% stacking gel. (D) SDS-PAGE of proteins eluted from α-chitin column under nonreducing condition. Lane 1, molecular weight markers; lanes 2 and 3, BGL24. (E) SDS-PAGE in presence of reducing agent. Lanes 1 and 2, BGL24; lane 3, molecular weight markers.

In the presence of a reducing agent such as 2-mercaptoethanol or DTT, a strong band of ~24 kDa was observed along with a minor band at ~44 kDa (Fig. 5.1E). These results suggest that BGL24 is a homodimer wherein the two subunits are connected via disulfide bonds and that they could not be fully cleaved even by strong reducing agents.

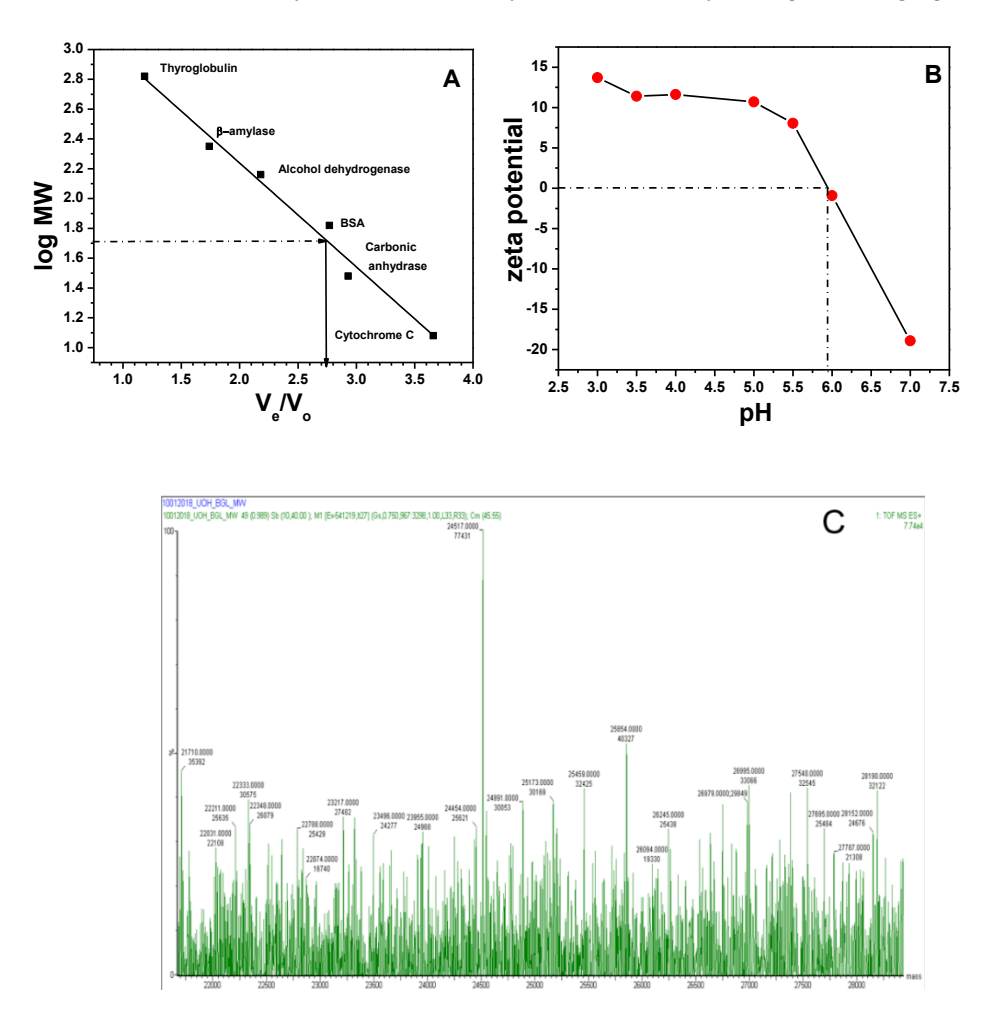


**Fig. 5.2.** Determination of molecular weight and isoelectric point of BGL24. (A) Molecular weight of native BGL24 was determined to be ~50 kDa from gel filtration chromatography on Sephadex G-100. (B) The isoelectric point (pI) of BGL24 was estimated as 5.95 from a plot of zeta potential versus pH . (C) Deconvoluted MALDITOF mass spectrum of BGL24. The most intense peak at m/z value of 24517 indicates that the subunit molecular weight of BGL24 is 24,517 Daltons.

Further purification using size exclusion chromatography and reverse phase HPLC yielded a major peak corresponding to >95 % of total protein loaded (Fig. 5.1B) which is in agreement with the conclusion drawn from SDS-PAGE analysis (see lane 2 of Fig. 5.1D). Gel filtration chromatography of BGL24 on Sephadex G-100 yielded the molecular weight of the native protein as  $\sim 50$  kDa (Fig. 5.2A). The isoelectric point of BGL24 was estimated as 5.95 from a plot of zeta potential versus pH (Fig. 5.2B).

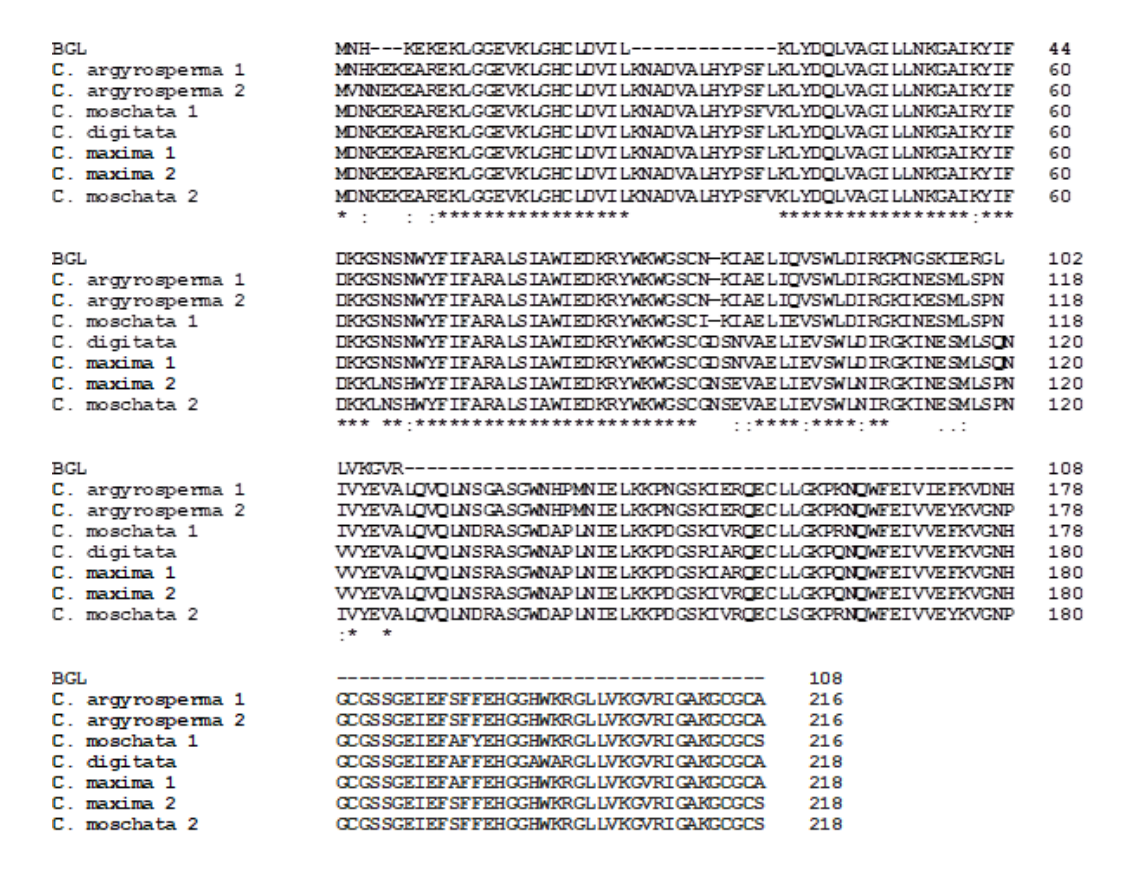


**Fig. 5.3.** Multiple sequence alignment of the partial amino acid sequence of BGL24 with the primary structure of other 24 kDa PP2-type Cucurbitaceae phloem exudate lectins/proteins. Sequences of *C. argyrosperma* 1 (AAM82558.1), *C. argyrosperma* 2 (AAA33118.1), *C. moschata* 1 (AAF74345.1), *C. moschata* 2 (XP\_022927327.1), *C. digitata* (AAM82559.1), *C. maxima* 1 (XP\_023001604.1), and *C. maxima* 2 (CAA80364.1) were taken from NCBI gene bank. Multiple sequence alignment was performed using Clustal Omega (<a href="https://www.ebi.ac.uk/Tools/msa/clustalo/">https://www.ebi.ac.uk/Tools/msa/clustalo/</a>).

The band corresponding to ~24 kDa in the SDS-PAGE was excised and subjected to mass spectrometric analysis to obtain the exact mass of the protein. The MALDI-TOF mass spectrum, as shown in Fig. 5.2C, indicates that the subunit mass of BGL24 is 24517 Da.

In order to obtain information on the amino acid sequence of BGL24, the band corresponding to BGL24 was cut from the SDS-PAGE gel and in-gel tryptic digestion was carried out. MS/MS analysis showed that tryptic digestion yielded a number of peptides with masses ranging between 651.35 and 2767.09. The exact masses of several of these peptides could be matched to the calculated masses of predicted tryptic peptides in the primary structure of the phloem lectin from *Cucurbita argyrosperma* subsp. *sororia* (NCBI access no. AAM82558.1) based on Mascot search with a top score of 206. Multiple sequence alignment, shown in Fig. 5.3, suggests that BGL24 exhibits high homology with a number of other Cucurbitaceae phloem exudate lectins as well.

#### 5.4.2. Lectin Activity and Carbohydrate Specificity

Hemagglutination assays revealed that BGL24 exhibits strong lectin activity and agglutinates human (A, B, O) as well as rabbit erythrocytes with equal efficiency. Divalent metal ions ( $Ca^{2+}$ ,  $Mg^{2+}$ ,  $Mn^{2+}$ ,  $Sn^{2+}$ ,  $Zn^{2+}$ ) did not exhibit any significant effect on the hemagglutination assay, suggesting that BGL24 does not require any divalent metal ions for its activity. This was further supported by the observation that dialysis against EDTA did not affect the hemagglutination activity of BGL24. In order to investigate the carbohydrate specificity of BGL24, hemagglutination assays were performed in the presence of various mono, di, and oligosaccharides. Similar to the results obtained previously for the other PP2-type lectins from Cucurbitaceae, none of the mono- or disaccharides (except chitobiose) could inhibit the hemagglutination activity of BGL24 even at 125 mM concentration. Chitooligosaccharides at very low concentration inhibited the hemagglutination activity with high efficiency. Chitotriose exhibited 50% inhibition of the hemagglutination activity (IC<sub>50</sub>) at the low concentration of 0.2 mM whereas chitotetraose (IC<sub>50</sub> = 50  $\mu$ M), chitopentaose and chitohexaose (IC<sub>50</sub> =

 $25~\mu M$ ) inhibited hemagglutination activity at even lower concentrations, suggesting that BGL24 exhibits high specificity for chitooligosaccharides.

## 5.4.3. Temperature and pH Effect on the Hemagglutination Activity

Thermal inactivation of BGL24 was probed by incubating the protein sample at different temperatures for 60 minutes followed by cooling to room temperature and testing its activity by hemagglutination assay. These experiments indicated that activity of the lectin was retained fully when incubated up to 70 °C, but decreases drastically to ~10% when incubated at 80 °C. Incubation at temperatures above 80 °C led to a complete loss of the lectin activity.

Effect of varying the pH on the lectin activity of BGL24 was investigated by dialyzing it against buffers of different pH and then testing its activity by the hemagglutination assay. These studies showed that BGL24 exhibits the highest activity in the pH range of 5.0-8.0. At pH 3.0-4.0 the lectin activity decreased to about 50% as compared to that at pH 7.4 whereas at pH 2.0 the activity decreased further to 30%.

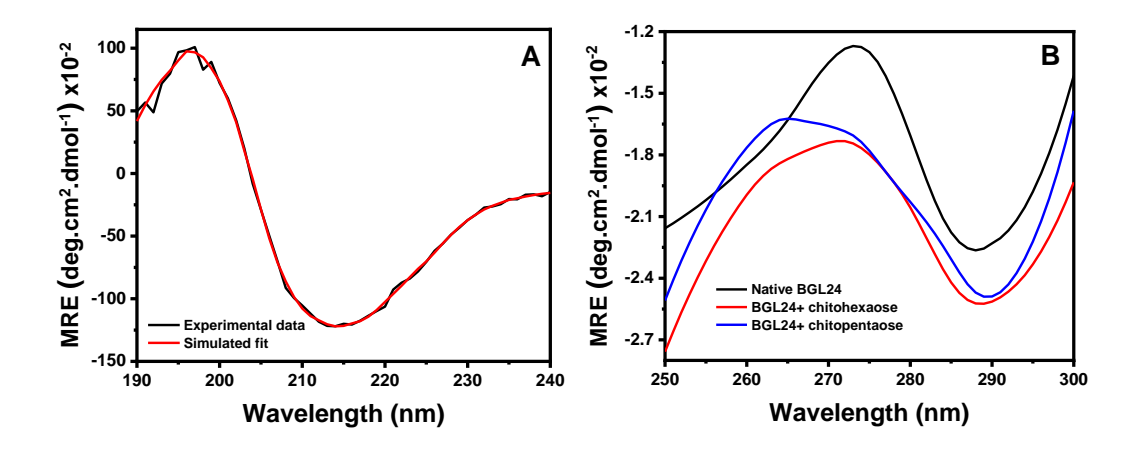


**Fig. 5.4.** CD spectra of BGL24 in the (A) far-UV (190-240 nm) and near-UV (250-300 nm) regions. Spectra were obtained in the near UV region in the presence of 1.0 mM concentrations of chitopentaose and chitohexaose also (indicated in blue and red, respectively).

## 5.4.4. Secondary Structure of BGL24: CD Spectroscopic Studies

The far-UV CD spectrum of BGL24 under native protein (Fig. 5.4A, black line) showed a sharp negative band centered around 216 nm and a positive band at 193 nm, suggesting that BGL24 contains  $\beta$ -sheet as the predominant secondary structure, with very little  $\alpha$ helical content. Quantitative information on the various secondary structural elements was obtained by further analysis of the far-UV CD spectral data using three different methods CONTILL, SELCON3 and CDSSTR, available online at DICHROWEB (www.cryst.bbk.ac.uk/cd web/HTML). The average results obtained from these three programs suggested that BGL24 contains 41.3% β-sheets, 21.7% β-turns, 3.8% α-helices and 33.1% unordered structures (Table 5.1). The simulated fit obtained from the CDSSTR analysis shown in Fig. 5.4A (red line) is in good agreement with the experimental spectrum. The secondary structure of BGL24 thus contains high percentage of β-sheet. In this respect it resembles several other Cucurbitaceae phloem exudate lectins, such as PPL, CPL and snake gourd phloem lectin (SGPL), which contain 35.8, 38.9, and 39.2% β-sheet, respectively, with low α-helical content [Narahari and Swamy, 2010; Nareddy et al., 2018; Narahari et al., 2011]. Similarly, two phloem exudate lectins from Coccinia indica, CIA17 and CIA24 also have high percentage of β-sheet (42.2 and 40.5% β-sheet, respectively) in their secondary structure [Bobbili et al., 2018a, b].

**Table 5.1.** Secondary structure analysis of BGL24 from CD spectra and comparison with values predicted by DICHROWEB software.

Method	Percent secondary structure				
	α-Helix	β-Sheet	β-Turns	Unordered	
CDSSTR	5.0	40.0	21	34.0	
CONTINLL	4.6	40.7	22.2	32.5	
SELCON3	1.9	43.3	21.9	32.9	
AVERAGE	3.8	41.3	21.7	33.1	

The near UV CD spectrum of BGL24 showed a maximum at 274 nm with a shoulder at 260 nm and a minimum at 288 nm (Fig. 5.4B), which can be ascribed to the contribution from the side chains of aromatic amino acids phenylalanine, tyrosine and tryptophan [Rabbani et al., 2011]. Binding of chitooligosaccharides led to changes in the intensity and position of both these bands, suggesting that the orientation and position of some of the aromatic side chains are perturbed by carbohydrate binding.

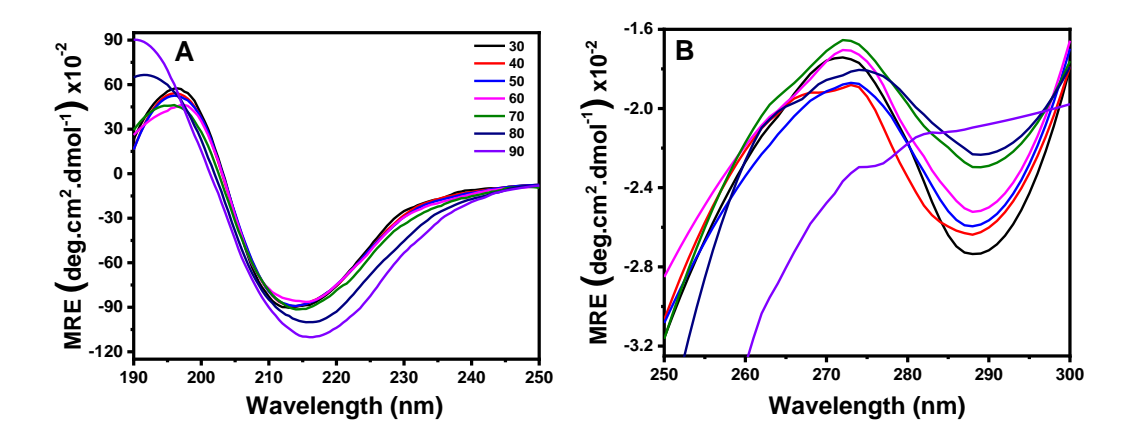


**Fig. 5.5.** CD spectra of BGL24 at different temperatures. (A) Far-UV region; (B) near-UV region. Color code indicates the temperatures (in °C) at which the spectra were recorded.

# 5.4.5. Thermal and pH Stability: CD Spectroscopic and DSC Studies

In order to investigate the thermal stability of BGL24, CD spectra of the protein were recorded at various temperatures between 30 and 90 °C (Fig. 5.5). Very little changes in the shape and intensity of CD spectra were observed in the far-UV region when the sample was heated from 30 to 70 °C, whereas moderate changes were seen between 70 and 90 °C, suggesting that the secondary structure of BGL24 is quite stable up to 70 °C and undergoes only marginal changes below 90 °C (Fig. 5.5A). Interestingly, considerable changes in the spectral intensity were seen in the near-UV CD spectra of BGL24 even in the 40-70 °C range, suggesting that the tertiary structure of the protein undergoes changes continuously as the temperature is increased. Notably, drastic

changes were observed in the near-UV spectra between 70 and 90 °C, clearly indicating that the protein undergoes significant changes in the tertiary structure above 70 °C (Fig. 5.5B). In comparison, the secondary structure of SGPL was unaltered between 30 and 60 °C and PPL was thermally stable up to 80 °C [Narahari and Swamy, 2010; Narahari et al., 2011a]. Both the secondary and tertiary structures of CIA17 and CPL was unaltered even at 95 °C [Bobbili et al., 2018a; Nareddy et al., 2018]. These observations indicate that the thermal stability of BGL24 is comparable to that of PPL but less than that of CIA17 and CPL.

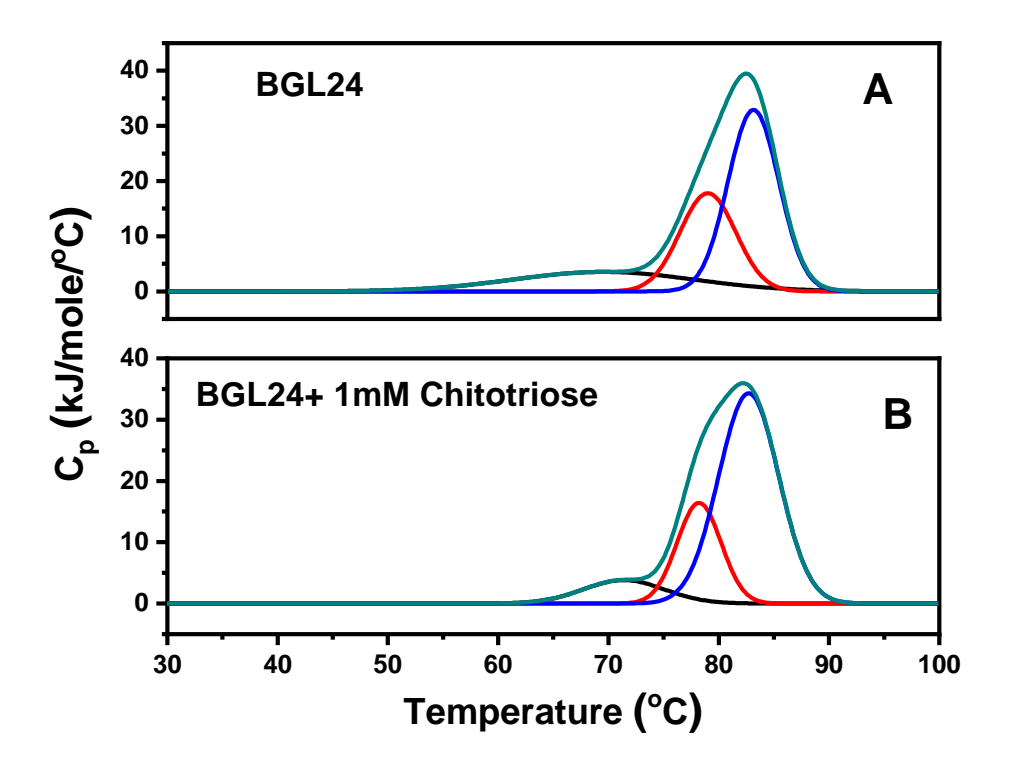


**Fig. 5.6.** DSC thermograms of BGL24. Heating scans of (A) native BGL24, and (B) BGL24 in the presence of 1 mM chitotetraose. Scan rate: 1°/min (Celsius scale). Deconvolution of the original thermograms (green lines) using the NanoAnalyze software provided by TA Systems yielded three underlying peaks (indicated by black, red and blue lines).

In order to obtain quantitative thermodynamic information on the thermal unfolding of BGL24 and the effect of carbohydrate binding on it, DSC studies were performed on the lectin in the absence as well as presence of chitooligosaccharides at 1 mM concentration. Native BGL24 in double distilled water exhibits three partially overlapping endothermic components, centered at  $\sim 69.5$ , 79.0 and 83.2 °C, respectively (Fig. 5.6A). The thermal unfolding of BGL24 was found to be an irreversible process. Similar to the native protein, thermograms obtained in presence of chitooligosaccharides, (GlcNAc)<sub>3-6</sub> could be resolved into three components, with the position of the endotherms remaining nearly unchanged. The transition temperatures and enthalpies ( $\Delta H_c$ ) corresponding to all the three transitions are listed in Table 5.2.

**Table 5.2.** Thermodynamic parameters associated with the thermal unfolding of BGL24 and the effect of chitooligosaccharide binding.

Sample description	T <sub>m</sub> (°C)	$\Delta H_{\rm c}$ (kJ mol <sup>-1</sup> )			
BGL24					
Transition 1	69.5	72.6			
Transition 2	79.0	112.5			
Transition 3	83.2	190.0			
BGL24 + chitotriose	BGL24 + chitotriose				
Transition 1	71.4	35.0			
Transition 2	78.2	82.0			
Transition 3	82.7	234.9			
BGL24 + chitotetraose	BGL24 + chitotetraose				
Transition 1	73.6	12.0			
Transition 2	77.5	48.3			
Transition 3	81.9	260.0			
BGL24 + chitopentaose					
Transition 1	73.3	27.6			
Transition 2	78.2	52.6			
Transition 3	82.01	258.1			
BGL24 + chitohexaose					
Transition 1	71.5	17.0			
Transition 2	81.1	131.1			
Transition 3	83.3	295.4			

The three components of the DSC thermograms obtained with native BGL24 and in the presence of chitooligosaccharides could be analysed in the following manner. The first endothermic component may be assigned to the dissociation of the higher oligomeric forms of the protein to dimers, whereas the second component could be assigned to the dissociation of the homodimeric protein into monomers which remain in the folded state or in a nearly folded state [Rabbani et al., 2012]. However, the two protomers would still be connected via a disulfide bridge, but without significant non-covalent interactions between them. The third endothermic component can be attributed to the unfolding of the monomer.

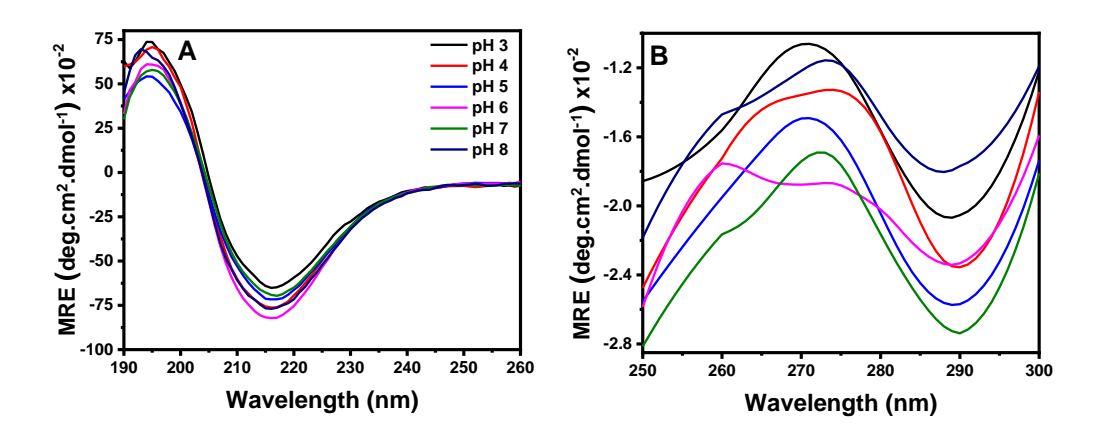


**Fig. 5.7.** CD spectra of BGL24 recorded at different pH. (A) Far-UV region, (B) near UV region. Color code given in panel A indicates the pH at which each spectrum was recorded (for both panels A and B).

Change in pH can alter protein structure either by disrupting hydrogen bonds between the amino acid residues or by disturbing salt bridges between the positively and negatively charged side chains of amino acids [Rabbani et al., 2014]. The effect of changing pH on the structure of BGL24 was also investigated by recording both far-UV and near-UV CD spectra after dialysing the protein sample against buffers of different pH (between 3.0 and 8.0). The far-UV CD spectrum of the protein exhibited only minor changes (Fig. 5.7A), suggesting that the secondary structure of BGL24 was mostly unaltered when the pH was varied between 3.0 and 8.0, and that the secondary structure

of BGL24 is quite stable over a wide pH range. In this respect it is comparable to *Cucumis sativus* phloem exudate lectin, which was reported to retain its secondary structure in pH range of 3.0-8.0 [Nareddy et al., 2018].

The secondary structure of two Cucurbitaceae seed lectins, *Momordica charantia* lectin (MCL) and *Trichosanthes dioica* seed lectin (TDSL) was also reported to be stable secondary structure over a broad pH range [Kavitha and Swamy, 2009; Kavitha et al., 2009a]. In contrast, major changes were observed in the near-UV CD spectrum of BGL24 (Fig. 5.7B), which did not exhibit any systematic trends with pH change, indicating that changes in the tertiary structure do not follow any particular order with change in pH [Rabbani et al., 2015].

# 5.4.6. Binding of MeUmbβ(GlcNAc)<sub>3</sub> and Unlabeled Chitooligosaccharides to BGL24: Fluorescence Titrations

The emission spectra of MeUmb $\beta$ (GlcNAc)<sub>3</sub> in the absence and in the presence of different concentrations of BGL24, recorded at 20 °C, are shown in Fig. 5.8A. Spectrum 1, which has the highest fluorescence intensity, corresponds to MeUmb $\beta$ (GlcNAc)<sub>3</sub> in buffer alone whereas the remaining spectra with decreasing intensities correspond to those recorded in the presence of increasing concentrations of the lectin. From this figure it is observed that the fluorescence intensity of the 4-methylumbelliferyl sugar was significantly quenched upon binding to BGL24. The fluorescence titration data was analysed by plotting  $F_o/(F_o-F_c)$  vs 1/[P]<sub>t</sub> where  $F_o$ ,  $F_c$  and  $\Delta F$  represent initial fluorescence intensity of MeUmb $\beta$ (GlcNAc)<sub>3</sub> alone, fluorescence intensity at any point of the titration (corrected for dilution) and the corresponding change in fluorescence intensity, respectively. Such plots obtained at various temperatures between 15 and 35 °C showed that the fluorescence intensity of MeUmb $\beta$ (GlcNAc)<sub>3</sub> is totally quenched at saturation binding by BGL24. This suggests that the quantum yield of the fluorescent sugar becomes zero upon binding to BGL24. Consistent with this, no significant change in the emission maximum was seen upon binding of the fluorescent sugar to the protein.

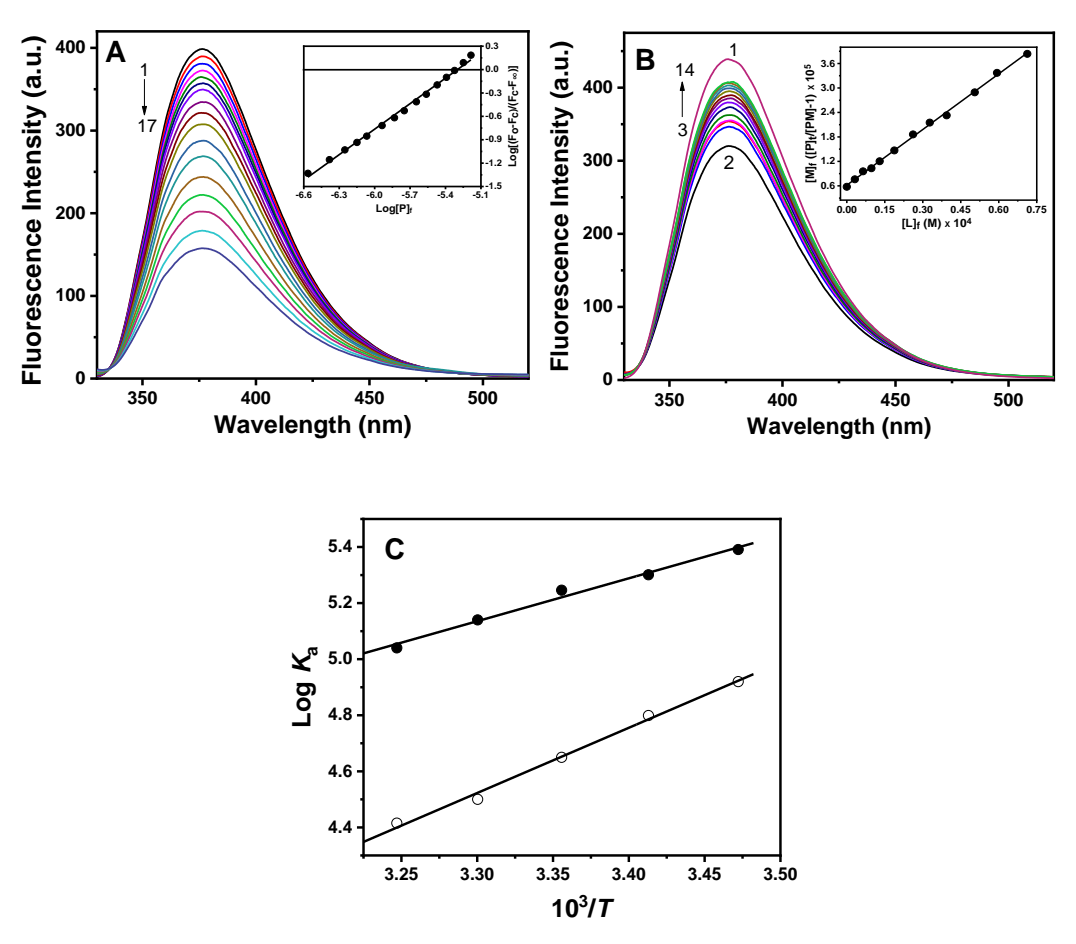


**Fig. 5.8.** Fluorescence titration of MeUmbβ(GlcNAc)<sub>3</sub> with BGL24 and reversal titration with chitotriose at 20 °C. (A) Fluorescence emission spectra of MeUmbβ(GlcNAc)<sub>3</sub> in the absence and presence of BGL24. Spectrum 1 corresponds to MeUmbβ(GlcNAc)<sub>3</sub> alone and spectra 2-17 correspond to those recorded in the presence of increasing concentration of BGL24. *Inset*, double logarithmic plot of the titration data according to Eq. 5.2. The X-intercept of the plot gives  $pK_a$  of the binding equilibrium, from which the association constant  $K_a$  was estimated as  $2.46 \times 10^5$  M<sup>-1</sup>. (B) Fluorescence emission spectra of MeUmbβ(GlcNAc)<sub>3</sub> in the absence and presence of BGL24 and chitotriose. Spectrum 1 refers to the chromophoric ligand alone, spectrum 2 corresponds to the mixture of MeUmbβ(GlcNAc)<sub>3</sub> and BGL24, whereas spectra 3-14 were obtained in the presence of increasing concentration of chitotriose. From the plot in the *Inset*, the association constants of  $K_M = 1.298 \times 10^5$  M<sup>-1</sup> for the indicator ligand and  $K_L = 0.63 \times 10^{-1}$  for the indicator ligand and  $K_L = 0.63 \times 10^{-1}$  for the indicator ligand and  $K_L = 0.63 \times 10^{-1}$  for the indicator ligand and  $K_L = 0.63 \times 10^{-1}$  for the indicator ligand and  $K_L = 0.63 \times 10^{-1}$  for the indicator ligand and  $K_L = 0.63 \times 10^{-1}$  for the indicator ligand and  $K_L = 0.63 \times 10^{-1}$  for the indicator ligand and  $K_L = 0.63 \times 10^{-1}$  for the indicator ligand and  $K_L = 0.63 \times 10^{-1}$  for the indicator ligand and  $K_L = 0.63 \times 10^{-1}$  for the indicator ligand and  $K_L = 0.63 \times 10^{-1}$  for the indicator ligand and  $K_L = 0.63 \times 10^{-1}$  for the indicator ligand and  $K_L = 0.63 \times 10^{-1}$  for the indicator ligand and  $K_L = 0.63 \times 10^{-1}$  for the indicator ligand and  $K_L = 0.63 \times 10^{-1}$  for the indicator ligand and  $K_L = 0.63 \times 10^{-1}$  for the indicator ligand and  $K_L = 0.63 \times 10^{-1}$  for the indicator ligand and  $K_L = 0.63 \times 10^{-1}$  for the indicator ligand  $K_L = 0.63 \times 10^{-1}$  for the indicator ligand  $K_L = 0.63 \times 10^{-1}$  for the indica

 $10^5$  M<sup>-1</sup> for the inhibitory ligand have been obtained. (C) van't Hoff plots for MeUmbβ(GlcNAc)<sub>3</sub> ( $\bullet$ ) and (GlcNAc)<sub>3</sub> ( $\circ$ ).

The titration data was then analysed further according to the following equation [Chipman et al., 1967; Komath et al., 2001; Sanadi and Surolia, 1994]:

$$\log [(F_0 - F_c)/(F_c - F_\infty)] = pK_a + \log [P]_f$$
(5.1)

where  $F_{\infty}$  is the fluorescence intensity when all the fluorescent ligand is bound to the protein and  $[P]_f$  is the free protein concentration, given by the expression:

$$[P]_{f} = [P]_{t} - [M]_{t} \times [(F_{o} - F_{c})/(F_{c} - F_{\infty})]$$
(5.2)

where [P]<sub>t</sub> and [M]<sub>t</sub> are the total concentrations of the protein and the fluorescently labeled ligand, respectively. From the X-intercepts of plots of log [(F<sub>o</sub>-F<sub>c</sub>)/(F<sub>c</sub>-F<sub> $\infty$ </sub>)] vs log [P]<sub>f</sub> the association constants,  $K_a$  for the binding of MeUmb $\beta$ (GlcNAc)<sub>3</sub> to BGL24 were determined at different temperatures. From a van't Hoff plot of these temperature dependent values of  $K_a$  (see Table 5.3), the enthalpy of binding ( $\Delta H$ ) and entropy of binding ( $\Delta S$ ) for this interaction were obtained as -29.3 kJ mol<sup>-1</sup> and +1.67 J mol<sup>-1</sup>K<sup>-1</sup>, respectively.

**Table 5. 3.** Association constants ( $K_a$ ) for the binding of MeUmb(GlcNAc)<sub>3</sub> to BGL24 at different temperatures.

Temperature (°C)	$K_{\rm a} \times 10^{-5}  ({\rm M}^{-1})$
15	2.46
20	2.00
25	1.76
30	1.38
35	1.10

The interaction of the nonfluorescent chitooligosaccharides (chitotriose, chitoteraose, chitopentaose and chitohexaose) to BGL24 was investigated by monitoring the increase in fluorescence intensity of a mixture of the lectin and MeUmb $\beta$ (GlcNAc)<sub>3</sub>

on addition of the inhibitory ligands according to Eq. 5.3 [Komath et al., 2001; Sanadi and Surolia, 1994]:

$$\{[P]_{\ell}[PM]-1\} [M]_f = (K_L/K_M) [L]_f + 1/K_M$$
(5.3)

where  $[P]_t$ , [PM],  $[M]_f$ , and  $[L]_f$  correspond to the concentrations of the total protein, the protein-indicator ligand complex, free indicator ligand and free inhibiting ligand, respectively. The intercept and slope of the straight line obtained from the plot of  $\{[P]_t/[PM]-1\}$   $[M]_f$  vs  $[L]_f$  yield the association constants for both the indicator ligand  $(K_M)$  and inhibitory ligand  $(K_L)$ . The values thus obtained are listed in Table 5.4.

**Table 5.4.** Association constants,  $K_L$  and  $K_M$  for the binding of chitooligosaccharides and MeUmb $\beta$ (GlcNAc)<sub>3</sub> to BGL24 determined from reversal titrations. Values in parentheses are standard deviations from 2-4 independent titrations.

Ligand	T (°C)	$K_{\rm L} \times 10^{-4}  ({ m M}^{-1})$	$K_{\rm M} \times 10^{-4}  ({ m M}^{-1})$
(GlcNAc) <sub>3</sub>	15	8.4 (± 3.2)	12.0 (± 0.3)
,,	20	6.3 (± 1.3)	11.4 (± 1.6)
,,	25	4.5 (± 0.4)	$9.9 (\pm 0.2)$
,,	30	$3.4 (\pm 0.3)$	$8.6 (\pm 0.4)$
,,	35	$2.6 (\pm 0.5)$	$6.7 (\pm 0.5)$
(GlcNAc) <sub>4</sub>	20	14.3 (± 2.8)	12.0 (± 2.4)
(GlcNAc) <sub>5</sub>	20	15.3 (± 2.1)	11.2 (± 2.5)
(GlcNAc) <sub>6</sub>	20	17.9 (± 2.3)	10.9 (± 1.7)

The data presented in Table 5.4 shows that the binding constants for the association of chitooligosaccharides with BGL24 increase considerably when the oligosaccharide size is increased from triose  $(6.3 \times 10^4 \text{ M}^{-1})$  to tetraose  $(1.43 \times 10^5 \text{ M}^{-1})$ , whereas only marginal increases are observed with pentaose  $(1.53 \times 10^5 \text{ M}^{-1})$  and

hexaose  $(1.79 \times 10^5 \text{ M}^{-1})$ . These results are consistent with the results of hemagglutination-inhibition presented in Section 5.4.3. In addition, these results suggest that the lectin combining site most likely accommodates a tetrasaccharide and the marginal increase in binding affinity when the oligosaccharide size is increased beyond tetraose most likely arises due to increase in statistical probability of binding.

From the temperature dependent association constants presented in Table 5.4, the thermodynamic parameters for the BGL24-chitotriose interaction were obtained by means of a van't Hoff plot as  $\Delta H = -44.6 \text{ kJ mol}^{-1}$ ,  $\Delta S = -60.5 \text{ J mol}^{-1}\text{K}^{-1}$ . These values clearly suggest that chitooligosaccharide binding to BGL24 is driven by enthalpic forces with negative contribution from entropy. A comparison of the enthalpy and entropy of binding for MeUmb $\beta$ (GlcNAc)<sub>3</sub> and chitotriose reveals that although the enthalpy of binding for the unlabeled chitotriose is about 1.5-fold higher than the value obtained for the fluorescently labeled sugar, due to the large negative contribution from binding entropy the association constant becomes 3-fold weaker. Thus the stronger binding of MeUmb $\beta$ (GlcNAc)<sub>3</sub> as compared to (GlcNAc)<sub>3</sub> is due to a smaller negative contribution from entropy of binding for the methylumbelliferyl glycoside.

It is interesting to compare the association constants and the corresponding thermodynamic parameters for the binding of chitotriose and its 4-methylumbelliferyl derivative to BGL24 with those obtained for the interaction of these two ligands with other Cucurbitaceae phloem lectins reported earlier. Fluorescence spectroscopic titrations yielded the association constant for the binding of MeUmb $\beta$ (GlcNAc)<sub>3</sub> to *Coccinia indica* agglutinin (CIA) at 25 °C is  $2.82 \times 10^5$  M<sup>-1</sup>, which is about 60% higher than the value of  $1.76 \times 10^5$  M<sup>-1</sup> obtained for BGL24 in the present study [Sanadi and Surolia, 1994]. Association constants in the range of  $9.6 \times 10^4$  -  $1.95 \times 10^5$  M<sup>-1</sup> were obtained by ITC measurements at 25 °C for the binding of chitotriose to several Cucurbitaceae phloem exudate lectins such as CPL, PPL, CIA17, CIA24 and SGPL [Anantharam et al., 1986; Nareddy et al., 2017; Rabbani et al., 2014; Narahari et al., 2011; Bobbili et al., 2019]. The association constant of  $6.3 \times 10^4$  M<sup>-1</sup> obtained here for the BGL24-chitotriose

interaction is smaller than all these values, but about 8-fold higher than the value of  $8.0 \times 10^3 \, \text{M}^{-1}$  obtained for the binding of chitotriose to LAA at 25 °C.

For Luffa acutangula agglutinin (LAA), the binding constants are  $1.26 \times 10^4$ , 9.7  $\times$  10<sup>4</sup> and 6.5  $\times$  10<sup>5</sup> M<sup>-1</sup> for chitotriose, chitotetraose and chitopentaose, respectively, indicating that increasing the chitooligosaccharide size results in additional interactions of the ligand with the lectin combining site [Anantharam et al., 1986; Anantharam et al., 1985]. The dimeric PPL and SGPL bind to (GlcNAc)<sub>3-5</sub> with binding constants ranging between  $1.26 \times 10^5$  and  $1.53 \times 10^5$  M<sup>-1</sup>, and  $1.7 \times 10^5$  and  $3.6 \times 10^5$  M<sup>-1</sup>, respectively, at 25 °C as determined by isothermal titration calorimetric (ITC) studies [Narahari et al., 2011; Rabbani et al., 2015]. The association constants for CPL were in the range of 1.11 to  $1.92 \times 10^5$  M<sup>-1</sup> for chitotriose to chitopentaose [Nareddy et al., 2018]. For CIA17, the binding constant increases for triose, tetraose and pentaose with K<sub>a</sub> values ranging between  $3.5 \times 10^5$  to  $4.3 \times 10^5$  M<sup>-1</sup> [Bobbili et al., 2019], and for CIA24, the affinity towards chitotriose is moderate ( $K_a = 2.7 \times 10^4 \,\mathrm{M}^{-1}$ ) which increases for to  $1.13 \times 10^5 \,\mathrm{M}^{-1}$ for chitopentaose [Bobbili et al., 2018b]. These observations clearly indicate that the affinity towards higher oligosaccharides increses for all the lectins cited here, but for PPL, CPL and CIA17, a dramatic increase in the association constant was observed for chitohexaose. BGL24 binds chitooligisacharides in a specific manner and the affinity towards the (GlcNAc)<sub>3-6</sub> is similar to the homodimeric CIA24 and SGPL.

# 5.4.7. Cytotoxicity

Cytotoxicity of BGL24 towards normal splenocytes and epithelial, triple negative breast cancer cells (MDA-MB-231) was evaluated colorimetrically by measuring changes in the absorption intensity at 570 nm due to the formation of purple-coloured formazan, resulting from the reduction of MTT by the cellular oxidoreductase enzymes [Rabbani et al., 2018]. The cytotoxicity of jacalin was also assessed to compare its effect with that of BGL24 on the two cell lines. The results of these studies, presented in Fig. 5.9 show that cell viability of MDA-MB-231 cell line decreased to 82% upon treatment with a relatively low concentration (125  $\mu$ g/mL) of BGL24 whereas only a marginal decrease (cell viability = 94%) was observed upon incubation with the same concentration of

jacalin. Upon incubation with higher doses (1 mg/mL), the cell viability decreased to 63% for BGL24 and 68% for jacalin. Although the viability of normal splenocytes was almost unaffected with 125  $\mu$ g/mL of either lectin, at 1 mg/mL concentration of the lectins, viability of normal cells decreased to 80% when incubated with jacalin, whereas the corresponding value for BGL24 was 88%. These results demonstrate that BGL24 exhibits higher cytotoxicity against MDA-MB-231 cancer cell line than jacalin, but lower cytotoxicity on normal splenocytes.

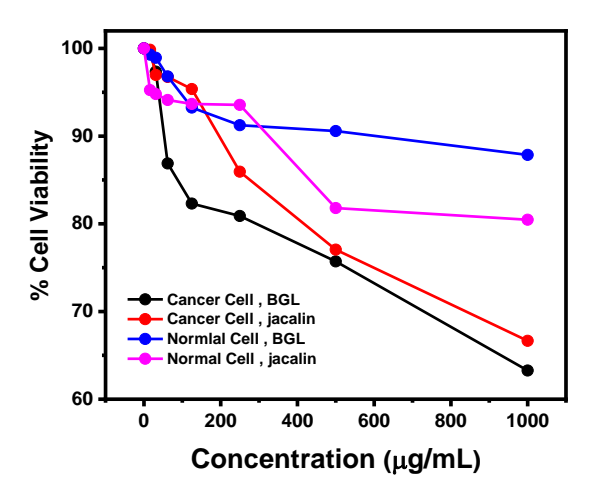


**Fig. 5.9.** Effect of jacalin and BGL24 on the viability of normal spleenocytes and MDA-MB-231 breast cancer cells. Cell viability was estimated by the MTT assay after treating both the cells with different concentrations of each lectin for 72 hrs.

Lectins are thought to play a major role in plant defense against viral, bacterial, fungal and insect attack by interacting with the carbohydrate structures present on the cell surfaces of these infectious agents [Peumans and Van Damme, 1995]. In our previous work, cell viability assays revealed that jacalin and mulberry latex galactose-specific lectin (MLGL), an α-D-galactose specific jacalin related lectin (gJRL) exhibit cytotoxicity against epithelial (MDCK) as well as breast cancer cells (MCF7) [Datta et al., 2016]. It was proposed that this could be due to an interaction between the lectins and tumor associated TF-antigen, expressed on the breast cancer cell surface [Cazet et al., 2010; Datta et al., 2016]. PP2-type lectins such as *Luffa acutangula* agglutinin and *Coccinia indica* agglutinin have been shown to bind to *N*-linked oligosaccharides

containing core chitobiose structure [Anantharam et al., 1986; Sanadi and Surolia, 1994]. It is likely that the cytotoxicity of BGL24 and other PP2-type, chitooligosaccharide-binding lectins is mediated by their interaction with *N*-linked oligosaccharides attached to the cell surface glycoproteins on the target cells. Since our results demonstrate that BGL24 is more cytotoxic against MDA-MB-231 cancer cells than normal splenocytes as compared to jacalin, BGL24 might be exhibiting the cytotoxity by interacting with the *N*-linked glycans expressed more on the cell surface of the breast cancer cells than the norman splenocytes. Further work is required to investigate the mechanism of cytotoxicity of BGL24 in more detail and also to explore its potential in therapeutic applications to treat malignant tumors.

#### 5.5. Conclusions

In summary, in the present work, a chitooligosaccharide binding, PP2-type lectin (BGL24) was purified from the phloem exudate of bottle gourd (Lagenaria siceraria) by affinity chromatography. BGL24 is a homodimer in which the two subunits of ~24 kDa mass are connected via disulfide linkage(s). At higher concentrations, BGL24 self assembles to form oligomers of higher molecular weight. BGL24 is highly homologous to other Cucurbitaceae phloem exudate PP2-type lectins and proteins with high β-sheet content. CD spectroscopic studies showed that the secondary structure of BGL24 is stable up to >70°C and over a broad pH range (3.0-8.0). At physiological pH, BGL24 undergoes irreversible thermal unfolding and the unfolding thermogram could be resolved into three overlapping endotherms centered at ~69.5, 79.0 and 83.2 °C, respectively. Fluorescence titrations on the binding of MeUmbβ(GlcNAc)<sub>3</sub> to BGL24 and reversal titrations with chitooligosaccharides revealed that the association constants for the binding of the fluorescently labeled sugar is about 3-fold higher than the unlabeled chitotriose, which could be attributed to a smaller negative entropic contribution associated with the labeled sugar. Further, the association constants for the unlabeled chitooligosaccharides were found to increase significantly from trisaccharide to tetrasaccharide, but only marginally with further increase in the oligosaccharide size. The cyctotoxicity of BGL24 towards epithelial, triple negative breast cancer cells (MDA- MB-231) is higher than that for normal splenocytes. Further studies are required to investigate the anticancer activity of BGL24 in more detail, and to investigate its role in long distance trafficking of nutrients, sugars, RNA etc as well as in wound sealing mechanism to protect the plant against pathogen attack. Such studies are currently underway in our laboratory.

## General Discussion, Conclusions and Future Prospects



#### 6.1. General Discussion and Conclusions

The thesis primarily describes the structure and conformational dynamics, (un)folding pathway and carbohydrate binding of *Coccinia indica* agglutinin (CIA17), a PP2 type phloem exudate lectin from ivy gourd. In addition, the purification and characterization of a new PP2 like lectin from the phloem exudate of bottle gourd (*Lagenaria siceraria*) and thermodynamic analysis of its chitooligosaccharide binding are also reported.

Phloem is the major integral component of the entire plant communication system through which the photoassimilates and other organic molecules are transported over long distances. Phloem sap contains many structurally distinct protein bodies, collectively called as phloem proteins (P-proteins) among which PP1 and PP2 are the major proteins. PP1 is the structural filamentous protein whereas PP2 proteins are involved in plant defence mechanism, in wound sealing and antipathogenic responses. They are thought to interact with RNA molecules to form ribonucleoprotein (RNP) complexes and transport them from cell to cell [Dinant et al., 2003, Read and Northcote, 1983; Will et al., 2013; Beneteau et al., 2010; Will et al., 2006; Gómez and Pallás, 2004; Gómez et al., 2005; Zhang et al., 2013]. While PP1 proteins do not exhibit any ligand binding ability, PP2 proteins have been shown to exhibit lectin activity. Cucurbitaceae fruits are highly enriched with these PP2 lectins which have a common chitin binding domain and bind to chiooligisaccharides specifically. The potential involvement of these PP2 type lectins in plant growth and development, as well as plant defence responses make it important to understand their structure-function relationship.

Unfolding of an oligomeric protein is still an unsolved and challenging problem since its complexity arises from different kinds of inter-subunit interactions as well as intramolecular interactions. For example, soyabean agglutinin and concanavalin A exist as tetramers which unfold in a two-state manner with the folded-unfolded state in equilibrium whereas unfolding process of another tetrameric lectin, peanut agglutinin or *Erythrina cristagalli* lectin involves several intermediate states [Gaikwad et al., 2002; Reddy et al., 1999; Sen and Mandal, 2014; Sinha et al., 2005]. Although several phloem exudate lectins have been purified and characterized, there have been no reports on the (un)folding

dynamics of any of them, several of which have been shown to exist as polydisperse aggregates in solution. In this context, *Coccinia indica* agglutinin (CIA17) will be very interesting to study with respect to the unfolding dynamics since CIA17 was reported to form larger soluble aggregates in solution. The question that arises here is whether CIA17 unfolds in a single step process with the folded and unfolded state in the equilibrium or it undergoes the formation one or more intermediates and if the intermediates formed what will be the nature of those intermediates?

Chapter 2 addresses the above questions and presents a detailed mechanism of thermal and chemical unfolding of Coccinia indica agglutinin (CIA17), a chitooligosacharide-specific phloem exudate lectin. The results obtained demonstrate that CIA17 is a highly thermostable protein with an unfolding temperature of  $T_{\rm m} \sim 109$  °C (midpoint of transition). Thermal unfolding of CIA17 is a complex process involving three transitions with T<sub>m</sub> ~98, 106 and 109 °C which could be assigned to the dissociation of protein oligomers into constituent dimers followed by the dissociation of the dimers into monomers, and complete unfolding of the monomers. Chemical unfolding of CIA17 also involves two distinct steps which could be attributed to the dissociation of the dimeric protein into monomers and unfolding of the monomers. The difference observed in the thermal and chemical unfolding pathway of the protein is possibly due the large differences in the concentrations of CIA17 used in the DSC and fluorescence studies, employed in the thermal and chemical unfolding studies, respectively, emphasising the fact that CIA17 forms oligomers in a concentration dependent manner. The hypothesis "concentration dependent oligomerization of CIA17" was probed by fluorescence correlation spectroscopic (FCS) studies. The results showed that the protein exists as a monomer below 1 nM concentration, but associates to form dimers at higher concentrations with a dissociation constant (K<sub>D</sub>) of ~2.9 nM. The dimers associate to yield tetramers with a K<sub>D</sub> of ~47 µM, which further associate to form higher oligomers with further increase in concentration. The phloem sap contains ~6-8 mg/ml of the protein which has utmost strong propensity to form higher oligomers (≥ tetramer). The phloem fluid oozing out of the wound (or cut) is a clear liquid consisting of those large soluble oligomers/aggregates

which associate further to form a jelly like substance through the formation of disulphide linkages upon exposure to the air and thus seals the wound. Incubation of the protein with 10 mM DTT results in a single monomer to dimer equilibrium suggesting that the blocking of the disulfide linkages with strong reducing agents prevents the formation of higher oligomers. These are the novel results which describe the proposed role of CIA17 as a key player in the defence response of the plant against microbes and insects.

The complexity observed in the thermal and chemical unfolding of CIA17 prompted us to investigate the effect of changing pH on the conformation, structural dynamics as well as carbohydrate-binding activity of CIA17 and the results of detailed studies on this aspect have been reported in *Chapter 3*. The secondary structure of CIA17 remains almost unaltered over a wide pH range (8.5-2.0) while the tertiary structure of the protein was significantly modulated with the change in pH as indicated by CD spectroscopic studies. Intensity of the protein intrinsic fluorescence and the average fluorescence lifetime decrease with decrease in pH which indicated perturbations in the local conformation of the lectin (near Trp residues). CIA17 contains nine tryptophan residues which are neither totally buried inside the hydrophobic interior of the protein nor completely exposed on the hydrophilic surface, but are most likely distributed across various degrees of exposure to the aqueous medium. At pH 2.0 the Trp accessibility increased largely towards external charged quenchers such as iodide and cesium ion when compared to that of the native protein indicating that low pH (pH 2.0) induced considerable perturbation in the protein structure. This conformational change of the protein was accompanied by the exposure of hydrophobic regions on the protein surface as indicated by change in the ANS fluorescence spectra in presence of the lectin at different pH. Further, results of FCS studies indicated considerable change in the size and conformational dynamics of the protein at low pH. At pH 2.0 the lectin exists as a monomer over the concentration range of 10-200 nM and forms dimers at higher concentrations (K<sub>D</sub> ≈ 387 nM) but couldn't form higher oligomers even at significantly higher concentrations ( $\sim$ 57  $\mu$ M) unlike the native protein (at pH 7.4). The unfolding temperature decreases from 109 °C to 72 °C as the pH decreases from 7.4 to 2.0 and the unfolding of the pH 2.0 intermediate involves a two steps process: the homo-dimeric lectin dissociates into monomeric molten-globule-like state followed by the complete unfolding of the monomers. The first transition due to the dissociation of oligomer to dimeric constituents which was observed for the native protein (pH 7.4) was not observed for the lectin at pH 2.0. The intermediate retains a considerable degree of chitooligosaccharide binding ability.

The presence of different solutes and macromolecules makes the intracellular environment very different from the dilute buffer medium where most of the biophysical/biochemical studies have been carried out so far. The crowded environment can influence the conformation, structure as well as the activity of proteins. The effect of molecular crowding on the structure and function of lectins, specifically phloem exudate lectins is yet to be unraveled. In order to understand the effect of macromolecular crowding on the conformational features of the protein and how it affects carbohydrate binding properties of CIA17, polymeric dextrans of different sizes such as D6, D40 and D70 have been employed as crowding agents in the work presented in Chapter 4. The results obtained demonstrated the secondary structure of CIA17 remains essentially unaffected in the presence of higher molecular weight dextrans (D70 and D40) while appreciable changes were observed in the presence of D6. The tertiary structure of the protein was significantly modulated by all three crowders as indicated by the crowder-induced quenching of the intrinsic protein fluorescence. While the larger dextrans, D70 and D40 induced modest quenching (~10%) of the protein fluorescence by a predominantly static pathway, D6 induced maximum quenching (37%) involving both static and collisional quenching processes. The crowder-induced perturbation of the local conformation of the lectin was further investigated by monitoring the Trp accessibility in presence of crowding agents towards the external quenchers like acrylamide and iodide ion. Least quenching observed for both the quenchers in presence of D6 among the three crowders employed is possibly due to the highest excluded volume effect and lower availability of some of the fluorophores which are quenched directly by D6 molecules via a collisional pathway. Association constant for the CIA17-chitotriose interaction increased by 33% and 260% in the presence of D40 and D70, whereas it decreased by 33% in presence of D6. The higher binding affinity in presence of D40 and D70 is possibly due to the more compact structure

and due to the increased effective concentration of the protein and sugar which result from the replacement of water structure from the bulk by the crowder molecule under excluded volume effect. On the other hand, D6 being smaller in size, can possibly penetrate into the protein interior and disrupt the water structure from the bulk as well as from the binding pocket, weaken water mediated H-bonding interaction between the protein and sugar molecules, which results in a decrease in the binding constant. These observations demonstrate that the structure, conformation as well as carbohydrate binding characteristics of the lectin are affected to different extent in differently crowded environments which is relevant to understanding how protein-carbohydrate interactions can be modulated under physiological conditions *in vivo*.

Chapter 5 reports the purification and characterization of a new PP2-type lectin, BGL24 from the phloem exudate of bottle gourd (Lagenaria siceraria). BGL24 was purified using affinity chromatography on  $\alpha$ -chitin and the protein eluted as a single peak which gives a single band on native PAGE. SDS-PAGE analysis under nonreducing and reducing conditions indicated that the protein exists as homo-dimer with a subunit mass of ~24 kDa and the subunits are interconnected with a disulfide linkage which couldn't be cleaved fully even by the use of strong reducing agents like DTT. BGL24 agglunitates human erythrocytes and exhibits high specificity for chitooligosaccharides. The isoelectric point of BGL24 was estimated from zeta potential measurements as 5.95. Partial amino acid sequence obtained by mass spectrometric studies indicated that BGL24 is highly homologous with other PP2-type phloem exudate lectins. The lectin contains  $\beta$ -sheet predominantly with low α-helical content in its secondary structure. BGL24 is thermally quite stable with an unfolding temperature of ~82 °C at physiological pH, and undergoes irreversible thermal unfolding. Similar to the unfolding of CIA17, the unfolding thermogram of BGL24 consisted of three overlapping endotherms centered at ~69.5, 79.0 and 83.2 °C, respectively, which can be attributed to the dissociation of oligomer to dimer, dimer dissociating to monomer followed by the unfolding of monomer. Fluorescence titrations employing 4-methylumbelliferyl-β-D-N,N',N''-triacetylchitotrioside as an indicator ligand revealed that the association constants for BGL24-chitooligosaccharide interaction increase considerably when the ligand size is increased from chitotriose to

chitotetraose, whereas only marginal increase was observed when the size of the oligosaccharide was further increased to chitopentaose and chitohexaose. BGL24 is more cytotoxic against MDA-MB-231 cancer cells than normal splenocytes. The cytotoxicity might be mediated by the interaction of BGL24 with the *N*-linked glycans of the glycoconjugates expressed on the cell surface. The observation perhaps can be related to the antipathogenic responses of the plant.

#### **6.2. Future Directions**

The role of PP2 lectins in wound sealing is still not clearly understood. The phloem sap that oozes out through the cut/wound of the surface of the plant tissues (e.g., raw fruits) can form jelly like substances in air i.e., under oxidative environment. This process perhaps involves the formation of disulfide linkages between two PP2 proteins or between PP2 protein and PP1 protein, resulting in a larger filamentous structure. Although the concentration dependent oligomerization of CIA17, a PP2 type lectin has been investigated in detail, PP1-PP2 interaction is not studied so far. Therefore, it will be interesting to isolate, purify and characterize the PP1 protein from the same fruit along with the purification of PP2 lectin and investigate PP1-PP2 interaction in detail.

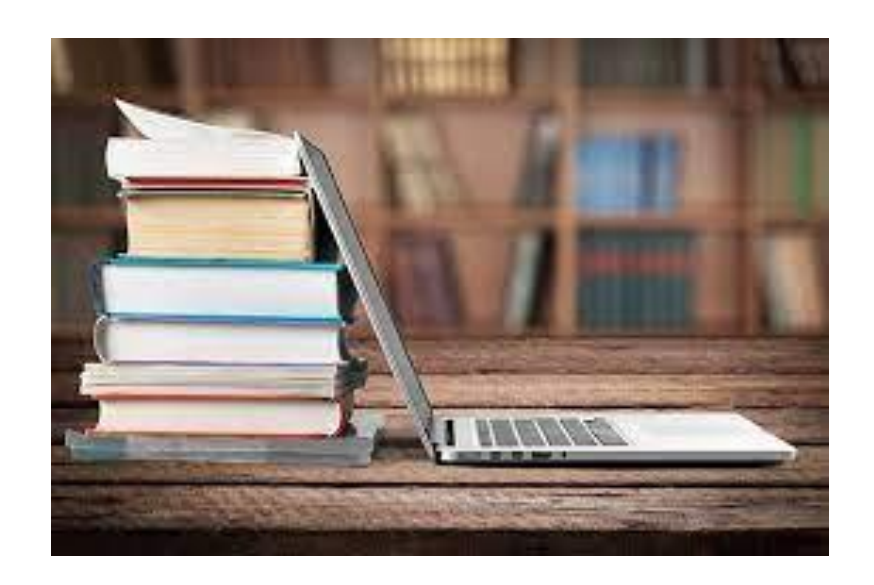
PP2 proteins have been reported to exhibit characteristics such as long-distance translocation, RNA-binding activity and capacity to increase plasmodesmata exclusion size, which suggests that certain phloem proteins could be involved in RNA transport within the plants. How these RNA molecules translocate through the phloem is not well understood, though recent evidence indicates the presence of translocatable RBPs in the phloem, which act as potential components of long-distance RNA transport system. In view of this, Thermodynamic parameters associated with the RNA binding of several reported phloem lectins should also be studied, which can provide clues to understand the role of phloem lectins in RNA transport.

Although phloem conducts several organic molecules other than photoassimilates e.g., phytohormones, methyl jasmonate etc from source to sink tissue, the involvement of the PP2 lectins in transport of non-carbohydrate organic molecules is not well understood.

In view of this, the non-carbohydrate ligands binding of several reported phloem lectins can be studied further.

Crowders have been shown to increase protein aggregation and/or oligomerization. Many lectins, especially PP2 lectins have been shown to oligomerize at higher concentration. How molecular crowding will affect the oligomerization will be interesting to investigate in future.

## References



Ahmad, I.; Irshad, M.; Rizvi, M. M. A. Nutritional and Medicinal Potential of *Lagenaria siceraria*. *Int. J. Veg. Sci.* **2011**, *17*, 157-170.

Alexov, E. Numerical Calculations of the pH of Maximal Protein Stability. The Effect of the Sequence Composition and Three-Dimensional Structure. *Eur J Biochem.* **2004**, *271*, 173-85.

Ali, M. H.; Imperiali, B. Protein Oligomerization: How and Why. *Bioorg. Med. Chem.* **2005**, *13*, 5013–5020.

Anantharam, V.; Patanjali, S. R.; Surolia, A. A Chitotetrose Specific Lectin from Luffa acutangula: Physico-Chemical Properties and the Assignment of Orientation of Sugars in the Lectin Binding Site. J. Biosci. **1985**, *8*, 403-411.

Anantharam, V.; Patanjali, S. R.; Swamy, M. J.; Sanadi, A. R.; Goldstein, I. J.; Surolia, A. Isolation, Macromolecular Properties, and Combining Site of a Chito-Oligosaccharide-Specific Lectin from the Exudate of Ridge Gourd (*Luffa acutangula*). *J. Biol. Chem.* **1986**, 261, 14621–14627.

Balachandran, S.; Xiang, Y.; Schobert, C.; Thomson, G. A.; Lucas, W. J. Phloem Sap Proteins from *Cucurbita maxima* and *Ricinus communis* have the Capacity to Traffic Cell to Cell through Plasmodesmata. *Proc. Natl. Acad. Sci. USA* **1997**, *94*, 14150-14155.

Basak, S.; Chattopadhyay, K. Studies of Protein Folding and Dynamics Using Single Molecule Fluorescence Spectroscopy. *Phys. Chem. Chem. Phys.* **2014**, *16*, 11139-11149.

Beneteau, J.; Renard, D.; Marche, L.; Douville, E.; Lavenant, L.; Rahbe, Y.; Dupont, D.; Vilaine, F.; Dinant, S. Binding Properties of the N-Acetylglucosamine and High-Mannose N-Glycan PP2-A1 Phloem Lectin in *Arabidopsis*. *Plant Physiol.* **2010**, *153*, 1345-1361.

Benton, L. A.; Smith, A. E.; Young, G. B.; Pielak, G. J. Unexpected Effects of Macromolecular Crowding on Protein Stability. *Biochemistry* **2012**, *51*, 9773-9775.

Berg, J. M.; Tymoczko, J. L.; Stryer, L. Biochemistry. 5th edition. New York: W H Freeman; 2002. Chapter 3, Protein Structure and Function.

Beyenbach, J.; Weber, C.; Kleinig, H. Sieve-Tube Proteins from *Cucurbita maxima*. *Planta* **1974**, *119*, 113-124.

Bhanu, K.; Komath, S. S.; Maiya, B. G.; Swamy, M. J. Interaction of Porphyrins with Concanavalin A and Pea Lectin. *Curr Sci.* **1997**, *73*, 598-602.

Bhuyan, A. K.; Udgaonkar, J. B. Folding of Horse Cytochrome C in the Reduced State. *J. Mol. Biol.* **2001**, *312*, 1135–1160.

Bobbili, K. B.; Bandari, S.; Grobe, K.; Swamy, M. J. Mutational Analysis of the Pumpkin (*Cucurbita maxima*) Phloem Exudate Lectin, PP2 Reveals Ser-104 is Crucial for Carbohydrate Binding. *Biochem. Biophys. Res. Commun.* **2014**, *450*, 622-627

Bobbili, K. B.; Singh, B.; Narahari, A.; Bulusu, G.; Surolia, A.; Swamy, M. J. Chitooligosaccharide Binding to CIA17 (*Coccinia indica* agglutinin). Thermodynamic Characterization and Formation of Higher Order Complexes. *Int. J. Biol. Macromol* **2019**, 137, 774-782.

Bobbili, K. B.; Pohlentz, G.; Narahari, A.; Sharma, K.; Surolia, A.; Mormann, M.; Swamy, M. J. *Coccinia indica* Agglutinin, a 17 kDa PP2 Like Phloem Lectin: Affinity Purification, Primary Structure and Formation of Self-Assembled Filaments. *Int. J. Biol. Macromol.* **2018a**, *108*, 1227–1236.

Bobbili, K. B.; Datta, D.; Mondal, S.; Polepalli, S.; Pohlentz, G.; Mormann, M.; Swamy, M. J. Purification, Chitooligosaccharide Binding Properties and Thermal Stability of CIA24, a New PP2-Like Phloem Exudate Lectin from Ivy Gourd (*Coccinia indica*). *Int. J. Biol. Macromol.* **2018b**, *110*, 588–597.

Bogoeva, V. P.; Radeva, M. A.; Atanasova, L. Y.; Stoitsova, S. R.; Boteva, R. N. Fluorescence Analysis of Hormone Binding Activities of Wheat Germ Agglutinin. *Biochim. Biophys. Acta. Prot. Proteom.* **2004**, *1698*, 213-218.

Bonetti, D.; Camilloni, C.; Visconti, L.; Longhi, S.; Brunori, M.; Vendruscolo, M.; Gianni, S. Identification and Structural Characterization of an Intermediate in the Folding of the Measles Virus X Domain. *J. Biol Chem.* **2016**, *291*, 10886-10892.

Bostwick, D. E.; Skaggs, M. I.; Thompson, G. A. Organization and Characterization of *Cucurbita* Phloem Lectin Genes. *Plant Mol. Biol.* **1994**, *26*, 887-897.

Bueter, C. L.; Specht, C. A.; Levitz, S. M. Innate Sensing of Chitin and Chitosan. *PLOS Pathog.* **2013**, *9*, e1003080.

Bundle, D. R.; Young, N. M. Carbohydrate-Protein Interactions in Antibodies and Lectins. *Curr. Opin. Struct. Biol.* **1992**, *2*, 666-673.

Bychkova, V. E.; Ptitsiyn, O. B. Folding Intermediates are Involved in Genetic Diseases. *FEBS Letters* **1995**, *359*, 15076-15078.

Cazet, A.; Julien, S.; Bobowoski, M.; Burchell, J.; Delannoy, P. Tumor-Associated Carbohydrate Antigens in Breast Cancer. *Breast Cancer Res.* **2010**, *12*, 204.

Chakraborty, M.; Kuriata, A. M.; Henderson, J. N.; Salvucci, M. E.; Wachter, R. M.; Levitus, M. Protein Oligomerization Monitored by Fluorescence Fluctuation Spectroscopy: Self Assembly of Rubisco Activase. *Biophys. J.* **2012**, *103*, 949-958.

Charlton, L., Barnes, C., Li, C., Orans, J., Young, G., and Pielak, G. Residue-Level Interrogation of Macromolecular Crowding Effects on Protein Stability. *J. Am. Chem. Soc.* **2008**, *130*, 6826–6830.

Chattopadhyay, K.; Saffarian, S.; Elson, E. L.; Frieden, C. Measuring Unfolding of Proteins in the Presence of Denaturant Using Fluorescence Correlation Spectroscopy. *Biophys. J.* **2005**, 88, 1413–1422.

Chen, C. S.; Chen, C. Y.; Ravinath, D. M.; Bungahot, A.; Cheng, C. P.; You, R. I. Functional Characterization of Chitin-Binding Lectin from Solanum integrifolium Containing Anti-Fungal and Insecticidal Activities. *BMC Plant Biol.* **2018**, *18*, 1-11.

Chen, H.; Ahsan, S. S.; Santiago-Berrios, M. B.; Abruña, H. D.; Webb, W. W. Mechanisms of Quenching of Alexa Fluorophores by Natural Amino Acids. *J. Am. Chem. Soc.* **2010**, *132*, 7244–7245.

Chen, Y.; Barkley, M. D. Toward Understanding Tryptophan Fluorescence in Proteins. *Biochemistry* **1998**, *37*, 9976-9982.

Cheung, M. S.; Klimov, D.; Thirumalai, D. Molecular Crowding Enhances Native State Stability and Refolding Rates of Globular Proteins. *Proc. Natl. Acad. Sci. U. S. A.* **2005**, *102*, 4753-4758.

Chipman, D. M.; Grisaro, V.; Sharon, N. Binding of Oligosaccharides Containing N-Acetylglucosamine and N-Acetylmuramic Acid to Lysozyme: The Specificity of Binding Subsites. *J. Biol. Chem.* **1967**, *242*, 4388-4394.

Choi, J.; Kim, S.; Tachikawa, T.; Fujitsukaa, M.; Majima, T. Unfolding Dynamics of Cytochrome C Revealed by Single-Molecule and Ensemble-Averaged Spectroscopy. *Phys. Chem. Chem. Phys.* **2011**, *13*, 5651-5658.

Christiansen, A.; Wang, Q.; Samiotakis, A.; Cheung, M. S.; Wittung-Stafshede, P. Factors Defining Effects of Macromolecular Crowding on Protein Stability: An in Vitro/in Silico Case Study Using Cytochrome C. *Biochemistry* **2010**, *49*, 6519–6530.

Cole, N.; Ralston, G. B. Enhancement of Self-Association of Human Spectrin by Polyethylene Glycol. *Int. J. Biochem.* **1994**, *26*, 799-804.

Dam, T. K.; Brewer, C. F. Thermodynamic Studies of Lectin-Carbohydrate Interactions by Isothermal Titration Calorimetry. *Chem. Rev.* **2002**, *102*, 387–430.

Das, N.; Sen, P. Structural, Functional, and Dynamical Responses of a Protein in a Restricted Environment Imposed by Macromolecular Crowding. *Biochemistry* **2018**, *57*, 6078-6089.

Das, S; De, A; Samanta, A. Ambient Condition Mg<sup>2+</sup> Doping Producing Highly Luminescent Green- and Violet-Emitting Perovskite Nanocrystals with Reduced Toxicity and Enhanced Stability. *J. Phys. Chem. Letters* **2020**, *11*, 1178-1188.

Datta, D.; Pohlentz, G.; Schulte, M.; Kaiser, M.; Goycoolea, F. M.; Müthing, J.; Mormann, M.; Swamy, M. J. Physico-Chemical Characteristics and Primary Structure of an Affinity-Purified A-D-Galactose-Specific, Jacalin-Related Lectin from the Latex of Mulberry (*Morus indica*). *Arch. Biochem. Biophys.* **2016**, *609*, 59-68.

Dhara, A.; Samiotakis, A.; Ebbinghausa, S.; Nienhausa, L.; Homouz, D.; Gruebele, M.; Cheung, M. S. Structure, Function and Folding of Phosphoglycerate Kinase are Strongly Perturbed by Macromolecular Crowding. *Proc. Natl. Acad. Sci. U.S.A.* **2010**, *107*, 17586-17591.

Dimick, S. M.; Powell, S. C.; McMahon, S. A.; Moothoo, D. N.; Naismith, J. H.; Toone, E. J. On the Meaning of Affinity: Cluster Glycoside Effects and Concanavalin A. *J. Am. Chem. Soc.* **1999**, *121*, 10286-10296.

Dinant, S.; Clark, A. M.; Zhu, Y.; Vilaine, F.; Palauqui, J. C.; Kusiak, C.; Thompson, G. A. Diversity of the Super Family of Phloem Lectins (Phloem Protein 2) in Angiosperm. *Plant Physiol.* **2003**, *131*, 114-128.

Drickamer, K.; Taylor, M. E. Biology of Animal Lectins. *Annu Rev cell biology*, **1993**, 9, 237-264.

Duy, C.; Fitter, J. How Aggregation and Conformational Scrambling of Unfolded States Govern Fluorescence Emission Spectra. *Biophys. J.* **2006**, *90*, 3704-3711.

Eftink, M. R. The Use of Fluorescence Methods to Monitor Unfolding Transitions in Proteins. *Biophys. J.* **1994**, 66, 482-501.

Ellis, R. J. Macromolecular Crowding: Obvious but Under Appreciated. *Trends Biochem. Sci.* **2001**, *26*, 597-604.

Elgavish, S.; Shaanan, B. Lectin-Carbohydrate Interactions: Different Folds, Common Recognition Principles. *Trends Biochem. Sci.* **1997**, *12*, 462-467.

Esau, K.; Cronshaw, J. Tubular Components in Cells of Healthy and Tobacco Mosaic Virus-Infected *Nicotiana*. *Virology* **1967**, *33*, 26-35.

Fan, Y. Q.; Liu, H. J.; Li, C.; Luan, Y. S.; Yang, J. M.; Wang, Y-L. Effects of Macromolecular Crowding on Refolding of Recombinant Human Brain-Type Creatine Kinase. *Int. J. Biol. Macromol.* **2012**, *51*, 113-118.

Feige, M. J.; Groscurth, S.; Marcinowski, M.; Yew, Z. T.; Truffault, V.; Paci, E.; Kessler, H.; Buchner, J. The Structure of a Folding Intermediate Provides Insight into Differences in Immunoglobulin Amyloidogenicity. *Proc. Natl. Acad. Sci.* **2008**, *105*, 13373-13378.

Fujimoto, Z.; Tateno, H.; Hirabayashi, J. Lectin Structures: Classification Based on the 3-D Structures. *Methods Mol. Biol.* **2014**, *1200*, 579-606.

Gaikwad, S. M.; Gurjar, M. M.; Khan, M. I. *Artocarpus hirsuta* lectin. Differential Modes of Chemical and Thermal Denaturation. *Eur. J. Biochem.* **2002**, *269*, 1413-1417.

Gegg, C. V.; Roberts, D. D.; Segel, I. H.; Etzler, M. E. Characterization of the Adenine Binding Sites of Two Dolichos biflorus Lectins. *Biochemistry* **1992**, *31*, 6938-6942.

Golecki, B.; Schulz, A.; Thompson, G. A. Translocation of Structural P Proteins in the Phloem. *The Plant Cell* **1999**, *11*, 127–140.

Gómez, G.; Pallás, V. Identification of an in Vitro Ribonucleoprotein Complex between a Viroid RNA and a Phloem Protein from Cucumber Plants. *Mol. Plant Microbe Interact.* **2001**, *14*, 910-913.

Gómez G.; Pallás, V. A Long-Distance Translocatable Phloem Protein from Cucumber forms a Ribonucleo Protein Complex *in Vivo* with Hop Stunt Viroid RNA. *J. Virol.* **2004**, 78, 10104-10110.

Gómez, G.; Torres, H.; Pallás, V. Identification of Translocatable RNA Binding Phloem Proteins from Melon, Potential Components of the Long-Distance RNA Transport System. *Plant J.* **2005**, *41*, 107-116.

Goto, Y.; Takahashi, N.; Fink, A. L. Mechanism of Acid-Induced Folding of Proteins. *Biochemistry.* **1990**, *29*, 3480-3488.

Gout, E.; Bligny, R.; Douce, R. Regulation of Intracellular pH Values in Higher Plant Cells. Carbon-13 and Phosphorus-31 Nuclear Magnetic Resonance Studies. *J. Biol. Chem.* **1992**, *267*, 13903-13909.

Griffin, M. D. W.; Gerrard, J. A.; The Relationship between Oligomeric State and Protein Function. In: Matthews J. M. (eds) Protein Dimerization and Oligomerization in Biology. *Adv. Exp. Med. Biol.* **2012**, 747.

Harada, R.; Sugita, Y.; Feig, M. Protein Crowding Affects Hydration Structure and Dynamics. *J. Am. Chem. Soc.* **2012**, *134*, 4842-4849.

Hashimoto K, Panchenko AR. Mechanisms of Protein Oligomerization, the Critical Role of Insertions and Deletions in Maintaining Different Oligomeric States. *Proc. Natl. Acad. Sci. U. S. A.* **2010**, *107*, 20352-20357.

Hatters, D. M.; Minton, A. P.; Howlett, G. J. Macromolecular Crowding Accelerates Amyloid Formation by Human Apolipoprotein C-II. *J. Biol. Chem.* **2002**, *277*, 7824-7830.

Henzler-Wildman, K.; Kern, D. Dynamic Personalities of Proteins. *Nature* **2007**, 450, 964-972.

Heo, J-Ok.; P, Roszak.; Furuta, K. M.; Helariutta, Y. Phloem Development: Current Knowledge and Future Perspectives. *Am. J. Bot.* **2014**, *9*, 1393-1402.

Hirsch, A. M. Role of Lectins (and rhizobial exopolysaccharides) in Legume Nodulation. *Curr. Opin. Plant Biol.* **1999**, *2*, 320-326.

Hong, J.; Gierasch, L. M. Macromolecular Crowding Remodels the Energy Landscape of a Protein by Favoring a More Compact Unfolded State. *J. Am. Chem. Soc.* **2010**, *132*, 10445-10452.

Inomata, K.; Ohno, A.; Tochio, H.; Isogai, S.; Tenno, T.; Nakase, I.; Takeuchi, T.; Futaki, S.; Ito, Y.; Hiroaki, H.; Shirakawa, M. High-Resolution Multi-Dimensional NMR Spectroscopy of Proteins in Human Cells. *Nature* **2009**, *458*, 106–109.

Ishizawa, K. Intracellular pH Regulation of Plant Cells Under Anaerobic Conditions. In: van Dongen J., Licausi F. (eds) Low-Oxygen Stress in Plants. *Plant Cell Monographs. Springer* **2014**, *21*, 55-74.

Jorgensen, R. A.; Atkinson, R. G.; Forster, R. L. S.; Lucas, W. J.; An RNA Based Information Super High Way in Plants. *Science* **1998**, *279*, 1486-1487.

Jiang, M.; Guo, Z. H. Effects of Macromolecular Crowding on the Intrinsic Catalytic Efficiency and Structure of Enterobactin-Specific Isochorismate Synthase. *J. Am. Chem. Soc.* **2007**, *129*, 730-31.

Jiang, Y.; Zhang, C-Xi.; Chen, R.; He, S. Y. Challenging Battles of Plants with Phloem-Feeding Insects and Prokaryotic Pathogens. *Proc. Natl. Acad. Sci. U. S. A.* **2019**, *116*, 23390-23397.

Junqueira, M.; Spirin, V.; Balbuena, T. S.; Thomas, H.; Adzhubei, I.; Sunyaev, S. Protein Identification Pipeline for the Homology-Driven Proteomics. *J. Proteomics* **2008**, *71*, 346-356.

Kamakaka, R. T.; Biggins, S. Histone Variants: Deviants? Genes Dev. 2005, 19, 295-316.

Kapusta, P. Absolute Diffusion Coefficients: Compilation of Reference Data for FCS Calibration. Rev 1; Technical Note; PicoQuant GmbH, **2010**.

Kasprzewska, A. Plant Chitinases-Regulation and Function. *Cell Mol. Biol. Lett.* **2003**, 8, 809-824.

Kavitha, M.; Sultan, N. A. M.; Swamy, M. J. Fluorescence Studies on the Interaction of Hydrophobic Ligands with *Momordica charantia* (bitter gourd) Seed Lectin. *J. Photochem. Photobiol. B: Biol.* **2009**, *94*, 59-64.

Kavitha, M.; Swamy, M. J. Spectroscopic and Differential Scanning Calorimetric Studies on the Unfolding of Trichosanthes Dioica Seed Lectin. Similar Modes of Thermal and Chemical Denaturation. *Glycoconjugate J.* **2009**, *26*, 1075-1084.

Kehr, J. Phloem Sap Proteins: Their Identities and Potential Roles in the Interaction between Plants and Phloem-Feeding Insects. *J. Exp. Bot.* **2006**, *57*, 767-774.

Khan, F.; Ahmad, A.; Khan, M. I. Chemical, Thermal and pH-Induced Equilibrium Unfolding Studies of *Fusarium solani* lectin. *IUBMB Life*, **2007**, *59*, 34 - 43.

Khan, J. M.; Qadeer, A.; Ahmad, E.; Ashraf, R.; Bhushan, B.; Chaturvedi, S. K.; Rabbani, G.; Khan, R. H. Monomeric Banana Lectin at Acidic pH Overrules Conformational Stability of Its Native Dimeric Form. *PLoS ONE* **2013**, *8*, e62428.

Khurana, R.; Udgaonkar, J. B. Equilibrium Unfolding Studies of Barstar: Evidence for an Alternative Conformation which Resembles a Molten Globule. *Biochemistry* **1994**, *33*, 106-115.

Kijne, J. W. Functions of Plant Lectins. Chemtracts-Biochem. Mol. Biol. 1996, 6, 180-187.

Kim, J. S.; Yethiraj, A. Crowding Effects on Protein Association: Effect of Interactions between Crowding Agents. *J. Phys. Chem. B* **2011**, *115*, 347-353.

Kleining, H.; Thones, J.; Dorr, I.; Kollmann, R. Filament Formation in Vitro of a Sieve Tube Protein from *Cucurbita maxima* and *Cucurbita pepo. Planta* **1975**, *127*, 163–170.

Knoblauch, M.; Peters W. S.; Münch, Morphology, Microfluidics - Our Structural Problem with the Phloem. *Plant Cell Environ.* **2010**, *33*, 1439-52.

Komath, S. S.; Kenoth, R.; Swamy, M. J. Thermodynamic Analysis of Saccharide Binding to Snake Gourd (Trichosanthes anguina) Seed Lectin. Fluorescence and Absorption Spectroscopic Studies. *Eur. J. Biochem.* **2001**, 268,111-119.

Komath, S. S.; Kavitha, M.; Swamy, M. J. Beyond Carbohydrate Binding: New Directions in Plant Lectin Research. *Org. Biomol. Chem.* **2006**, *4*, 973-988.

Kozer, N.; Kuttner, Y. Y.; Haran, G.; Schreiber, G. Protein-Protein Association in Polymer Solutions: from Dilute to Semidilute to Concentrated. *Biophys J.* **2007**, *92*, 2139-49.

Kumar, C. S.; Swamy, M. J. A pH Switch Regulates the Inverse Relationship between Membranolytic and Chaperone-like Activities of HSP-1/2, a Major Protein of Horse Seminal Plasma. Biochemistry. **2016**, *55*, 3650-3657.

Kumar, A.; Venkatesu, P. Overview of the Stability of  $\alpha$ -Chymotrypsin in Different Solvent. *Chem. Rev.* **2012**, *112*, 4283–4307.

Kumar, G.; Mishra, P.; Anantharam, V.; Surolia, A. *Luffa acutangula* Agglutinin: Primary Structure Determination and Identification of a Tryptophan Residue Involved in its Carbohydrate-Binding Activity Using Mass Spectrometry. *IUBMB Life* **2015**, *67*, 943–953.

Kumari, N.; Yadav, S. Modulation of Protein Oligomerization: An Overview. *Prog. Biophys. Mol. Biol.* **2019**, *149*, 99-113.

Kundu, A.; Kundu, S.; Chattopadhyay, K. The Presence of Non-Native Helical Structure in the Unfolding of a Beta-Sheet Protein MPT63. *Protein Science* **2017**, *26*, 536-549.

Kuwajima, K. The Molten Globule State of R-lactalbumin. *FASEB J.* **1996**, *10*, 102–109. Colón, W.; Roder, H. Kinetic Intermediates in the Formation of the Cytochrome *C* Molten Globule. *Nat. Struct. Mol. Biol.* **1996**, *3*, 1019–1025.

Laemmli, U. K. Most Commonly Used Discontinuous Buffer System for SDS Electrophoresis, *Nature* **1970**, 227, 680-685.

Lee, J. R.; Boltz, K. A.; Lee, S. Y. Molecular Chaperone Function of *Arabidopsis thaliana* Phloem Protein2-A1, Encodes a Protein Similar to Phloem Lectin. *Biochem. Biophys. Res. Commun.* **2014**, *443*, 18-21.

Lehninger, A. L; Nelson, D. L; Cox, M. M, Lehninger Principles of Biochemistry. 4<sup>th</sup> ed. W. H. Freeman and Company, **2004**.

Lemieux, R. U. How Water Provides the Impetus for Molecular Recognition in Aqueous Solution. *Acc. Chem. Res.* **1996**, *29*, 373-380.

Lis, H.; Sharon, N. The Biochemistry of Plant Lectins (Phytohemagglutinins). *Annu. Rev. Biochem.* **2003**, *42*, 541-574.

Liu, S. A Review on Protein Oligomerization Process. *Int. J. Precis. Eng. Manuf.* **2015**, *16*, 2731–2760.

Lodish, H.; Berk, A.; Zipursky, S. L.; Matsudaira, P.; Baltimore, D.; Darnell, J. Protein Glycosylation in the ER and Golgi Complex. *Molecular Cell Biology*. 4<sup>th</sup> ed. New York: W. H. Freeman; **2000**. Section 17.7, (https://www.ncbi.nlm.nih.gov/books/NBK21744/)

Lucas, W. J.; Yoo, B. C.; Kragler, F. RNA as a Long-Distance Information Macromolecule in Plants. *Nat. Rev. Mol. Cell Biol.* **2001**, *2*, 849-57.

Ma, B.; Wolfson, H. J.; Nussinov, R. Protein Functional Epitopes: Hot Spots, Dynamics and Combinatorial Libraries. *Curr. Opin. Struct. Biol.* **2001**, *11*, 364-369.

Maliarik, M. J.; Goldstein, I. J. Photoaffinity Labelling of the Adenine Binding Sites of the Lectins from Lima Bean, *Phaseolutus lunatus* and the Kidney Bean, *Phaseolus vulgaris*. *J. Biol. Chem.* **1988**, *263*, 11274-11279.

Malik, A.; Kundu, J.; Mukherjee, S.; Chowdhury, P. Myoglobin Unfolding in Crowding and Confinement. *J. Phys. Chem. B* **2012**, *116*, 12895-12904.

Marcos, M. J.; Villar, E.; Gavilanes, F.; Zhadan, G. G.; Shnyrov, V. L. Compact Residual Structure in Lentil Lectin at pH 2. *Eur. J. Biochem.* **2000**, 267, 2127-2132.

Miklos, A. C.; Li, C. G.; Sharaf, N. G.; Pielak, G. J. Volume Exclusion and Soft Interaction Effects on Protein Stability under Crowded Conditions. *Biochemistry* **2010**, *49*, 6984-6991.

Miklos, A. C.; Sarkar, M.; Wang, Y.; Pielak, G. J. Protein Crowding Tunes Protein Stability. *J. Am. Chem. Soc.* **2011**, *133*, 7116-7120.

Minton, A. P. The Influence of Macromolecular Crowding and Macromolecular Confinement on Biochemical Reactions in Physiological Media. *J. Biol. Chem.* **2001**, 276, 10577-80.

Mojumdar, S. S.; Chowdhury, R.; Chattoraj, S.; Bhattacharyya, K. Role of Ionic Liquid on the Conformational Dynamics in the Native, Molten Globule, and Unfolded States of Cytochrome C: a Fluorescence Correlation Spectroscopy Study. *J. Phys. Chem. B* **2012**, *116*, 12189-98.

Mondal, S.; Swamy, M. J. Purification, Biochemical/Biophysical Characterization and Chitooligosaccharide Binding to BGL24, a New PP2-Type Phloem Exudate Lectin from Bottle Gourd (*Lagenaria siceraria*). *Int. J. Biol. Macromol.* **2020**, *164*, 3656–3666.

Mondal, S.; Bobbili, K. B.; Paul, S.; Swamy, M. J. DSC and FCS Studies Reveal the Mechanism of Thermal and Chemical Unfolding of the Phloem Exudate Lectin CIA17, a

Polydisperse Oligomeric Protein from *Coccinia indica. J. Phys. Chem. B.* **2021**, *125*, 7117–7127.

Moran-Zorzano, M. T.; Viale, A. M.; Munoz, F. J.; Alonso-Casajus, N.; Eydallin, G. G.; Zugasti, B.; Baroja-Fernández, E.; Pozueta-Romero, J. Escherichia coli AspP Activity is Enhanced by Macromolecular Crowding and by Both Glucose1,6-Bisphosphate and Nucleotide-Sugars. *FEBS Lett.* **2007**, *581*, 1035-1040.

Moremen, K. W.; Tiemeyer, M.; Nairn, A. V. Vertebrate Protein Glycosylation: Diversity, Synthesis and Function. *Nat. Rev. Mol. Cell. Biol.* **2012**, *13*, 448-462.

Mortel, K. H.; Weatherman, R. V.; Kiessling, L. L. Recognition Specificity of Neoglycopolymers Prepared by Ring-Opening Metathesis Polymerization. *J. Am. Chem. Soc.* **1996**, *118*, 2297-2298.

Münch E. Die Stoffbewegungen in der Pflanze. Gustav Fischer, Jena, Germany, 1930.

Narahari, A.; Swamy, M. J. Tryptophan Exposure and Accessibility in the Chitooligosaccharide-Specific Phloem Exudate Lectin from Pumpkin (*Cucurbita maxima*). A Fluorescence Study. *J. Photochem. Photobiol. B.* **2009**, *97*, 40-47.

Narahari, A.; Swamy, M. J. Rapid Affinity-Purification and Physicochemical Characterization of Pumpkin (*Cucurbita maxima*) Phloem Exudate Lectin. *Biosci. Rep.* **2010**, *30*, 341-349.

Narahari, A.; Nareddy, P. K.; Swamy, M. J. A New Chitooligosaccharide Specific Lectin from Snake Gourd (*Tricosanthes anguina*) Phloem Exudate. Purification, Physico-Chemical Characterization and Thermodynamics of Saccharide Binding. *Biochimie* **2011a**, *93*, 1676–1684.

Narahari, A.; Singla, H.; Nareddy, P. K.; Bulusu, G.; Surolia, A.; Swamy, M. J. Isothermal Titration Calorimetric and Computational Studies on the Binding of Chito-Oligosaccharides to Pumpkin (*Cucurbita maxima*) Phloem Exudate Lectin. *J. Phys. Chem. B* **2011b**, *115*, 13710–13717.

Nareddy, P. K.; Swamy, M. J. Differential Scanning Calorimetric and Spectroscopic Studies on the Thermal and Chemical Unfolding of Cucumber (*Cucumis sativus*) Phloem Exudate Lectin. *Int. J. Biol. Macromol.* **2018**, *106*, 95–100.

Nareddy, P. K.; Bobbili, K. B.; Swamy, M. J. Purification, Physico-Chemical Characterization and Thermodynamics of Chitooligosaccharide Binding to Cucumber (*Cucumis sativus*) Phloem Lectin. *Int. J. Biol. Macromol.* **2017**, *95*, 910–919.

Newberry, R. W.; Raines R. T. Secondary Forces in Protein Folding. *ACS Chem. Biol.* **2019**, *14*, 1677-1686.

Nooren, I. M.; Thornton, J. M. Structural Characterisation and Functional Significance of Transient Protein-Protein Interactions. *J. Mol. Biol.* **2003**, *325*, 991-1018.

O'Brien, E. P.; Brooks, B. R.; Thirumalai, D. Effects of pH on Proteins: Predictions for Ensemble and Single-Molecule Pulling Experiments. *J. Am. Chem. Soc.* **2012**, *134*, 979-987.

Ohtsubo, K.; Marth J. D. Glycosylation in Cellular Mechanisms of Health and Disease. *Cell* **2006**, *126*, 855-867.

Oparka, K. J.; Cruz, S. S. The Great Escape: Phloem Transport and Unloading of Macromolecules. *Annu. Rev. Plant Physiol. Plant Mol. Biol.* **2000**, *51*, 323-347.

Owens, R. A.; Blackburn, M.; Ding, B. Possible Involvement of the Phloem Lectin in Long-Distance Viroid Movement. *Mol. Plant-Microbe Interact.* **2001**, *14*, 905–909.

Pabbathi, A.; Ghosh, S.; Samanta, A. FCS Study on the Structural Stability of Lysozyme in the Presence of Morpholinium Salts. *J. Phys. Chem. B.* **2013**, *117*, 16587–16593.

Pace, C. N. Determination and Analysis of Urea and Guanidine Hydrochloride Denaturation Curves. *Methods Enzymol.* **1986**, *131*, 166-280.

Pallas, V.; Gómez, G. Phloem RNA-Binding Proteins as Potential Components of the Long-Distance RNA Transport System, *Front. Plant Sci.* **2013**, *4*, 130.

Patel, A. K.; Singh, V. K.; Bergmann, U.; Jagannadham, M. V.; Kursula P. Purification, Crystallization and Preliminary X-ray Crystallographic Analysis of MIL, a Glycosylated Jacalin Related Lectin from Mulberry (*Morus indica*) Latex. *Acta. Crysta. Sect. F: Struct. Biol. Cryst. Comm.* **2011**, *67*, 608-612.

Perham, M.; Stagg, L; Wittung-Stafshede, P. Macromolecular Crowding Increases Structural Content of Folded Proteins. *FEBS Lett.* **2007**, *581*, 5065-5069.

Peumans, W. J.; Van Damme, E. J. M. Lectins as Plant Defense Proteins. *Plant Physiol*, **1995**, *109*, 347-352.

Peumans, W. J.; Van Damme, E. J.; Barre, A.; Rougé, P. Classification of Plant Lectins in Families of Structurally and Evolutionary Related Proteins. *Adv. Exp. Med. Biol.* **2001**, 491, 27-54.

Pilobello, K. T.; Mahal L. K. Deciphering the Glycocode: The Complexity and Analytical Challenge of Glycomics. *Curr. Opin. Chem. Biol.* **2007**, *11*, 300-305.

Prajapati, R. S.; Indu, S.; Varadarajan. R. Identification and Thermodynamic Characterization of Molten Globule States of Periplasmic Binding Proteins. *Biochemistry*, **2007**, *46*, 10339–10352.

Privalov, P. L. Intermediate States in Protein Folding. J. Mol. Biol. 1996, 258, 707-725.

Puchkov, E. O. Intracellular Viscosity: Methods of Measurement and Role in Metabolism. *Biochem. (Moscow) Supp. Series A: Membrane and Cell Biol.* **2013**, *7*, 270–279.

Rabbani, G.; Ahmed, N.; Zaidi, N.; Khan, R. H. pH Dependent Conformational Transitions in Conalbumin (Ovotransferrin), a Metalloproteinase from Egg White. *Cell. Biochem. Biophys.* **2011**, *61*, 551-560.

Rabbani, G.; Ahmed, N.; Zaidi, N.; Fatima, S.; Khan, R. H. pH Induced Molten Globule State of Rhizopus Niveus Lipase is More Resistant Against Thermal and Chemical Denaturation than Its Native State. *Cell. Biochem. Biophys.* **2012**, *62*, 487-499.

Rabbani, G.; Lee, E. J.; Ahmed, K.; Baig, M. H.; Choi, I. Binding of Tolperisone Hydrochloride with Human Serum Albumin: Effects on the Conformation, Thermodynamics and Activity of HSA. *Mol. Pharm.* **2018**, *15*, 1445-1456.

Rabbani, G.; Kaur, J.; Ahmed, E.; Zaidi, N.; Khan, R. H.; Jain, S. K. Structural Characteristics of Thermostable Immunogenic Outer Membrane Protein from Salmonella Enterica Serovar Typhi. *Appl. Microbiol. Biotechnol.* **2014**, *98*, 2533-2543.

Rabbani, G.; Ahmed, E.; Khan, M. V.; Ashraf, M. T.; Bhat, R.; Khan, R. H. Impact of Structural Stability of Cold Adapted Candida Antarctica Lipase B (CalB): In Relation to pH, Chemical and Thermal Denaturation. *RSC Adv.* **2015**, *5*, 20115-20131.

Radford, S.; Dobson, C.; Evans, P. The Folding of Hen Lysozyme Involves Partially Structured Intermediates and Multiple Pathways. *Nature* **1992**, *358*, 302-307.

Rajagopalan, S.; Huang, F.; Fresht, A. R. Single-Molecule Characterization of Oligomerization Kinetics and Equilibria of the Tumor Suppressor p53. *Nucleic Acids Res.* **2011**, *39*, 2294-2303.

Rajendran, A.; Nakano, S.; Sugimoto, N. Molecular Crowding of the Cosolutes Induces an Intramolecular i-Motif Structure of Triplet Repeat DNA Oligomers at Neutral pH. *Chem. Commun.* **2010**, *46*, 1299-1301.

Read, S. M.; Northcote, D. H. Subunit Structure and Interactions of the Phloem Proteins of *Cucurbita maxima* (Pumpkin). *Eur. J. Biochem.* **1983**, *134*, 561-569.

Reddy, G. B.; Bharadwaj, S.; Surolia, A. Thermal Stability and Mode of Oligomerization of the Tetrameric Peanut Agglutinin: A Differential Scanning Calorimetry Study. *Biochemistry* **1999**, *38*, 4464–4470.

Redfield, C.; Smith, R. A. G.; Dobson, C. M. Structural Characterization of a Highly-Ordered 'Molten Globule' at Low pH. *Nat. Struct. Mol. Biol.* **1994**, *1*, 23–29

Reily, C.; Stewart, T. J.; Renfrow, M. B.; Novak, J. Glycosylation in Health and Disease. *Nat. Rev. Nephrol.* **2019**, *15*, 346–366.

Roberts, D. D.; Goldstein, I. J. Hydrophobic Binding Properties of the Lectin from Lima Beans (*Phaseolus lunatus*). J. Biol. Chem. **1982**, 257, 11274-11277.

Roberts, D. D.; Goldstein, I. J. Binding of Hydrophobic Ligands to Plant Lectins: Titration with Arylaminonaphthalenesulfonates. *Arch. Biochem. Biophys.* **1983**a, 224, 479-484.

Roberts, D. D.; Goldstein, I. J. Adenine Binding Sites of the Lectin from Lima Beans (*Phaseolus lunatus*). J. Biol. Chem. **1983b**, 258, 13820-13824.

Roberts, J. K. M.; Ray, P. M.; Jardetzky, N. W.; Jardetzky. O. Estimation of Cytoplasmic and Vacuolar pH in Higher Plant Cells by 31p NMR. *Nature* **1980**, 283, 870-872.

Roberts, J. K. M.; Wemmer, D.; Ray, P. M.; Jardetzky. O. Regulation of Cytoplasmic and Vacuolar pH in Major Root Tips under Different Experimental Conditions. *Plant Physiol.* **1982**, *69*, 1344-1347.

Robertson, A. D.; Murphy K. P. Protein Structure and the Energetics of Protein Stability. *Chem. Rev.* **1997**, *97*, 1251–1267.

Royer, C. A. Probing Protein Folding and Conformational Transitions with Fluorescence. *Chem. Rev.* **2006**, *106*, 1769–1784.

Rüdiger, H.; Gabius, H. J. Plant Lectins: Occurrence, Biochemistry, Functions and Applications. *Glycoconj. J.* **2001**, *18*, 589-613.

Russo, N. V. D.; Estrin, D. A.; Martı, M. A.; Roitberg, A. E. pH-Dependent Conformational Changes in Proteins and Their Effect on Experimental pk<sub>a</sub>s: The Case of Nitrophorin 4. *PLoS Comput Biol.* **2012**, 8, e1002761.

Sabnis, D. D.; Hart, J. W. The Isolation and Some Properties of a Lectin (Haemagglutinin) from Cucurbita Phloem Exudate. *Planta* **1978**, *142*, 97-101.

Samiotakis, A.; Wittung-Stafshede, P.; Cheung, M. S. Folding, Stability and shape of Proteins in crowded Environments: Experimental and Computational Approaches. *Int. J. Mol. Sci.* **2009**, *10*, 572-588.

Sanadi, A. R.; Surolia, A. Studies on a Chitooligosaccharide-Specific Lectin from *Coccinia indica*. Thermodynamics and Kinetics of Umbelliferyl Glycoside Binding. *J. Biol. Chem.* **1994**, 269, 5072-5077.

Sanadi, A. R.; Ananthram, V.; Surolia, A. Elucidation of the Combining Site of *Coccinia indica* Agglutinin (CIA) by Thermodynamic Analyses of its Ligand Binding. *Pure & Appl. Chem.* **1998**, *70*, 677-686.

Sarkar, M.; Li, C.; Pielak, G. Soft Interactions and Crowding. *Biophys. Rev.* **2013a**, *5*, 187-194.

Sarkar, M.; Smith, A.; Pielak, G. Impact of Reconstituted Cytosol on Protein Stability. *Proc. Natl. Acad. Sci. U. S. A.* **2013b**, *110*, 19342-19347.

Sasaki, Y.; Miyoshi, D.; Sugimoto N. Regulation of DNA Nucleases by Molecular Crowding. *Nucleic Acids Res.* **2007**, *35*, 4086-4093.

Schepper, V. De.; Swaef, T. De.; Bauweraerts, I.; Steppe, K. Phloem Transport: A Review of Mechanisms and Controls. *J. Exp. Bot*, **2013**, *64*, 4839-4850.

Schlumbaum, A.; Vandorpe, P. A Short History of *Lagenaria siceraria* (Bottle Gourd) in the Roman Provinces: Morphotypes and Archaeogenetics, *Veg. Hist. Archaeobot.* **2012**, 21, 499-509.

Schulz, A.; Alosi, M. C.; Sabnis, D.D.; Park, R. B. A Phloem-Specific Lectin-Like Protein is Located in Pine Sieve-Element Plastids by Immunocytochemistry. *Planta* **1989**, *179*, 506-515.

Sen, D.; Mandal, D. K. A Comparative Study of Unfolding of *Erythrina Cristagalli* Lectin in Chemical Denaturant and Fluoroalcohols. *Protein Pept. Lett.* **2014**, *21*, 80-89.

Senske, M.; Tork, L.; Born, B.; Havenith, M.; Herrmann, C.; Ebbinghaus, S. Protein Stabilization by Macromolecular Crowding through Enthalpy Rather than Entropy. *J. Am. Chem. Soc.* **2014**, *136*, 9036–9041.

Shahid, S.; Hassan, M. I.; Islam, A.; Ahmad, F. Size-Dependent Studies of Macromolecular Crowding on the Thermodynamic Stability, Structure and Functional

Activity of Proteins: in Vitro and in Silico Approaches. *Biochim. Biophys. Acta. Gen. Subj.* **2017**, *1861*, 178-197.

Sharma, V.; Surolia, A. Analyses of Carbohydrate Recognition by Legume Lectins: Size of the Combining Site Loops and Their Primary Specificity. *J. Mol. Biol.* **1997**, 267, 433-445.

Sharon, N. Bacterial Lectins, Cell-Cell Recognition and Infectious Disease. *FEBS Lett.* **1987**, *217*, 145-157.

Sharon, N. Lectin-Carbohydrate Complexes of Plants and Animals: An Atomic View. *Trends Biochem. Sci*, **1993**, *18*, 221-226.

Sharon, N.; Lis, H. History of Lectins: From Hemagglutinins to Biological Recognition Molecules. *Glycobiology* **2004**, *14*, 53-62.

Sharon, N.; Lis, H. Lectins: Cell-Agglutinating and Sugar-Specific Proteins. *Science* **1972**, *177*, 949-959.

Sherman, E.; Itkin, A.; Kuttner, Y. Y.; Rhoades, E.; Amir, D.; Haas, E.; Haran, G. Using Fluorescence Correlation Spectroscopy to Study Conformational Changes in Denatured Proteins. *Biophys. J.* **2008**, *94*, 4819-4827.

Shevchenko, A.; Tomas, H.; Havlis, J.; Olsen, J. V.; Mann, M. In-Gel Digestion for Mass Spectrometric Characterization of Proteins and Proteomes. *Nat. Protoc.* **2006**, *1*, 2856-2860.

Singh, P.; Chowdhury, P. K. Crowding-Induced Quenching of Intrinsic Tryptophans of Serum Albumins: A Residue-Level Investigation of Different Conformations. *J. Phys. Chem. Lett.* **2013**, *4*, 2610-2617.

Singh, P.; Chowdhury, P. K. Unravelling the Intricacy of the Crowded Environment through Tryptophan Quenching in Lysozyme. *J. Phys. Chem. B* **2017**, *121*, 4687-4699.

Sinha, S.; Mitra, N.; Kumar, G.; Bajaj, K.; Surolia, A. Unfolding Studies on Soybean Agglutinin and Concanavalin A Tetramers: A Comparative Account. *Biophys. J.* **2005**, *88*, 1300-1310.

Spiro, R. G. Protein Glycosylation: Nature, Distribution, Enzymatic Formation, and Disease Implications of Glycopeptide Bonds. *Glycobiology*, **2002**, *12*, 43R-56R.

Stagg, L.; Zhang, S-Q.; Cheung, M. S.; Wittung-Stafshede, P. Molecular Crowding Enhances Native Structure and Stability of  $\alpha/\beta$  Protein Flavodoxin. *Proc. Natl. Acad. Sci. U. S. A.* **2007**, *104*, 18976-18981.

Sultan, N. A. M.; Swamy, M. J. Energetics of Carbohydrate Binding to *Momordica charantia* (Bitter Gourd) Lectin: An Isothermal Titration Calorimetric Study. *Arch. Biochem. Biophys.* **2005**, *437*, 115-125.

Surolia, A.; Sharon, N.; Schwarz, F. P. Thermodynamics of Monosaccharide and Disaccharide Binding to *Erythrina corallodendron* Lectin. *J. Biol. Chem.* **1996**, *271*, 17697-17703.

Swaminathan, C. P.; Surolia, N.; Surolia, A. Role of Water in the Specific Binding of Mannose and Mannooligosaccharides to Concanavalin A. *J. Am. Chem. Soc.* **1998,** *120,* 5153-5159.

Swaminathan, R.; Periasamy, N.; Udgaonkar, J. B.; Krishnamoorthy, G. Molten Globule-like Conformation of Barstar: A Study by Fluorescence Dynamics. *J. Phys. Chem.* **1994**, 98, 9270-9278.

Talley, K.; Alexov, E. On the pH-Optimum of Activity and Stability of Proteins. *Proteins* **2010**, *78*, 2699-2706.

Tan, P. H.; Sandmaier, B. M.; Stayton, P. S. Contributions of a Highly Conserved VH/VL Hydrogen Bonding Interaction to scFv Folding Stability and Refolding Efficiency. *Biophys. J.* **1998**, *75*, 1473-1482.

Tanaka, Y.; Tsumoto, K.; Yasutake, Y.; Umetsu, M.; Yao, M.; Fukada, H.; Tanaka, I.; Kumagai, I. How Oligomerization Contributes to the Thermostability of an Archaeon Protein. *J. Biol. Chem.* **2004**, *279*, 32957-32967.

Tanford, C. Protein Denaturation. Adv. Prot. Chem. 1968, 23, 69-282.

Tejavath, K. K.; Nadimpalli, S. K. Purification and Characterization of a Class II α-mannosidase from Moringa Oleifera Seed Kernels. *Glycoconj. J.* **2014**, *31*, 485-496.

Thompson, G. A.; Schulz, A. Macromolecular Trafficking in the Phloem. *Trends Plant Sci.* **1999**, *4*, 354-360.

Tsytlonok, M.; Itzhaki, L. S. The How's and Why's of Protein Folding Intermediates. *Arch. Biochem. Biophys.* **2013**, *531*, 14-23.

Mitra, N.; Sinha, S.; Ramya, T. N.C.; Surolia, A. N-linked Oligosaccharides as Outfitters for Glycoprotein Folding, Form and Function. *Trends in Biochem. Sci.* **2006**, *31*, 156-163.

Van Damme, E. J. M.; Peumans, W. J.; Barre, A.; Rougé, P. Plant Lectins: A Composite of Several Distinct Families of Structurally and Evolutionary Related Proteins with Diverse Biological Roles. *Crit. Rev. Plant Sci.* **1998**, *17*, 575-692.

Van Damme, E. J. M.; Hause, B.; Hu, J.; Barre, A.; Rougé, P.; Proost, P.; Peumans, W. J. Two Distinct Jacalin-Related Lectins with a Different Specificity and Subcellular Location are Major Vegetative Storage Proteins in the Bark of the Black Mulberry Tree. *Plant Physiol.* **2002**, *130*, 757-769.

Varki, A.; Cummings, R. D.; Esko, J. D.; Freeze, H. H.; Stanley, P.; Bertozzi, C. R.; Hart, G. W.; Etzler, M. E. Essentials of Glycobiology. 2nd ed. *Cold Spring Harbor Laboratory Press*, 2009. Available from: https://www.ncbi.nlm.nih.gov/books/NBK1908/

Vigneshwaran, V.; Thirusangu, P.; Madhusudana, S.; Krishna, V.; Pramod, S. N.; Prabhakar, B. T. The Latex Sap of the 'Old World Plant' *Lagenaria siceraria* with Potent Lectin Activity Mitigates Neoplastic Malignancy Targeting Neovasculature and Cell Death. *Int. Immunopharmacol.* **2016**, *39*, 158-171.

Voet, D.; Voet, J. G. Biochemistry, 4th ed., John Wiley and Sons, Inc, USA. 2011

Wagner, C.; Kiefhaber, T. Intermediates can Accelerate Protein Folding. *Proc. Natl. Acad. Sci. U. S. A.* **1999**, *96*, 6716-6721.

Weis, W. L.; Drickamer, K. Structural Basis of Lectin-Carbohydrate Recognition. *Annu. Rev. Biochem.* **1996**, 65, 441-473

Wilkins, D. K.; Grimshaw, S. B.; Receveur, V.; Dobson, C. M.; Jones, J. A.; Smith, L. J. Hydrodynamic Radii of Native and Denatured Proteins Measured by Pulse Field Gradient NMR Techniques. *Biochemistry* **1999**, *38*, 16424-16431.

Will, T.; Van Bel, A. J. E. Physical and Chemical Interactions Between Aphids and Plants. *J. Exp. Bot.* **2006**, *57*, 729-737.

Will, T.; Furch, A. C. U.; Zimmermann, M. R. How Phloem-Feeding Insects Face the Challenge of Phloem-Located Defenses. *Front Plant. Sci.* **2013**, *4*, 336.

Wu, L. C; Peng, Z. Y. Kim, P. S. Bipartite Structure of the α-lactalbumin Molten Globule. *Nat Struct Mol Biol.* **1995**, *2*, 281-286.

Yadav, R.; Sengupta, B.; Sen, P. Conformational Fluctuation Dynamics of Domain I of Human Serum Albumin in the Course of Chemically and Thermally Induced Unfolding Using Fluorescence Correlation Spectroscopy. *J. Phys. Chem. B* **2014**, *118*, 5428-5438.

Yang, A. S.; Honig, B. On the pH Dependence of Protein Stability. *J. Mol. Biol.* **1993**, 231, 459-474.

Yetişir, H.; Şakar, M.; Serçe, S. Collection and Morphological Characterization of Lagenaria Siceraria Germplasm from the Mediterranean Region of Turkey, Genet. *Resour. Crop Evol.* **2008**, *55*, 1257-1266.

Zhang, C. L.; Shi, H. J.; Chen, L.; Wang, X. M.; Lu, B. B.; Zhang, S. P.; Liang, Y. A.; Liu, R. X.; Qian, J.; Sun, W. W.; You, Z. Z.; Dong, H. S. Harpin-Induced Expression and Transgenic Overexpression of the Phloem Protein Gene AtPP2-A1 in *Arabidopsis* Repress Phloem Feeding of the Green Peach Aphid *Myzus persicae*. *BMC Plant Biol*. **2011**, *11*, 11-30.

Zhou, H. X.; Rivas, G.; Minton, A. P. Macromolecular Crowding and Confinement: Biochemical, Biophysical, and Potential Physiological Consequences. *Annu. Rev. Biophys.* **2008**, *37*, 375-97.

Zohu, B.; Tian, K.; Jing, G. An in Vitro Peptide Folding Model Suggests the Presence of the Molten Globule State During Nascent Peptide Folding. *Protein Engineering*. **2000**, *13*, 35-39.

Zimmerman, S. B.; Minton, A. P. Macromolecular Crowding: Biochemical, Biophysical, and Physiological Consequences. *Annu. Rev. Biophys. Biomol. Struct.* **1993**, *22*, 27-65.

# Biophysical Studies on the Structure, Conformational Dynamics and Carbohydrate Binding of Cucurbitaceae Phloem Exudate Lectins

by Saradamoni Mondal

Submission date: 28-Dec-2021 11:55AM (UTC+0530)

**Submission ID:** 1736035909

**File name:** Saradamoni-Mondal-Thesis\_For-Plagiarism-Check.pdf (1.47M)

Word count: 29673

Character count: 161682

Biophysical Studies on the Structure, Conformational Dynamics and Carbohydrate Binding of Cucurbitaceae Phloem Exudate Lectins

**ORIGINALITY REPORT** 

32%

6%

.

1%

SIMILARITY INDEX

INTERNET SOURCES

**PUBLICATIONS** 

STUDENT PAPERS

PRIMARY SOURCES

Saradamoni Mondal, Kishore Babu Bobbili,
Sumanta Paul, Musti J. Swamy. "DSC and FCS
Studies Reveal the Mechanism of Thermal
and Chemical Unfolding of CIA17, a
Polydisperse Oligomeric Protein from ", The
Journal of Physical Chemistry B, 2021

22%

Prof. Musti J. Swamy
School of Chemistry

Prof. Musti J. Swamy
School of Chemistry
University of Hyderabad
Hyderabad – 500 046, India

Saradamoni Mondal, Musti J. Swamy.
"Purification, biochemical/biophysical characterization and chitooligosaccharide binding to BGL24, a new PP2-type phloem exudate lectin from bottle gourd (Lagenaria siceraria)", International Journal of Biological Macromolecules, 2020

1 %

publication James

Prof. Musti J. Swamy School of Chemistry University of Hyderabad Hyderabad – 500 046, India

Publication

baadalsg.inflibnet.ac.in

Internet Source

1 %

4

Debparna Datta, Musti J. Swamy.
"Fluorescence and circular dichroism studies

1 %

on the accessibility of tryptophan residues and unfolding of a jacalin-related  $\alpha$ - d-galactose-specific lectin from mulberry ( Morus indica )", Journal of Photochemistry and Photobiology B: Biology, 2017

**Publication** 

Kishore Babu Bobbili, Bipin Singh, Akkaladevi Narahari, Gopalakrishnan Bulusu, A. Surolia, Musti J. Swamy. "Chitooligosaccharide binding to CIA17 (Coccinia indica agglutinin). Thermodynamic characterization and formation of higher order complexes", International Journal of Biological Macromolecules, 2019

1 %

Publication

Publication

Akkaladevi Narahari, Hitesh Singla, Pavan Kumar Nareddy, Gopalakrishnan Bulusu, Avadhesha Surolia, Musti J. Swamy. "Isothermal Titration Calorimetric and Computational Studies on the Binding of Chitooligosaccharides to Pumpkin () Phloem Exudate Lectin ", The Journal of Physical Chemistry B, 2011

<1%

Akkaladevi Narahari, Musti J. Swamy.
"Tryptophan exposure and accessibility in the chitooligosaccharide-specific phloem exudate lectin from pumpkin (Cucurbita maxima). A

<1%

### fluorescence study", Journal of Photochemistry and Photobiology B: Biology, 2009

Publication

Akkaladevi Narahari, Pavan Kumar Nareddy, Musti J. Swamy. "A new chitooligosaccharide specific lectin from snake gourd (Trichosanthes anguina) phloem exudate. Purification, physico-chemical characterization and thermodynamics of saccharide binding", Biochimie, 2011

<1%

- Publication
- Awanish Kumar, Pannuru Venkatesu.
  "Overview of the Stability of α-Chymotrypsin in Different Solvent Media", Chemical Reviews, 2012
  Publication

<1%

Pavan Kumar Nareddy, Kishore Babu Bobbili, Musti J. Swamy. "Purification, physicochemical characterization and thermodynamics of chitooligosaccharide binding to cucumber (Cucumis sativus) phloem lectin", International Journal of Biological Macromolecules, 2017

<1%

Kishore Babu Bobbili, Debparna Datta, Saradamoni Mondal, Sirilatha Polepalli et al. "Purification, chitooligosaccharide binding

<1%

properties and thermal stability of CIA24, a new PP2-like phloem exudate lectin from ivy gourd (Coccinia indica)", International Journal of Biological Macromolecules, 2018 **Publication** 

Nilimesh Das, Pratik Sen. "Structural, 12 Functional, and Dynamical Responses of a Protein in a Restricted Environment Imposed by Macromolecular Crowding", Biochemistry, 2018

Publication

Pavan Kumar Nareddy, Musti J. Swamy. 13 "Differential scanning calorimetric and spectroscopic studies on the thermal and chemical unfolding of cucumber (Cucumis sativus ) phloem exudate lectin", International Journal of Biological Macromolecules, 2018 Publication

<1%

<1%

Jun Soo Kim, Arun Yethiraj. "Crowding Effects 14 on Protein Association: Effect of Interactions between Crowding Agents", The Journal of Physical Chemistry B, 2011 **Publication** 

<1%

R. K. Sreejith, C. G. Suresh, Siddharth H. Bhosale, Varsha Bhavnani, Avinash Kumar, Sushama M. Gaikwad, Jayanta K. Pal. "Conformational Transitions of the Catalytic Domain of Heme-Regulated Eukaryotic

<1%

## Initiation Factor 2α Kinase, a Key Translational Regulatory Molecule", Journal of Fluorescence, 2011

Publication

16	www.biomeddefine.com Internet Source	<1%
17	"Protein Folding Handbook", Wiley, 2005 Publication	<1%
18	www.nature.com Internet Source	<1%
19	www.ncbi.nlm.nih.gov Internet Source	<1%
20	www.science.gov Internet Source	<1%
21	en.wikipedia.org Internet Source	<1%
22	pubs.acs.org Internet Source	<1%
23	www.physics.fsu.edu Internet Source	<1%
24	www.researchgate.net Internet Source	<1%
25	Amanda E. Hargrove, Sonia Nieto, Tianzhi Zhang, Jonathan L. Sessler, Eric V. Anslyn. "Artificial Receptors for the Recognition of	<1%

# Phosphorylated Molecules", Chemical Reviews, 2011

Publication

26	www.scribd.com Internet Source	<1%
27	Amrita Kundu, Sangeeta Kundu, Krishnananda Chattopadhyay. "The presence of non-native helical structure in the unfolding of a beta- sheet protein MPT63", Protein Science, 2017 Publication	<1%
28	Nathan Sharon, Halina Lis. "Lectins", Springer Science and Business Media LLC, 2007 Publication	<1%
29	Sneha Sudha Komath, Mannem Kavitha, Musti J. Swamy. "Beyond carbohydrate binding: new directions in plant lectin research", Organic & Biomolecular Chemistry, 2006 Publication	<1%
30	www.tandfonline.com Internet Source	<1%
31	Irina M. Kuznetsova, Konstantin K. Turoverov, Vladimir N. Uversky. "Use of the Phase Diagram Method to Analyze the Protein Unfolding-Refolding Reactions: Fishing Out the "Invisible" Intermediates", Journal of Proteome Research, 2004	<1%

Kishore Babu Bobbili, Gottfried Pohlentz,
Akkaladevi Narahari, Kaushal Sharma et al.
"Coccinia indica agglutinin, a 17 kDa PP2 like
phloem lectin: Affinity purification, primary
structure and formation of self-assembled
filaments", International Journal of Biological
Macromolecules, 2018

<1%

**Publication** 

Sylvie Dinant, Anna M. Clark, Yanmin Zhu, Françoise Vilaine, Jean-Christophe Palauqui, Chantal Kusiak, Gary A. Thompson. "Diversity of the Superfamily of Phloem Lectins (Phloem Protein 2) in Angiosperms", Plant Physiology, 2003

<1%

Publication

Yanjuan Jiang, Chuan-Xi Zhang, Rongzhi Chen, Sheng Yang He. "Challenging battles of plants with phloem-feeding insects and prokaryotic pathogens", Proceedings of the National Academy of Sciences, 2019

<1%

Publication

Kumar, C. Sudheer, D. Sivaramakrishna, Sanjay K. Ravi, and Musti J. Swamy. "Fluorescence investigations on choline phospholipid binding and chemical unfolding of HSP-1/2, a major protein of horse seminal plasma", Journal of Photochemistry and Photobiology B Biology, 2016.

<1%

36	Dolev Rimmerman, Denis Leshchev, Darren J. Hsu, Jiyun Hong, Baxter Abraham, Robert Henning, Irina Kosheleva, Lin X. Chen. " Probing Cytochrome Folding Transitions upon Phototriggered Environmental Perturbations Using Time-Resolved X-ray Scattering ", The Journal of Physical Chemistry B, 2018 Publication	<1%
37	dspace.ncl.res.in:8080 Internet Source	<1%
38	www.esp.org Internet Source	<1%
39	academic.oup.com Internet Source	<1%
40	"The Molecular Immunology of Complex Carbohydrates —2", Springer Science and Business Media LLC, 2001 Publication	<1%
41	Sk Saddam Hossain, Sneha Paul, Anunay Samanta. "Structural Stability and Conformational Dynamics of Cytochrome c in Hydrated Deep Eutectic Solvents", The Journal of Physical Chemistry B, 2021	<1%
42	Alexis D. Richaud, Guangkuan Zhao, Samir Hobloss, Stéphane P. Roche, "Folding in Place:	<1%

Hobloss, Stéphane P. Roche. "Folding in Place:

Design of β-Strap Motifs to Stabilize the Folding of Hairpins with Long Loops", The Journal of Organic Chemistry, 2021

Publication

Mullah Muhaiminul Islam, Sahadev Barik,
Naupada Preeyanka, Moloy Sarkar.
"Interaction of Lysozyme with Monocationic
and Dicationic Ionic Liquids: Toward Finding a
Suitable Medium for Biomacromolecules", The
Journal of Physical Chemistry B, 2020

<1%

- Publication
- Nabil Ali Mohammed Sultan, M. Kavitha, Musti J. Swamy. "Purification and physicochemical characterization of two galactose-specific isolectins from the seeds of ", IUBMB Life, 2009

<1%

- Publication
- Supratik Sen Mojumdar, Rajdeep Chowdhury, Shyamtanu Chattoraj, Kankan Bhattacharyya. "Role of Ionic Liquid on the Conformational Dynamics in the Native, Molten Globule, and Unfolded States of Cytochrome C: A Fluorescence Correlation Spectroscopy Study", The Journal of Physical Chemistry B, 2012

<1%

Publication

Sumra Shahid, Md. Imtaiyaz Hassan, Asimul Islam, Faizan Ahmad. "Size-dependent studies of macromolecular crowding on the thermodynamic stability, structure and functional activity of proteins: in vitro and in silico approaches", Biochimica et Biophysica Acta (BBA) - General Subjects, 2017

<1%

Publication

**Publication** 

Kishore Babu Bobbili, Shyam Bandari, Kay Grobe, Musti J. Swamy. "Mutational analysis of the pumpkin (Cucurbita maxima) phloem exudate lectin, PP2 reveals Ser-104 is crucial for carbohydrate binding", Biochemical and Biophysical Research Communications, 2014

<1%

Qin Tian, Wei Wang, Chen Miao, Hao Peng, Bo Liu, Fangwei Leng, Lei Dai, Fang Chen, Jinku Bao. "Purification, characterization and molecular cloning of a novel mannose-binding lectin from rhizomes of Ophiopogon japonicus with antiviral and antifungal activities", Plant Science, 2008

<1%

Rolf Misselwitz, Karin Welfle, Christoph Krafft, Claudio O. Gualerzi, Heinz Welfle. "
Translational Initiation Factor IF2 from: a

<1%

## Spectroscopic and Microcalorimetric Study of the C-Domain ", Biochemistry, 1997

Publication

Narahari, A.. "A new chitooligosaccharide specific lectin from snake gourd (Trichosanthes anguina) phloem exudate. Purification, physico-chemical characterization and thermodynamics of saccharide binding", Biochimie, 201110

Publication

www.pubmedcentral.nih.gov

<1%

<1%

Bhaswati Sengupta, Nilimesh Das, Pratik Sen. "Elucidation of µs dynamics of domain-III of human serum albumin during the chemical and thermal unfolding: A fluorescence correlation spectroscopic investigation", Biophysical Chemistry, 2017

<1%

Vijay M. Krishnamurthy, George K. Kaufman, Adam R. Urbach, Irina Gitlin et al. "Carbonic

<1%

Adam R. Urbach, Irina Gitlin et al. "Carbonic Anhydrase as a Model for Biophysical and Physical-Organic Studies of Proteins and Protein–Ligand Binding", Chemical Reviews, 2008

Publication

56

Publication

Ravindra Singh Prajapati, S. Indu, Raghavan Varadarajan. " Identification and

# Thermodynamic Characterization of Molten Globule States of Periplasmic Binding Proteins ", Biochemistry, 2007

Publication

aip.scitation.org

Internet Source

<ul> <li>V. Anbazhagan, Rajani S. Damai, Aniruddha Paul, Musti J. Swamy. "Interaction of the major protein from bovine seminal plasma, PDC-109 with phospholipid membranes and soluble ligands investigated by fluorescence approaches", Biochimica et Biophysica Acta (BBA) - Proteins and Proteomics, 2008 Publication</li> <li>worldwidescience.org Internet Source</li> <li>M. Kavitha. "Spectroscopic and differential scanning calorimetric studies on the unfolding of Trichosanthes dioica seed lectin. Similar modes of thermal and chemical denaturation", Glycoconjugate Journal, 02/03/2009</li> </ul>	57	Seed Proteins, 1999. Publication	<1%
<ul> <li>Internet Source</li> <li>Www.mdpi.com         </li> <li>M. Kavitha. "Spectroscopic and differential scanning calorimetric studies on the unfolding of Trichosanthes dioica seed lectin. Similar modes of thermal and chemical denaturation", Glycoconjugate Journal,</li> </ul>	58	Paul, Musti J. Swamy. "Interaction of the major protein from bovine seminal plasma, PDC-109 with phospholipid membranes and soluble ligands investigated by fluorescence approaches", Biochimica et Biophysica Acta (BBA) - Proteins and Proteomics, 2008	<1%
M. Kavitha. "Spectroscopic and differential scanning calorimetric studies on the unfolding of Trichosanthes dioica seed lectin. Similar modes of thermal and chemical denaturation", Glycoconjugate Journal,	59		<1%
scanning calorimetric studies on the unfolding of Trichosanthes dioica seed lectin. Similar modes of thermal and chemical denaturation", Glycoconjugate Journal,	60		<1%
Publication	61	scanning calorimetric studies on the unfolding of Trichosanthes dioica seed lectin. Similar modes of thermal and chemical denaturation", Glycoconjugate Journal, 02/03/2009	<1%

63	A. A. Moosavi-Movahedi. "Formation of the Molten Globule-Like State of Cytochrome c Induced by n-Alkyl Sulfates at Low Concentrations", Journal of Biochemistry, 01/01/2003 Publication	<1%
64	Jagtap, D.D "Disulphide bond reduction and S-carboxamidomethylation of PSP94 affects its conformation but not the ability to bind immunoglobulin", BBA - Proteins and Proteomics, 200706 Publication	<1%
65	Jerson L. Silva, Andrea C. Oliveira, Tuane C. R. G. Vieira, Guilherme A. P. de Oliveira, Marisa C. Suarez, Debora Foguel. "High-Pressure Chemical Biology and Biotechnology", Chemical Reviews, 2014 Publication	<1%
66	pubs.rsc.org Internet Source	<1%

#### List of Publications

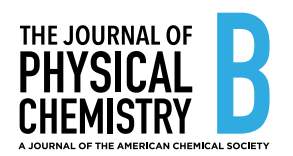
- Mondal, S.; Bobbili, K. B.; Paul, S.; Swamy, M. J. DSC and FCS Studies Reveal the Mechanism of Thermal and Chemical Unfolding of the Phloem Exudate Lectin CIA17, a Polydisperse Oligomeric Protein from *Coccinia indica. J. Phys. Chem. B* 2021, 125, 26, 7117-7127
- Mondal, S.; Swamy, M. J. Purification, Biochemical/Biophysical Characterization and Chitooligosaccharide Binding to BGL24, a New PP2-Type Phloem Exudate Lectin from Bottle Gourd (*Lagenaria siceraria*). Int. J. Biol. Macromol. 2020, 164, 3656-3666.
- Venugopal\*, A.; Mondal\*, S.; Ranganatha, K. S.; Datta, D.; Kumar, N. S.; Swamy, M. J. Purification and biochemical/biophysical characterization of two hexosaminidases from the fresh water mussel, *Lamellidens corrianus*. *Int. J. Biol. Macromol.* 2019, 149, 754–766.
   \*These two authors equally contributed.
- 4. Datta, D., Pohlentz, G., **Mondal, S.** Mormann, M.; Swamy, M. J. Macromolecular properties and partial amino acid sequence of a Kunitz-type protease inhibitor from okra (*Abelmoschus esculentus*) seeds. *J. Biosci.* **2019**, *44*, 35.
- Bobbili, K. B.; Datta, D.; Mondal, S.; Polepalli, S.; Pohlentz, G.; Mormann, M.; Swamy, M. J. Purification, Chitooligosaccharide Binding Properties and Thermal Stability of CIA24, a New PP2-Like Phloem Exudate Lectin from Ivy Gourd (Coccinia indica). Int. J. Biol. Macromol. 2018, 110, 588–597.
- 6. Sen, K. D.; **Mondal**, **S.** Exact Energy-Density Relationships for Sum of Screened Coulomb Potentials. (Therotical and Quantum chemistry at the dawn of the 21<sup>st</sup> century, chapter:17) eBook ISBN: 9781351170963.

#### To Be Communicated

- 1. **Mondal, S.**; Swamy, M. J. Macromolecular Crowding Significantly Affects the Conformational Features and Carbohydrate Binding Properties of CIA17, a PP2-type Lectin from *Coccinia indica*. (Submitted for publication)
- 2. **Mondal, S.**; Das, S.; Barik, S.; Swamy, M. J. Effect of pH on the Local/Global Structure of CIA17 and Its Carbohydrate Binding. Presence of a Molten Globule-Like State at low pH.
- 3. Swamy, M. J.; **Mondal, S.**; Bobbili, K. B.; Narahari A.; Datta, D. Cucurbitaceae Phloem Exudate Lectins: Purification, Molecular Characterization and Carbohydrate Binding Characteristics.
- 4. Swamy, M. J.; **Mondal, S**. Subunit Association, Thermal and Chemical Unfolding of Cucurbitaceae Phloem Exudate Lectins. A Review
- Mondal, S.; Swamy, M. J. Thermal, Chemical and pH Unfolding of BGL24, a Chitooligosachharide Specific PP2-Type Lectin from the Phloem Exudate of Bottle Gourd.
- 6. **Mondal, S.**; Venugopal, A.; Ranganatha, K. S.; Kumar, N. S.; Swamy, M. J. Fluorescence Spectroscopic Studies on Hexosaminidases (HexA and HexB) from Edible Fresh Water Mussel, *Lamellidens corrianus*.

#### **Conferences/ Presentations**

- Subunit Association and (un)folding Dynamics of CIA17 at low pH: A Spectroscopic and Microscopic study
  - <u>Poster Presentation:</u> FCS-2021, Organized by IISER Thiruvananthapuram and RGCB Thiruvananthapuram under the aegis of the Fluorescence Society.
- Unravelling the effect of macromolecular crowding on the structure and carbohydrate binding of phloem exudate lectin.
  - **Oral Presentation:** 18<sup>th</sup> annual in-house symposium CHEMFEST-2021, Held at School of Chemistry, University of Hyderabad. (Best oral presentation award).
- Calorimetric and spectroscopic investigation on thermal, pH and chemical unfolding of CIA17, a PP2-like phloem lectin.
  - **Poster Presentation:** 17<sup>th</sup> annual in-house symposium CHEMFEST-2020, Held at School of Chemistry, University of Hyderabad.
- Affinity purification and physico-chemical characterization of BGL24, a chitooligosaccharide binding PP2-type phloem exudate lectin from bottle gourd (*Lagenaria siceraria*).
  - **Poster Presentation:** 43<sup>rd</sup> Indian Biophysical Society Annual Meeting, Organized by Indian Institute of Science Education and Research Kolkata (IISER, Kolkata), February, 2019.
- Affinity purification and physico-chemical characterization of BGL24, a chitooligosaccharide binding PP2-type phloem exudate lectin from bottle gourd (*Lagenaria siceraria*).
  - **Poster Presentation:** 16<sup>th</sup> annual in-house symposium CHEMFEST-2019, Held at School of Chemistry, University of Hyderabad. (Best poster award).



pubs.acs.org/JPCB Article

# DSC and FCS Studies Reveal the Mechanism of Thermal and Chemical Unfolding of CIA17, a Polydisperse Oligomeric Protein from *Coccinia Indica*

Saradamoni Mondal, Kishore Babu Bobbili, Sumanta Paul, and Musti J. Swamy\*



Cite This: J. Phys. Chem. B 2021, 125, 7117–7127



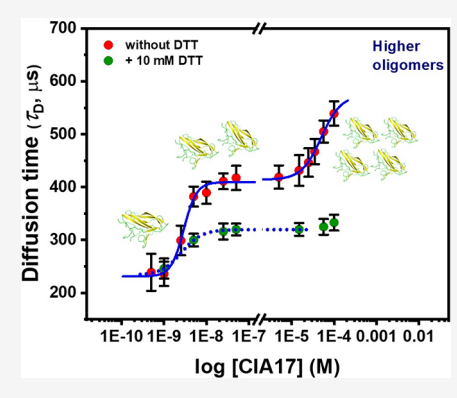
**ACCESS** 

III Metrics & More



Supporting Information

**ABSTRACT:** The mechanism of thermal and chemical unfolding of *Coccinia indica* agglutinin (CIA17), a chitooligosacharide-specific phloem exudate lectin, was investigated by biophysical approaches. DSC studies revealed that the unfolding thermogram of CIA17 consists of three components ( $T_{\rm m} \sim 98$ , 106, and 109 °C), which could be attributed to the dissociation of protein oligomers into constituent dimers, dissociation of the dimers into monomers, and unfolding of the monomers. Intrinsic fluorescence studies on the chemical denaturation by guanidinium thiocyanate and guanidinium chloride indicated the presence of two distinct steps in the unfolding pathway, which could be assigned to dissociation of the dimeric protein into monomers and unfolding of the monomers. Results of fluorescence correlation spectroscopic studies could be interpreted in terms of the following model: CIA17 forms oligomeric structures in a concentration dependent manner, with the protein existing as a monomer below 1 nM concentration but associating to form dimers at higher



concentrations ( $K_{\rm D} \approx 2.9$  nM). The dimers associate to yield tetramers with a  $K_{\rm D}$  of  $\sim 50~\mu{\rm M}$ , which further associate to form higher oligomers with further increase in concentration. These results are consistent with the proposed role of CIA17 as a key player in the defense response of the plant against microbes and insects.

#### 1. INTRODUCTION

Despite numerous studies on protein (un)folding dynamics, a detailed understanding of the complexity of structural/ conformational changes that occur during protein folding/ unfolding is still an important and largely unsolved problem. 1-3 Although the pathway of protein folding is often described by a simple two-state model (native  $\leftrightarrow$  unfolded), recent studies employing different single-molecule techniques revealed the presence of intermediate state(s) even for single-domain, monomeric proteins.<sup>4–6</sup> Characterizing the nature of such intermediate states is crucial for understanding protein folding since the intermediate states can direct folding and accelerate the transition to the native state restricting the conformational space available for the unfolded state. 4,7,8 While a number of studies have been reported on the unfolding of single-domain/subunit proteins, unfolding studies on oligomeric proteins have been rather limited. The stability of oligomeric proteins can be greatly influenced by intersubunit interaction as well as intramolecular interactions. In this context, while some oligomeric legume lectins showed two-state unfolding with a folded multisubunit native protein and unfolded polypeptides in equilibrium, several globular proteins are known to deviate from the two-state behavior and exhibit well-populated intermediate states. 9-12 Although the unfolding of several legume lectins has been investigated, there have been no reports on the folding/unfolding processes of phloem exudate lectins, several of which have been shown to exist as polydisperse aggregates in solution. 13-15

The phloem proteins (P-proteins) are highly abundant in the Cucurbitaceae genere and appear as amorphous, crystalline, or tubular structures under microscopy. 16-19 Phloem proteome, primarily composed of phloem protein 1 (PP1) and phloem protein 2 (PP2), is the major integral component for the entire plant communication system by which water, minerals, nutrients, and biological macromolecules such as amino acids, sugars, peptides, proteins, and RNAs are transported over long distances. 16,19-21 PP2 proteins together with the filamentous phloem protein, PP1, appear to be synthesized in companion cells and transported into the sieve elements via plasmodesmata pores.<sup>22</sup> Under conditions of oxidative stress, e.g., when the tissue is wounded by insects and phloem exudate is exposed to air, PP1 and PP2 proteins associate to form cross-liked filaments connected via disulfide bonds and finally yield an insoluble gel which seals the wound and prevents microorganisms and fungi from entering the plant

Received: March 9, 2021 Revised: June 14, 2021 Published: June 25, 2021





tissue, thus protecting the plants from pathogenic attack.<sup>23–29</sup> While PP1 proteins do not exhibit any ligand-binding ability, PP2 proteins have been shown to exhibit lectin activity and also interact with different RNA molecules to form ribonucleoprotein (RNP) complexes and transport them from cell to cell.<sup>28,30,31</sup> Therefore, it is important to carry out systematic investigations on them in order to obtain a molecular level understanding of their biological functions.

In view of the above, PP2-type phloem exudate lectins have been purified from several Cucurbitaceae species such as ridge gourd (*Luffa acutangula*), <sup>32,33</sup> pumpkin (*Cucurbita maxima*), <sup>23,34–37</sup> snake gourd (*Trichosanthes anguina*), <sup>38</sup> cucumber (*Cucumis sativus*), <sup>39,40</sup> ivy gourd (*Coccinia indica*), <sup>41–43</sup> and bottle gourd (*Lagenaria siceraria*) <sup>15</sup> and are characterized in considerable detail. The PP2 lectins from various Cucurbitaceae species are highly homologous with respect to their amino acid sequence and contain a highly conserved "chitin-binding domain" whose conformation is locked by a disulfide bond between two cysteine residues.

Coccinia indica agglutinin (CIA17), purified from the phloem exudate of unripe ivy gourds (Coccinia indica), is a homodimeric PP2-type lectin with a subunit molecular mass of  $\sim$ 17 kDa. <sup>13</sup> This protein exists in a polydisperse, oligomeric form with the size of the oligomer increasing with concentration. Each subunit of the lectin is made up of 152 amino acid residues and contains an extended binding site which specifically recognizes chitooligosaccharides. <sup>13,42</sup> CIA17 is a predominantly  $\beta$ -sheet protein and exhibits high thermal stability with its secondary and tertiary structures remaining essentially unaltered up to 90 °C as indicated by CD spectroscopic investigations reported earlier. <sup>13</sup>

In the present study, thermal unfolding of CIA17 was further investigated in the absence as well as in the presence of ligands (chitooligosaccharides) using differential scanning calorimetry (DSC). Since CIA17 contains nine tryptophan residues in its primary structure, <sup>13</sup> chaotrope-induced unfolding of this protein was studied using fluorescence spectroscopy by monitoring changes in tryptophan emission characteristics in the presence of varying concentrations of chemical denaturants. The concentration dependent oligomerization as well as guanidinium chloride (GdmCl)-induced unfolding pathway was probed using fluorescence correlation spectroscopy (FCS).

#### 2. MATERIALS AND METHODS

- **2.1. Materials.** Unripe ivy gourds were purchased from local vendors.  $\beta$ -Chitin from squid pen (Sigma) was a kind gift from Prof. A. R. Podile, School of Life Sciences, University of Hyderabad. 2-Mercaptoethanol ( $\beta$ ME),  $\alpha$ -chitin, chitooligosaccharides, ammonium persulfate, acrylamide, GdmCl, guanidinium thiocyanate (GdmSCN), urea, and dithiothreitol (DTT) were purchased from Sigma (St. Louis, MO). Alexa Fluor 488 carboxylic acid succinimide ester (A488) was obtained from Invitrogen (Carlsbad, CA). All other chemicals and reagents were procured from local suppliers and were of the highest purity available.
- **2.2. Purification of CIA17.** CIA17 was purified by sequential affinity chromatography on  $\alpha$ -chitin and  $\beta$ -chitin as described earlier and was found to be pure by sodium dodecyl sulfate-polyacrylamide gel electrophoresis (SDS-PAGE). The concentration of the purified protein was estimated from its  $A_{280 \text{ nm}}$  value of 3.08 for a 1.0 mg/mL solution at 1.0 cm path length. This would correspond to a molar extinction coefficient of 53 700 M<sup>-1</sup> cm<sup>-1</sup>.

- 2.3. Differential Scanning Calorimetry. DSC measurements were carried out on a Nano DSC instrument from TA systems (New Castle, DE). Protein samples of 0.5–1.0 mg/mL (29-58 μM) concentration, dialyzed against 10 mM sodium phosphate buffer, pH 7.0 were heated from 10 to 120 °C at a scan rate of 60°/h. The dialysate was used as the reference. To investigate the effect of ligand binding on the thermal unfolding of the protein, CIA17 was preincubated with 4.37 mM chitotriose before the DSC scan. Sample and reference solutions were properly degassed prior to the DSC experiment to eliminate bubbling effects. The reproducibility of baselines was verified by multiple scans, and the reversibility of protein unfolding was investigated by scanning the samples twice in succession. After corrections were made for buffer contributions, the thermograms were analyzed using the Gaussian Modeler software supplied by TA Systems.
- **2.4. Fluorescence Spectroscopy.** Fluorescence spectra were recorded on a Spex Fluoromax-4 fluorescence spectrometer (Jobin-Yvon Ltd., Edison, NJ). CIA17 samples of  $1.11~\mu\mathrm{M}$  concentration were irradiated with 295 nm light to excite tryptophan residues selectively, and emission spectra were recorded in the wavelength range of  $300-400~\mathrm{nm}$  using excitation and emission slits of 5 nm width.

Chemical unfolding of CIA17 induced by various chaotropic agents was studied by monitoring changes in the intrinsic fluorescence properties of the protein when the concentration of the denaturants was varied. In these experiments, CIA17 samples were incubated overnight with different concentrations of denaturants (GdmCl, GdmSCN, and urea), and emission spectra of the protein were recorded as described above for the native protein. All spectra were corrected by subtracting buffer scans recorded under identical conditions. To investigate the role of disulfide bonds in stabilizing the protein structure, studies were also performed in the presence of 10 mM DTT.

2.5. Fluorescence Correlation Spectroscopy. FCS measurements were carried out with an Alexa 488 labeled CIA17 (A488-CIA17). The lectin was labeled with Alexa Fluor 488 carboxylic acid succinimide ester (A488) following the procedure provided by the manufacturer (Molecular Probes, Invitrogen). The labeling reaction was carried out in 0.1 M carbonate buffer, pH 8.3 at room temperature by incubating a mixture of CIA17 and A488 at a dye/protein ratio of 2 for 2 h in the dark. To stop the labeling reaction, the reaction mixture was incubated with freshly prepared 1.2 M hydroxylamine, pH 8.5. The labeled protein (A488-CIA17) was separated from the free dye by passing the reaction mixture through a Sephadex G-25 column (30  $\times$  1.3 cm), pre-equilibrated with 20 mM sodium phosphate buffer, pH 7.4. The absorbance spectra of the free dye and the labeled protein are shown in Figure S1. The concentrations of the protein and dye were estimated by measuring the absorbance of the conjugate in phosphate buffer at 495 and 280 nm using their molar extinction coefficients of  $73\,000\,\mathrm{M}^{-1}\,\mathrm{cm}^{-1}$  (A488) and  $53\,700\,\mathrm{M}^{-1}\,\mathrm{cm}^{-1}$  (CIA17). The degree of labeling ([dye]/[protein]) was estimated as 0.44.

**2.6. FCS Instrumentation and Methods.** FCS measurements were carried out using a time-resolved confocal fluorescence microscope, MicroTime 200, PicoQuant. A pulsed diode laser ( $\lambda_{\rm ex}$  = 485 nm with fwhm 144 ps) was used as the excitation source. The excitation light was reflected by a dichroic mirror and focused onto the sample placed on a coverslip using a water immersion objective (Olympus UPlansApo 60×/1.2 NA). The fluorescence signal of the

sample collected by the same objective was directed to pass through the same dichroic mirror and a 510 LP filter followed by a pinhole of 50  $\mu$ m diameter. The signal was then passed through a 50/50 beam splitter and entered into the two PDM series single-photon avalanche diodes (SPADs) from Pico-Quant. The FCS measurements were performed by placing a highly diluted (0.5-50 nM) solution of A488-CIA17 on a coverslip placed on the top of the objective. For denaturation study, the labeled protein (25 nM concentration) was incubated with increasing concentrations (0-7.5 M) of GdmCl. To investigate oligomer formation by the lectin at higher concentrations, the labeled protein (10 nM) was mixed with different concentrations of unlabeled protein (final concentration 250 nM $-100 \mu M$ ) and incubated for 30-120min before FCS measurements. The duration of each measurement was 600 s, and each point represented in the plot is the average of three independent measurements.

**2.7. FCS Data Analysis.** The fluctuations of the fluorescence intensity were measured within a small detection volume (1.2 fL) and a temporal range from nanoseconds to seconds by using a focused laser beam and pinhole. All the FCS data were analyzed using SymphoTime software provided by PicoQuant. Fluorescence fluctuations detected by two SPAD detectors were then cross-correlated via the second-order autocorrelation function, given by

$$G(\tau) = \frac{\langle \delta F(t) \delta F(t+\tau) \rangle}{\langle F(t) \rangle^2} \tag{1}$$

where  $\langle F(t) \rangle$  is the average fluorescence intensity and  $\delta F(t)$  and  $\delta F(t+\tau)$  are the fluctuations of the fluorescence intensity from the mean value at time t and  $t+\tau$ , which are given by

$$\delta F(t) = F(t) - \langle F(t) \rangle$$

and

$$\delta F(t+\tau) = F(t+\tau) - \langle F(t) \rangle$$

The correlation function of a molecule diffusing freely is given by

$$G(\tau) = \frac{1}{N} \left( 1 + \frac{\tau}{\tau_{\rm D}} \right)^{-1} \left( 1 + \frac{\tau}{\kappa^2 \tau_{\rm D}} \right)^{-1/2}$$
 (2)

The correlation function of a molecule undergoing conformational changes (or any other reactions/changes) that result in changes in the fluorophore brightness along with the diffusion is given by

$$G(\tau) = \frac{1 - I + I \exp(\tau/\tau_{\rm R})}{N(1 - I)} \left(1 + \frac{\tau}{\tau_{\rm D}}\right)^{-1} \left(1 + \frac{\tau}{\kappa^2 \tau_{\rm D}}\right)^{-1/2}$$
(3)

In the above equations, N represents the number of molecules in the observation volume,  $\tau_{\rm D}$ ,  $\tau$ , and  $\tau_{\rm R}$  are the diffusion time, lag time, and relaxation time, respectively.  $\kappa$  (= $\omega_z/\omega_{xy}$ ) is the structural parameter where  $\omega_z$  and  $\omega_{xy}$  are the longitudinal and transverse radii of the observation volume, and I is the associated amplitude. The excitation volume was estimated as 1.2 fL using the known diffusion coefficient of Rhodamine 6G (422  $\mu$ m² s<sup>-1</sup>) in water (average of values obtained by two different methods). Although the same excitation wavelength was used in the calibration experiments with Rhodamine 6G and in the studies with A488 and A488-CIA17, it should be noted that the differences in the emission spectra of the two

probes can still introduce a slight difference in the estimation of the excitation volume. However, these differences are not expected to affect the main results obtained here and the conclusions drawn from them. All the measurements were carried out at room temperature ( $\sim$ 25 °C). The diffusion coefficient (D) was calculated employing the  $\tau_D$  value in eq 4:

$$\tau_{\rm D} = \frac{\omega_{\rm xy}^2}{4D} \tag{4}$$

According to the Stokes-Einstein equation, the hydrodynamic radius  $(R_h)$  can be estimated from the measured value of D of the species diffusing in the smaller volume as follows:

$$D = \frac{k_{\rm B}T}{6\pi\eta R_{\rm h}} \tag{5}$$

where  $\eta$  is the viscosity and T is the temperature at which measurements were carried out.

The progressive addition of GdmCl changes the viscosity and refractive index of the solution that affect the actual determination of the size and the relaxation time of the protein. Hence the hydrodynamic radius was estimated using the following eqs 6 and 7, respectively, after correcting the viscosity and refractive index mismatch: 46-48

$$\frac{R_{\rm h}^{\rm sample}}{R_{\rm h}^{\rm A488}} = \frac{\tau_{\rm D}^{\rm sample}}{\tau_{\rm D}^{\rm A488}} \tag{6}$$

$$\tau_{\rm R}^{\rm corr} = \tau_{\rm R}^{\rm uncorr} \times \frac{\tau_{\rm D}^{\rm buff}}{\tau_{\rm D}^{\rm sample}}$$
(7)

where  $R_{\rm h}^{\rm A488}$  and  $R_{\rm h}^{\rm sample}$  are the hydrodynamic radii of free A488 and A488-CIA17, respectively, and  $\tau_{\rm D}^{\rm A488}$  is the diffusion time of free A488.  $\tau_{\rm R}^{\rm corr}$  and  $\tau_{\rm R}^{\rm uncorr}$  are the viscosity-corrected and uncorrected relaxation time component, respectively.  $\tau_{\rm D}^{\rm buff}$  and  $\tau_{\rm D}^{\rm sample}$  correspond to the diffusion time of A488-CIA17 in buffer and in different experimental conditions, respectively. The  $R_{\rm h}$  of A488 was estimated as 5.63 (±0.23) Å from the diffusion coefficient of 435 (±19)  $\mu{\rm m}^2$  s<sup>-1</sup>, which in turn was estimated from the cross-correlation data shown in Figure S4.

#### 3. RESULTS AND DISCUSSION

3.1. DSC Studies on the Thermal Stability of CIA17. In order to investigate the thermal unfolding of CIA17 and the effect of ligand binding on it, DSC studies were performed on the protein in 10 mM phosphate buffer, pH 7.0 in the absence and presence of 1 mM chitotriose. The thermogram of native CIA17 consists of three overlapping endothermic components centered at 98.3, 105.9, and 108.6 °C (Figure 1A), where the lowest temperature component was found to be the broadest among them. The broad transition is consistent with the polydisperse nature of the oligomeric structures as observed from AFM studies.<sup>13</sup> When the native protein was heated to 110 °C and immediately cooled to 10 °C and reheated, no endotherm was observed indicating that the unfolding process is irreversible. However, when the sample was heated to 103 °C (midpoint of transition 2), cooled to 10 °C, and reheated, only two peaks were seen; the first peak centered at 98.3 °C was not observed (Figure 1B). Although thermograms obtained in the presence of chitotriose could also be resolved into three components similar to native CIA17, small but distinct shifts to higher temperatures were observed in the position of all three endotherms (Figure 1C). Transition

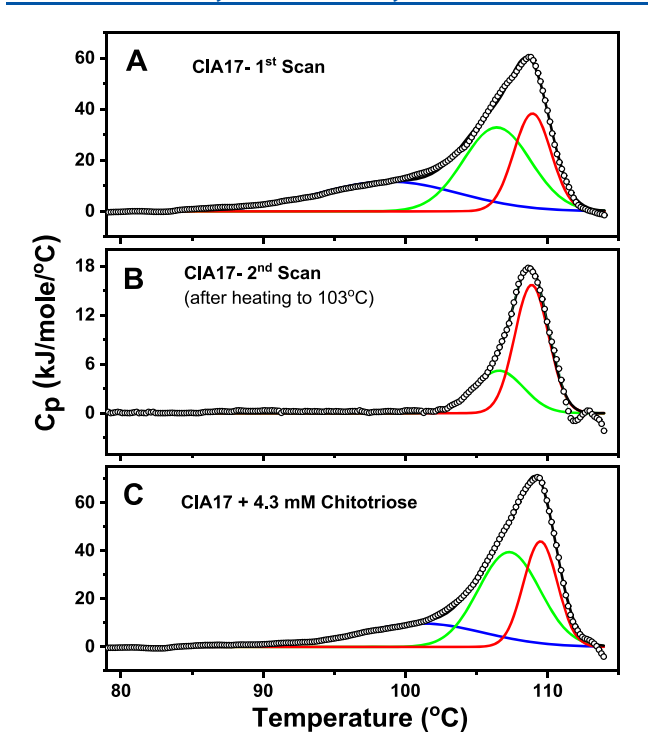


**Figure 1.** DSC thermograms of CIA17 at pH 7.0: (A) first heating scan; (B) second heating scan of the protein that was heated to 103 °C and cooled to 10 °C; (C) first heating scan in the presence of 4.37 mM chitotriose. The data points are shown as open circles. The blue, green, and red lines indicate the three individual transitions obtained from the fit, whereas the black line corresponds to the sum of the three individual transitions.

temperatures obtained by analyzing the thermograms are given in Table 1.

Table 1. Transition Temperatures of the Different Transitions in the Thermal Unfolding of CIA17 Obtained from Differential Scanning Calorimetric Studies<sup>a</sup>

sample/scan description	transition assignment	$T_{\rm m}$ (°C)	
native CIA17			
transition 1	oligomer to dimer	98.3	
transition 2	dimer to monomer	105.9	
transition 3	monomer unfolding	108.6	
second heating scan after cooling	from 103 °C		
transition 1	dimer to monomer	106.7	
transition 3	monomer unfolding	108.9	
CIA17 + 4.3 mM chitotriose			
transition 1	oligomer to dimer	101.1	
transition 2	dimer to monomer	107.3	
transition 3	monomer unfolding	109.5	
<sup>a</sup> Buffer: 10 mM sodium phosphate, pH 7.0.			

The complex thermogram of CIA17 containing three underlying components can be explained as follows. Our previous AFM studies have shown that in the concentration range used in the present DSC studies (0.5-1.0 mg/mL, which is approximately 29-58  $\mu$ M of the protein) CIA17 exists as a mixture of soluble, oligomeric aggregates. 13 Therefore, we assign transition 1 to reversible dissociation of the oligomeric aggregates into dimers. Transition 1 is not seen in DSC scans performed with low concentrations of the protein (see Figure S2), which is in agreement with our previous AFM studies, which indicated that oligomerization of CIA17 is concentration dependent. 13 Further, this transition is not seen when the sample is heated to 103 °C (midpoint of the second transition), cooled to 10 °C, and reheated, suggesting that most likely the formation of the soluble aggregates is a slow process. Transition 2, centered at ~105.9 °C, can be assigned to the dissociation of dimers into monomers, whereas transition 3, centered at ~108.6 °C, is assigned to the irreversible unfolding of the monomers. Oligomerization could be responsible for the hyperthermal stability of CIA17, with the residues at the interface of oligomerization acting as hot spots, which enhance thermal stability via oligomerization. 49

The thermal stability of CIA17 was not significantly affected in the presence of chitooligosaccharides, which could be due to a relatively weak association between the lectin and the oligosaccharides at the high temperatures where these transitions occur. The three transitions that are observed in the DSC thermograms of CIA17 (see Figure 1A) can be represented by Scheme I:

$$(A_2)_n \leftrightarrow nA_2 \rightarrow 2nA \rightarrow 2nU$$
 (I)

where n is the degree of oligomerization. A plausible pictorial representation of these thermal transitions is given in Figure 2.

3.2. Chemical Unfolding of CIA17. The addition of chaotropic agents to protein solutions in aqueous media disrupts the hydrogen bond network between water molecules both in the bulk as well as in the hydration shells around hydrophobic amino acids, which weakens the hydrophobic effect and destabilizes the protein structure, resulting in its unfolding. We have investigated the effect of three chemical denaturants, namely, urea, GdmCl, and GdmSCN, on the structure of CIA17 by monitoring fluorescence emission characteristics of the protein. Chemical unfolding of many proteins was studied by monitoring changes in the tryptophan fluorescence characteristics such as fluorescence intensity, quantum yield, emission maximum, fluorescence lifetime, etc., resulting from the addition of increasing concentrations of the denaturants. 50 Although fluorescence intensity exhibits proportionality to the population of the microstates (i.e., folded, unfolded), which is crucial to derive thermodynamic parameters from the spectroscopic data, complexity arises in some cases due to various factors including very small

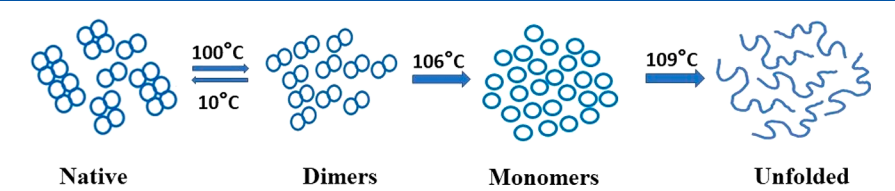


Figure 2. Plausible schematic representation of the thermal unfolding of CIA17. In the first transition, centered at  $\sim$ 98.3 °C, the oligomers reversibly dissociate into dimers. In the second transition, centered at  $\sim$ 105.9 °C, the dimers irreversibly dissociate into monomers. In the final transition, centered at 108.6 °C, the monomers undergo complete, irreversible unfolding.

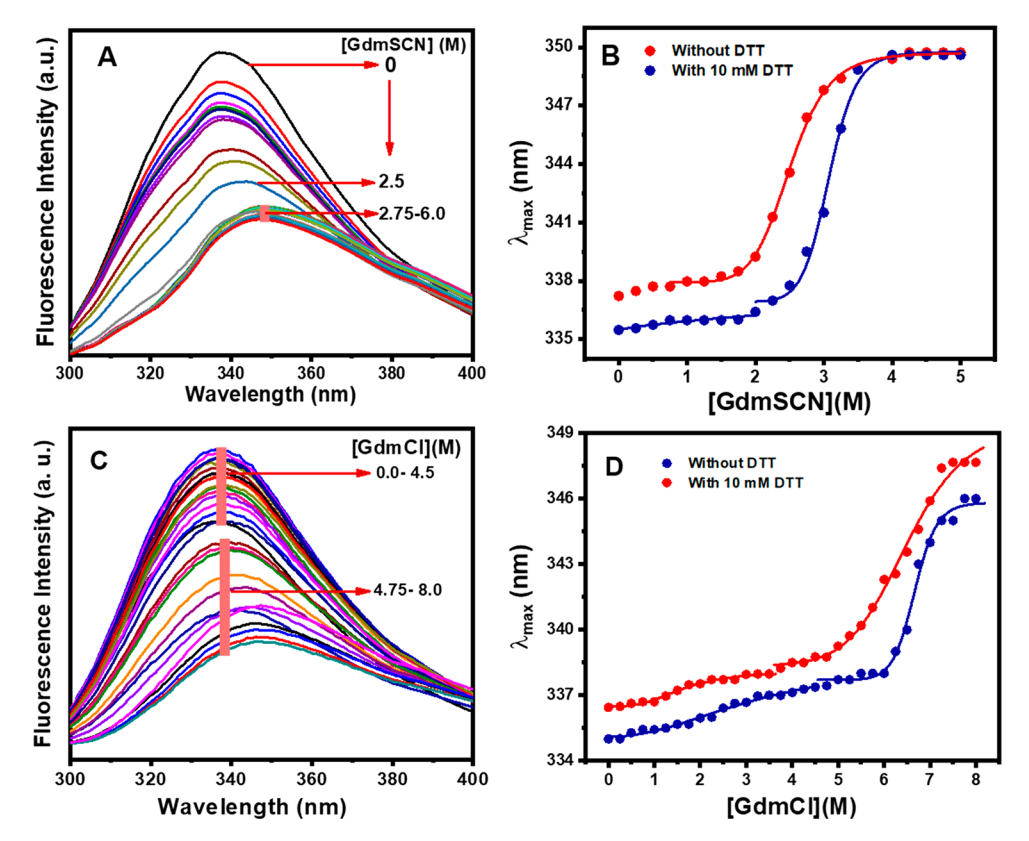


Figure 3. Fluorescence emission spectra of CIA17 in the absence and in the presence of GdmCl (A) and GdmSCN (C). Emission maximum ( $\lambda_{max}$ ) of CIA17 vs denaturant concentration for (B) GdmCl and (D) GdmSCN. Blue and red  $\bullet$  symbols represent data points for experiments performed in the absence and in the presence of 10 mM DTT. Solid lines in (B) and (D) correspond to sigmoidal fits of the data obtained using the Botzmann model and the Levenberg–Marquardt iteration algorithm available in the MicroCal Origin software.

differences in the signal intensity between the folded and unfolded states, which make precise measurements difficult. 51,52 The emission maximum ( $\lambda_{max}$ ) of native CIA17 is seen at 335 nm upon excitation at 295 nm. This suggests that the nine tryptophan residues in CIA17 are neither totally buried inside the hydrophobic core of the protein nor fully exposed on the hydrophilic surface but are probably distributed in different states of exposure to the aqueous solvent. The fluorescence emission of some of these could be quenched by neighboring amino acid residues such as Lys, Arg, Asp, Glu, Asn, and His by excited state proton transfer and/or electron transfer mechanisms.<sup>53</sup> Further, different denaturants may affect the fluorescence intensity as each of the chaotropic agents used here was reported to affect the lifetime of the indole moiety differently. 54 In the case of CIA17, while major transitions centered around 3.4 and 2.3 M GdmSCN could be discerned in experiments performed in the absence and in the presence of 10 mM DTT, respectively, there was too much scatter in the intensity data in the unfolding studies carried out using GdmCl (Figure S3). In view of these considerations, which make it difficult to investigate the chemical unfolding of CIA17 by monitoring changes in the fluorescence intensity, we have monitored changes in the emission  $\lambda_{\rm max}$  of the lectin in the presence of denaturants. While the emission maximum also does not give an accurate picture of the unfolding process, at least the general trends can be assessed more reliably since the emission  $\lambda_{\text{max}}$  only increases when the protein unfolds, whereas the emission intensity can increase, decrease, or remain unaltered.

Fluorescence spectra of CIA17 incubated with different concentrations of GdmSCN and a plot depicting the emission maximum of CIA17 as a function of the denaturant concentration are shown in Figure 3A and 3B, respectively. Similar data corresponding to GdmCl-induced unfolding are presented in Figure 3C and 3D, respectively. The main unfolding event appears to be a two-state transition with a transition midpoint at 3.1 M GdmSCN, and the  $\lambda_{max}$  of the protein exhibits a red shift to 349 nm as the concentration of the chaotrope is gradually increased to ~4 M, indicating complete exposure of Trp residues to the aqueous solvent (Figures 3 A and 3B). Interestingly, a smaller, yet distinct event is seen between 0 and 2 M GdmSCN. Considering that this event is associated with only a small shift ( $\sim$ 2 nm) in  $\lambda_{max}$ (Figure 3B), this transition can be ascribed to the dissociation of the dimeric protein into monomers, which does not change the structure of the folded protomers and hence is not expected to significantly alter the emission  $\lambda_{\text{max}}$ . Incubation of the protein with 10 mM DTT prior to treatment with GdmSCN lowered the midpoint of the main unfolding event to  $\sim 2.5$  M GdmSCN, whereas the minor transition appears to have reached completion before 1.0 M GdmSCN.

Qualitatively very similar results were obtained with GdmCl (Figure 3C, 3D), except that the midpoint of the main unfolding transition was observed at significantly higher concentrations of the chaotrope for the studies conducted in the presence and in the absence of 10 mM DTT (~6.4 and 6.8 M, respectively). The corresponding minor transitions, attributed to the dissociation of the dimeric CIA17 into monomers, were found to be centered at around 1.4 and 2.5 M

GdmCl, respectively (Figure 3D). Urea was found to be the least effective in denaturing CIA17. In the absence of DTT, incubation with 10 M urea led to only a 2–3 nm red shift in the emission maximum, although upon reduction with 10 mM DTT the emission  $\lambda_{\rm max}$  of CIA17 shifted to 345 nm (Figure S4). These observations are consistent with the general understanding that urea is a weaker chemical denaturant than guanidinium salts. <sup>55</sup>

Results obtained from chemical unfolding studies on CIA17, performed in the absence and in the presence of DTT, can be explained in terms of additional stability imparted by the disulfide bonds connecting cysteine residues to the overall structure of the protein. CIA17 contains three cysteine residues among which C34 and C51 form an intramolecular disulfide bond, whereas C125 near the C-terminal end remains exposed to the surface and most likely participates in the formation of intermolecular disulfide linkages with other PP2 molecules as well as PP1 proteins, which promote the formation of crosslinked, extended structures that seal the wounds inflicted by insect bites. The present results, obtained from the chaotropeinduced unfolding studies, suggest that these intra- and intermolecular disulfide bonds undergo cleavage when incubated with 10 mM DTT, which facilitates the complete unfolding of CIA17 upon treatment with the chaotropic agents, GdmSCN and GdmCl. Thus, the present studies indicate that disulfide linkages play an important role in the tertiary and quaternary structures of CIA17.

It is instructive to compare the results of thermal unfolding studies with those obtained from chemical denaturation studies. While the DSC studies indicated that the thermal unfolding of CIA17 involves three distinct steps, only two wellresolved steps could be identified in the chemical unfolding studies with both GdmCl and GdmSCN. This difference can be explained on the basis of differences in the concentrations of CIA17 used in the DSC and fluorescence studies, employed in the thermal and chemical unfolding studies, respectively. Our previous AFM studies have shown that at the relatively high concentration of 0.5–1.0 mg ( $\sim$ 29–58  $\mu$ M) used in the DSC studies CIA17 exists as relatively large, yet soluble aggregated structures, whereas at the concentration of  $\sim 1-2$  $\mu$ M used in the fluorescence studies it exists as small globular structures. 13 Therefore, it appears that the first component in the DSC thermogram of native CIA17, centered at ~98.3 °C, is the dissociation of such large soluble aggregates of the protein into dimers. Since such large aggregates are not present in the low concentration protein samples used in the fluorescence measurements; only two transitions have been observed in the chemical denaturation studies. The formation of higher oligomers or aggregation at higher concentrations was further investigated by probing the size of the native protein using fluorescence correlation spectroscopy (FCS).

# 3.3. Fluorescence Correlation Spectroscopic Studies. The fluorescence-correlated data for the CIA17-A488 conjugate in 15 mM phosphate buffer is shown in Figure 4. The cross-correlation data was better fitted to eq 3, which includes the contribution of an exponential term in addition to the simple diffusion to the fluorescence intensity fluctuation than to eq 2, which corresponds to a single-diffusion component model. The correlation data for free Alexa488 was well fitted to the single-diffusion model (Figure S5), and the laser intensity used for all the FCS measurements was $\sim 10-12~\mu W$ , which rules out the possibility of fluorescence fluctuation due to intersystem crossing. Considering these aspects, the second

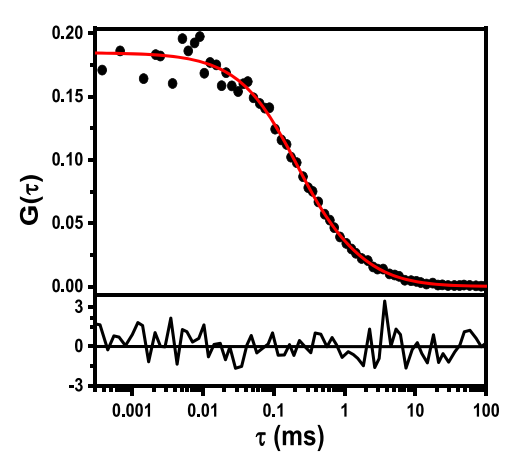


**Figure 4.** Correlation data of A488-labeled CIA17. The red solid line is the fit to eq 2, simple diffusion with a second-order exponential component. The bottom panel shows the residual distribution for the fit

term  $(\tau_R)$  in the correlation function can be attributed to the conformational fluctuations in the protein that modulate the interaction between amino acid residues Trp and Tyr of the protein and the fluorophore because side chains of these two amino acids have been demonstrated to efficiently quench the fluorescence emission of Alexa fluorophores when they come in close proximity. Besides nine Trp and three Tyr residues, each CIA17 subunit also has two His and six Met residues, which can quench the fluorescence emission intensity of the dye to different degrees when the protein undergoes conformational fluctuations. This in turn can lead to fluctuations in the observed fluorescence intensity. The quenching of the fluorescence intensity and the decrease in the average lifetime of the free A488 in the CIA17-A488 conjugate are shown in Figures S6 and S7.

From FCS measurements performed on the labeled CIA17 in the concentration range of 5–50 nM, the average hydrodynamic radius ( $R_{\rm h}$ ) of the native protein was estimated as 2.91 ( $\pm$ 0.23) nm, which is significantly higher than 2.04 nm predicted for the monomeric protein by the following empirical equation:<sup>58</sup>

$$R_{\rm h} = 4.75 n^{0.29} \,\text{Å} \tag{8}$$

where n is the number of amino acid residues in the protein. The higher  $R_{\rm h}$  value obtained from the FCS measurements suggests that the lectin exists in an oligomeric form in the concentration range of 5–50 nM. A significant change in the average diffusion time  $(\tau_{\rm D})$  from 332  $(\pm 23)$  to 236  $(\pm 21)$   $\mu s$  was observed with the progressive dilution of the labeled protein to  $\leq$ 0.8 nM. Consequently, the  $R_{\rm h}$  value decreases to  $\sim$ 2.13  $(\pm 0.15)$  nm indicating that CIA17 exists essentially as a monomer at concentrations below 1 nM.

In order to investigate the formation of higher oligomers or aggregates at higher concentrations, the CIA17-A488 conjugate (10 nM) was mixed with unlabeled CIA17 to yield varying concentrations (250 nM $-100~\mu$ M) of the total protein. FCS measurements were carried out after 30–120 min incubation with the same experimental setup. The normalized correlation curves and the variation of the hydrodynamic radius of the native protein as a function of total protein (labeled + unlabeled protein) concentration are shown in Figure 5, and the autocorrelation profiles along with fits are shown in Figure S8. Despite the complexity of oligomerization,

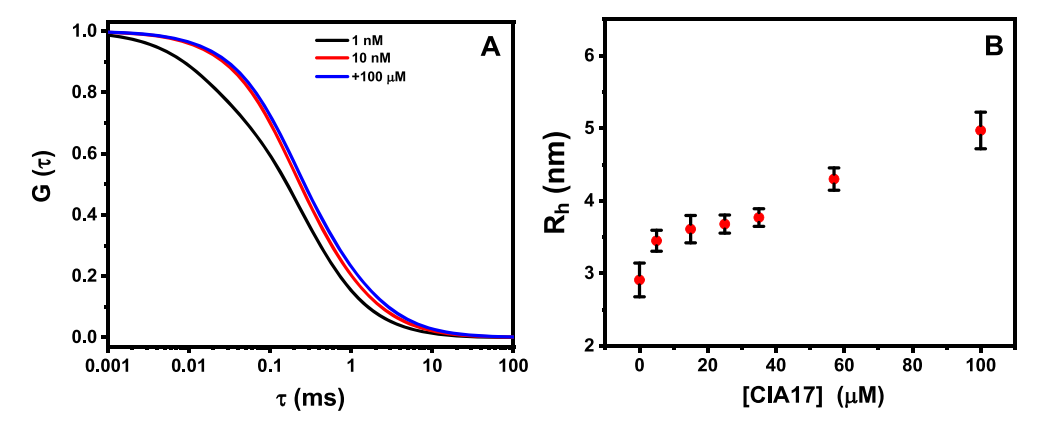
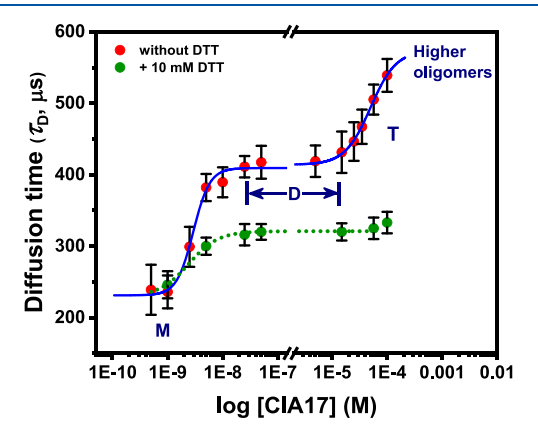


Figure 5. (A) Normalized correlation curves of the A488-CIA17 conjugate with increasing concentration of unlabeled CIA17. (B) Variation of  $R_h$  with increasing concentration of protein. Error bars represent SD values estimated from a minimum of four measurements.

all the correlation data could be fitted satisfactorily to eq 3. The  $R_{\rm h}$  value increases to 3.4 (±0.33) nm at  $\geq$ 5  $\mu$ M of total protein. Only a marginal change was observed over the concentration range of 5–40  $\mu$ M. The  $R_{\rm h}$  value increases to 4.3 (±0.2) nm at 57  $\mu$ M and 4.97 (±0.25 nm) nm when the protein concentration reached 100  $\mu$ M.

The average degree of oligomerization (k) was determined from the relative diffusion coefficients ( $D_k$ , k = 1, 2, 3, ...) of different oligomers. According to the Stokes-Einstein equation, the diffusion coefficient of a spherical particle is inversely proportional to the cubic root of its volume. The AFM images of CIA17 reported earlier<sup>13</sup> indicate that small oligomers are nearly spherical, and at higher concentrations they further self-assemble leading to the formation of filamentous structures. Considering the near-spherical shape of the oligomers, it can be written as  $D_k = D_1 k^{-1/3}$ , where k is the number of subunits present in the oligomer.<sup>59</sup> The diffusion coefficient was found to decrease to 84 ( $\pm 14$ )  $\mu$ m<sup>2</sup> s<sup>-1</sup> when the concentration of the total protein (labeled + unlabeled) was varied between 5 and 50 nM, whereas it was estimated as 115 ( $\pm$ 21)  $\mu$ m<sup>2</sup> s<sup>-1</sup> at concentrations  $\leq$ 0.8 nM. The  $D_k/D_1$  value remained nearly unchanged within error at an average value of 0.86 over the wide concentration range of 5 nM-5  $\mu$ M, implying that CIA17 exists as a homodimer over this concentration range. The ratio decreases to 0.71 ( $\pm$ 0.12) in the concentration range  $10-40 \mu M$  of the unlabeled protein suggesting the formation of tetramers (dimer of dimers).

Figure 6 shows a plot of diffusion time of CIA17 as a function of log [CIA17]. For the native protein in the absence of any reducing agent, the plot shows two well-separated equilibria corresponding to association of monomers to give a dimer and dimers combining to yield tetramers. Sigmoidal fits of the data using the Botzmann model and the Levenberg-Marquardt iteration algorithm available in the MicroCal Origin software yielded the dissociation constants  $(K_D)$  for the M  $\leftrightarrow$ D and D  $\leftrightarrow$  T equilibria as 2.9 ( $\pm$ 0.4) nM and 49.9 ( $\pm$ 6.9)  $\mu$ M, respectively. The diffusion coefficient was found to be 56  $\mu \text{m}^2 \text{ s}^{-1}$  at a protein concentration of 57  $\mu \text{M}$  and 49.3  $\mu \text{m}^2 \text{ s}^{-1}$ at 100  $\mu$ M of the total protein with corresponding  $D_k/D_1$  ratios of 0.54 and 0.48, respectively. The k value was estimated to be  $\sim$ 8–12 when the concentration of the total protein was varied between 50 and 100  $\mu$ M, which suggests that the homodimeric CIA17 self-assembles leading to the formation of larger aggregates at higher protein concentrations. Very interestingly, when the CIA17 samples were preincubated with 10 mM DTT, only one equilibrium was observed which overlapped



**Figure 6.** Binding curves showing the  $M \leftrightarrow D$  and  $D \leftrightarrow T$  equilibria of CIA17. The change in diffusion time is plotted against the logarithm of the total protein concentration. From a nonlinear regression of the data (blue lines), the dissociation constants  $(K_D)$  for the  $M \leftrightarrow D$  and  $D \leftrightarrow T$  equilibria were estimated as 2.9  $(\pm 0.4)$  nM and 49.9  $(\pm 6.9)$   $\mu$ M for native CIA17 (without DTT), whereas in the presence of 10 mM DTT the  $K_D$  value for the  $M \leftrightarrow D$  equilibrium was estimated as 2.4  $(\pm 0.8)$  nM. See the text for details.

with the monomer-dimer equilibrium seen in the absence of the reducing agent. The  $K_D$  value for this equilibrium was estimated as 2.4 (±0.8) nM, which is comparable to that observed for the native CIA17. While the diffusion time observed for the monomer in the presence of DTT was similar to that determined for the native protein, the  $\tau_{\rm D}$  value corresponding to the dimer was, however, considerably lower than that determined for the native protein dimer. This suggests that the reduction of the disulfide bonds leads to changes in the shape of the protein, which in turn alter its diffusion time. Additionally, it is seen that the presence of DTT prevents the formation of higher oligomers (beyond dimer), clearly indicating that disulfide bond formation is required for the formation of large oligomeric structures of the protein which take part in the formation of polymeric structures that may play a role in wound sealing on the surface of the fruit.

The dissociation constants of  $\sim$ 2.9 nM estimated here for the CIA dimer dissociating into monomers and  $\sim$ 50  $\mu$ M estimated for the tetramer to dissociate to yield dimers are about 1 and 3 orders of magnitude higher than the values of 0.55 and 50 nM, respectively, estimated for the corresponding equilibria of the tumor suppressor protein p53. Additionally, it is also interesting to note that in the case of p53 the  $K_D$ 

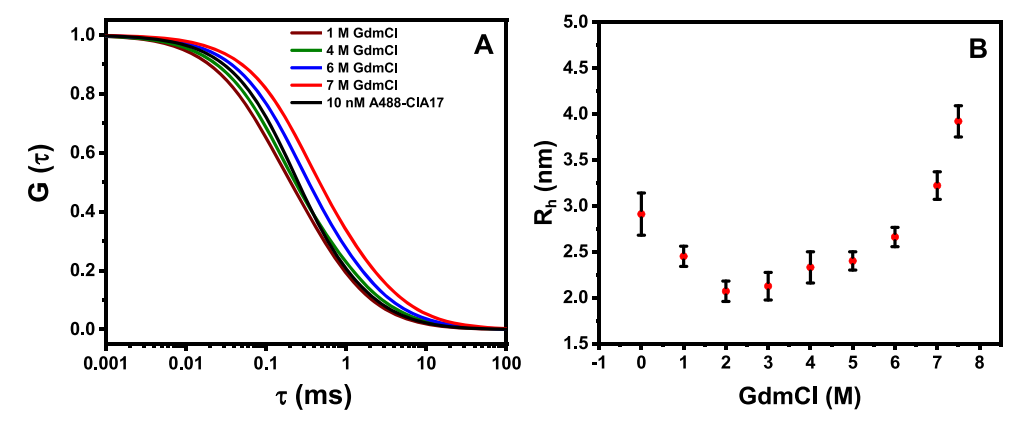


Figure 7. (A) Normalized correlation curves of the A488-CIA17 conjugate with increasing concentration of unlabeled CIA17. (B) Variation of the  $R_h$  value with increasing concentration of GdmCl.

values for the dimer  $\leftrightarrow$  tetramer equilibrium are approximately 100-fold higher than that estimated for the monomer  $\leftrightarrow$  dimer equilibrium, whereas for CIA17 the  $K_{\rm D}$  values for the two equilibria differ by  $\sim$ 17 000 fold.

3.4. Effect of GdmCl on the Size and Conformational **Dynamics of CIA17.** The normalized fluorescence correlation profile and the variation of the hydrodynamic radius of the native protein with the increase in denaturant (GdmCl) concentration is shown in Figure 7, and the autocorrelation profiles along with the fits are shown in Figure S9. In contrast to what is expected for a monomeric protein, the R<sub>h</sub> value decreases with the increase in the concentration of GdmCl up to 2 M, followed by a steady increase in the  $R_h$  value with a gradual increase in the concentration (3 to 7.5 M) of the denaturant. For the native protein, an  $R_h$  value of ~2.91  $(\pm 0.23)$  nm was calculated from the diffusion time of 25 nM A488-CIA17. At 2 M GdmCl, Rh decreases to ~2.07 nm, which is close to the R<sub>h</sub> value of 2.04 nm predicted for the monomer by eq 8. With further increase in the denaturant concentration, R<sub>h</sub> increases steadily, and a sharp change to a value of 3.92 nm occurs at 7.5 M concentration. This matched well with the  $R_h$  value of 3.87 nm predicted for the unfolded protein (with n amino acid residues) from the following empirical equation:<sup>58</sup>

$$R_{\rm h} = 2.21 {\rm n}^{0.57} \,{\rm Å} \tag{9}$$

This clearly suggests that the lectin completely unfolds when incubated with 7.5 M GdmCl. Results of steady state fluorescence measurements (section 3.2) suggested that chemical unfolding of CIA17 by GdmCl is a three-state process. Similarly, the FCS data could be interpreted as follows: in the first transition (0–2 M GdmCl) the dimeric protein dissociates to give monomers, and the second transition (3–7.5 M GdmCl) is the denaturation of monomers to yield the unfolded protein. The above changes in the hydrodynamic radius of the protein as the concentration of the denaturant is varied are consistent with the following model. CIA17 exists as a homodimer at the concentration used in these studies (25 nM), and its chaotropic-induced denaturation can be described by the three-state model shown in Scheme II:

$$A_2 \overset{K_1}{\leftrightarrow} 2I \overset{K_2}{\leftrightarrow} 2U \tag{II}$$

where  $A_2$  is the dimeric native protein, I is the monomeric intermediate, and U is the unfolded protein.

The variation of the relaxation time  $(\tau_R)$  monitored as a function of the GdmCl concentration is shown in Figure 8.

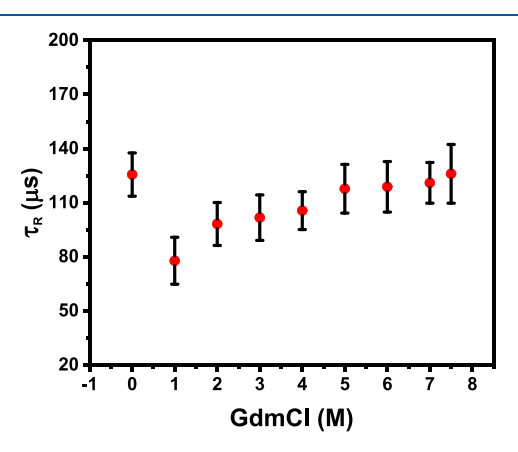


Figure 8. Variation of  $\tau_R$  as a function of the GdmCl concentration.

The figure indicates that  $\tau_{\rm R}$  decreases from 126 (±12) to 78 (±13)  $\mu{\rm s}$  upon the addition of 1 M GdmCl and then gradually increases and finally reaches 126 (±16)  $\mu{\rm s}$  at 7.5 M of GdmCl. The sharp decrease in relaxation time at low GdmCl concentrations (0–1 M) may be due to the partial dissociation of dimers to monomers. The constant increase in  $\tau_{\rm R}$  as the concentration of GdmCl increases is possibly due to the increase in the average distance of the fluorophore and Trp residues during the unfolding process.

It is interesting to compare the results of thermal and chemical unfolding studies on CIA17 with those obtained with cucumber (*Cucumis sativus*) phloem lectin (CPL), another dimeric phloem exudate lectin isolated from the Cucurbitaceae. While the present studies have shown that unfolding thermograms of CIA17 could be resolved into three components, suggesting the presence of intermediate states in the unfolding process, thermal unfolding of CPL could be analyzed in terms of a single transition from a fully folded state to a completely unfolded state. Similarly, the chemical unfolding of CIA17 by GdmCl and GdmSCN could be resolved into two transitions, whereas the denaturation of CPL by GdmCl could be explained in terms of a single unfolding transition.

#### 4. CONCLUSIONS

In summary, the present DSC studies on the thermal unfolding of CIA17 show that it is a highly thermostable protein with a  $T_{\rm m}$  of ~109 °C for the complete unfolding of the protein at physiological pH. The overall thermal unfolding of the protein is a complex process involving the dissociation of oligomeric aggregates into dimers, followed by further dissociation of the dimers into monomers which then undergo complete unfolding to yield the fully denatured protein. Fluorescence spectroscopic studies on the chaotrope-induced unfolding of CIA17 by GdmSCN and GdmCl revealed at least two components in the unfolding process, which could be attributed to the dissociation of the dimeric protein into monomers and the complete unfolding of the monomeric subunits. Results of fluorescence correlation spectroscopic studies show that CIA17 exists in the monomeric form below 1 nM, and the monomers associate to give dimers at higher concentrations ( $K_D \sim 2.9$  nM), which again associate to tetramers with a further increase in concentration ( $K_D \sim 50$  $\mu$ M). Higher oligomers are formed when the concentration is increased. The concentration of CIA17 under physiological conditions is  $\sim 6-8$  mg/mL, or  $\sim 340-450$   $\mu$ M (S. Mondal and M. J. Swamy, unpublished results). The present results show that it is considerably higher than the concentrations required for the formation of higher oligomers (≥tetramer). However, since the phloem fluid oozing out of the wound (or cut) on the fruit is a clear liquid, these oligomers must be in soluble form inside the plant. However, upon exposure to air upon coming out, the proteins in the phloem fluid associate to form a jellylike substance which seals the wound. The exposure to air must involve disulfide bond formation (oxidation), and the results presented in this study show that blocking the disulfide bond formation by using DTT in the sample prevents the formation of higher oligomers. These results are relevant for understanding the role of the phloem proteins in protecting the plant from insect/pest attack.

#### ASSOCIATED CONTENT

#### Supporting Information

The Supporting Information is available free of charge at https://pubs.acs.org/doi/10.1021/acs.jpcb.1c02120.

Absorption spectra of Alexa Flour 488 labeled CIA17 (Figure S1); DSC thermograms of CIA17 at varying concentrations of the protein (Figure S2); GdmCl induced unfolding of CIA17 (Figure S3); fluorescence emission spectra of urea-induced unfolding of CIA17 in the absence and in the presence of 10 mM DTT (Figure S4); steady state fluorescence spectra and the lifetime decay of the free A488 and in the CIA17-A488 conjugate (Figures S6, S7); fluorescence autocorrelation curves of free A488 and A488-CIA17 as a function of the total protein (labeled + unlabeled protein) concentration and in the presence of chotropic denaturant at varying concentrations (Figures S5, S8, and S9) (PDF)

#### AUTHOR INFORMATION

#### **Corresponding Author**

Musti J. Swamy - School of Chemistry, University of Hyderabad, Hyderabad 500 046, India; o orcid.org/0000-0002-3108-3633; Phone: +91-40-2313-4807;

Email: mjswamy@uohyd.ac.in, mjswamy1@gmail.com;

Fax: +91-40-2301-2460

#### **Authors**

Saradamoni Mondal - School of Chemistry, University of Hyderabad, Hyderabad 500 046, India

Kishore Babu Bobbili - School of Chemistry, University of Hyderabad, Hyderabad 500 046, India; o orcid.org/0000-0002-9645-6832

Sumanta Paul – School of Chemistry, University of Hyderabad, Hyderabad 500 046, India; o orcid.org/0000-0003-4825-0984

Complete contact information is available at: https://pubs.acs.org/10.1021/acs.jpcb.1c02120

#### **Author Contributions**

Writing-part of the original draft, formal analysis, and investigation (S.M.); writing—part of the original draft, formal analysis, and investigation (K.B.B.); investigation (S.P.); funding acquisition, conceiving ideas, planning and supervision of research, and writing—reviewing and editing (M.J.S.).

The authors declare no competing financial interest.

#### ACKNOWLEDGMENTS

This work was supported by a midcareer award from the University Grants Commission (UGC) (New Delhi, India) to M.J.S. We thank DST (India) for support under the FIST and PURSE programs and UGC (India) for support under the CAS and UPE-II programs of the School of Chemistry and the University of Hyderabad. We are grateful to Prof. A. Samanta for providing access to the TCSPC fluorescence spectrometer. S.M. and K.B.B. were supported by Senior Research Fellowships from CSIR (India). S.P. is a Senior Research Fellow of the UGC (India). University of Hyderabad is an Institution of Eminence (IoE) of UGC (India). We acknowledge financial support to UoH IoE by MHRD (F11/9/2019-U3(A)).

#### ABBREVIATIONS

AFM, atomic force microscopy; CD, circular dichroism; CIA17, Coccinia indica agglutinin; DSC, differential scanning calorimetry; DTT, dithiothreitol; GdmCl, guanidinium chloride; GdmSCN, guanidinium thiocyanate; PP1, phloem protein 1; PP2, phloem protein 2; RNP, ribonucleoprotein;  $T_{\rm m}$ , melting (unfolding) temperature

#### REFERENCES

- (1) Royer, C. A. Probing Protein Folding and Conformational Transitions with Fluorescence. Chem. Rev. 2006, 106, 1769-1784.
- (2) Choi, J.; Kim, S.; Tachikawa, T.; Fujitsuka, M.; Majima, T. Unfolding Dynamics of Cytochrome C Revealed by Single-Molecule and Ensemble-Averaged Spectroscopy. Phys. Chem. Chem. Phys. 2011, 13, 5651-5658.
- (3) Pace, C. N. Determination and Analysis of Urea and Guanidine Hydrochloride Denaturation Curves. Methods Enzymol. 1986, 131,
- (4) Privalov, P. L. Intermediate States in Protein Folding. J. Mol. Biol. 1996, 258, 707-725.
- (5) Basak, S.; Chattopadhyay, K. Studies of Protein Folding and Dynamics Using Single Molecule Fluorescence Spectroscopy. Phys. Chem. Chem. Phys. 2014, 16, 11139-11149.
- (6) Yadav, R.; Sengupta, B.; Sen, P. Conformational Fluctuation Dynamics of Domain I of Human Serum Albumin in the Course of Chemically and Thermally Induced Unfolding Using Fluorescence Correlation Spectroscopy. J. Phys. Chem. B 2014, 118, 5428-5438.
- (7) Bhuyan, A. K.; Udgaonkar, J. B. Folding of Horse Cytochrome C in the Reduced State. J. Mol. Biol. 2001, 312, 1135-1160.

- (8) Bonetti, D.; Camilloni, C.; Visconti, L.; Longhi, S.; Brunori, M.; Vendruscolo, M.; Gianni, S. Identification and Structural Characterization of an Intermediate in the Folding of the Measles Virus X Domain. *J. Biol. Chem.* **2016**, *291*, 10886–10892.
- (9) Reddy, G. B.; Bharadwaj, S.; Surolia, A. Thermal Stability and mode of Oligomerization of the Tetrameric Peanut Agglutinin: A Differential Scanning Calorimetry Study. *Biochemistry* **1999**, 38, 4464–4470.
- (10) Sen, D.; Mandal, D. K. A Comparative Study of Unfolding of *Erythrina Cristagalli* Lectin in Chemical Denaturant and Fluoroalcohols. *Protein Pept. Lett.* **2013**, *21*, 80–89.
- (11) Sinha, S.; Mitra, N.; Kumar, G.; Bajaj, K.; Surolia, A. Unfolding Studies on Soybean Agglutinin and Concanavalin A Tetramers: a Comparative Account. *Biophys. J.* **2005**, *88*, 1300–131.
- (12) Gaikwad, S. M.; Gurjar, M. M.; Khan, M. I. Artocarpus hirsuta lectin. Differential Modes of Chemical and Thermal Denaturation. Eur. J. Biochem. 2002, 269, 1413–1417.
- (13) Bobbili, K. B.; Pohlentz, G.; Narahari, A.; Sharma, K.; Surolia, A.; Mormann, M.; Swamy, M. J. *Coccinia indica* Agglutinin, a 17 kDa PP2 Like Phloem Lectin: Affinity Purification, Primary Structure and Formation of Self-Assembled Filaments. *Int. J. Biol. Macromol.* **2018**, 108, 1227–1236.
- (14) Bobbili, K. B.; Datta, D.; Mondal, S.; Polepalli, S.; Pohlentz, G.; Mormann, M.; Swamy, M. J. Purification, Chitooligosaccharide Binding Properties and Thermal Stability of CIA24, a New PP2-Like Phloem Exudate Lectin from Ivy Gourd (*Coccinia indica*). *Int. J. Biol. Macromol.* **2018**, *110*, 588–597.
- (15) Mondal, S.; Swamy, M. J. Purification, Biochemical/Biophysical Characterization and Chitooligosaccharide Binding to BGL24, a New PP2-Type Phloem Exudate Lectin from Bottle Gourd (*Lagenaria siceraria*). Int. J. Biol. Macromol. 2020, 164, 3656–3666.
- (16) Kehr, J. Phloem Sap Proteins: Their Identities and Potential Roles in the Interaction between Plants and Phloem-Feeding Insects. *J. Exp. Bot.* **2006**, *57*, 767–774.
- (17) Esau, K.; Cronshaw, J. Tubular Components in cells of Healthy and Tobacco Mosaic Virus-Infected. *Virology* **1967**, *33*, 26–35.
- (18) Kleinig, H.; Thones, J.; Dorr, I.; Kollmann, R. Filament Formation in vitro of a Sieve Tube Protein from *Cucurbita maxima* and *Cucurbita pepo. Planta* 1975, 127, 163–170.
- (19) Thompson, G. A.; Schulz, A. Macromolecular Trafficking in the Phloem. *Trends Plant Sci.* **1999**, *4*, 354–360.
- (20) Golecki, B.; Schulz, A.; Thompson, G. A. Translocation of Structural P Proteins in the Phloem. Plant Cell 1999, 11, 127-140.
- (21) Oparka, K. J.; Cruz, S. S. The great escape: Phloem Transport and Unloading of Macromolecules. *Annu. Rev. Plant Physiol. Plant Mol. Biol.* **2000**, *51*, 323–347.
- (22) Dinant, S.; Clark, A. M.; Zhu, Y.; Vilaine, F.; Palauqui, J. C.; Kusiak, C.; Thompson, G. A. Diversity of the Super Family of Phloem Lectins (Phloem Protein 2) in Angiosperm. *Plant Physiol.* **2003**, *131*, 114–128.
- (23) Read, S. M.; Northcote, D. H. Subunit Structure and Interactions of the Phloem Proteins of *Cucurbita maxima* (Pumpkin). *Eur. J. Biochem.* **1983**, 134, 561–569.
- (24) Will, T.; Furch, A. C. U.; Zimmermann, M. R. How Phloem-Feeding Insects Face the Challenge of Phloem-Located Defenses. *Front. Plant Sci.* **2013**, *4*, 336.
- (25) Beneteau, J.; Renard, D.; Marche, L.; Douville, E.; Lavenant, L.; Rahbe, Y.; Dupont, D.; Vilaine, F.; Dinant, S. Binding Properties of the N-Acetylglucosamine and High-Mannose N-Glycan PP2-A1 Phloem Lectin in *Arabidopsis. Plant Physiol.* **2010**, *153*, 1345–1361.
- (26) Will, T.; Van Bel, A. J. E. Physical and Chemical Interactions Between Aphids and Plants. *J. Exp. Bot.* **2006**, *57*, 729–737.
- (27) Gómez, G.; Pallás, V. A Long-Distance Translocatable Phloem Protein from Cucumber forms a Ribonucleo Protein Complex *in vivo* with Hop Stunt Viroid RNA. *J. Virol.* **2004**, 78, 10104–10110.
- (28) Gómez, G.; Torres, H.; Pallás, V. Identification of Translocatable RNA Binding Phloem Proteins from Melon. Potential Components of the Long Distance RNA Transport System. *Plant J.* **2005**, *41*, 107–116.

- (29) Zhang, C.; Shi, H.; Chen, L.; Wang, X.; Lü, B.; Zhang, S.; Liang, Y.; Liu, R.; Qian, J.; Sun, W.; You, Z.; Dong, H. H. Harpin-Induced Expression and Transgenic Overexpression of the Phloem Protein Gene AtPP2-A1 in Arabidopsis Repress Phloem Feeding of the Green Peach Aphid *Myzus persicae*. *BMC Plant Biol.* **2011**, *11*, 11–30.
- (30) Owens, R. A.; Blackburn, M.; Ding, B. Possible involvement of the Phloem Lectin in Long-Distance Viroid Movement. *Mol. Plant-Microbe Interact.* **2001**, *14*, 905–909.
- (31) Pallás, V.; Gómez, G. Phloem RNA-Binding Proteins as Potential Components of the Long-Distance RNA Transport System. *Front. Plant Sci.* **2013**, *4*, 130.
- (32) Anantharam, V.; Patanjali, S. R.; Swamy, M. J.; Sanadi, A. R.; Goldstein, I. J.; Surolia, A. Isolation, Macromolecular Properties, and Combining Site of a Chito-Oligosaccharide-Specific Lectin from the Exudate of Ridge Gourd (*Luffa acutangula*). *J. Biol. Chem.* **1986**, 261, 14621–14627.
- (33) Kumar, G.; Mishra, P.; Anantharam, V.; Surolia, A. Luffa acutangula Agglutinin: Primary Structure Determination and Identification of a Tryptophan Residue Involved in its Carbohydrate-Binding Activity Using Mass Spectrometry. IUBMB Life 2015, 67, 943–953.
- (34) Narahari, A.; Swamy, M. J. Rapid Affinity-Purification and Physicochemical Characterization of Pumpkin (*Cucurbita maxima*) Phloem Exudate Lectin. *Biosci. Rep.* **2010**, *30*, 341–349.
- (35) Narahari, A.; Singla, H.; Nareddy, P. K.; Bulusu, G.; Surolia, A.; Swamy, M. J. Isothermal Titration Calorimetric and Computational Studies on the Binding of Chito-Oligosaccharides to Pumpkin (Cucurbita maxima) Phloem Exudate Lectin. J. Phys. Chem. B 2011, 115, 4110.
- (36) Bostwick, D. E.; Skaggs, M. I.; Thompson, G. A. Organization and Characterization of *Cucurbita* Phloem Lectin Genes. *Plant Mol. Biol.* **1994**, *26*, 887–897.
- (37) Bobbili, K. B.; Bandari, S.; Grobe, K.; Swamy, M. J. Mutational Analysis of the Pumpkin (*Cucurbita maxima*) Phloem Exudate Lectin, PP2 Reveals Ser-104 is Crucial for Carbohydrate Binding. *Biochem. Biophys. Res. Commun.* **2014**, 450, 622–627.
- (38) Narahari, A.; Nareddy, P. K.; Swamy, M. J. A New Chitooligosaccharide Specific Lectin from Snake Gourd (*Tricosanthes anguina*) Phloem Exudate. Purification, Physico-Chemical Characterization and Thermodynamics Of Saccharide Binding. *Biochimie* **2011**, 93, 1676–1684.
- (39) Nareddy, P. K.; Bobbili, K. B.; Swamy, M. J. Purification, Physico-Chemical Characterization and Thermodynamics of Chitooligosaccharide Binding to Cucumber (*Cucumis sativus*) Phloem Lectin. *Int. J. Biol. Macromol.* **2017**, *95*, 910–919.
- (40) Nareddy, P. K.; Swamy, M. J. Differential Scanning Calorimetric and Spectroscopic Studies on the Thermal and Chemical Unfolding Of Cucumber (*Cucumis sativus*) Phloem Exudate Lectin. *Int. J. Biol. Macromol.* **2018**, *106*, 95–100.
- (41) Sanadi, A. R.; Surolia, A. Studies on a Chitooligosaccharide-Specific Lectin from *Coccinia indica*. Thermodynamics and Kinetics of Umbelliferyl Glycoside Binding. *J. Biol. Chem.* **1994**, 269, 5072–5077.
- (42) Bobbili, K. B.; Singh, B.; Narahari, A.; Bulusu, G.; Surolia, A.; Swamy, M. J. Chitooligosaccharide Binding to CIA17 (*Coccinia indica agglutinin*). Thermodynamic Characterization and Formation of Higher Order Complexes. *Int. J. Biol. Macromol.* **2019**, 137, 774–782.
- (43) Sanadi, A. R.; Ananthram, V.; Surolia, A. Elucidation of the Combining Site of *Coccinia indica* Agglutinin (CIA) by Thermodynamic Analyses of its Ligand Binding. *Pure Appl. Chem.* **1998**, *70*, 677–686.
- (44) Kapusta, P. Absolute Diffusion Coefficients: Compilation of Reference Data for FCS Calibration, Rev. 1; Technical Note; PicoQuant GmbH: Berlin, Germany, 2010.
- (45) Foo, Y. H.; Naredi-Rainer, N.; Lamb, D. C.; Ahmed, S.; Wohland, T. Factors Affecting the Quantification of Biomolecular Interactions by Fluorescence Cross-Correlation Spectroscopy. *Biophys. J.* **2012**, *102*, 1174–1183.

- (46) Sherman, E.; Itkin, A.; Kuttner, Y. Y.; Rhoades, E.; Amir, D.; Haas, E.; Haran, G. Using Fluorescence Correlation Spectroscopy to Study Conformational Changes in Denatured Proteins. *Biophys. J.* **2008**, *94*, 4819–4827.
- (47) Chattopadhyay, K.; Saffarian, S.; Elson, E. L.; Frieden, C. Measuring Unfolding of Proteins in the Presence of Denaturant Using Fluorescence Correlation Spectroscopy. *Biophys. J.* **2005**, *88*, 1413–1422.
- (48) Mojumdar, S. S.; Chowdhury, R.; Chattoraj, S.; Bhattacharyya, K. Role of Ionic Liquid on the Conformational Dynamics in the Native, Molten Globule, and Unfolded States of Cytochrome C: a Fluorescence Correlation Spectroscopy Study. *J. Phys. Chem. B* **2012**, *116*, 12189–12198.
- (49) Tanaka, Y.; Tsumoto, K.; Yasutake, Y.; Umetsu, M.; Yao, M.; Fukada, H.; Tanaka, I.; Kumagai, I. How Oligomerization Contributes to the Thermostability of an Archaeon Protein. *J. Biol. Chem.* **2004**, 279, 32957–32967.
- (50) Eftink, M. R. The Use of Fluorescence Methods to Monitor Unfolding Transitions in Proteins. *Biophys. J.* **1994**, *66*, 482–501.
- (51) Duy, C.; Fitter, J. How Aggregation and Conformational Scrambling of Unfolded States Govern Fluorescence Emission Spectra. *Biophys. J.* **2006**, *90*, 3704–3711.
- (52) Tan, P. H.; Sandmaier, B. M.; Stayton, P. S. Contributions of a Highly Conserved VH/VL Hydrogen Bonding Interaction to scFv Folding Stability and Refolding Efficiency. *Biophys. J.* **1998**, *75*, 1473–1482
- (53) Chen, Y.; Barkley, M. D. Toward Understanding Tryptophan Fluorescence in Proteins. *Biochemistry* **1998**, *37*, 9976–9982.
- (54) Swaminathan, R.; Periasamy, N.; Udgaonkar, J. B.; Krishnamoorthy, G. Molten Globule-like Conformation of Barstar: A Study by Fluorescence Dynamics. *J. Phys. Chem.* **1994**, *98*, 9270–9278.
- (55) Tanford, C. Protein Denaturation. Adv. Protein Chem. 1968, 23, 121–282.
- (56) Chen, H.; Ahsan, S. S.; Santiago-Berrios, M. B.; Abruña, H. D.; Webb, W. W. Mechanisms of Quenching of Alexa Fluorophores by Natural Amino Acids. *J. Am. Chem. Soc.* **2010**, *132*, 7244–7245.
- (57) Pabbathi, A.; Ghosh, S.; Samanta, A. FCS Study on the Structural Stability of Lysozyme in the Presence of Morpholinium Salts. *J. Phys. Chem. B* **2013**, *117*, 16587–16593.
- (58) Wilkins, D. K.; Grimshaw, S. B.; Receveur, V.; Dobson, C. M.; Jones, J. A.; Smith, L. J. Hydrodynamic Radii of Native and Denatured Proteins Measured by Pulse Field Gradient NMR Techniques. *Biochemistry* **1999**, *38*, 16424–16431.
- (59) Chakraborty, M.; Kuriata, A. M.; Henderson, J. N.; Salvucci, M. E.; Wachter, R. M.; Levitus, M. Protein Oligomerization Monitored by Fluorescence Fluctuation Spectroscopy: Self Assembly of Rubisco Activase. *Biophys. J.* **2012**, *103*, 949–958.
- (60) Rajagopalan, S.; Huang, F.; Fersht, A. R. Single-Molecule Characterization of Oligomerization Kinetics and Equilibria of the Tumor Suppressor p53. *Nucleic Acids Res.* **2011**, *39*, 2294–2303.

FISEVIER

Contents lists available at ScienceDirect

#### International Journal of Biological Macromolecules

journal homepage: http://www.elsevier.com/locate/ijbiomac



# Purification, biochemical/biophysical characterization and chitooligosaccharide binding to BGL24, a new PP2-type phloem exudate lectin from bottle gourd (*Lagenaria siceraria*)



Saradamoni Mondal, Musti J. Swamy \*

School of Chemistry, University of Hyderabad, Hyderabad 500046, India

#### ARTICLE INFO

Article history:
Received 7 July 2020
Received in revised form 25 August 2020
Accepted 31 August 2020
Available online 2 September 2020

Keywords: Cucurbitaceae Carbohydrate binding protein Phloem protein 2

#### ABSTRACT

Phloem Protein 2 (PP2), highly abundant in the sieve elements of plants, plays a significant role in wound sealing and anti-pathogenic responses. In this study, we report the purification and characterization of a new PP2-type lectin, BGL24 from the phloem exudate of bottle gourd (*Lagenaria siceraria*). BGL24 is a homodimer with a subunit mass of ~24 kDa and exhibits high specificity for chitooligosaccharides. The isoelectric point of BGL24 was estimated from zeta potential measurements as 5.95. Partial amino acid sequence obtained by mass spectrometric studies indicated that BGL24 exhibits extensive homology with other PP2-type phloem exudate lectins. CD spectroscopic measurements revealed that the lectin contains predominantly  $\beta$ -sheets, with low  $\alpha$ -helical content. CD spectroscopic and DSC studies showed that BGL24 exhibits high thermal stability with an unfolding temperature of ~82 °C, and that its secondary structure is essentially unaltered between pH 3.0 and 8.0. Fluorescence titrations employing 4-methylumbelliferyl- $\beta$ -D-N,N',N''-triacetylchitotrioside as an indicator ligand revealed that the association constants for BGL24-chitooligosaccharide interaction increase considerably when the ligand size is increased from chitotriose to chitotetraose, whereas only marginal increase was observed for chitopentaose and chitohexaose. BGL24 exhibited moderate cytotoxicity against MDA-MB-231 breast cancer cells, whereas its effect on normal splenocytes was marginal.

© 2020 Elsevier B.V. All rights reserved.

#### 1. Introduction

Lectins are a unique class of non-enzymatic proteins of non-immune origin that bind carbohydrates in a highly specific and reversible manner [1–3]. They are highly abundant in nature and are found in a variety of plants and animals, as well as microbes and fungi [4,5]. Their distinct carbohydrate binding properties make them important tools in biological, biomedical and clinical research [5,6].

In plants, lectins are present in different parts including seeds, bark, leaves, roots/tubers, latex as well as the phloem exudate. Phloem in vascular plants is the major integral part of the whole communication system by which water, nutrients, minerals, amino acids, sugars, peptides and proteins, and RNAs are transported over long distances [7,8]. PP1 and PP2 are highly abundant proteins in the phloem sap. PP2 proteins associate with the polymers of phloem filament protein (PP1) through disulfide linkages and move from companion cells to the sieve tube via plasmodesmata and play a major role in long-distance trafficking [9–17]. Under stress, the PP2 proteins, which exhibit lectin activity, immobilize microorganisms and fungi to the cross-linked filaments,

resulting in a sealing of the wounded sieve tubes. The PP2 proteins thus play a key role in wound sealing and anti-pathogenic responses [18]. Besides PP2 proteins, a wide range of chitin-binding lectins and chitinases are present in plants, which also appear to play a role in plant resistance against pathogens [19–21].

The Cucurbitaceae phloem exudate lectins (PP2 proteins) are soluble cytoplasmic proteins with extended binding chitooligosaccharides [B (1-4) linked oligomers acetylglucosamine (GlcNAc)] [5]. Chitin is a major polysaccharide present in the fungal cell wall, exoskeletons of insects, eggs of nematodes etc. [22,23]. Cucurbitaceae PP2 lectins have a common "chitin binding domain", composed of cysteine-rich amino acid residues. In addition to their strong and specific recognition of chitooligosaccharides, some of these proteins have been shown to bind to N-glycans, probably through the core chitobiose (GlcNAc\beta14GlcNAc) moieties and also interact with viroid RNA in a nonspecific manner [14,24-27]. In the last couple of decades several PP2-type lectins have been purified from the phloem exudate of Cucurbitaceae species and characterized in considerable detail. These include Luffa acutangula agglutinin (LAA) [27-29], two homodimeric lectins from the phloem exudate of Coccinia indica fruits, CIA17 and CIA24 with subunit masses of 17 and 24 kDa, respectively [24,25,29], pumpkin (*Cucurbita maxima*) phloem exudate lectin (PPL)

<sup>\*</sup> Corresponding author. E-mail address: mjswamy@uohyd.ac.in (M.J. Swamy).

[18,26,30], *Cucumis sativus* phloem lectin (CPL) [31,32], and AtPP2-A1 from *Arabidopsis thaliana* [9]. In earlier literature CIA17 was referred to as CIA as the presence of the 24 kDa protein in this species was unknown at that time [24]. Upon biological stress and/or injury, Cucurbitaceae plants ooze the phloem through the wound, which very quickly coagulates to form elastic-like substance. Analysis of the biochemical composition of the phloem exudate revealed that it contains a variety of macromolecules including lectins.

Lagenaria siceraria, commonly known as bottle gourd, belongs to the Cucurbitaceae family [33]. L. siceraria is a rich wellspring of dietary prebiotics and is believed to improve the probiotic populaces that influence enteric microbial metabolism prompting synthesis and release of beneficial biomolecules [33–36]. Recently Vigneswaran and coworkers have reported the anti-proliferative activity of crude L. siceraria latex sap [36]. The potential pharmacological activity of the different parts of L. siceraria to treat various diseases made them important for detailed biochemical and biophysical characterization.

In the present work, we report the purification of a PP2-type lectin (bottle gourd lectin, BGL24) from the phloem exudate of bottle gourd by affinity chromatography on chitin. Information on the primary and secondary structure of the lectin was obtained by mass spectrometric and circular dichroism (CD) spectroscopic studies, whereas its carbohydrate binding specificity was identified to be directed towards chitooligosaccharides by hemagglutination-inhibition assay. The effect of temperature and pH on the stability as well as on the lectin activity of BGL24 was also explored. Additionally, thermodynamic parameters governing the binding of a fluorescently labeled chitooligosaccharide, 4-methylumbelliferyl- $\beta$ -D-N,N',N''-triacetylchitotrioside [MeUmb $\beta$ (GlcNAc) $_3$ ] to this lectin were characterized by fluorescence titrations monitoring changes in the fluorescence intensity of the 4-

methlyumbelliferyl moiety upon titration with BGL24, whereas the

binding of unlabeled chitooligosaccharides was investigated by using

MeUmbβ(GlcNAc)<sub>3</sub> as an indicator ligand (cf. [24]).

#### 2. Materials and methods

#### 2.1. Materials

Unripe bottle gourds (*Lagenaria siceraria*) were purchased from local vegetable vendors. Chitin (from crab shells), dithiothreitol (DTT), galactose, glucose, mannose, fucose, methyl- $\alpha$ -D-glucopyranoside, methyl- $\alpha$ -D-galactopyranoside, methyl- $\alpha$ -D-mannopyranoside, *N*-acetyl-D-glucosamine, cellobiose, lactose, melibiose, lactulose, 4-methylumbelliferyl- $\beta$ -D-N,N',N"-triacetylchitotrioside and all the chitooligosaccharides were obtained from Sigma Chemical Co. (St. Louis, MO, USA). All other chemicals and reagents used were of the highest purity available from local suppliers.

#### 2.2. Extraction and purification of BGL24

Bottle gourd fruits were washed thoroughly with double distilled water and dried. Then 2–3 mm deep longitudinal incisions were made on the clean surface of the fruit as described earlier for other Cucurbitaceae fruits [24–27] and the phloem exudate oozing out from the incisions was collected into previously prepared ice-cold 20 mM sodium phosphate buffer (pH 7.4) containing 150 mM NaCl and 3 mM DTT (PBS-DTT) [31,32]. The phloem exudate collected in PBS-DTT was centrifuged at 4057g for 20 min at 4 °C in an Eppendorf 5810R centrifuge. The supernatant was directly subjected to affinity chromatography on a chitin column which was pre-equilibrated with PBS-DTT. The flowthrough obtained was reloaded to ensure complete binding of the protein. The column was then washed with PBS-DTT extensively to remove unbound proteins, monitoring absorbance of the eluent at 280 nm. When absorbance fell below 0.05 at 280 nm, the proteins bound to the chitin column were eluted with 16 mM acetic acid at room temperature and fractions of ~6 mL were collected. The absorbance of each fraction was assessed at 280 nm. Fractions of higher absorbance were pooled and dialyzed against distilled water followed by 20 mM phosphate buffer. Homogeneity of the affinity-purified protein was assessed by native PAGE as well as by SDS-PAGE under reducing/denaturing and non-reducing conditions [37].

#### 2.3. Size exclusion chromatography

The affinity purified protein dialyzed against 20 mM sodium phosphate buffer (pH 7.4) containing 150 mM NaCl (PBS) was further subjected to gel-filtration chromatography. About 100 mL of Sephadex G-100 matrix was packed in a long glass column (1.5 cm  $\times$  100 cm) and equilibrated with PBS. The void volume (Vo) and the resolution of the column were previously measured by the passage of blue-dextran and the standard protein marker successively. About 1 mL of BGL24 sample (2.5 mg/mL) was loaded on the column and eluted with the extraction buffer. After discarding the void volume, 1 mL fractions were collected and the absorbance of each fraction was measured at 280 nm. The molecular weight (MW) of the native protein was determined from a plot of log MW vs  $\rm V_e/\rm V_o$  and comparing the elution volume of the protein with that of standard proteins as described earlier [38]. In this plot  $\rm V_o$  is the void volume and  $\rm V_e$  is the elution volume.

#### 2.4. Reverse phase HPLC

Reverse phase HPLC was performed on a Shimadzu UFLC system (Kyoto, Japan) equipped with a diode array detector. Affinity purified BGL24 was dialyzed against water and subjected to chromatography on a semi-preparative C-18 column (250 mm  $\times$  10 mm) of 10  $\mu$ m particle size [39]. The column was eluted with an increasing gradient of 0.1% trifluoroacetic acid (TFA) as solvent A and 66% acetonitrile in 0.1% TFA as solvent B using a 70-minute program with a constant flow rate of 5 mL/min. The purity of the protein was assessed by SDS-PAGE [37].

#### 2.5. Zeta potential measurements

In order to determine the isoelectric point of BGL24, zeta potential of the protein was measured at different pH using a Malvern Zetasizer Nano ZS (Malvern Instrument Ltd., UK) fitted with a red laser ( $\lambda = 632.8$  nm) [39]. A 10 µg/mL concentration protein solution in PBS was titrated with 0.1 M HCl to obtain the desired pH within the range of 2.0–8.0 at 25 °C. For every sample of different pH, measurements were done in triplicate using a disposable folded capillary cell (DTS1070) provided by Malvern and average values have been reported.

#### 2.6. Hemagglutination and hemagglutination-inhibition assays

Hemagglutination and hemagglutination-inhibition assays were carried out in 96 well ELISA microtiter plates as described earlier [39]. In brief, BGL24 was serially two-fold diluted into successive wells in each row of the ELISA plate. To each well containing 50 µL of serially diluted lectin in PBS, 50 µL of 4% of human erythrocyte suspension (A, B, O) were added and mixed, which resulted in a final volume of 100 µL. After incubation at 4 °C for 1 h, the hemagglutination titer was visually scored. The effect of divalent metal ions on the lectin activity was assessed by performing the hemagglutination assay in the presence of 1 mM concentration of various divalent metal ions (Ca<sup>2+</sup>, Mg<sup>2+</sup>, Mn<sup>2+</sup>, Sn<sup>2+</sup>, Zn<sup>2+</sup>). Activity of the protein was also assessed after dialyzing against 10 mM EDTA, followed by dialysis against PBS. To investigate the effect of temperature on the lectin activity, samples were preincubated at the desired temperature (25-95 °C) for 60 min, cooled to room temperature and the hemagglutination assay was performed as described above. To investigate the effect of pH, lectin samples used were dialysed against the buffer of desired pH (3.0-8.0) together with erythrocytes that were suspended in the same buffer.

Hemagglutination-inhibition assays were performed in the following manner. A stock solution of sugar was serially two-fold diluted in a microtiter plate to give a final volume of 40  $\mu L$  in each well. Then 10  $\mu L$  of lectin was added to each well, mixed and incubated at 4 °C for ~15 min. Then 50  $\mu L$  of 4% erythrocyte suspension was added and mixed. After incubation for 1 h at 4 °C, the hemagglutination titer was visually scored. The following sugars were used in the hemagglutination-inhibition assay: galactose, glucose, mannose, fucose, methyl- $\alpha$ -D-glucopyranoside, methyl- $\alpha$ -D-galactopyranoside, methyl- $\alpha$ -D-mannopyranoside, N-acetyl-D-glucosamine, cellobiose, lactose, melibiose, lactulose and chitooligosaccharides, (GlcNAc) $_{3\text{-}6}$ -

#### 2.7. Mass spectrometric studies

Partial amino acid sequence of BGL24 was obtained by MALDI-TOF mass spectrometry. Samples for MS analysis were prepared as follows. Bands corresponding to BGL24 were excised from SDS-PAGE gels (electrophoresis being performed under reducing conditions) and cut into small pieces and the protein was subjected to in-gel digestion by trypsin according to Shevchenko et al. [40]. Details of the methodology adopted for in-gel digestion and peptide extraction have been described in an earlier publication [31]. In the final step, the proteolytic peptides were extracted by adding extraction buffer (water/acetonitrile, 1:2 v/v with 5% formic acid added) to each tube and incubating for 15 min at 37 °C in a shaker. The supernatant was collected into a fresh tube and dried in vacuo.

The residue obtained in the above step was dissolved in trifluoroacetic acid and acetonitrile buffer and spotted along with  $\alpha$ -cyano-4-hydroxycinnamic acid (HCCA) matrix onto the target plate. After air drying of the spot, mass spectra were recorded using a Bruker Ultraflex III MALDI-TOF/TOF mass spectrometer (Bruker Daltonics) which was calibrated with peptide standards (bradykinin, angiotensin-I, angiotensin-II, bombesin, ACTH and somatostatin). Peaks with high relative abundance were further analysed by Mascot search.

The intact molecular mass of BGL24 was determined from the mass spectrum recorded on an Autoflex II MALDI TOF-TOF instrument from Bruker Daltonics as described earlier [41]. Protein sample extracted from a reducing SDS-PAGE gel band corresponding to 24 kDa was used for estimating the exact mass. The following instrumental settings were employed. Laser frequency: 60 Hz (laser power 90%); acceleration voltage: 20 kV; lens voltage: 6 kV; mass range: 20000 to 30,000 *m/z*. The instrument was calibrated using a high molecular weight standard (Protein standard II, Bruker).

#### 2.8. Multiple sequence alignment

Amino acid sequences of several tryptic peptides of BGL24 were obtained from Mascot analysis by matching their masses with those predicted for tryptic peptides of phloem lectin 2 of *Cucurbita argyosperma*. Amino acid sequences of other homologous proteins were obtained from the NCBI protein database (www.ncbi.nlm.nih. gov/protein). Pairwise sequence alignment was done with *Cucurbita argyrosperma* ssp. phloem protein using bioinformatics (https://www.ebi.ac.uk/Tools/psa/). Multiple sequence alignment with other PP2-type lectins and phloem proteins was carried out using Clustal Omega software (https://www.ebi.ac.uk/Tools/msa/clustalo/).

#### 2.9. Circular dichroism spectroscopy

All CD spectra were recorded on an Aviv 420 spectropolarimeter (Lakewood, NJ, USA) that was connected with a Peltier thermostat for temperature regulation [31,39]. The concentration of BGL24 used was ~0.1 OD and 1.0 OD for measurements in the far UV (250–190 nm) and near UV (300–250 nm) regions, respectively. Samples were placed in a rectangular quartz cuvette of 2 mm path length and the slit width

was 2 nm. All spectra reported are the averages of 5 scans obtained at a scan rate of 20 nm/min. In order to investigate the thermal unfolding as well as the pH-induced unfolding of BGL24, CD spectra were recorded at different temperatures (30–90 °C) and at different pH (3.0–8.0). To obtain the desired pH condition, the BGL24 samples were dialyzed against appropriate buffers among the following: 20 mM KCl-HCl (pH 2.0), 20 mM glycine-HCl (pH 3.0), 20 mM sodium acetate (pH 4.0–5.0), 20 mM sodium phosphate (pH 6.0–7.0), 20 mM Tris-HCl (pH 8.0–9.0).

#### 2.10. Differential scanning calorimetry

DSC measurements were performed on a NanoDSC differential scanning calorimeter from TA instruments (New Castle, Delaware, USA) equipped with a sample cell and a reference cell. BGL24 in water was taken in the sample cell whereas water was loaded in the reference cell. DSC scans were also run with BGL24 that was preincubated with 1 mM chitotetraose. Thermograms obtained were analysed by fitting the data to a Gaussian model available in the NanoAnalyze DSC analysis software provided by the manufacturer.

### 2.11. Fluorescence studies on the binding of MeUmb $\beta$ (GlcNAc) $_3$ to BGL24 and reversal titrations with chitooligosaccharides

All the fluorescence spectroscopic measurements were performed on a Jasco FP-8500 spectrofluorometer equipped with a Jasco ETC-815 Peltier device for temperature regulation. A 2.0 mL solution of 3.81  $\mu$ M 4-methylumbelliferyl- $\beta$ -D-N,N',N''-triacetylchitotrioside

[MeUmb $\beta$ (GlcNAc) $_3$ ] in a 1  $\times$  1  $\times$  4.5-cm quartz cuvette was excited at 318 nm and emission spectra were recorded between 330 and 520 nm. Slit widths of 2.5 nm were used on both the monochromators. The umbelliferyl sugar was titrated by the addition of small aliquots from a 1.97 mg/mL (~82  $\mu$ M) BGL24 stock solution and emission spectra was recorded in the wavelength range of 330–520 nm after 2 min incubation. In order to obtain the thermodynamic parameters of binding, titrations were carried out at five different temperatures between 15 and 35 °C. The association constants were determined from the Chipman plot as described in [24,42,43].

Binding of unlabeled chitooligosaccharides to BGL24 was investigated by studying their ability to reverse the binding of MeUmbβ(GlcNAc)<sub>3</sub> from its complex with BGL24. In these reversal experiments, the fluorescence spectrum of MeUmbβ(GlcNAc)<sub>3</sub> (3.81 μM) was recorded first and then it was incubated with a defined quantity of BGL24 (~3.5 μM), following which the fluorescence spectrum of the sample was recorded again. The mixture was then titrated by adding small aliquots of the unlabeled chitooligosaccharide from a concentrated (1.5–3.0 mM) stock solution at a constant temperature. This led to an increase in the fluorescence intensity of the indicator ligand due to its dissociation from the complex with BGL24. The association constants for both the indicating and inhibitory ligands were obtained by analyzing the titration data (changes in the fluorescence intensity of the indicator ligand) as described earlier [42,43]. In order to obtain the thermodynamic parameters some of the titrations were performed at different temperatures.

#### 2.12. Cell culture

Normal splenocytes and triple negative breast cancer cells (MDA-MB-231) were maintained in a 37 °C incubator (Sanyo MCO-19AIC, Panasonic Biomedical Sales Europe BV, AZ Etten Leur, Netherlands) in 5%  $\rm CO_2$  and humid atmosphere. Both types of cells were cultured in 9.6 cm² culture flasks in MEM medium supplemented with 2 mM glutamine, 10% foetal bovine serum (FBS) and 1% penicillin-streptomycin. Cells were counted and seeded at a density of 1  $\times$  10⁴ cells/cm² in each well of a 96 well cell culture plate.

#### 2.13. MTT cell viability assay

The cytotoxicity of BGL24 towards normal splenocytes and MDA-MB-231 cells was assessed by MTT cell-viability assay as described previously [39] and the results were compared with those obtained with jacalin (*Artocarpus integrifolia* lectin). Briefly, in each well of a 96-well cell culture plate, 100  $\mu$ L of cell suspension was transferred and kept overnight. Then 100  $\mu$ L of each lectin was added in different concentrations (0–1 mg/mL) to different wells. After incubation at 37 °C for 72 h, the supernatant was removed from the cells and 100  $\mu$ L of fresh medium was added, followed by the addition of 25  $\mu$ L of 5 mg/mL MTT in PBS. The plates were then incubated for 4 h and the supernatant was removed. Then 100  $\mu$ L of DMSO was added to each well and after 15 min of shaking at 300 rpm the absorbance was measured at 570 nm. The respective untreated medium was used as the negative control.

#### 3. Results and discussion

#### 3.1. Affinity chromatographic purification of BGL24

BGL24 was purified from the phloem exudate of bottle gourd (*Lagenaria siceraria*) by affinity chromatography on  $\alpha$ -chitin. A single peak was obtained when the lectin was eluted with 16 mM acetic acid from the  $\alpha$ -chitin column in about 85% overall yield (Fig. 1A, Table S1). In native PAGE under non-reducing and non-denaturing condition, the affinity purified protein showed a single band (Fig. 1C). SDS-PAGE under non-reducing condition showed an intense band corresponding to ~44 kDa (Fig. 1D, lane 2). When larger amounts of the

protein were loaded, weaker bands corresponding to higher molecular weights were also seen (Fig. 1D, lane 3), suggesting that BGL24 selfassembles noncovalently to form higher oligomeric structures similar to another Cucurbitaceae phloem exudate lectin, CIA17 [25]. In the presence of a reducing agent such as 2-mercaptoethanol or DTT, a strong band of ~24 kDa was observed along with a minor band at ~44 kDa (Fig. 1E). These results suggest that BGL24 is a homodimer wherein the two subunits are connected via disulfide bonds and that they could not be fully cleaved even by the strong reducing agents. Further purification using size exclusion chromatography and reverse phase HPLC yielded a major peak corresponding to >95% of total protein loaded (Fig. 1B) which is in agreement with the conclusion drawn from SDS-PAGE analysis (cf. lane 2 of Fig. 1D). Gel filtration chromatography of BGL24 on Sephadex G-100 yielded the molecular weight of the native protein as ~50 kDa (Fig. 2A). The isoelectric point of BGL24 was estimated as 5.95 from a plot of zeta potential versus pH (Fig. 2B).

The band corresponding to ~24 kDa in the SDS-PAGE was excised and subjected to mass spectrometric analysis to obtain the exact mass of the protein. The MALDI-TOF mass spectrum, shown in Fig. S2, indicates that the subunit mass of BGL24 is 24,517 Da.

In order to obtain information on its amino acid sequence, the band corresponding to BGL24 was cut from the SDS-PAGE gel and in-gel tryptic digestion was carried out. MS/MS analysis showed that tryptic digestion yielded a number of peptides with masses ranging between 651.35 and 2767.09. The exact masses of several of these peptides could be matched to the calculated masses of predicted tryptic peptides in the primary structure of the phloem lectin from *Cucurbita argyrosperma* subsp. *sororia* (NCBI access no. AAM82558.1) based on Mascot search with a top score of 206 (Table S2). Pairwise sequence

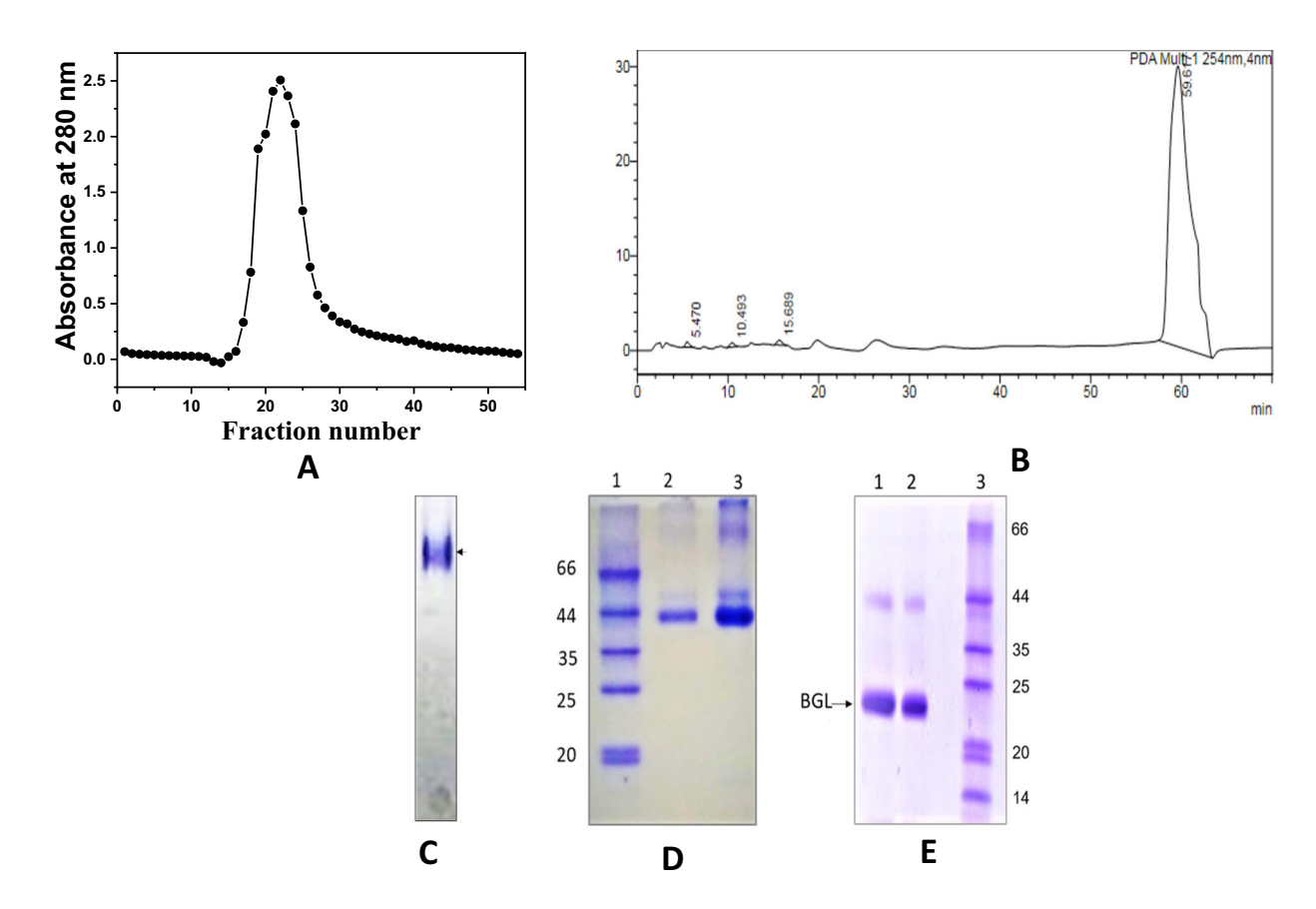


Fig. 1. Chromatographic purification and gel electrophoresis analysis of BGL24. (A) Elution profile of BGL24 from  $\alpha$ -chitin affinity chromatography. Protein bound to  $\alpha$ -chitin was eluted with 16 mM acetic acid and 6 mL fractions were collected. (B) Reverse phase HPLC chromatogram of affinity purified BGL24. The major peak eluting at 59.6 min corresponds to BGL24. (C) Native-PAGE of affinity purified protein on 10% resolving gel and 2.5% stacking gel. (D) SDS-PAGE of proteins eluted from  $\alpha$ -chitin column under nonreducing condition. Lane 1, molecular weight markers; lanes 2 and 3, BGL24. (E) SDS-PAGE in presence of reducing agent. Lanes 1 and 2, BGL24; lane 3, molecular weight markers.

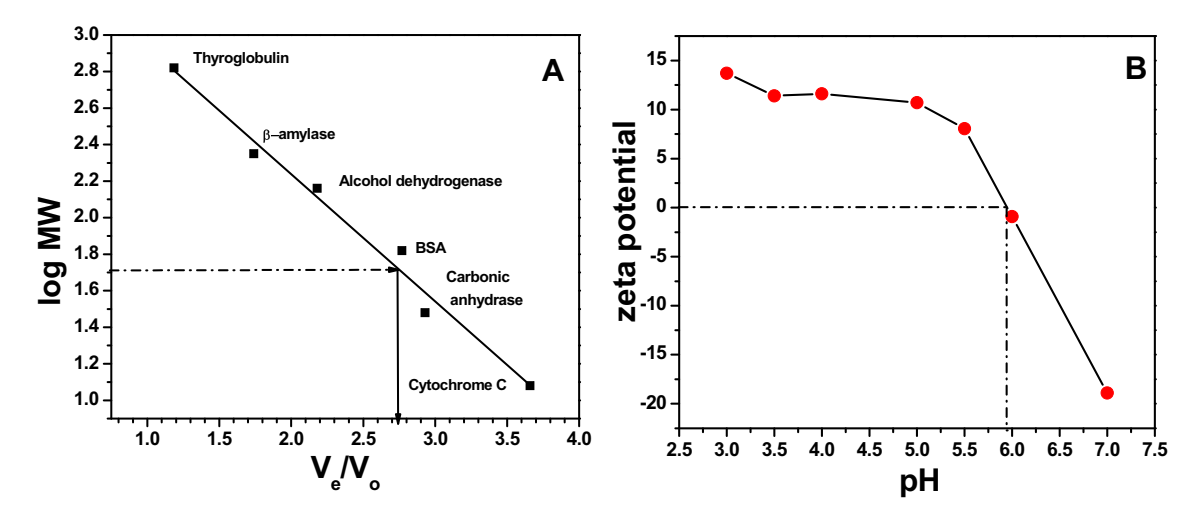


Fig. 2. Determination of molecular weight and isoelectric point of BGL24. (A) Molecular weight of native BGL24 was determined to be ~50 kDa from gel filtration chromatography on Sephadex G-100. The elution profile of BGL24 is given in Fig. S1. (B) The isoelectric point (pl) of BGL24 was estimated as 5.95 from a plot of zeta potential versus pH.

alignment of the peptides obtained for BGL24 with the primary structure of *Cucurbita argyrosperma* phloem lectin is shown in Fig. S3. Multiple sequence alignment, shown in Fig. 3, suggests that BGL24 exhibits high homology with a number of other Cucurbitaceae phloem proteins and lectins as well.

#### 3.2. Lectin activity and carbohydrate specificity

Hemagglutination assays revealed that BGL24 exhibits strong lectin activity and agglutinates human (A, B, O) as well as rabbit erythrocytes with equal efficiency. Divalent metal ions (Ca<sup>2+</sup>, Mg<sup>2+</sup>, Mn<sup>2+</sup>, Sn<sup>2+</sup>,

BGL C. argyrosperma C. argyrosperma C. moschata 1 C. digitata C. maxima 1 C. maxima 2 C. moschata 2	MNHKEKEKLGGEVKLGHCLDVIL	44 60 60 60 60 60
BGL C. argyrosperma C. argyrosperma C. moschata 1 C. digitata C. maxima 1 C. maxima 2 C. moschata 2	DKKSNSNWYFIFARALSIAWIEDKRYWKWGSCN-KIAELIQVSWLDIRKPNGSKIERGL DKKSNSNWYFIFARALSIAWIEDKRYWKWGSCN-KIAELIQVSWLDIRGKINESMLSPN DKKSNSNWYFIFARALSIAWIEDKRYWKWGSCN-KIAELIQVSWLDIRGKIKESMLSPN DKKSNSNWYFIFARALSIAWIEDKRYWKWGSCI-KIAELIEVSWLDIRGKINESMLSPN DKKSNSNWYFIFARALSIAWIEDKRYWKWGSCGDSNVAELIEVSWLDIRGKINESMLSQN DKKSNSNWYFIFARALSIAWIEDKRYWKWGSCGDSNVAELIEVSWLDIRGKINESMLSQN DKKLNSHWYFIFARALSIAWIEDKRYWKWGSCGNSEVAELIEVSWLNIRGKINESMLSPN DKKLNSHWYFIFARALSIAWIEDKRYWKWGSCGNSEVAELIEVSWLNIRGKINESMLSPN *** **:*******************************	102 118 118 118 120 120 120
BGL C. argyrosperma C. argyrosperma C. moschata 1 C. digitata C. maxima 1 C. maxima 2 C. moschata 2	LVKGVR	108 178 178 178 180 180 180
BGL C. argyrosperma C. argyrosperma C. moschata 1 C. digitata C. maxima 1 C. maxima 2 C. moschata 2	GCGSSGEIEFSFFEHGGHWKRGLLVKGVRIGAKGCGCA 216 GCGSSGEIEFSFFEHGGHWKRGLLVKGVRIGAKGCGCA 216 GCGSSGEIEFAFYEHGGHWKRGLLVKGVRIGAKGCGCA 216 GCGSSGEIEFAFFEHGGWARGLLVKGVRIGAKGCGCA 218 GCGSSGEIEFAFFEHGGHWKRGLLVKGVRIGAKGCGCA 218 GCGSSGEIEFAFFEHGGHWKRGLLVKGVRIGAKGCGCA 218 GCGSSGEIEFSFFEHGGHWKRGLLVKGVRIGAKGCGCS 218	

**Fig. 3.** Multiple sequence alignment of the partial amino acid sequence of BGL24 with the primary structure of other 24 kDa PP2-type Cucurbitaceae phloem exudate lectins/proteins. Sequences of *C. argyrosperma* 1 (AAM82558.1), *C. argyrosperma* 2 (AAA33118.1), *C. moschata* 1 (AAF74345.1), *C. moschata* 2 (XP\_022927327.1), *C. digitata* (AAM82559.1), *C. maxima* 1 (XP\_023001604.1), and *C. maxima* 2 (CAA80364.1) were taken from NCBI gene bank. Multiple sequence alignment was performed using Clustal Omega (https://www.ebi.ac.uk/Tools/msa/clustalo/).

Zn<sup>2+</sup>) did not exhibit any significant effect on the hemagglutination assay, suggesting that BGL24 does not require any divalent metal ions for its activity. This was further supported by the observation that dialysis against EDTA did not affect the hemagglutination activity of BGL24. In order to investigate the carbohydrate specificity of BGL24, hemagglutination assays were performed in the presence of various mono, di, and oligosaccharides. Similar to the previous results obtained for the other PP2-type lectins from Cucurbitaceae, none of the mono- or disaccharides (except chitobiose) could inhibit the hemagglutination activity of BGL24 even at 125 mM concentration. Chitooligosaccharides at very low concentration inhibited the hemagglutination activity with high efficiency. Chitotriose exhibited 50% inhibition of the hemagglutination activity (IC<sub>50</sub>) at the low concentration of 0.2 mM whereas chitotetraose  $(IC_{50} = 50 \mu M)$ , chitopentaose and chitohexaose  $(IC_{50} = 25 \mu M)$ inhibited hemagglutination activity at even lower concentrations, suggesting that BGL24 exhibits high specificity for chitooligosaccharides.

#### 3.3. Temperature and pH effect on the hemagglutination activity

Thermal inactivation of BGL24 was probed by incubating the protein sample at different temperatures for 60 min followed by cooling to room temperature and testing its activity by hemagglutination assay. These experiments indicated that activity of the lectin was retained fully when incubated up to 70 °C, but decreases drastically to ~10% when incubated at 80 °C. Incubation at temperatures above 80 °C led to a complete loss of the lectin activity (Fig. S4A).

Effect of varying the pH on the lectin activity of BGL24 was investigated by dialyzing it against buffers of different pH and then testing its activity by the hemagglutination assay. These studies showed that BGL24 exhibits the highest activity in the pH range of 5.0–8.0. At pH 3.0–4.0 the lectin activity decreased to about 50% as compared to that at pH 7.4 whereas at pH 2.0 the activity decreased further to 30% (see Fig. S4B).

#### 3.4. Secondary structure of BGL24: CD spectroscopic studies

The far-UV CD spectrum of the native protein (Fig. 4A, black line) showed a sharp negative band centered around 216 nm and a positive band at 193 nm, suggesting that BGL24 contains  $\beta$ -sheet as the predominant secondary structure, with very little  $\alpha$ -helical content. Quantitative information on the various secondary structural elements was obtained by further analysis of the far-UV CD spectral data using three different methods CONTILL, SELCON3 and CDSSTR, available online at DICHROWEB (www.cryst.bbk.ac.uk/cd web/HTML). The average results

obtained from these three programs suggested that BGL24 contains 41.3%  $\beta$ -sheets, 21.7%  $\beta$ -turns, 3.8%  $\alpha$ -helices and 33.1% unordered structures (Table S3). The simulated fit obtained from the CDSSTR analysis shown in Fig. 4A (red line) is in good agreement with the experimental spectrum. The secondary structure of BGL24 thus contains high percentage of  $\beta$ -sheet. In this respect it resembles several other Cucurbitaceae phloem exudate lectins, such as PPL, CPL and snake gourd phloem lectin (SGPL), which contain 35.8, 38.9, and 39.2%  $\beta$ -sheet, respectively, with low  $\alpha$ -helical content [26,31,44]. Similarly, two phloem exudate lectins from *Coccinia indica*, CIA17 and CIA24 also have high percentage of  $\beta$ -sheet (42.2 and 40.5%  $\beta$ -sheet, respectively) in their secondary structure [25,29].

The near UV CD spectrum of BGL24 showed a maximum at 274 nm with a shoulder at 260 nm and a minimum at 288 nm (Fig. 4B), which can be ascribed to the contribution from the side chains of aromatic amino acids phenylalanine, tyrosine and tryptophan [45]. Binding of chitooligosaccharides led to changes in the intensity and position of both these bands, suggesting that the orientation and position of some of the aromatic side chains are perturbed by carbohydrate binding.

#### 3.5. Thermal and pH stability: CD spectroscopic and DSC studies

In order to investigate the thermal stability of BGL24, CD spectra of the protein were recorded at various temperatures between 30 and 90 °C (Fig. 5). Very little changes in the shape and intensity of CD spectra were observed in the far-UV region when the sample was heated from 30 °C to 70 °C, whereas moderate changes were seen between 70 and 90 °C, suggesting that the secondary structure of BGL24 is quite stable up to 70 °C and undergoes only marginal changes below 90 °C (Fig. 5A). Interestingly, considerable changes in the spectral intensity were seen in the near-UV CD spectra of BGL24 even in the 40-70 °C range, suggesting that the tertiary structure of the protein undergoes changes continuously as the temperature is increased. Notably, drastic changes were observed in the near-UV spectra between 70 and 90 °C, clearly indicating that the protein undergoes significant changes in the tertiary structure above 70 °C (Fig. 5B). In comparison, the secondary structure of SGPL was unaltered between 30 and 60 °C and PPL was thermally stable up to 80 °C [26,44]. Both the secondary and tertiary structures of CIA17 and CPL were unaltered even at 95 °C [25,32]. These observation indicate that the thermal stability of BGL24 is comparable to that of PPL but less than that of CIA17 and CPL.

In order to obtain quantitative thermodynamic information on the thermal unfolding of BGL24 and the effect of carbohydrate binding on it, DSC studies were performed on the lectin in the absence as well as

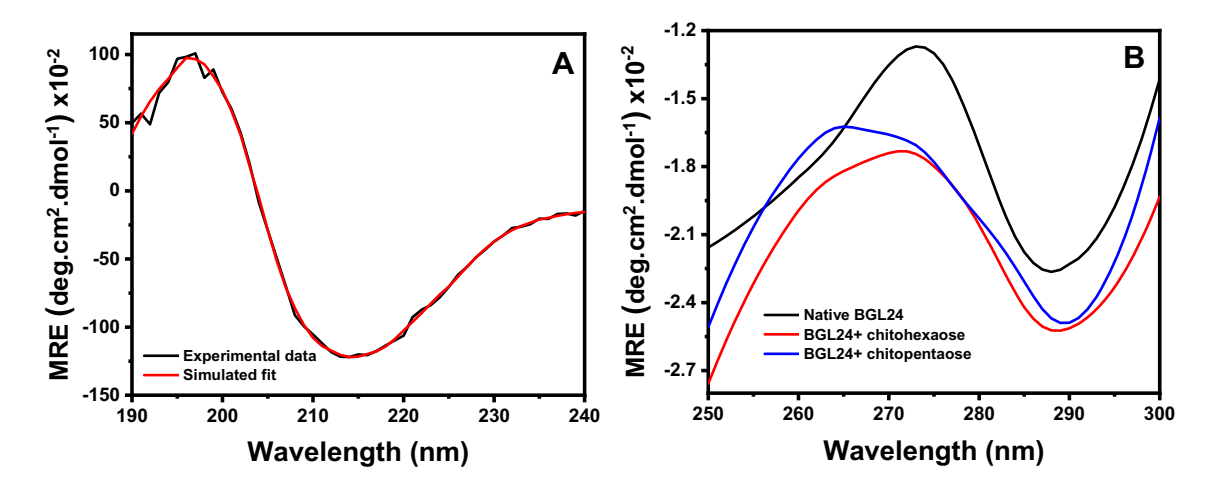


Fig. 4. CD spectra of BGL24 in the (A) far-UV (190–240 nm) and near UV (250–300 nm) regions. Spectra were obtained in the near UV region in the presence of 1.0 mM concentrations of chitopentaose and chitohexaose also (indicated in blue and red, respectively).

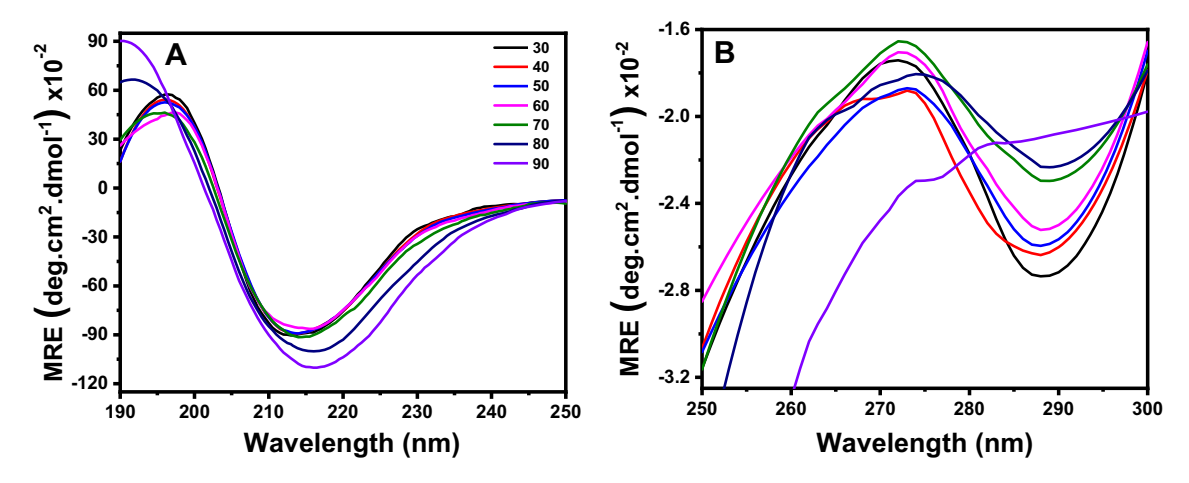
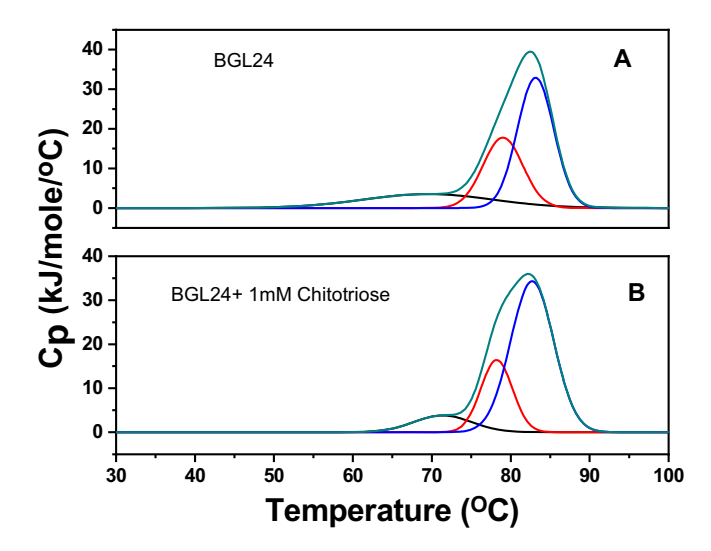


Fig. 5. CD spectra of BGL24 at different temperatures. (A) Far-UV region; (B) near UV region. Color code indicates the temperatures (in °C) at which the spectra were recorded.

presence of chitooligosaccharides at 1 mM concentration. Native BGL24 in double distilled water exhibits three partially overlapping endothermic components, centered at ~69.5, 79.0 and 83.2 °C, respectively (Fig. 6A). The thermal unfolding of BGL24 was found to be an irreversible process. Similar to the native protein, thermograms obtained in presence of chitooligosaccharides, (GlcNAc)<sub>3-6</sub> could be resolved into three components, with the position of the endotherms remaining nearly unchanged. The transition temperatures and enthalpies ( $\Delta H_c$ ) corresponding to all the three transitions are listed in Table 1.

The three components of the DSC thermograms obtained with native BGL24 and in the presence of chitooligosaccharides could be analysed in the following manner. The first endothermic component may be assigned to the dissociation of the higher oligomeric forms of the protein to dimers, whereas the second component could be assigned to the dissociation of the homodimeric protein into monomers which remain in the folded state or in a nearly folded state (cf. [46]). However, the two protomers would still be connected via a disulfide bridge, but without significant non-covalent interactions between them. The third endothermic component can be attributed to the unfolding of the monomer.



**Fig. 6.** DSC thermograms of BGL24. Heating scans of (A) native BGL24, and (B) BGL24 in the presence of 1 mM chitotetraose are shown. Scan rate:  $1^{\circ}$ /min (Celsius scale). Deconvolution of the original thermograms (green lines) using the NanoAnalyze software provided by TA Systems yielded three underlying peaks (indicated by black, red and blue lines).

Change in pH can alter protein structure either by disrupting hydrogen bonds between the amino acid residues or by disturbing salt bridges between the positively and negatively charged side chains of amino acids [47]. The effect of changing pH on the structure of BGL24 was also investigated by recording both far-UV and near-UV CD spectra after dialysing the protein sample against buffers of different pH (between 3.0 and 8.0). The far-UV CD spectrum of the protein exhibited only minor changes (Fig. 7A), suggesting that the secondary structure of BGL24 was mostly unaltered when the pH was varied between 3.0 and 8.0, and that the secondary structure of BGL24 is quite stable over a wide pH range. In this respect it is comparable to *Cucumis sativus* phloem exudate lectin, which was reported to retain its secondary structure in pH range of 3.0–8.0 (32).

Two Cucurbitaceae seed lectins, *Momordica charantia* lectin (MCL) and *Trichosanthes dioica* seed lectin (TDSL) were also reported to exhibit stable secondary and tertiary structure over a broad pH range [48,49]. In contrast, major changes were observed in the near-UV CD spectrum of BGL24 (Fig. 7B), which did not exhibit any systematic trends with pH change, indicating that changes in the tertiary structure do not follow any particular order with change in pH (cf. [50]).

**Table 1**Thermodynamic parameters associated with the thermal unfolding of BGL24 and the effect of chitooligosaccharide binding.

Sample description	T <sub>m</sub> (°C)	$\Delta H_{\rm c}$ (kJ mol <sup>-1</sup> )
BGL24		
Transition 1	69.5	72.6
Transition 2	79.0	112.5
Transition 3	83.2	190
BGL24 + chitotriose		
Transition 1	71.4	35.0
Transition 2	78.2	82.0
Transition 3	82.7	234,9
BGL24 + chitotetraose		
Transition 1	73.6	12.0
Transition 2	77.5	48.3
Transition 3	81.9	260
BGL24 + chitopentaose		
Transition 1	73.3	27.63
Transition 2	78.2	52.6
Transition 3	82.01	258.1
BGL24 + chitohexaose		
Transition 1	71.5	17.01
Transition 2	81.1	131.1
Transition 3	83.3	295.4

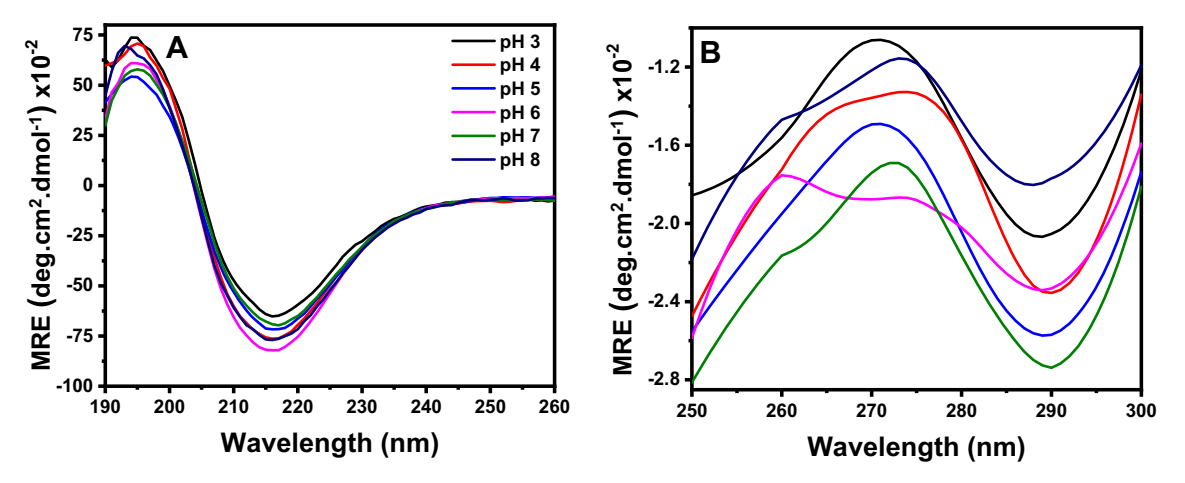


Fig. 7. CD spectra of BGL24 recorded at different pH. (A) Far-UV region, (B) near UV region. Color code given in panel A indicates the pH at which each spectrum was recorded (for both panels A and B).

3.6. Binding of MeUmb $\beta$ (GlcNAc) $_3$  and unlabeled chitooligosaccharides to BGL24: fluorescence titrations

The emission spectra of MeUmb\(\beta\)(GlcNAc)<sub>3</sub> in the absence and in the presence of different concentrations of BGL24, recorded at 20 °C, are shown in Fig. 8A. Spectrum 1, which has the highest fluorescence intensity, corresponds to MeUmb\(\beta(\text{GlcNAc})\_3\) in buffer alone whereas the remaining spectra with decreasing intensities correspond to those recorded in the presence of increasing concentrations of the lectin. From this figure it is observed that the fluorescence intensity of the 4methylumbelliferyl sugar was significantly quenched upon binding to BGL24. The fluorescence titration data was analysed by plotting  $F_0/(F_0$  $F_c$ ) vs  $1/[P]_t$  where  $F_o$ ,  $F_c$  and  $\Delta F$  represent initial fluorescence intensity of MeUmbβ(GlcNAc)<sub>3</sub> alone, fluorescence intensity at any point of the titration (corrected for dilution) and the corresponding change in fluorescence intensity, respectively. Such plots obtained at various temperatures between 15 and 35 °C showed that the fluorescence intensity of MeUmbβ(GlcNAc)<sub>3</sub> is totally quenched at saturation binding by BGL24 (see Fig. S4 for a representative plot for the data obtained at 20 °C). This suggests that the quantum yield of the fluorescent sugar becomes zero upon binding to BGL24. Consistent with this, no significant change in the emission maximum was seen upon binding of the fluorescent sugar to the protein. The titration data was then analysed further according to the following equation [24,42,43]:

$$\log [(F_0 - F_c)/(F_c - F_\infty)] = pK_a + \log [P]_f$$
 (1)

where  $F_{\infty}$  is the fluorescence intensity when all the fluorescent ligand is bound to the protein and  $[P]_f$  is the free protein concentration, given by the expression:

$$[P]_f = [P]_t - [M]_t \times [(F_o - F_c)/(F_c - F_{\infty})] \tag{2}$$

where  $[P]_t$  and  $[M]_t$  are the total concentrations of the protein and the fluorescently labeled ligand, respectively. From the X-intercepts of plots of  $\log [(F_o-F_c)/(F_c-F_\infty)]$  vs  $\log [P]_f$  the association constants,  $K_a$  for the binding of MeUmb $\beta$ (GlcNAc) $_3$  to BGL24 were determined at different temperatures. From a van't Hoff plot of these temperature dependent values of  $K_a$  (see Table 2), the enthalpy of binding ( $\Delta H$ ) and entropy of binding ( $\Delta S$ ) for this interaction were obtained as -29.3 kJ mol $^{-1}$  and +1.67 J mol $^{-1}$  K $^{-1}$ , respectively.

The interaction of the nonfluorescent chitooligosaccharides (chitotriose, chitoteraose, chitopentaose and chitohexaose) to BGL24 was investigated by monitoring the increase in fluorescence intensity

of a mixture of the lectin and MeUmb $\beta$ (GlcNAc)<sub>3</sub> on addition of the inhibitory ligands (cf. [24,43]):

$$\{[P]_f/[PM]-1\} [M]_f = (K_L/K_M) [L]_f + 1/K_M$$
 (3)

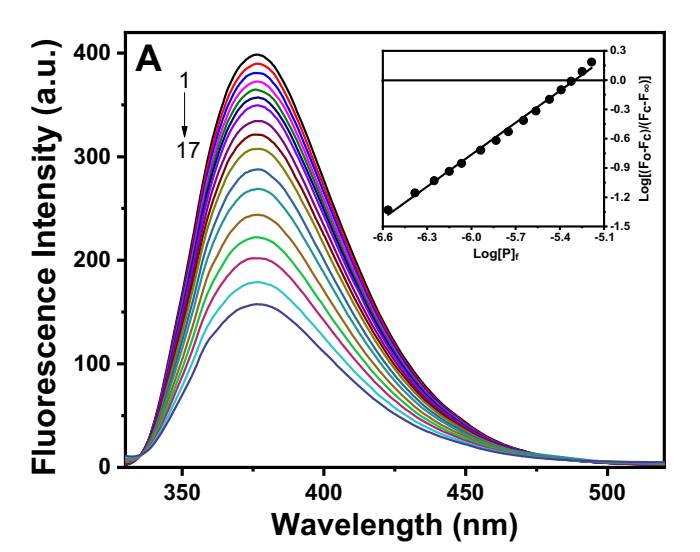
where  $[P]_t$ , [PM],  $[M]_f$ , and  $[L]_f$  correspond to the concentrations of the total protein, the protein-indicator ligand complex, free indicator ligand and free inhibiting ligand, respectively. The intercept and slope of the straight line obtained from the plot of  $\{[P]_t/[PM]-1\}$   $[M]_f$  vs  $[L]_f$  yield the association constants for both the indicator ligand  $(K_M)$  and inhibitory ligand  $(K_L)$ . The values thus obtained are listed in Table 3.

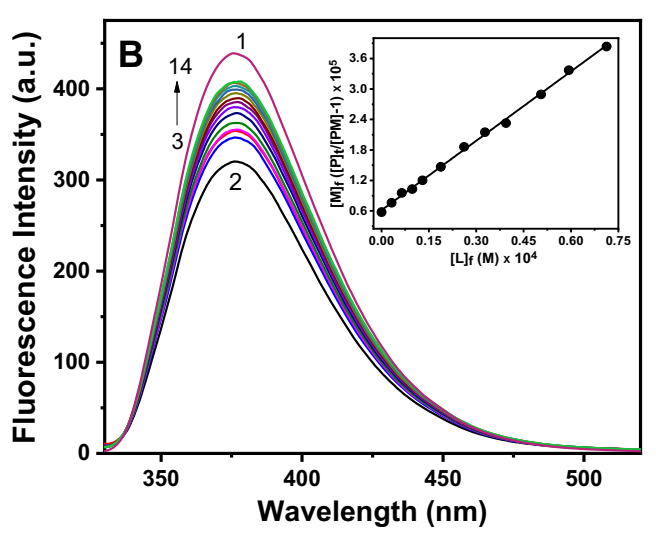
The data presented in Table 3 shows that the binding constants for the association of chitooligosaccharides with BGL24 increase considerably when the oligosaccharide size is increased from triose  $(6.3 \times 10^4~{\rm M}^{-1})$  to tetraose  $(1.43 \times 10^5~{\rm M}^{-1})$ , whereas only marginal increases are observed with pentaose  $(1.53 \times 10^5~{\rm M}^{-1})$  and hexaose  $(1.79 \times 10^5~{\rm M}^{-1})$ . These results are consistent with the results of hemagglutination-inhibition presented in Section 3.2. In addition, these results suggest that the lectin combining site most likely accommodates a tetrasaccharide and the marginal increase in binding affinity when the oligosaccharide size is increased beyond tetraose most likely arises due to increase in statistical probability of binding

From the temperature dependent association constants presented in Table 3, the thermodynamic parameters for the BGL24-chitotriose interaction were obtained by means of a van't Hoff plot as  $\Delta H = -44.6 \text{ kJ} \text{ mol}^{-1}, \Delta S = -60.5 \text{ J mol}^{-1} \text{ K}^{-1}$ . These values clearly suggest that the chitooligosaccharide binding to BGL24 is driven by enthalpic forces with negative contribution from entropy. A comparison of the enthalpy and entropy of binding for MeUmb $\beta$ (GlcNAc) $_3$  and chitotriose reveals that although the enthalpy of binding for the unlabeled chitotriose is about 1.5 fold higher than the value obtained for the fluorescently labeled sugar, due to the large negative contribution from binding entropy the association constant becomes 3-fold weaker. Thus the stronger binding of MeUmb $\beta$ (GlcNAc) $_3$  as compared to (GlcNAc) $_3$  is due to a smaller negative contribution from entropy of binding for the methylumbelliferyl glycoside.

It is interesting to compare the association constants and the corresponding thermodynamic parameters for the binding of chitotriose and its 4-methylumbelliferyl derivative to BGL24 with those obtained for the interaction of these two ligands with other Cucurbitaceae phloem lectins reported earlier. Fluorescence spectroscopic titrations yielded the association constant for the binding of MeUmb $\beta$ (GlcNAc) $_3$  to Coccinia indica agglutinin (CIA) at 25 °C as  $2.82 \times 10^5$  M $^{-1}$ , which is

about 60% higher than the value of  $1.76 \times 10^5 \, \mathrm{M}^{-1}$  obtained for BGL24 in the present study [24]. Association constants in the range of  $9.6 \times 10^4$ – $1.95 \times 10^5 \, \mathrm{M}^{-1}$  were obtained by ITC measurements at 25 °C for the binding of chitotriose to several Cucurbitaceae phloem exudate lectins such as CPL, PPL, CIA17, CIA24 and SGPL [27,31,45,51,52].





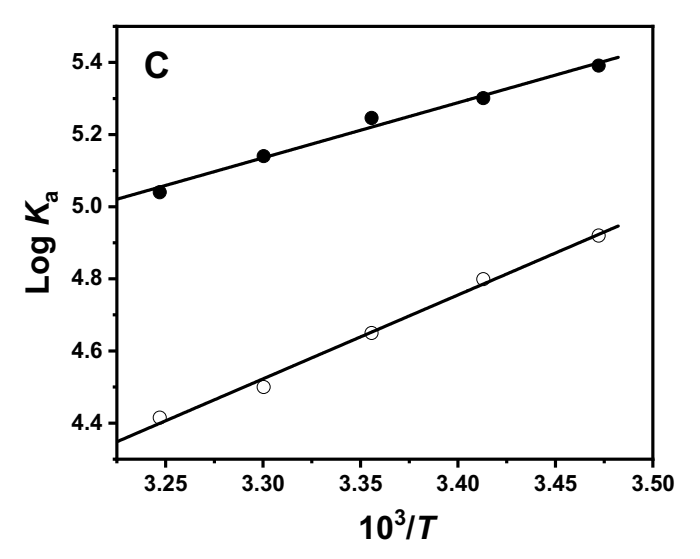


**Table 2**Association constants  $(K_a)$  for the binding of MeUmb(GlcNAc)<sub>3</sub> to BGL24 at different temperatures.

Temperature (°C)	$K_{\rm a} \times 10^{-5}  ({\rm M}^{-1})$
15	2.46
20	2.00
25	1.76
30	1.38
35	1.10

**Table 3** Association constants,  $K_L$  and  $K_M$  for the binding of chitooligosaccharides and MeUmb $\beta$ (GlcNAc) $_3$  to BGL24 determined from reversal titrations. Values in parentheses are standard deviations from 2 to 4 independent titrations.

Ligand	T (°C)	$K_{\rm L} \times 10^{-4}  ({ m M}^{-1})$	$K_{\rm M} \times 10^{-4}  ({ m M}^{-1})$
(GlcNAc) <sub>3</sub>	15	8.4 (±3.2)	12.0 (±0.3)
	20	$6.3 (\pm 1.3)$	$11.4 (\pm 1.6)$
	25	$4.5~(\pm 0.4)$	$9.9 (\pm 0.2)$
	30	$3.4 (\pm 0.3)$	$8.6 (\pm 0.4)$
	35	$2.6~(\pm 0.5)$	$6.7 (\pm 0.5)$
(GlcNAc) <sub>4</sub>	20	$14.3 (\pm 2.8)$	$12.0~(\pm 2.4)$
(GlcNAc) <sub>5</sub>	20	$15.3 (\pm 2.1)$	$11.2 (\pm 2.5)$
(GlcNAc) <sub>6</sub>	20	$17.9 (\pm 2.3)$	$10.9 (\pm 1.7)$

The association constant of  $6.3 \times 10^4~\text{M}^{-1}$  obtained here for the BGL24-chitotriose interaction is smaller than all these values, but about 8-fold higher than the value of  $8.0 \times 10^3~\text{M}^{-1}$  obtained for the binding of chitotriose to LAA at 25 °C.

For Luffa acutangula agglutinin (LAA), the binding constants are  $1.26 \times 10^4$ ,  $9.7 \times 10^4$  and  $6.5 \times 10^5$  M<sup>-1</sup> for chitotriose, chitotetraose and chitopentaose, respectively, indicating that increasing the chitooligosaccharide size results in additional interactions of the ligand with the lectin combining site [27,53]. The dimeric PPL and SGPL bind to  $(GlcNAc)_{3-5}$  with binding constants ranging between  $1.26 \times 10^5$  and  $1.53 \times 10^5 \,\mathrm{M}^{-1}$ , and  $1.7 \times 10^5 \,\mathrm{and} \,3.6 \times 10^5 \,\mathrm{M}^{-1}$ , respectively, at 25 °C as determined by isothermal titration calorimetric (ITC) studies [44,50]. The association constants for CPL were in the range of 1.11 to  $1.92 \times 10^5 \, \text{M}^{-1}$  for chitotriose to chitopentaose [31]. For CIA17, the binding constant increases for tri, tetra and pentaose ranging between  $3.5 \times 10^5$  to  $4.3 \times 10^5$  M<sup>-1</sup> [52], and for CIA24, the affinity towards chitotriose is moderate ( $K_a = 2.7 \times 10^4 \,\mathrm{M}^{-1}$ ) and the  $K_a$  value increases for tetraose and pentaose up to  $1.13 \times 10^5 \,\mathrm{M}^{-1}$  [29]. These observations clearly indicate that the affinity towards higher oligosaccharides increses for all the lectins cited here, but for PPL, CPL and CIA17, a dramatic increase in the association constant was observed for chitohexaose. BGL24 binds chitooligisacharides in a specific manner and the affinity towards the  $(GlcNAc)_{3-6}$  is similar to the homodimeric CIA24 and SGPL.

Fig. 8. Fluorescence titration of MeUmbβ(GlcNAc)<sub>3</sub> with BGL24 and reversal titration with chitotriose at 20 °C. (A) Fluorescence emission spectra of MeUmbβ(GlcNAc)<sub>3</sub> in the absence and presence of BGL24. Spectrum 1 corresponds to MeUmbβ(GlcNAc)<sub>3</sub> alone and spectra 2–17 correspond to those recorded in the presence of increasing concentration of BGL24. *Inset*, double logarithmic plot of the titration data according to Eq. (1). The X-intercept of the plot gives  $pK_a$  of the binding equilibrium, from which the association constant  $K_a$  was estimated as 2.46 × 10<sup>5</sup> M<sup>-1</sup>. (B) Fluorescence emission spectra of MeUmbβ(GlcNAc)<sub>3</sub> in the absence and presence of BGL24 and chitotriose. Spectrum 1 refers to the chromophoric ligand alone, spectrum 2 corresponds to the mixture of MeUmbβ(GlcNAc)<sub>3</sub> and BGL24, whereas spectra 3–14 were obtained in the presence of increasing concentration of chitotriose. From the plot in the *Inset*, the association constants of  $K_M = 1.298 \times 10^5$  M<sup>-1</sup> for the indicating and  $K_L = 0.63 \times 10^5$  M<sup>-1</sup> for the inhibitory ligand have been obtained. (C) van't Hoff plots for MeUmbβ(GlcNAc)<sub>3</sub> ( $\blacksquare$ ) and (GlcNAc)<sub>3</sub> ( $\bigcirc$ ).

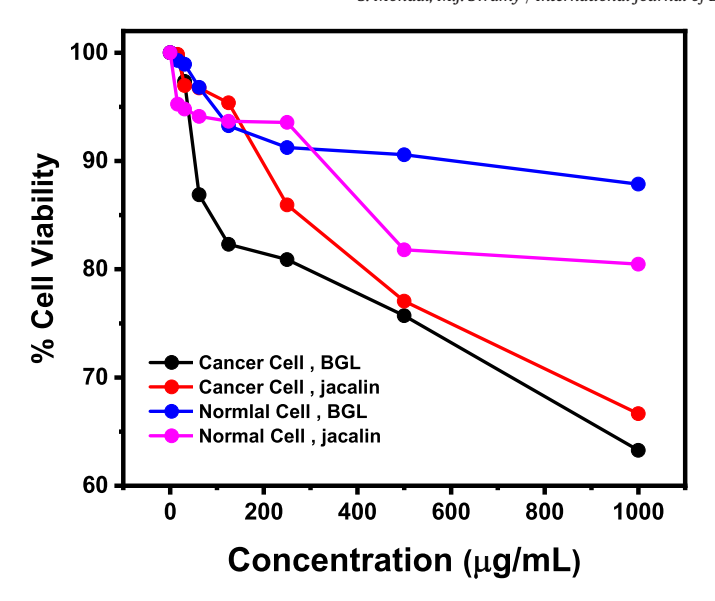


**Fig. 9.** Effect of jacalin and BGL24 on the viability of normal spleenocytes and MDA-MB-231 breast cancer cells. Cell viability was estimated by the MTT assay after treating both the cells with different concentrations of each lectin for 72 h.

#### 3.7. Cytotoxicity

Cytotoxicity of BGL24 towards normal splenocytes and epithelial, triple negative breast cancer cells (MDA-MB-231) was evaluated colorimetrically by measuring changes in the absorption intensity at 570 nm due to the formation of purple-coloured formazan, resulting from the reduction of MTT by the cellular oxidoreductase enzymes [54]. The cytotoxicity of jacalin was also assessed to compare its effect with that of BGL24 on the two cell lines. The results of these studies, presented in Fig. 9 show that cell viability of MDA-MB-231 cell line decreased to 82% upon treatment with a relatively low concentration (125 µg/mL) of BGL24 whereas only a marginal decrease (cell viability = 94%) was observed upon incubation with the same concentration of jacalin. Upon incubation with higher doses (1 mg/mL), the cell viability decreased to 63% for BGL24 and 68% for jacalin. Although the viability of normal splenocytes was almost unaffected with 125 µg/mL of either lectin, at 1 mg/mL concentration of the lectins, viability of normal cells decreased to 80% when incubated with jacalin, whereas the corresponding value for BGL24 was 88%. These results demonstrate that BGL24 exhibits higher cytotoxicity against MDA-MB-231 cancer cell line than jacalin, but lower cytotoxicity on normal splenocytes.

Lectins are thought to play a major role in plant defense against viral, bacterial, fungal and insect attack, possibly by interacting with the carbohydrate structures present on the cell surfaces of these infectious agents [55]. In our previous work, cell viability assays revealed that jacalin and mulberry latex galactose-specific lectin (MLGL), an  $\alpha$ -Dgalactose specific jacalin related lectin (gJRL) exhibit cytotoxicity against epithelial (MDCK) as well as breast cancer cells (MCF7) [39]. It was proposed that this could be due to an interaction between the lectins and tumor associated TF-antigen, expressed on the breast cancer cell surface [39,56]. PP2-type lectins such as Luffa acutangula agglutinin and Coccinia indica agglutinin have been shown to bind to N-linked oligosaccharides containing core chitobiose structure [24,27]. It is likely cytotoxicity of BGL24 and other PP2-type, chitooligosaccharide-binding lectins is mediated by their interaction with N-linked oligosaccharides attached to the cell surface glycoproteins on the target cells. Since our results demonstrate that BGL24 is more cytotoxic against MDA-MB-231 cancer cells than normal splenocytes as compared to jacalin, BGL24 might be exhibiting the cytotoxity by interacting with the N-linked glycans expressed more on the cell surface of the breast cancer cells than the norman splenocytes. Further work is required to investigate the mechanism of cytotoxicity of BGL24 in more detail and also to explore its potential in therapeutic applications to treat malignant tumors.

In summary, in the present work, a chitooligosaccharide binding, PP2-type lectin (BGL24) was purified from the phloem exudate of bottle-gourd (Lagenaria siceraria) by affinity chromatography. BGL24 is a homodimer in which the two subunits of ~24 kDa mass are connected via disulfide linkage(s). At higher concentrations, BGL24 self assembles to form oligomers of higher molecular weight. BGL24 is highly homologous to other Cucurbitaceae phloem exudate PP2-type lectins and proteins with high β-sheet content. Circular dichroism spectral studies showed that the secondary structure of BGL24 is stable up to >70 °C and over a broad pH range (3.0-8.0). At physiological pH, BGL24 undergoes irreversible thermal unfolding and the unfolding thermogram could be resolved into three overlapping endotherms centered at ~69.5, 79.0 and 83.2 °C, respectively. Fluorescence titrations on the binding of MeUmb\(\beta\) (GlcNAc)<sub>3</sub> to BGL24 and reversal titrations with chitooligosaccharides revealed that the association constants for the binding of the fluorescently labeled sugar is about 3-fold higher than the unlabeled chitotriose, which could be attributed to a smaller negative entropic contribution associated with the labeled sugar. Further, the association constants for the unlabeled chitooligosaccharides were found to increase significantly from trisaccharide to tetrasaccharide, but only marginally with further increase in the oligosaccharide size. The cyctotoxicity of BGL24 towards epithelial, triple negative breast cancer cells (MDA-MB-231) is higher than that for normal splenocytes. Further studies are required to investigate the anticancer activity of BGL24 in more detail, and to investigate its role in long distance trafficking of nutrients, sugars, RNA etc. as well as in wound sealing mechanism to protect the plant against pathogen attack. Such studies are currently underway in our laboratory.

#### **CRediT authorship contribution statement**

**Saradamoni Mondal**: Conceptualization; Data curation; Formal analysis; Investigation; Methodology; Writing - original draft.

**Musti J. Swamy**: Project administration; Resources; Supervision; Funding acquisition; Writing - review & editing.

#### **Declaration of competing interest**

The authors declare that they have no conflicts of interest with the contents of this article.

#### Acknowledgments

This work was supported by a mid-career award from the University Grants Commission (India) to MJS. We thank the UGC (India) for its support through the UPE-II grant to the University of Hyderabad and the CAS program to the School of Chemistry. Support from the Department of Science and Technology under the FIST program to the School of Chemistry is gratefully acknowledged. We thank Dr. Pradip Paik (School of Engineering Sciences and Technology, University of Hyderabad) and his student Ms. Somedutta Maity for their help in cell culture and MTT assay.

#### Appendix A. Supplementary data

Purification table (Table S1), Mascot search based assignment of amino acid sequences (Table S2), secondary structure analysis of BGL24 (Table S3), gel filtration of BGL24 on Sephadex G-100 (Fig. S1), deconvoluted MALDI-TOF mass spectrum of BGL24 (Fig. S2), pairwise sequence alignment of BGL24 peptides with the primary structure of phloem lectin from *Cucurbita argyrosperma* subsp. sororia (Fig. S3),

effect of temperature and pH on the hemagglutination activity of BGL24 (Fig. S4), plot of  $F_o/(F_o-F_c)$  vs  $1/[P]_t$  for the interaction MeUmb $\beta$ (GalNAc) $_3$  with BGL24 at 20 °C (Fig. S5). Supplementary data to this article can be found online at https://doi.org/10.1016/j. ijbiomac.2020.08.246.

#### References

- N. Sharon, H. Lis, Lectins: cell-agglutinating and sugar-specific proteins, Science 177 (1972) 949–959.
- [2] H. Lis, N. Sharon, Lectins: carbohydrate-specific proteins that mediate cellular recognition, Chem. Rev. 98 (2002) 637–674.
- [3] H. Lis, N. Sharon, The biochemistry of plant lectins (phytohemagglutinins), Annu. Rev. Biochem. 42 (2003) 541–574.
- [4] N. Sharon, H. Lis, History of lectins: from hemagglutinins to biological recognition molecules, Glycobiology 14 (2004) 53–62.
- [5] W.J. Peumans, E.J. Van Damme, A. Barre, P. Rougé, Classification of plant lectins in families of structurally and evolutionary related proteins, Adv. Exp. Med. Biol. 491 (2001) 27–54.
- [6] E.J.M. Van Damme, W.J. Peumans, A. Barre, P. Rougé, Plant lectins: a composite of several distinct families of structurally and evolutionary related proteins with diverse biological roles, Crit. Rev. Plant Sci. 17 (1998) 575–692.
- [7] J. Kehr, Phloem sap proteins: their identities and potential roles in the interaction between plants and phloem-feeding insects, J. Exp. Bot. 57 (2006) 767–774.
- [8] P. Sashi, K.K. Singarapu, A.K. Bhuyan, Solution NMR structure and backbone dynamics of partially disordered *Arabidopsis thaliana* phloem protein 16-1, a putative mRNA transporter, Biochemistry 57 (2018) 912–924.
- [9] S. Dinant, A.M. Clark, Y. Zhu, F. Vilaine, J.C. Palauqui, C. Kusiak, G.A. Thompson, Diversity of the superfamily of phloem lectins (phloem protein 2) in angiosperms, Plant Physiol. 131 (2003) 114–128.
- [10] G.A. Thompson, A. Schulz, Macromolecular trafficking in the phloem, Trends Plant Sci. 4 (1999) 354–360.
- [11] K.J. Oparka, S.S. Cruz, The great escape: phloem transport and unloading of macro-molecules, Annu. Rev. Plant Physiol. Plant Mol. Biol. 51 (2000) 323–347.
- [12] B. Golecki, A. Schulz, G.A. Thompson, Translocation of structural P proteins in the phloem, Plant Cell 11 (1999) 127–140.
- [13] R.A. Owens, M. Blackburn, B. Ding, Possible involvement of the phloem lectin in long-distance viroid movement, Mol. Plant-Microbe Interact. 14 (2001) 905–909.
- [14] V. Pallas, G. Gómez, Phloem RNA-binding proteins as potential components of the long-distance RNA transport system, Front. Plant Sci. 4 (2013) 130.
- [15] T. Will, A.C.U. Furch, M.R. Zimmermann, How phloem-feeding insects face the challenge of phloem-located defenses, Front. Plant Sci. 4 (2013) 336.
- [16] J. Beneteau, D. Renard, L. Marche, E. Douville, L. Lavenant, Y. Rahbe, D. Dupont, F. Vilaine, S. Dinant, Binding properties of the N-acetylglucosamine and highmannose N-glycan PP2-A1 phloem lectin in *Arabidopsis*, Plant Physiol. 153 (2010) 1345–1361.
- [17] T. Will, A.J.E. Van Bel, Physical and chemical interactions between aphids and plants, J. Exp. Bot. 57 (2006) 729–737.
- [18] S.M. Read, D.H. Northcote, Subunit structure and interactions of the phloem proteins of *Cucurbita maxima* (pumpkin), Eur. J. Biochem. 134 (1983) 561–569.
- [19] A. Kasprzewska, Plant chitinases-regulation and function, Cell. Mol. Biol. Lett. 8 (2003) 809–824.
- [20] Z. Fujimoto, H. Tateno, J. Hirabayashi, Lectin structures: classification based on the 3-D structures, Methods Mol. Biol. 1200 (2014) 579–606.
- [21] J.H. Wong, T.B. Ng, R.C.F. Cheung, X.J. Ye, H.X. Wang, S.K. Lam, P. Lin, Y.S. Chan, E.F. Fang, P.H.K. Ngai, L.X. Xia, X.Y. Ye, Y. Jiang, F. Liu, Proteins with antifungal properties and other medicinal applications from plants and mushrooms, Appl. Microbiol. Biotechnol. 87 (2010) 1221–1235.
- [22] C.S. Chen, C.Y. Chen, D.M. Ravinath, A. Bungahot, C.P. Cheng, R.I. You, Functional characterization of chitin-binding lectin from *Solanum integrifolium* containing anti-fungal and insecticidal activities, BMC Plant Biol. 18 (2018) 1–11.
- [23] C.L. Bueter, C.A. Specht, S.M. Levitz, Innate sensing of chitin and chitosan, PLoS Pathog. 9 (2013), e1003080.
- [24] A.R. Sanadi, A. Surolia, Studies on a chitooligosaccharide-specific lectin from Coccinia indica. Thermodynamics and kinetics of umbelliferyl glycoside binding, J. Biol. Chem. 269 (1994) 5072–5077.
- [25] K.B. Bobbili, G. Pohlentz, A. Narahari, K. Sharma, A. Surolia, M. Mormann, M.J. Swamy, Coccinia indica agglutinin, a 17 kDa PP2 like phloem lectin: affinity purification, primary structure and formation of self-assembled filaments, Int. J. Biol. Macromol. 108 (2018) 1227–1236.
- [26] A. Narahari, M.J. Swamy, Rapid affinity-purification and physicochemical characterization of pumpkin (*Cucurbita maxima*) phloem exudate lectin, Biosci. Rep. 30 (2010) 341–349.
- [27] V. Anantharam, S.R. Patanjali, M.J. Swamy, A.R. Sanadi, I.J. Goldstein, A. Surolia, Isolation, macromolecular characterization and the combining site of a chito-oligosaccharide binding lectin from the fruits of ridge gourd (*Luffa acutangula*), J. Biol. Chem. 261 (1986) 14621–14627.
- [28] G. Kumar, P. Mishra, V. Anantharam, A. Surolia, Luffa acutangula agglutinin: primary structure determination and identification of a tryptophan residue involved in its carbohydrate-binding activity using mass spectrometry, IUBMB Life 67 (2015) 943–953
- [29] K.B. Bobbili, D. Datta, S. Mondal, S. Polepalli, G. Pohlentz, M. Mormann, M.J. Swamy, Purification, chitooligosaccharide binding properties and thermal stability of CIA24,

- a new PP2-like phloem exudate lectin from ivy gourd (*Coccinia indica*), Int. J. Biol. Macromol. 110 (2018) 588–597.
- [30] D.E. Bostwick, M.I. Skaggs, G.A. Thompson, Organization and characterization of Cucurbita phloem lectin genes, Plant Mol. Biol. 26 (1994) 887–897.
- [31] P.K. Nareddy, K.B. Bobbili, M.J. Swamy, Purification, physico-chemical characterization and thermodynamics of chitooligosaccharide binding to cucumber (*Cucumis sativus*) phloem lectin, Int. J. Biol. Macromol. 95 (2017) 910–919.
- [32] P.K. Nareddy, M.J. Swamy, Differential scanning calorimetric and spectroscopic studies on the thermal and chemical unfolding of cucumber (*Cucumis sativus*) phloem exudate lectin, Int. J. Biol. Macromol. 106 (2018) 95–100.
- [33] H. Yetişir, M. Şakar, S. Serçe, Collection and morphological characterization of Lagenaria siceraria germplasm from the Mediterranean region of Turkey, Genet. Resour, Crop. Evol. 55 (2008) 1257–1266.
- [34] A. Schlumbaum, P. Vandorpe, A short history of *Lagenaria siceraria* (bottle gourd) in the Roman provinces: Morphotypes and archaeogenetics, Veg. Hist. Archaeobotany 21 (2012) 499–509.
- [35] I. Ahmad, M. Irshad, M.M.A. Rizvi, Nutritional and medicinal potential of Lagenaria siceraria, Int. J. Veg. Sci. 17 (2011) 157–170.
- [36] V. Vigneshwaran, P. Thirusangu, S. Madhusudana, V. Krishna, S.N. Pramod, B.T. Prabhakar, The latex sap of the 'Old World Plant' *Lagenaria siceraria* with potent lectin activity mitigates neoplastic malignancy targeting neovasculature and cell death, Int. Immunopharmacol. 39 (2016) 158–171.
- [37] U.K. Laemmli, Most commonly used discontinuous buffer system for SDS electrophoresis, Nature 227 (1970) 680–685.
- [38] K.K. Tejavath, S.K. Nadimpalli, Purification and characterization of a class II  $\alpha$ -mannosidase from *Moringa oleifera* seed kernels, Glycoconj. J. 31 (2014) 485–496.
- [39] D. Datta, G. Pohlentz, M. Schulte, M. Kaiser, F.M. Goycoolea, J. Müthing, M. Mormann, M.J. Swamy, Physico-chemical characteristics and primary structure of an affinity-purified α-D-galactose-specific, jacalin-related lectin from the latex of mulberry (Morus indica), Arch. Biochem. Biophys. 609 (2016) 59–68.
- [40] A. Shevchenko, H. Tomas, J. Havlis, J.V. Olsen, M. Mann, In-gel digestion for mass spectrometric characterization of proteins and proteomes, Nat. Protoc. 1 (2006) 2856–2860.
- [41] M. Junqueira, V. Spirin, T.S. Balbuena, H. Thomas, I. Adzhubei, S. Sunyaev, Protein identification pipeline for the homology-driven proteomics, J. Proteome 71 (2008) 346–356.
- [42] D.M. Chipman, V. Grisaro, N. Sharon, Binding of oligosaccharides containing *N*-acetylglucosamine and *N*-acetylmuramic acid to lysozyme: the specificity of binding subsites, J. Biol. Chem. 242 (1967) 4388–4394.
- [43] S.S. Komath, R. Kenoth, M.J. Swamy, Thermodynamic analysis of saccharide binding to snake gourd (*Trichosanthes anguina*) seed lectin. Fluorescence and absorption spectroscopic studies, Eur. J. Biochem. 268 (2001) 111–119.
- [44] A. Narahari, P.K. Nareddy, M.J. Swamy, Purification, physico-chemical characterization and thermodynamics of chitooligosaccharide binding to a new lectin from the phloem exudate of snake gourd (*Trichosnathes anguina*), Biochimie 93 (2011) 1076–1084.
- [45] G. Rabbani, E. Ahmed, N. Zaidi, R.H. Khan, pH dependent conformational transitions in conalbumin (ovotransferrin), a metalloproteinase from egg white, Cell Biochem. Biophys. 61 (2011) 551–560.
- [46] G. Rabbani, E. Ahmed, N. Zaidi, S. Fatima, R.H. Khan, pH induced molten globule state of *Rhizopus niveus* lipase is more resistant against thermal and chemical denaturationthan its native state, Cell Biochem. Biophys. 62 (2012) 487–499.
- [47] G. Rabbani, J. Kaur, E. Ahmed, N. Zaidi, R.H. Khan, S.K. Jain, Structural characteristics of thermostable immunogenic outer membrane protein from *Salmonella enterica* serovar Typhi, Appl. Microbiol. Biotechnol. 98 (2014) 2533–2543.
- [48] M. Kavitha, N.A.M. Sultan, M.J. Swamy, Fluorescence studies on the interaction of hydrophobic ligands with *Momordica charantia* (bitter gourd) seed lectin, J. Photochem. Photobiol. B Biol. 94 (2009) 59–64.
- [49] M. Kavitha, M.J. Swamy, Spectroscopic and differential scanning calorimetric studies on the unfolding of *Trichosanthes dioica* seed lectin. Similar modes of thermal and chemical denaturation, Glycoconj. J. 26 (2009) 1075–1084.
- [50] G. Rabbani, E. Ahmed, M.V. Khan, M.T. Ashraf, R. Bhat, R.H. Khan, Impact of structural stability of cold adapted *Candida antarctica* lipase B (CalB): in relation to pH, chemical and thermal denaturation, RSC Adv. 5 (2015) 20115–20131.
- [51] A. Narahari, H. Singla, G. Bulusu, A. Surolia, M.J. Swamy, Isothermal titration calorimetric and computational modeling studies on chitooligosaccharide binding to pumpkin (*Cucurbita maxima*) phloem exudate lectin, J. Phys. Chem. B 115 (2011) 4110–4117.
- [52] K.B. Bobbili, A. Narahari, B. Singh, G. Bulusu, A. Surolia, M.J. Swamy, Chitooligosaccharide binding to CIA17 (*Coccinia indica* agglutinin). Thermodynamic characterization and formation of higher order complexes, Int. J. Biol. Macromol. 137 (2019) 774–782.
- [53] V. Anantharam, S.R. Patanjali, A. Surolia, A chitotetrose specific lectin from Luffa acutangula: Physico-chemical properties and the assignment of orientation of sugars in the lectin binding site, J. Biosci. 8 (1985) 403–411.
- [54] G. Rabbani, E.J. Lee, K. Ahmed, M.H. Baig, I. Choi, Binding of tolperisone hydrochloride with human serum albumin: effects on the conformation, thermodynamics and activity of HSA, Mol. Pharm. 15 (2018) 1445–1456.
- [55] W.J. Peumans, E.J.M. Van Damme, Lectins as plant defense proteins, Plant Physiol. 109 (1995) 347–352.
- [56] A. Cazet, S. Julien, M. Bobowoski, J. Burchell, P. Delannoy, Tumor-associated carbohydrate antigens in breast cancer, Breast Cancer Res. 12 (2010) 204.